Daniel Dizdarevic

Symmetries and Symmetrisation in Quantum and Electromagnetic Multi-Mode Systems for Balancing Gain and Loss

Von der Fakultät Mathematik und Physik der Universität Stuttgart
zur Erlangung der Würde eines Doktors der Naturwissenschaften
(Dr. rer. nat.) genehmigte Abhandlung

Vorgelegt von Daniel Dizdarevic aus Göppingen

Hauptberichter Apl. Prof. Dr. Jörg Main
Institut für Theoretische Physik I
Universität Stuttgart

Mitberichter Apl. Prof. Dr. Johannes Roth
Institut für Funktionelle Materie und Quantentechnologien
Universität Stuttgart

Tag der mündlichen Prüfung: 31. Mai 2021

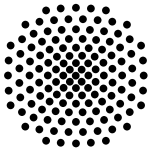

Universität Stuttgart
Institut für Theoretische Physik I

2021

Daniel Dizdarevic

Symmetries and Symmetrisation in Quantum and Electromagnetic Multi-Mode Systems for Balancing Gain and Loss

Dissertation, 2021

Hauptberichter: Apl. Prof. Dr. Jörg Main
Mitberichter: Apl. Prof. Dr. Johannes Roth

Universität Stuttgart

Institut für Theoretische Physik I
Pfaffenwaldring 57
70569 Stuttgart

I am the most incurably lazy devil that ever stood in shoe leather — that is, when the fit is on me, for I can be spry enough at times.

Sherlock Holmes

—A Study in Scarlet

Abstract

Losses usually are an undesirable effect in physics. However, in combination with gain, novel and unexpected features occur. This is because gain and loss can effectively be described via an imaginary potential, which renders a Hamiltonian non-Hermitian. Although there are similarities to standard quantum mechanics, non-Hermitian quantum mechanics exhibits unique mathematical features like bi-orthogonal and self-orthogonal states. Such systems can be used to describe open quantum systems efficiently; though, the overall probability is not conserved in general. However, by balancing gain and loss, stable stationary states with intriguing properties can be realised.

Balanced gain and loss occurs in combination with anti-unitary symmetries, which are related to time reversal. The simplest and most powerful symmetry in this regard is $\mathcal{PT}$ symmetry, which acted as the driving force behind the development of non-Hermitian quantum mechanics in the last two decades. Researchers produced some astounding results involving $\mathcal{PT}$ symmetry, like unidirectionally invisible structures and optimal robust wireless power transfer. Due to the generality of the $\mathcal{PT}$ operator, $\mathcal{PT}$ symmetry is applicable to almost any physical system, though, it is broken even for small perturbations. In the absence of symmetries, balanced gain and loss can still be achieved by means of symmetrisation or semi-symmetrisation, which are introduced in this thesis. Symmetrised non-Hermitian systems show similar features as symmetric ones, but they allow for a broader range of applications. Symmetrisation allows for the description of physical multi-well potentials with gain and loss. Yet, the lack of obvious symmetries or recognisable patterns makes symmetrised systems hard to understand intuitively.

The relations between symmetries and symmetrisation are discussed in detail and both concepts are explicitly applied to one-dimensional multi-mode quantum systems, for which a simple mat-

rix model is used as an example. Analytical symmetrised solutions are derived and it is explicitly demonstrated how symmetrisation can be used to systematically find two-mode systems with a stable stationary ground state. Further, it is shown that models with just two modes are only semi-symmetrisable, whereas they can be perfectly $\mathcal{PT}$-symmetric. Semi-symmetrisation is also applied to multi-mode systems for the realisation of multi-mode chains and to spatially extended Gaussian multi-well potentials. Gaussian potentials can be used in experimental realisations with Bose–Einstein condensates involving non-linear contact interactions; these can be used to realise a self-stabilising mechanism of stationary states, thus making the system robust with respect to small perturbations.

By deriving a mathematically equivalent model for inductively coupled electric resonant circuits, the concepts of symmetries and symmetrisation can be transferred from the quantum realm to the classical field of electrodynamics. While this provides a simple and, in particular, accessible platform for experiments, the possibility of applications for wireless power transfer are also discussed briefly, which concludes this thesis.

Inhaltsangabe in deutscher Sprache

Verluste sind in der Physik häufig ein unerwünschter Nebeneffekt. In Kombination mit Gewinn können jedoch neuartige und unerwartete Eigenschaften auftreten. Der Grund hierfür ist, dass sich Gewinn und Verlust effektiv durch komplexe Potentiale beschreiben lassen, durch die ein Hamilton-Operator nicht-Hermitesch wird. Obwohl es Gemeinsamkeiten zum üblichen Formalismus der Quantenmechanik gibt, treten einzigartige mathematische Eigenschaften in der nicht-Hermiteschen Quantenmechanik auf, wie etwa biorthogonale und selbstorthogonale Zustände. Solche Systeme lassen sich zur effizienten Beschreibung offener Quantensysteme verwenden. Jedoch ist die Gesamtwahrscheinlichkeit hierbei im Allgemeinen nicht erhalten. Gleichen sich Gewinn und Verlust aus, so lassen sich aber stabile stationäre Zustände mit verblüffenden Eigenschaften erzeugen.

Ausgeglichener Gewinn und Verlust tritt im Zusammenhang mit antiunitären Symmetrien auf, die wiederum mit Zeitumkehr zusammenhängen. Die einfachste und zugleich einflussreichste Symmetrie in dieser Hinsicht ist die $\mathcal{PT}$-Symmetrie, welche in den letzten zwei Jahrzehnten als treibende Kraft hinter der Entwicklung der nicht-Hermiteschen Quantenmechanik fungierte. Forscherinnen und Forscher haben einige erstaunliche Ergebnisse im Zusammenhang mit $\mathcal{PT}$-Symmetrie erzielt, zu denen unter anderem unidirektional unsichtbare Strukturen und optimale und zugleich stabile, kabellose Energieübertragungen zählen. Aufgrund der Allgemeingültigkeit des $\mathcal{PT}$-Operators lässt sich $\mathcal{PT}$-Symmetrie auf nahezu jedes physikalische System anwenden; jedoch kann die Symmetrie bereits durch kleine Störungen gebrochen werden. Ohne Symmetrien lassen sich mithilfe von Symmetrisierung oder Semisymmetrisierung, zwei Konzepte, die in dieser Arbeit eingeführt werden, dennoch ausgeglichene Gewinne und Verluste erzeugen. Symmetrisierte,

nicht-Hermitesche Systeme weisen ähnliche Eigenschaften auf wie die symmetrischen, erlauben jedoch eine Vielzahl zusätzlicher Anwendungsmöglichkeiten. Mithilfe von Symmetrisierung lassen sich auch physikalische Mehrmuldenpotentiale mit Gewinnen und Verlusten beschreiben. Dennoch können symmetrisierte Systeme aufgrund des Fehlens erkennbarer Symmetrien und Muster nur schwer intuitiv gedeutet oder nachvollzogen werden.

Die Beziehung zwischen Symmetrien und Symmetrisierung wird im Detail besprochen und beide Konzepte werden explizit auf eindimensionale Mehrmuldenquantensysteme angewandt, die exemplarisch durch ein einfaches Matrixmodell beschrieben werden. Es werden analytische Lösungen für symmetrisierte Systeme hergeleitet und im Detail gezeigt, wie Symmetrisierung dazu genutzt werden kann, Zweimodensysteme mit einem stabilen stationären Grundzustand zu finden. Darüber hinaus wird gezeigt, dass Modelle mit nur zwei Moden nur semisymmetrisierbar sind, wohingegen diese problemlos $\mathcal{PT}$-symmetrisch sein können. Semisymmetrisierung wird außerdem auf Mehrmodensysteme zur Realisierung von Transportketten und auf räumlich ausgedehnte, Gauß-förmige Mehrmuldenpotentiale angewandt. Gauß-förmige Potentiale lassen sich für experimentelle Realisierungen mit Bose–Einstein-Kondensaten verwenden, welche nichtlineare Kontaktwechselwirkungen aufweisen. Diese Wechselwirkungen können für die Erzeugung eines Selbststabilisierungsmechanismus stabiler Zustände genutzt werden, wodurch das System stabil gegenüber kleinen Störungen wird.

Da sich ein mathematisch äquivalentes Modell für induktiv gekoppelte, elektrische Schwingkreise finden lässt, können Konzepte über Symmetrien und Symmetrisierung von der Quantenebene auf die klassische Theorie der Elektrodynamik übertragen werden. Obwohl das bereits einen einfachen und insbesondere einfach zugänglichen Aufbau für Experimente liefert, wird auch die Möglichkeit einer Anwendung für kabellose Energieübertragungen kurz diskutiert, um diese Arbeit damit abzuschließen.

Contents

Introduction

I

Come, Watson, come! The game is afoot.

Sherlock Holmes

—The Adventure of the Abbey Grange

Losses of any sort usually are an unwanted but common effect in physics. They lead to undesirable properties of physical systems, which do no longer follow certain conservation laws. The dissipation of energy due to friction is a common example of a mostly undesirable loss of energy in mechanical systems. Another example is the attenuation of light in optical media due to absorption and scattering, which lead to a loss of light intensity and provide a limiting factor in modern signal transmission techniques.

In theory, though, such issues can simply be resolved: On time reversal, loss becomes gain and the evolution of a physical system is completely reversed.[I] By connecting a system to its time-reversed copy, the amount of loss is balanced by an equal amount of gain, which restores the conservation of the energy, for example. Of course, this argumentation also works *vice versa*, meaning that an undesirable gain, like *electromagnetic interference* in electronic devices, for example, can also be balanced by an equal amount of loss via a time-reversed copy of the system.

Balanced gain and loss appears to be a simple concept at a first glance and — literally — means that *gain and loss* of some quantity are *balanced* in such a way that the overall amount of the quantity does not change. This statement is simple and simultaneously so general that it holds everywhere, in principle. To give an explicit example, which serves in a similar form as a motivation in Ref. [1], a system consisting of cats and boxes seems like a reasonable starting point. This is not only due to tradition — *e.g.* see Ref. [2] — but also because cats show a natural affinity for boxes [3–5]. Any box is thus expected to exhibit a natural gain of cats as shown in

[I] This also holds for irreversible processes, since time reversal, being just a theoretical concept, also affects the *second law of thermodynamics*.

Figure 1-1: Gain, loss

Fig. 1-1. Hence, the cat occupation of the box increases over time. To safely decrease the cat occupation, one could move the box to a higher position and cut a hole into its bottom. This leads to a loss of cats due to gravity as shown in Fig. 1-1, until the box is empty; this method can be considered to be safe, since the cats will probably land on their feet[2] [7; 9–12].

[2] The *falling cat problem* was studied already by James Clerk-Maxwell [6] and is an example of a non-holonomic system [7], in contrast to the *buttered toast phenomenon* [8], for example.

Since suitable mechanisms for gain and loss of cats in boxes were found, one may now couple them by allowing for an exchange of cats between a box with cat gain and a box with cat loss. This can be achieved by connecting the boxes via a tunnel as shown in Fig. 1-2, *i.e.* the cats can now tunnel between the boxes. If the cat distribution is characterised by $|🐈\rangle$, then its changes can formally be described by a model of the form

$$\frac{\mathrm{d}}{\mathrm{d}t}\,|🐈\rangle = B\,|🐈\rangle\ , \tag{1-1}$$

where B is a 2×2 matrix in which the diagonal and off-diagonal elements characterise the individual boxes and their coupling, respectively. Since there should occur repulsions if the cat density per box is high enough, a cat tunnelling current flows from the box with higher cat occupation to the box with lower cat occupation. Without gain or loss, this would lead the cats to become equally distributed over all boxes, which then corresponds to a cat equilibrium.

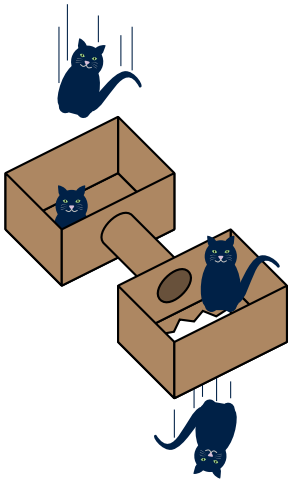

Figure 1-2: Balanced gain and loss

If gain and loss are balanced, *i.e.* the number of cats falling into one box is equal to the number of cats falling out of the other box per time, the overall number of cats in the boxes is conserved. Further, if the cat occupations are equal, a steady current flows from the box with gain to the box with loss. Although the cats are in perpetual motion, the cat occupation of each box appears to be constant under the assumption that the cats are indistinguishable; hence, the corresponding cat state $|🐈\rangle$ can be considered to be stationary.

Although the model (1-1) shown in Fig. 1-2 was introduced in a playful way, it encapsulates rather well the fundamental ideas which underlie this thesis. The model (1-1) corresponds to a one-dimensional, discrete two-mode system, which can be generalised to n modes by imagining n adjacently-connected boxes. Such static,

one-dimensional discrete systems occur in all fields of physics as discussed in the course of this thesis, and can, in principle, also be used to describe the dynamics of multi-dimensional lattices [13]. It should not have been surprising to see that balanced gain and loss of some quantity leads to a conservation, as there exist countless examples from everyday life to support this; one of them being that the amount of money a person owns does not change if income and expenses are balanced. Moreover, an interesting connection between gain, loss, and time reversal occurred, which, however, is no coincidence. In general, there exists a connection between the occurrence of stationary states and symmetries involving time reversal. The symmetries in the example above are obvious:

— gain and loss are balanced,

— the occupations are equal,

— the current and the occupations are conserved, *i.e.* they are symmetric in time.

However, there exist other systems with gain and loss, which — although possessing no apparent symmetries — yield stationary states as well. While gain and loss is also balanced, there exist fundamental differences between a symmetric system as discussed above, and such a symmetrised system. The discussion of concepts for balancing gain and loss and their applications in different physical systems is the foremost purpose of this thesis. Some more detailed motivations can be found in Chapters 3 and 9.

This thesis is organised in several parts, starting quite general and becoming more specialised with every chapter. First, Chapter 2 gives a rather general introduction to the concept of symmetries in physics. It is shown how physical theories can, in principle, be derived purely from symmetry considerations, which lays the foundations for the two other parts. The detailed discussion of time reversal in Section 2-3 a) is particularly important, as this concept is more subtle than it appears at first sight and takes a distinguished role among the symmetries in physics.

The first and major part of this thesis concerns quantum mechanics (QM) and introduces the reader to the idea of using non-

Hermitian operators, which leads to non-Hermitian quantum mechanics (NHQM). NHQM allows for an effective description of open quantum systems, *i.e.* quantum systems with gain and loss, for which different concepts of symmetry and symmetrisation to balance gain and loss are introduced. This involves discussions on linear and non-linear, discrete and continuous quantum systems. A brief overview of experimental methods to realise and investigate the considered systems with Bose–Einstein condensates (BECs) concludes the first part.

The second part of this thesis is much shorter and concerns the application of the results of the first part in electrodynamics (ED). In contrast to quantum systems, the considered models can rather easily be realised via inductively coupled resonant circuits. The derivation of the mathematically equivalent circuit model is of particular interest and represents the majority of the second part. Afterwards, the technical application of wireless power transfer (WPT) is briefly considered to demonstrate the model calculations with physical parameters.

In this theses different types of *natural units* are used, so that all quantities are dimensionless if not otherwise stated. For example, *Planck units* with $\hbar = c = 1$ are used for relativistic considerations, where the speed of light is the characteristic velocity. Such units are independent of the type of system which is considered. In contrast, in QM *atomic units* are useful, which are characterised by $\hbar = m = 1$, *i.e.* they are based specifically on systems with a characteristic mass m. Sloppily speaking, in the following, all of these quantities can be considered to be unity — "$\hbar = c = m = 1$" — if they are not appearing explicitly. In addition, a rich variety of notations is required and used throughout this thesis; some of them are common and some of them are not. An overview and summary of these notations can be found in Appendix A, which may be convenient to read beforehand.

Symmetry in physics

2

Symmetry is one of the most general and deep concepts in physics. Most of the theories in modern physics can be derived from symmetry principles directly. What is a symmetry in the first place, though?

Simply speaking, a *symmetry* occurs if a system is invariant under a certain operation. Such symmetry operations can be simple reflections or rotations. But in general, any mathematical operation can be a symmetry operation, some of which are rather abstract as shown in the course of this chapter. However, there are two different types of symmetries: Continuous symmetries are invariances with respect to infinitesimal operations. They are connected to conserved quantities or, *vice versa*, any conserved quantity in physics exists only because of a corresponding continuous symmetry, which is discussed in Section 2-1 c). In contrast, discrete symmetries are invariances with respect to finite operations like the flipping of signs of specific quantities. Although discrete symmetries seem to be much simpler at first sight, they involve some of the most fundamental symmetries in our universe and are deeply connected to the structure of quantum theory, as discussed in Sections 2-3 and 2-4.

At the end of this chapter, Section 2-5 introduces another and rather unusual symmetry. Supersymmetry (SUSY) describes the invariance of a theory under the exchange of bosons and fermions, the two different fundamental types of particles. While SUSY is known in the context of quantum field theories and the standard model, the focus in Section 2-5 lies on the general formalism in the context of QM, which forms the foundation of the discussions in Chapter 5.

2-1 Symmetry in Euclidean spaces

In this section the basic terminology and concepts of symmetry are introduced, starting with symmetry in Euclidean spaces. Most of the advanced concepts, which are discussed in the next sections and chapters, have simple analogues in the low-dimensional Euclidean spaces. This is particularly helpful to develop a more intuitive and clear understanding of the rather abstract mathematics behind group theory, which is used for the description of symmetries. For some more detailed introductions to the concepts of groups and symmetry see also Refs. [14; 15].

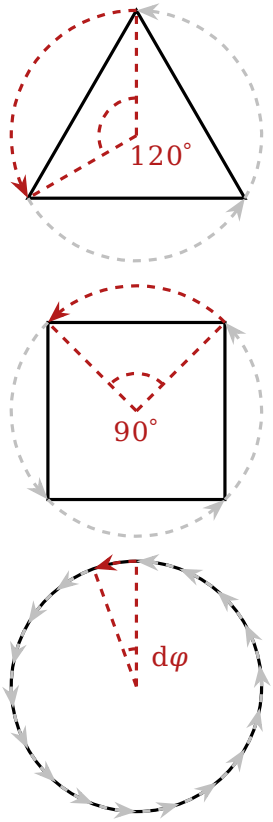

Figure 2-1: Different symmetric shapes

a) What is symmetry?

The term *symmetry* means that an object or a quantity is invariant under certain transformations. For example, an equilateral triangle is invariant under rotations of 120° around its centre of mass as shown in Fig. 2-1. If the corners are not labelled, then one does not even notice that such a transformation was applied at all. Therefore, the term *invariance* means that an object or a quantity is *exactly* the same as before. A similar but weaker concept is *covariance*, which means that only the *shape* of an object or quantity is the same after a transformation.

For example, a circle of radius r is defined by

$$x^2 + y^2 = r^2 \,, \tag{2-1}$$

where all points (x, y) on the circle are given by

$$\begin{pmatrix} x \\ y \end{pmatrix} = \begin{pmatrix} r\cos\varphi \\ r\sin\varphi \end{pmatrix}.$$

Obviously, a circle is invariant under rotations around its centre, which are transformations of φ because Eq. (2-1) does not depend on this parameter. However, a circle is merely covariant under isotropic stretching, which is a transformation of r, as such

transformations preserve only the shape of Eq. (2-1), but not its numerical value.

The rotational symmetry of a circle is an example of a *continuous symmetry*: For all possible rotation angles $\mathrm{d}\varphi \in [0, 2\pi)$ the circle looks the same. Moreover, the transformation parameter $\mathrm{d}\varphi$ can be arbitrarily small and thus arbitrarily close to the *identity transformation*, which does not alter the circle; in this case, the identity transformation is a rotation with $\mathrm{d}\varphi = 0$. Apart from such continuous symmetries there also exist *discrete symmetries*, in which only a finite number of transformation parameters exist for which the object appears unchanged.

Figure 2-1 shows that an equilateral triangle is invariant under rotations with $\varphi = 2\pi/3$ around its centre of mass. The same holds for a rotation with $\varphi = 4\pi/3$ and — trivially — for the rotation with $\varphi = 0$. However, the latter transformation is not really a symmetry because there is no object that changes if "nothing" is done; nevertheless the existence of such an identity transformations is important for the mathematical treatment of symmetries as discussed in the following. Other objects also possess similar discrete symmetries, like squares, which are symmetric with respect to rotations of $\varphi_n = n\pi/2$ for $n = 0, 1, 2, 3$.

For a moment, nothing happened. Then, after a second or so, nothing continued to happen.

Douglas Adams

b) Mathematical description of symmetry

In the previous section some examples for discrete and continuous symmetries in the plane were shown. To describe such symmetries mathematically, one must employ *group theory* and *Lie theory*.

A symmetry group $(S, \circ)$ of an object is a set of transformations S under which the object is invariant. The symmetry transformations then fulfil the group axioms with respect to the operation $\circ$:

— Closure: $s_1 \circ s_2 \in S \;\forall\; s_1, s_2 \in S$,

— Associativity: $s_1 \circ (s_2 \circ s_3) = (s_1 \circ s_2) \circ s_3 \;\forall\; s_1, s_2, s_3 \in S$,

— Existence of an identity: $\mathbb{1} \circ s = s = s \circ \mathbb{1} \;\forall\; s \in S$,

— Existence of an inverse: $s \circ s^{-1} = \mathbb{1} = s^{-1} \circ s \;\forall\; s \in S$.

The concept of symmetry groups is rather abstract but very powerful, since the properties of the group are independent of the objects on which the transformations can act. Therefore, symmetries can be studied separately and the knowledge can then be applied to whole classes of different objects with the same or similar symmetries.

Group theory

As an example of the description of a symmetry via group theory, one can consider all transformations $\mathbf{v}' = O(\mathbf{v})$ under which the Euclidean product

$$\mathbf{v} \cdot \mathbf{v} = \mathbf{v}^\mathsf{T} \mathbf{v} \tag{2-2}$$

is invariant. In the n-dimensional Euclidean space, transformations are described by $n \times n$ matrices and one finds

$$(\mathbf{v}')^\mathsf{T} \mathbf{v}' = \mathbf{v}^\mathsf{T} O^\mathsf{T} O \mathbf{v} \overset{!}{=} \mathbf{v} \cdot \mathbf{v} \,.$$

Transformation matrices which satisfy the condition

$$O^\mathsf{T} O = \mathbb{1} \tag{2-3}$$

are called *orthogonal* and do not change the length of vectors, *i.e.* the Euclidean product is invariant. The corresponding group is therefore called the n-dimensional orthogonal group $O(n)$.

However, there are two different types of orthogonal transformations. From Eq. (2-3) it follows that

$$\det\left(O^\mathsf{T} O\right) = \det O^\mathsf{T} \det O = \det^2 O = \det \mathbb{1} = 1 \,, \tag{2-4}$$

Therefore, there are either transformations with $\det O = 1$, which include only rotations, as they do not change the orientation of the underlying coordinate system, or transformations with $\det O = -1$, which include also reflections. The two types of transformations can be visualised by considering their actions on a geometric shape as shown in Fig. 2-2 at the example of a triangle; although both transformed triangles are congruent, their orientations are different.

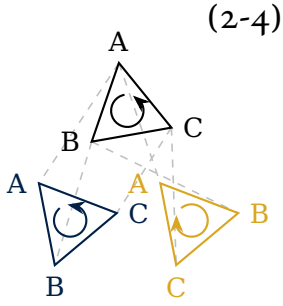

Figure 2-2: Transformations between congruent triangles

Lie theory

For continuous symmetries — like the rotational symmetry of a circle — the groups become *Lie groups*; they are not just groups, but also differentiable manifolds. For Lie groups it is sufficient to study infinitesimal transformations, *i.e.* transformations which are arbitrarily close to the identity transformation. An infinitesimal rotation $\mathrm{d}R$ can be expressed as

$$\mathrm{d}R = \mathbb{1} + \frac{\varphi}{N} G \tag{2-5}$$

with $N \to \infty$, where φ is a finite angle and G is another matrix called the *generator*. By applying the transformation (2-5) infinitely many times, a finite rotation

$$R(\varphi) = \lim_{N\to\infty} \left(\mathbb{1} + \frac{\varphi}{N} G\right)^N = \mathrm{e}^{G\varphi} \tag{2-6}$$

is obtained. Hence, G "generates" the finite transformations. Since one can obtain any finite transformations from infinitesimal ones, the Lie groups "look the same everywhere" and it is sufficient to study the structure in the vicinity of the identity. An important generator known from QM is the Hamiltonian, which generates the time evolution.

The generators of a Lie group form an algebra: The *Lie algebra* is a vector space $\mathfrak{S}$ with a bilinear, anti-commutative, binary operation $[\,,\,] : \mathfrak{S}\times\mathfrak{S} \to \mathfrak{S}$ called the Lie bracket, which also satisfies the Jacobi identity. The Lie bracket establishes the connection between the combination of elements of the Lie group and the combination of its generators via the Baker–Campbell–Hausdorff formula. An important property of a Lie algebra is that there always exists exactly one connected Lie group, which can be mapped to any of the other Lie groups being generated by the algebra. A well-known example of a Lie algebra is the angular momentum in QM. In this case, the Lie bracket is just the commutator and the corresponding Lie group describes rotations in three-dimensional space.

c) Noether's theorem

A connection between generators of continuous symmetries and conserved quantities — which are of utter importance to all physical theories — was found by Emmy Noether in 1918: Every conserved quantity is a generator of a symmetry group and *vice versa*.

To see this connection, one can consider a general Lagrangian[I] $\mathcal{L}(\phi, \partial_\mu \phi, t)$, where ϕ may be a generalised coordinate or even a field. A physical symmetry is a transformation, say $\phi \to \phi'(\phi, s)$ with a continuous parameter s so that $\phi'(\phi, 0) = \phi$, under which the Lagrangian is invariant,

$$\mathcal{L}\left(\phi', \partial_\mu \phi', t\right) = \mathcal{L}\left(\phi, \partial_\mu \phi, t\right).$$

It follows that

$$\frac{\mathrm{d}}{\mathrm{d}s}\mathcal{L}\left(\phi', \partial_\mu \phi', t\right) = \frac{\partial \mathcal{L}}{\partial \phi'}\frac{\partial \phi'}{\partial s} + \frac{\partial \mathcal{L}}{\partial\left(\partial_\mu \phi'\right)}\frac{\partial\left(\partial_\mu \phi'\right)}{\partial s} = 0\,. \tag{2-7}$$

The Euler–Lagrange equations also have to be invariant under a symmetry transformation, *i.e.*

$$\frac{\partial \mathcal{L}}{\partial \phi'} = \partial_\mu\left(\frac{\partial \mathcal{L}}{\partial\left(\partial_\mu \phi'\right)}\right).$$

Then, Eq. (2-7) can be written as

$$\partial_\mu\left(\frac{\partial \mathcal{L}}{\partial\left(\partial_\mu \phi'\right)}\frac{\partial \phi'}{\partial s}\right) \equiv \partial_\mu J^\mu = 0\,. \tag{2-8}$$

One immediately sees that a physical symmetry leads to a conserved quantity J^μ, which can in general be called *Noether current*; Eq. (2-8) can thus be understood as a *continuity equation*.

Examples of conserved quantities in physics are plentiful. As for the example mentioned above: The Hamiltonian is the generator of time evolutions, *i.e.* translations in time. The conserved quantity related to time translations via *Noether's theorem* is the energy.

[I] The formal notation $\partial_\mu \phi$ should indicate that this calculation is valid both in Euclidean spaces and in spacetime.

Representation theory

Since groups describe symmetry transformations in an abstract manner, they can act on all sorts of objects, which can be described via *representations*. A representation of a group is a mapping of the abstract group elements to a linear transformation acting on some vector space. This allows, for example, to apply the group $O(2)$, which is defined in the two-dimensional Euclidean space $\mathbb{R}^2$, to the three-dimensional Euclidean space $\mathbb{R}^3$, by finding the three-dimensional representations of its elements.

This short definition of representations should suffice for further purpose in this thesis. Although a thoroughful discussion of group theory, Lie theory, and representation theory would certainly be impossible to give in this scope, it would also distract the focus from the physical concepts which emerge as a *result* of the application of these mathematical tools. Therefore, the next section will give a short overview of how physical theories emerge naturally from simple assumptions about symmetry.

2-2 Physics from symmetry

In this section some of the most important concepts of physics are introduced and motivated from a symmetry perspective. Ref. [15] gives a thoroughful introduction and a detailed discussion on this subject and most of the following discussions represent selected summaries of topics discussed there.

a) The Lorentz group

One of the most fundamental symmetry groups in physics is the *Lorentz group* — the symmetry group of spacetime itself. This follows from the two basic assumptions that in all inertial[2] frames of reference

[2] *i.e.* non-accelerated

1) the laws of physics are the same (covariance),

Nothing travels faster than the speed of light, with the possible exception of bad news, which obeys its own special laws.

Douglas Adams

2) the vacuum velocity of light is the same (invariance).

These *principles of relativity* are the postulates Albert Einstein used in Ref. [16] to lay the foundations of relativity theory.

While the first assumption is relatively easy to accept, as it reflects everyday experiences, the second assumption seems rather odd. This is because life experience gives us an intuitive understanding of the *Newtonian* world, in which objects are moving at different velocities, the perception of which depends on the frame of reference. However, according to the laws of ED, the velocity at which light moves is independent of the frame of reference, so that it is not possible for a massive observer to travel alongside a beam of light and see it "frozen".[3] This contradicts our everyday experiences completely and leads to some absurd-looking phenomena, which are results of the fact that the perception of distances in space and in time depend on the frame of reference, *i.e.* they are *relative* instead of *absolute*.

[3] This is in fact the picture that brought Einstein to his conclusions [17].

However, by combining them into distances in four-dimensional spacetime,[4]

[4] Reminder: $c = 1$

$$s^2 = t^2 - x^2 - y^2 - z^2 \,, \tag{2-9}$$

one finds that this expression is the same in all frames of reference. Equation (2-9) is the inner product of spacetime and can be written as

$$s^2 = x_\mu \eta^{\mu\nu} x_\nu \,, \tag{2-10}$$

where the Greek indices refer to four-vectors governed by *Einstein's sum convention* and

$$\eta = \begin{pmatrix} 1 & & & \\ & -1 & & \\ & & -1 & \\ & & & -1 \end{pmatrix}$$

is the *metric of spacetime* $\mathbb{R}^{(1,3)}$. This definition is completely analogous to the Euclidean product (2-2), for which the metric is just the identity $\mathbb{1}$. However, in contrast to Euclidean products the

spacetime product (2-10) can also take negative values,[5] which describes distances of points in spacetime not being connected causally; that is, starting from one point, one would have to travel faster than light to reach the other point.

[5] *i.e.* it is *indefinite*

The transformations

$$\left(x'\right)_\mu = \Lambda^\nu_\mu x_\nu \,,$$

under which Eq. (2-10) is invariant, are defined by the condition

$$\Lambda^\mathsf{T} \eta \Lambda \stackrel{!}{=} \eta \,. \tag{2-11}$$

These are the *Lorentz transformations*, *i.e.* transformations between inertial systems. The Lorentz transformations are symmetries of spacetime. Their corresponding symmetry group is the *Lorentz group*[6] $O(1,3)$. As in Euclidean spaces, there are two types of Lorentz transformations with

[6] *cf.* the definition of the orthogonal group in Euclidean spaces: $O^\mathsf{T} \mathbb{1} O = \mathbb{1}$

$$(\det \Lambda)^2 = 1 \,,$$

which follows from the definition (2-11) directly. As discussed in Section 2-1 b), the transformations with $\det \Lambda = 1$ preserve the orientation of spacetime, while the transformations with $\det \Lambda = -1$ do not.

In contrast to Euclidean spaces, however, the time component plays a special role in the Lorentz group. Equation (2-11) yields

$$\Lambda^0_0 = \pm \sqrt{1 + \sum_n \left(\Lambda^n_0\right)^2} \,, \tag{2-12}$$

where n runs over the spatial components. Because of

$$\left(x'\right)_0 = t' = \Lambda^0_0 t + \sum_n \Lambda^n_0 x_n \,,$$

Eq. (2-12) determines the direction of time in the Lorentz transformation: For $\Lambda^0_0 > 0$, time is transformed "forwards", while transformations with $\Lambda^0_0 < 0$ include time reversal. With this knowledge one can further conclude that transformations with $\det \Lambda < 0$ and $\Lambda^0_0 \lessgtr 0$ include either only temporal or spatial reflections.

Table 2-1: The four different components of the Lorentz group

$\det \Lambda$	Λ^0_0	Op.
> 0	> 0	$\mathbb{1}$
< 0	> 0	$\mathcal{P}$
< 0	< 0	$\mathcal{CT}$
> 0	< 0	$\mathcal{CPT}$

It is useful to assign operators to these fundamental physical transformations:

— The *parity operator* $\mathcal{P}$ generates spatial inversions.

— The "*time-reversal*"[7] operator $\mathcal{CT}$ generates temporal inversions.

[7] The pure time-reversal operator $\mathcal{T}$ cannot be expressed as a Lorentz transformation *per se*, *cf.* Section 2-3 a).

While these operations are defined abstractly, their representations in four-dimensional spacetime read[8]

$$\mathcal{P} = \begin{pmatrix} 1 & & & \\ & -1 & & \\ & & -1 & \\ & & & -1 \end{pmatrix}, \quad \mathcal{CT} = \begin{pmatrix} -1 & & & \\ & 1 & & \\ & & 1 & \\ & & & 1 \end{pmatrix}.$$

[8] Note that the parity operator is also the metric of spacetime.

One also finds that there are transformations which invert time while preserving the orientation of spacetime as a whole. Such transformations are spacetime reflections and can be expressed with the operator $\mathcal{CPT}$.[9]

[9] *cf.* Section 2-3 b)

In conclusion, the Lorentz group consists of four components which are summarised in Table 2-1. Each component can be obtained by applying the corresponding operator onto the proper Lorentz group[10] with $\det \Lambda > 0$ and $\Lambda^0_0 > 0$. Because of this, the four components are disconnected, *i.e.* elements from different components cannot be transformed continuously into one another.

[10] The identity transformation preserves both the orientation of the coordinate system and the direction of time. Therefore, only such transformations can form a proper subgroup.

Generators

The Lorentz group possesses six symmetry generators,[11] which describe the possible transformations between inertial systems:

[11] *cf.* Eq. (2-6)

1) *Spatial rotations* can be described by

$$\Lambda_{\mathrm{R}}(\varphi) = \begin{pmatrix} 1 & \\ & R_m(\varphi) \end{pmatrix},$$

where $R_m(\varphi)$ are the three-dimensional Euclidean rotation matrices forming the special orthogonal group $SO(3)$. Since rotations in space are continuous, they can be generated by the three-

dimensional matrices[12] $J_m^{(3)}$,

$$R_m(\varphi) = \mathrm{e}^{\mathrm{i}J_m^{(3)}\varphi}\,,$$

which satisfy the relations

$$\left(J_m^{(3)}\right)^{\mathsf{T}} + J_m^{(3)} = 0\,,$$
$$\operatorname{tr} J_m^{(3)} = 0$$

following from Eqs. (2-3) and (2-4). Hence, the generators of rotations in spacetime read

$$J_m = \begin{pmatrix} 0 & \\ & J_m^{(3)} \end{pmatrix}.$$

[12] Note the additional imaginary unit in the exponential function, which is a common convention.

2) *Boosts* essentially are translations of four-momentum in spacetime. Such transformations are also continuous and can thus be written as

$$\Lambda_{\mathrm{B}} = \mathrm{e}^{\mathrm{i}K_m\theta} = \lim_{N\to\infty} \lambda_{\mathrm{B}}^N\,,$$

where $\lambda_{\mathrm{B}} = \mathbb{1} + \epsilon K_m$ with $|\epsilon| = |\mathrm{i}\theta/N| \ll 1$ are infinitesimal transformations generated by the matrices K_m. With Eq. (2-11) one finds that the generators K_μ of boosts must satisfy

$$K_m^{\mathsf{T}}\eta + \eta K_m = 0 \tag{2-13}$$

in the first order of ϵ.

With these generators the Lorentz transformations can in general be written as

$$\Lambda = \Lambda_{\mathrm{R}}\Lambda_{\mathrm{B}} = \mathrm{e}^{\mathrm{i}(\mathbf{J}\cdot\boldsymbol{\varphi}+\mathbf{K}\cdot\boldsymbol{\theta})}$$

with $\mathbf{J} = (J_1, J_2, J_3)^{\mathsf{T}}$ and $\mathbf{K} = (K_1, K_2, K_3)^{\mathsf{T}}$ satisfying

$$[J_k, J_l] = \mathrm{i}\epsilon_{klm}J_m\,,$$
$$[J_k, K_l] = \mathrm{i}\epsilon_{klm}K_m\,, \tag{2-14}$$

$$[K_k, K_l] = -\mathrm{i}\epsilon_{klm} J_m \,, \tag{2-15}$$

where the commutator is defined by $[A, B] = AB - BA$. Equation (2-14) shows that the commutators of rotations and boosts do not commutate. Moreover, because of Eq. (2-15) the boost generators are not even closed on themselves. Therefore, it is useful to define new generators

$$N_k^{\pm} = \frac{1}{2}(J_k \pm \mathrm{i} K_k)$$

satisfying

$$\left[N_k^{\pm}, N_l^{\pm}\right] = \mathrm{i}\epsilon_{klm} N_m^{\pm} \,, \tag{2-16}$$

$$\left[N_k^{+}, N_l^{-}\right] = 0 \tag{2-17}$$

which are closed because of Eq. (2-17). Each of these generators corresponds to an $SU(2)$ algebra defined by Eq. (2-16), respectively. The generators for the remaining components of the Lorentz group can be obtained by applying the corresponding operator from Table 2-1,

$$\begin{aligned} \mathcal{P} N_k^{\pm} &= N_k^{\mp} \,, \\ \mathcal{C}\mathcal{T} N_k^{\pm} &= N_k^{\mp} \,, \\ \mathcal{C}\mathcal{P}\mathcal{T} N_k^{\pm} &= N_k^{\pm} \,. \end{aligned} \tag{2-18}$$

The $SU(2)$ algebra is best known from QM because $SU(2)$ is the group of unitary 2×2 matrices with unit determinants describing rotations in $\mathbb{C}^2$. By choosing a distinguished direction, the eigenvectors of the corresponding generators form a $(2j+1)$-dimensional basis[13] with eigenvalues $\{-j, \dots, j\}$; this is possible only if j is either an integer or a half-integer. Hence, the $SU(2)$ algebra is suitable to describe the properties of spin and is therefore also called spin or angular momentum algebra.

[13] j can be obtained from the eigenvalues of the *Casimir operator* in this basis; an example being the squared angular momentum operator.

However, as discussed in Section 2-1 b), a group can be represented in various ways depending on the objects on which the group acts. The two lowest-dimensional representations are used in Section 2-2 b) to show how some of the fundamental theories in physics arise:

1) For $j = 0$ a *one-dimensional representation* is obtained, *i.e.* the vector space on which the group acts is one-dimensional. In this case, all generators must be zero to satisfy Eq. (2-16),

$$N_k^{\pm} = 0\,.$$

2) For $j = 1/2$ a *two-dimensional representation* is obtained, *i.e.* the vector space is two-dimensional in this case. This corresponds to the usual description of spin $1/2$ as discussed above with

$$|\uparrow\rangle = \begin{pmatrix} 1 \\ 0 \end{pmatrix},$$
$$|\downarrow\rangle = \begin{pmatrix} 0 \\ 1 \end{pmatrix}.$$

In this case, the generators are given by the three *Pauli matrices*

$$\sigma_1 = \begin{pmatrix} 0 & 1 \\ 1 & 0 \end{pmatrix}, \quad \sigma_2 = \begin{pmatrix} 0 & -\mathrm{i} \\ \mathrm{i} & 0 \end{pmatrix}, \quad \sigma_3 = \begin{pmatrix} 1 & 0 \\ 0 & -1 \end{pmatrix} \tag{2-19}$$

via

$$N_k^{\pm} = \frac{\sigma_\mathrm{k}}{2}\,. \tag{2-20}$$

b) Representations of the Lorentz group

In Section 2-2 a) it was shown that the Lorentz group contains two copies of the $SU(2)$ algebra. The $SU(2)$ algebra, on the other hand, can act either on scalars or vectors. With these results the most important representations of the Lorentz group[14] can be derived, which will give rise to some of the most fundamental physical theories. Since these representations stem from combinations of the two copies of the $SU(2)$ algebra, they can be labelled by (j_1, j_2).

[14] or more precisely, the representations of the *covering group* of the Lorentz group

The $(0, 0)$ representation

The combination of the lowest-dimensional representations of $SU(2)$ yields the lowest-dimensional representation of the Lorentz group with $j_1 = j_2 = 0$. The generators of the $SU(2)$ algebra are both zero, $N_k^+ = N_k^- = 0$. Hence, the corresponding transformations are given by

$$\Lambda = \prod_k \mathrm{e}^{\mathrm{i}N_k^+\phi_k^+}\,\mathrm{e}^{\mathrm{i}N_k^-\phi_k^-} = 1$$

which act on Lorentz scalars. The $(0, 0)$ representation is thus also called *scalar representation*. Here, ϕ_k are the components of the scalar field.

Using the non-interacting scalar Lagrangian

$$\mathcal{L} = \frac{1}{2}\left(\partial_\mu\phi\partial^\mu\phi - m^2\right)$$

and the Euler–Lagrange equations, one finds the *Klein–Gordon equation*

$$\left(\partial_\mu\partial^\mu + m^2\right)\phi = 0 \tag{2-21}$$

that corresponds to the equations of motion for massive, non-interacting bosons with spin 0. From Eq. (2-21) the Schrödinger equation can be derived, which is shown in Section 2-2 c).

The $(1/2, 0)$ and $(0, 1/2)$ representations

If different representations of $SU(2)$ are combined, then either the $(1/2, 0)$ representation with

$$N_k^+ = \frac{\sigma_\mathrm{k}}{2}\,,$$
$$N_k^- = 0$$

or the $(0, 1/2)$ representation with

$$N_k^+ = 0\,,$$

$$N_k^- = \frac{\sigma_k}{2}$$

are obtained. One can show that N_k^+ and N_k^- are exchanged under a parity transformation [15]; hence, a parity transformation causes a transition from the $(1/2, 0)$ to the $(0, 1/2)$ representation and *vice versa*. The objects, on which the Lorentz transformations in these representations act, possess two components and are called *Weyl spinors*. The Weyl spinors of the $(1/2, 0)$ representation are called *left-handed*, while those of the $(0, 1/2)$ representation are called *right-handed*.

A parity-symmetric theory can be constructed by combining both representations: The $(1/2, 0) \oplus (0, 1/2)$ representation acts on the *Dirac spinor field* $\underline{\psi}$, which contains both left-handed and right-handed Weyl spinors. The corresponding Lorentz-invariant Lagrangian reads

$$\mathcal{L} = \overline{\psi}\left(\mathrm{i}\gamma^\mu \partial_\mu - m\right)\underline{\psi}\,,$$

where $\overline{\psi} = \underline{\psi}^\dagger \gamma_0$ with the 4×4 *Dirac matrices* γ_k satisfying the *Dirac algebra*

$$\left\{\gamma^\mu, \gamma^\nu\right\} = 2\eta^{\mu\nu}\mathbb{1}\,.$$

By using the Euler–Lagrange equations, one obtains the *Dirac equation*

$$\left(\mathrm{i}\gamma^\mu \partial_\mu - m\right)\underline{\psi} = 0 \tag{2-22}$$

that describes massive, non-interacting fermions with spin 1/2.

The (1/2, 1/2) representation

Finally, by combining the two-dimensional representations of $SU(2)$ the $(1/2, 1/2)$ representation of the Lorentz group is obtained. Since the generators (2-20) commute, they act independently on the four-component objects. A reasonable choice for them are given by Hermitian 2×2 matrices, their basis given again by the Pauli matrices (2-19) together with the identity $\sigma_0 = \mathbb{1}$.

Further, one can show that the $(1/2, 1/2)$ representation transforms Hermitian matrices into Hermitian matrices [18]. The four independent components of a Hermitian matrix can be interpreted as the components of a vector, which then corresponds to the usual four-vector notation of relativity theory. Hence, the Lorentz transformations of special relativity belong to the $(1/2, 1/2)$ representation of the Lorentz group. However, this also reveals that four-vectors consist of two spinors of rank 2. Therefore, four-vectors are not the fundamental objects of spacetime and thus are not suited to describe all physical systems.

Using the non-interacting four-vector Lagrangian

$$\mathcal{L} = \frac{1}{4}\partial^\mu B^\nu \partial_\mu B_\nu - \frac{1}{4}\partial^\mu B^\nu \partial^\nu B_\mu + \frac{m^2}{2} B^\mu B_\mu \tag{2-23}$$

with a generalised electromagnetic four-potential B^μ [19] and the Euler–Lagrange equations, one finds the *Proca equation*

$$m^2 B^\mu = \frac{1}{2}\partial_\nu \left(\partial^\nu B^\mu - \partial^\mu B^\nu\right) \tag{2-24}$$

that describes massive, non-interacting bosons with spin 1. From Eq. (2-24) the Maxwell equations can be derived, which is shown in Section 2-2 c).

c) Derivation of physical theories

In this section the connection between the representations of the Lorentz group introduced in Section 2-2 b) and some of the "fundamental" physical theories are derived. While the close connection between relativity theory and ED is well-known,[15] also the Schrödinger equation can be derived from the Lorentz group in the non-relativistic approximation. That is, while these theories can formally be derived, their natural constants like the speed of light c or the reduced Planck constant $\hbar$ have to be determined experimentally.

[15] ED was, in fact, the first Lorentz-invariant field theory and inspired Einstein's special relativity.

Electrodynamics

The Proca equation (2-24) describes massive spin-1 fields. However, with $m = 0$ it can also be used to describe massless photons by

$$\partial_\mu G^{\mu\nu} = 0 \tag{2-25}$$

with the *dual electromagnetic tensor*

$$G^{\mu\nu} = \partial^\mu B^\nu - \partial^\nu B^\mu \,. \tag{2-26}$$

Photons are the exchange particles of electromagnetic interactions. Hence, Eqs. (2-25) and (2-26) correspond to the homogeneous Maxwell equations.

To derive the Maxwell equations in the presence of electrical charges and currents, the Lagrangian (2-23) must be coupled to the Dirac equation (2-22), which provides the required description of spin-1/2 fields. A detailed discussion of this topic may be found in Ref. [15]. However, here it is sufficient to note that the resulting Lagrangian is locally $U(1)$ invariant. The conserved quantity related to this symmetry according to Noether's theorem is the Noether current J^μ satisfying the continuity equation (2-8). Then, the inhomogeneous Maxwell equations read

$$\partial_\mu F^{\mu\nu} = J^\nu \,, \tag{2-27}$$

where J^μ corresponds to the electrical four-current and $F^{\mu\nu}$ is the *electromagnetic tensor* defined by

$$F^{\mu\nu} = \partial^\mu A^\nu - \partial^\nu A^\mu \,. \tag{2-28}$$

Since Eq. (2-28) is anti-symmetric, *i.e.* $F^{\mu\nu} = -F^{\nu\mu}$, the electromagnetic tensor contains just six independent components,

$$F^{k0} \equiv E^k \,,$$
$$F^{kl} \equiv -\epsilon^{klm} B^m \,,$$

where ϵ^{klm} is the *Levi–Civita symbol*. By separating Eq. (2-27) into its temporal and spatial parts, one finds

$$\nabla \cdot \mathbf{E} = J^0 \,, \tag{2-29}$$

$$\nabla \times \mathbf{B} - \partial_t \mathbf{E} = \mathbf{J} \,, \tag{2-30}$$

which are the inhomogeneous Maxwell equations in differential representation.

From here, also the homogeneous Maxwell equations can be derived: The derivative of the product of the electromagnetic tensor (2-28) and any *completely anti-symmetric tensor* is always zero.[16] A completely anti-symmetric tensor is, for example, given by the *Levi–Civita symbol*. Hence,

[16] *i.e.* Eq. (2-25)

$$G^{\mu\nu} \propto \epsilon^{\mu\nu\alpha\beta} F^{\alpha\beta}$$

satisfies Eq. (2-25), which analogously yields

$$\nabla \cdot \mathbf{B} = 0 \,, \tag{2-31}$$

$$\nabla \times \mathbf{E} + \partial_t \mathbf{B} = 0 \,. \tag{2-32}$$

Equations (2-29) to (2-32) are the Maxwell equations in differential representation and form the foundations of ED.

Quantum mechanics

In Section 2-2 a) the fundamental transformations of the Lorentz group were discussed, which are spatial rotations and boosts. However, physical theories should also be invariant with respect to the choice of the spacetime origin. The corresponding transformations are translations in spacetime. Therefore, by combining spatial rotations, boosts, and temporal and spatial translations the *Poincaré group* is obtained. The Poincaré group is the fundamental symmetry group of spacetime, underlying all physical theories.

In QM the concept of operators is of vital importance. The operators corresponding to physical quantities can be identified with the corresponding symmetry generators as discussed in Appendix B. With Eqs. (B-2) and (B-3) the Klein–Gordon equation (2-21) can

be written as

$$\left(\hat{p}^2 - E^2 + m^2\right)\phi = 0\,. \tag{2-33}$$

The solutions of Eq. (2-33) are given by plane waves

$$\phi(\hat{x}, t) = \mathrm{e}^{\mathrm{i}(\hat{p}\hat{x} - Et)} \tag{2-34}$$

with energies

$$E = \pm m\sqrt{1 + \frac{\hat{p}^2}{m^2}}$$

that can be either positive or negative. However, the negative energy solutions are neglected in the following.[17]

[17] This is the usual interpretation of a *Dirac sea*, in which all states with negative energies are assumed to be occupied already.

In the non-relativistic limit $|\hat{p}| \ll m$, where the kinetic energy of an object is much smaller than its rest energy, one finds

$$E = m\left[1 + \frac{\hat{p}^2}{2m^2} + O\left(\frac{\hat{p}^4}{m^4}\right)\right]. \tag{2-35}$$

With Eq. (2-35) the solutions (2-34) read

$$\phi(\hat{x}, t) \approx \mathrm{e}^{-\mathrm{i}mt}\,\mathrm{e}^{\mathrm{i}(\hat{p}\cdot\hat{x} - \frac{\hat{p}^2}{2m}t)} \equiv \mathrm{e}^{-\mathrm{i}mt}\psi(\hat{x}, t)\,. \tag{2-36}$$

The first term oscillates rapidly in comparison with the time dependence of ψ. By inserting Eq. (2-36) into the Klein–Gordon equation (2-21) and after some calculations [15] one finally finds the *Schrödinger equation* for a free particle[18]

$$\left(\mathrm{i}\partial_t + \frac{1}{2}\nabla^2\right)\psi(\hat{x}, t) = 0 \tag{2-37}$$

[18] *i.e.* for $\hbar = m = 1$; their values have to be determined by experimental means

with the non-relativistic kinetic energy $E = \hat{p}^2/2$.

Equation (2-37) describes the motion of a non-interacting particle in free space characterised by the wave function ψ. To describe the motion of a particle in an external potential V, one can simply add an additional term, *i.e.*

$$\left(\mathrm{i}\partial_t + \frac{1}{2}\nabla^2 - V(\hat{x}, t)\right)\psi(\hat{x}, t) = 0\,. \tag{2-38}$$

With Eqs. (B-1) to (B-4) and by rearranging the terms one obtains the usual *Schrödinger eigenvalue equation* in the presence of an external potential,

$$E\psi(\hat{x},t) = \left(\frac{\hat{p}^2}{2} + V(\hat{x},t)\right)\psi(\hat{x},t) \equiv \mathcal{H}\psi(\hat{x},t)\,. \tag{2-39}$$

Here, the Hamiltonian $\mathcal{H}$ is defined as the observable, physical operator corresponding the energy E. The probability of finding a quantum system in an eigenstate of $\mathcal{H}$ is determined by the absolute square of the corresponding eigenstate due to *Born's rule*.[19]

[19] This can also be motivated by symmetry considerations [20].

It should be noted that Eq. (2-39) does not further impose particular properties onto the Hamiltonian $\mathcal{H}$ or the potential V. The usual Hermiticity condition, which is sufficient to guarantee the reality of energy eigenvalues, is introduced as a postulate, *i.e.* it is not a necessary condition *per se*. This fact is further discussed and exploited in Chapter 4.

2-3 Fundamental symmetries in physical theories

A *fundamental symmetry* usually refers to a symmetry of nature which always holds. However, in this section the term will also be used for symmetries which are emerging from fundamental physical concepts and under which *most* physical systems are invariant. These symmetries are connected to the three fundamental operations of time reversal, parity inversion, and charge conjugation.

a) Time reversal

Time reversal is a fundamental symmetry operation in physics. Most physical theories are unchanged if all motions are reversed; they are *time-reversal symmetric*. Naively speaking, time-reversal

symmetry means that an object, which has been moving for a certain amount of time, will return to its initial state after the same amount of "reversed" time.

To get a glimpse on the notion of time reversal, one can consider a free particle moving in space. Intuitively, time reversal — in the literal sense — simply means that the parameter t is reversed, *i.e.* $t \to -t$. Time reversal also makes the particle move "backwards", *i.e.* $\mathbf{p} \to -\mathbf{p}$. A system is called time-reversal invariant if its equations of motions are invariant under these transformations. For a free particle, this is obviously the case, since its equation of motion depends quadratically on the momentum.

ED is also time-reversal invariant if all charges, which are creating the electromagnetic fields, are taken into account. To see this, one might consider the movement of a charged particle, like an electron with charge e, in the presence of a static, homogeneous external field perpendicular to the initial direction of motion. For an electric field $\mathbf{E}$ the electric force $\mathbf{F}_\mathrm{E} = e\mathbf{E}$ is independent of the motion of the electron. Therefore, the equations of motion for the electron are invariant under time reversal.

However, in the presence of a magnetic field $\mathbf{B}$ the Lorentz force $\mathbf{F}_\mathrm{L} = e/m_\mathrm{e}\mathbf{p}\times\mathbf{B}$ depends linearly on the momentum. Therefore, the equations of motion for the electron apparently are not invariant under time reversal. Figure 2-3 illustrates this scenario: The electron, starting from point A, will move in a clockwise circular motion to point B. If time and momentum are reversed, the electron will, however, not return to its initial position, but again moves in a clockwise circular motion to point C. This is due to the fact that the Lorentz force is changing its sign under time reversal. In order for the electron to return to its initial position, either the charge of the electron or the magnetic field have to be flipped in addition. In the former case, the corresponding symmetry operation is called *charge conjugation*[20] and it transforms particles into antiparticles and *vice versa*. In both cases, the Lorentz force and the canonical momentum $\mathbf{p} = \mathbf{p}_\mathrm{kin} - e\mathbf{A}$, which differs from the kinetic momentum $\mathbf{p}_\mathrm{kin}$ in the presence of a vector potential, is reversed; such effects do not necessarily require the physical presence of a magnetic field

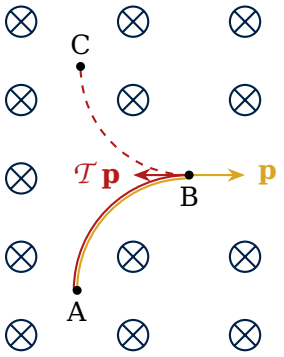

Figure 2-3: Time reversal in a magnetic field

[20] The related operator $\mathcal{C}$ is discussed in Section 2-3 b).

$\mathbf{B} = \nabla \times \mathbf{A}$, though, as the *Aharonov–Bohm effect* demonstrates [21–23], for example.

In reality, however, the magnetic field is inverted.[21] This may seem peculiar at first, but it can be understood by considering the simple physical process underlying the creation of a magnetic field. For this, consider electrons moving in a neutrally charged wire, *i.e.* the number of electrons equals the number of protons per area and time[22] as shown in Fig. 2-4. Despite the presence of a steady electric current, no electric field is created and so there is no effect on a charged particle in the vicinity of the wire. Now, consider a charged particle which is moving parallel to the electrons in the wire at the same velocity. In the frame of reference of the charged particle the electrons are resting, whereas the positively charged cores are moving. This causes their separating distances to contract slightly, thus increasing their density. Simultaneously, the electrons are spread out due to the assumption above; these opposite effects cause a charge imbalance as shown in Fig. 2-5. That is, for a moving particle the wire does no longer appear neutral and it thus experiences the effects of an electric field, so that the charged particle is either attracted or repelled. In the rest frame of the cores, this can effectively be described by the Lorentz force via a magnetic field.[23] On time reversal, both the motions of the charged particle and the motion of the electrons — and thus the current — are reversed. If time reversal does not act on the charges *per se*, the physical situation is unchanged and the direction of the electric force on the moving particle is preserved as required in Fig. 2-3. Thus, due to the definition of the Lorentz force, the magnetic field must be inverted, which is in agreement with the fact that the magnetic field is a consequence of the current in the wire in the first place.

However, the alternative, which involves a charge conjugation, is still worthwhile to discuss, as it actually corresponds to the Lorentz transformation $\mathcal{CT}$ defined in Section 2-2 a). Since $\mathcal{CT}$ inverts the time-component of four-vectors, it can be considered to be an operator for time reversal in its own right, but it necessarily also includes a charge conjugation.[24] This can easily be seen by applying $\mathcal{CT}$ to the four-current on the right-hand side of the

[21] *e.g.* see Ref. [24]

[22] It is assumed that this already includes effects due to length contraction.

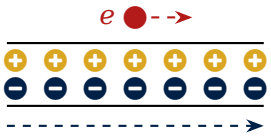

Figure 2-4: Neutral wire in the rest frame of its cores

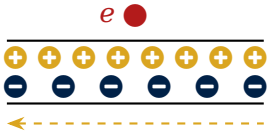

Figure 2-5: The wire in Fig. 2-4 in the rest frame of the electrons

[23] *i.e.* a magnetic field depends on the frame of reference

[24] hence the inclusion of the operator $\mathcal{C}$

Maxwell equations (2-27), for which the first component is the charge density. In fact, this example also shows that $\mathcal{CT}$ does not change the current because both the direction of movement and the charge are inverted simultaneously; hence, the magnetic field $\mathbf{B}$ is unchanged by the time-reversal $\mathcal{CT}$. The fundamental difference between the operators $\mathcal{T}$ and $\mathcal{CT}$ for time-reversal lies in the fact that the former is required to invert *trajectories*,[25] whereas the latter just inverts *vectors* in time; this may or may not be equivalent depending on the system. Therefore, the real time-reversal operator $\mathcal{T}$ can be — but does not necessarily has to be — a Lorentz transformation in a given situation.

[25] *cf.* Fig. 2-3

To summarise, on time reversal all motions are reversed, so that $\mathbf{j} \to -\mathbf{j}$ and $\mathbf{B} \to -\mathbf{B}$. Moreover, $\rho \to \rho$ and $\mathbf{E} \to \mathbf{E}$ because charges and thus the charge density ρ are unchanged. The Maxwell equations (2-29) to (2-32) are invariant with respect to these changes, which shows that ED is indeed time-reversal symmetric.[26] However, the Maxwell equations are also invariant under the Lorentz transformation $\mathcal{CT}$, *i.e.* ED is a Lorentz invariant theory as already mentioned in Section 2-2 c).

[26] Nevertheless, some physicists are claiming that it is not because both the electric and the magnetic fields must not be inverted, *e.g.* see Ref. [25]. However, this contradicts the discussions above.

In fact, most processes in the universe are time reversible concerning either classical physics but also on the quantum level.[27] This would imply that there exists no specific direction of time and that time reversal is a fundamental symmetry of nature. However, even on a macroscopic level there are systems violating time-reversal symmetry due to the *second law of thermodynamics*, which states that the entropy of an isolated system — *e.g.* the whole universe — never decreases over time; *i.e.* there exists an arrow of time. While the laws of thermodynamics are emergent properties of large numbers of particles, time-reversal symmetry is also violated by the fundamental laws of physics [26] as discussed in Section 2-3 b).

[27] That is, the quantum time-evolution operator is invariant under time reversal as shown in Section 2-4 b).

b) $\mathcal{CPT}$ symmetry

Apart from the time-reversal symmetry discussed in Section 2-3 a), there exist two other discrete fundamental symmetries, all three of which are illustrated in Fig. 2-6. To summarise:

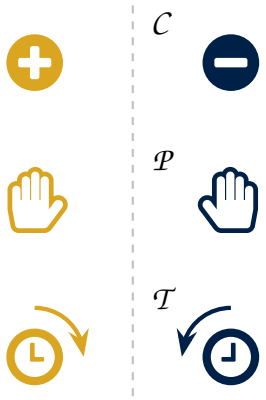

Figure 2-6: Illustration of the discrete fundamental symmetry operations

1) *Time-reversal symmetry* was introduced in Sections 2-2 a) and 2-3 a) and states that the evolution of a system is time reversible. In such systems there exists no arrow of time, *i.e.* an observer may not distinguish between future and past.

2) *Parity-inversion symmetry* was introduced in Section 2-2 a) and states that the laws of physics are indifferent to the "handedness" of objects; if the universe is mirrored, right-handed becomes left-handed and *vice versa*. In such systems there exists no preference for left-handedness or right-handedness, *i.e.* an observer may not be able to distinguish between the universe and its mirror image.

3) *Charge-conjugation symmetry* was briefly introduced in Section 2-3 a) and states that a system is invariant if all charges are exchanged with their anti-charges.[28] In such systems there exists no preferred type of charge, *i.e.* an observer may not distinguish between particles and antiparticles.

[28] This holds for the electrical charge and for all other types of charges arising in quantum field theory.

While most systems — both classical and quantum — respect these symmetries either separately or combined, they are not fundamental in the sense that they are not obeyed by all physical systems. There are particle decays caused by the weak force violating either one of these symmetries [27–29]. However, their combination $\mathcal{CPT}$ is considered to be a fundamental symmetry of all physical laws [30–32] and it is closely related to Lorentz invariance [33; 34]. In fact, the *$\mathcal{CPT}$ symmetry* holds for any theory which is invariant under Lorentz transformations and in which a vacuum exists with the same property; these are the very principles on which quantum field theories and the current understanding of our world are built upon. Therefore, this fact is also known as the *$\mathcal{CPT}$ theorem*.

2-4 Symmetry in quantum theories

In QM a system described by a Hamiltonian $\mathcal{H}$ is symmetric with respect to $\mathcal{S}$ if

$$[\mathcal{S}, \mathcal{H}] = \mathcal{S}\mathcal{H} - \mathcal{H}\mathcal{S} = 0\,. \tag{2-40}$$

That is, the Hamiltonian is invariant under the transformation $\mathcal{H}' = \mathcal{S}^{-1}\mathcal{H}\mathcal{S}$, *i.e.* $\mathcal{H}' = \mathcal{H}$. Such operators $\mathcal{S}$ can either be linear or anti-linear as stated by *Wigner's theorem*. For this thesis, the anti-linear operators are of particular interest. Therefore, Sections 2-3 a) and 2-4 b) introduce the anti-linear *time-reversal operator* and its related symmetry.

a) Wigner's theorem

Transformations T which leave the inner product of a Hilbert space unchanged, *i.e.*

$$\left|\left\langle T\psi' | T\psi\right\rangle\right| = \left|\left\langle \psi' | \psi\right\rangle\right|, \tag{2-41}$$

are of particular relevance in QM. These symmetry transformations of Hilbert spaces are represented by either *unitary* or *anti-unitary*[29] operators. This fact was first proven by Eugene Paul Wigner in 1931 [35] and is therefore called *Wigner's theorem*. Since then, this topic has been approached mathematically from several different directions [36–43]. Appendix C contains a simple derivation of Wigner's theorem following Ref. [43].

[29] anti-linear unitary

The interesting thing about Wigner's theorem is that, apart from the common linear operators O satisfying

$$O(a\,|\alpha\rangle + b\,|\beta\rangle) = aO\,|\alpha\rangle + bO\,|\beta\rangle\,,$$

also *anti-linear operators* $\mathcal{A}$ satisfying

$$\mathcal{A}(a\,|\alpha\rangle + b\,|\beta\rangle) = a^*\mathcal{A}\,|\alpha\rangle + b^*\mathcal{A}\,|\beta\rangle \tag{2-42}$$

can describe fundamental symmetries in QM. Anti-linear operators seem rather exotic and are usually not encountered in physical under-graduate courses. In fact, there exists only one physical transformation described by an anti-linear operator: *time reversal*, the properties and symmetries of which are discussed in Sections 2-3 a) and 2-4 b).

Unitary and anti-unitary transformations can also be understood in a geometric way by considering their analogues in the two-dimensional Euclidean space.[30] As discussed in Section 2-1 b), there are two different types of transformations which preserve the inner product of Euclidean spaces. Figure 2-2 shows the difference of these transformations when applied to geometric objects. In a similar manner the unitary and anti-unitary transformations of Wigner's theorem can be understood in complex spaces.[31]

[30] The exact analogue of Wigner's theorem in Euclidean spaces is called the *Mazur–Ulam theorem* [44].

[31] Rotations in real spaces can also be described by unitary matrices with determinants of either ± 1; this must not be confused with transformations of complex spaces.

Properties of anti-unitary operators

As can be concluded from the previous discussions, an anti-unitary operator $\mathcal{A}$ has the following properties:

1) $\mathcal{A}^\dagger$ is defined via

$$\left\langle \mathcal{A}\psi' \middle| \psi \right\rangle = \left\langle \psi' \middle| \mathcal{A}^\dagger \psi \right\rangle^* .$$

2) $\mathcal{A}$ preserves Eq. (2-41) by

$$\left\langle \mathcal{A}\psi' \middle| \mathcal{A}\psi \right\rangle = \left\langle \psi' \middle| \psi \right\rangle^* = \left\langle \psi \middle| \psi' \right\rangle .$$

3) $\mathcal{A}^2$ is unitary because

$$\left\langle \mathcal{A}^2\psi' \middle| \mathcal{A}^2\psi \right\rangle = \left\langle \mathcal{A}\psi' \middle| \mathcal{A}\psi \right\rangle^* = \left\langle \psi' \middle| \psi \right\rangle ,$$

which corresponds to the other possibility to preserve Eq. (2-41).

4) The operator

$$\mathcal{U} = \mathcal{A}\mathcal{K}$$

is unitary, where $\mathcal{K}$ is the anti-linear complex-conjugation operator. Note that the converse is also true: If $\mathcal{U}$ is unitary, then $\mathcal{A} = \mathcal{U}\mathcal{K}$ is anti-unitary.

b) The time-reversal operator

The classical time-reversal operator was introduced in Section 2-3 b). Its definition can be generalised to QM by replacing the momentum by its operator $\hat{p}$. However, time reversal takes a special role in QM, which becomes obvious if an argument by Eugene Wigner is considered [35]: A time-reversal invariant system, which evolved over a time t, returns to its initial state when it evolves "backwards" for the same amount of time t. In quantum mechanical terms this translates to time evolution followed by time reversal followed by time evolution followed by time reversal, *i.e.*[32]

[32] Time reversal is *involutory*: $\mathcal{T}^{-1} = \mathcal{T}$.

$$\mathcal{U}(t)\underbrace{\mathcal{T}\mathcal{U}(t)\mathcal{T}^{-1}}_{\stackrel{!}{=}\mathcal{U}^{-1}(t)} \stackrel{!}{=} \mathbb{1}\,, \tag{2-43}$$

with the time evolution operator

$$\mathcal{U}(t) = \mathrm{e}^{-\mathrm{i}\mathcal{H}t}\,.$$

Equation (2-43) shows that time evolution is, as desired, reversed under the time-reversal transformation. Further,

$$\mathcal{T}\mathrm{i}\mathcal{H}t\mathcal{T}^{-1} \stackrel{!}{=} -\mathrm{i}\mathcal{H}t\,, \tag{2-44}$$

which clearly shows that the action of $\mathcal{T}$ changes the sign of t.

Yet, since t is just a real number and not an operator, one may cancel it on both sides of Eq. (2-44),

$$\mathcal{T}\mathrm{i}\mathcal{H}\mathcal{T}^{-1} \stackrel{!}{=} -\mathrm{i}\mathcal{H}\,. \tag{2-45}$$

If $\mathcal{T}$ would be an ordinary linear operator, then it would not act on the imaginary unit i, which could be cancelled as well. However, then Eq. (2-45) cannot be satisfied if the energy is bound to be

positive. Because of Wigner's theorem, one must conclude that $\mathcal{T}$ must be an anti-linear operator for time-reversal invariant quantum systems, *i.e.* it must include a complex conjugation.

In fact, the property of being anti-linear is sufficient to define the operation of time reversal in QM entirely. Because of its definition[33] (B-2), any anti-linear operator changes the sign of momentum in the position-space representation. Moreover, since an anti-linear operator does not act on the real position x, the fundamental commutator (B-5) is preserved.

[33] *cf.* Appendix B

The former considerations reveal that the quantum time-reversal operator is anti-linear. However, its exact definition depends on the system. To understand this statement, one may first consider a free particle, which is a time-reversal invariant system. In this case, the time-reversal operator is simply given by

$$\mathcal{T} = \mathcal{K}\,, \tag{2-46}$$

with the complex-conjugation operator $\mathcal{K}$. However, the time-reversal operator is not always as simple as this. Its form heavily depends on the physical system under consideration.

To illustrate this, one can extend the example from above by introducing a spin.[34] The spin operator

$$\hat{\boldsymbol{\sigma}} = (\sigma_1, \sigma_2, \sigma_3)^\mathsf{T}$$

[34] Without any interactions such a system must still be invariant under time reversal.

contains the Pauli matrices, which span an additional two-dimensional Hilbert space. By using the relation

$$(\hat{\boldsymbol{\sigma}} \cdot \mathbf{a})(\hat{\boldsymbol{\sigma}} \cdot \mathbf{b}) = \mathbf{a} \cdot \mathbf{b} + \mathrm{i}\hat{\boldsymbol{\sigma}}(\mathbf{a} \times \mathbf{b})\,,$$

one finds that

$$\hat{\boldsymbol{\sigma}} \cdot \hat{\mathbf{p}} = |\hat{\mathbf{p}}|\,. \tag{2-47}$$

If the time-reversal operator (2-46) is applied to Eq. (2-47), the left-hand side becomes negative, while the right-hand side remains positive. Therefore, time reversal necessarily must flip the spin, *i.e.* $\hat{\boldsymbol{\sigma}} \to -\hat{\boldsymbol{\sigma}}$. Thus, the correct time-reversal operator for a spin

system is given by

$$\mathcal{T} = \mathrm{i}\sigma_2\mathcal{K}\,,$$

where the imaginary unit is necessary for time-reversal symmetry to be anti-unitary.

Properties of the time-reversal operator

From a physical point of view, the time-reversal operator is the most fundamental anti-linear operator in QM. Hence, every anti-linear operator can be written in terms of the time-reversal operator,

$$\mathcal{A} = O\mathcal{T}\,,$$

where O is a linear operator.

From a mathematical point of view, however, the time-reversal operator in turn can always be written in terms of the complex-conjugation operator $\mathcal{K}$,[35]

$$\mathcal{T} = O'\mathcal{K}\,,$$

where O' is another linear operator. Since both $\mathcal{T}$ and $\mathcal{K}$ are involutory, O' must also be involutory and satisfy the condition

$$\mathcal{T}^2 = O'\mathcal{K}O'\mathcal{K} = O'O'^* = \mathbb{1}\,.$$

[35] Complex conjugation is not a physically meaningful operation *per se*.

c) Time-reversal symmetry

To conclude this section, time-reversal symmetry in QM is discussed. As mentioned before, the Schrödinger equation (2-37) for a free particle is time-reversal invariant. The reason for this lies in the imaginary coefficient, which ensures that there is no distinct direction of time [45]. Time-reversal symmetry is necessary so that QM can be reduced to classical mechanics. To see this, it is convenient to compare the free Schrödinger equation to an almost identical equation describing the transfer of heat.

Any temperature gradient ∇T necessarily leads to a heat flux

$$\mathbf{q} = -k \nabla T \,,$$

where k describes the thermal conductivity. This heat flux satisfies the continuity equation

$$\frac{\partial Q}{\partial t} + \nabla \cdot \mathbf{q} = 0 \,,$$

where δQ describes the change in the internal heat energy per volume.

If no additional heat energy is generated and if thermal blackbody radiation is neglected, the change of the internal amount of heat contained in the volume depends only on the change in temperature,

$$\frac{\mathrm{d}Q}{\mathrm{d}t} = mc \frac{\mathrm{d}T}{\mathrm{d}t} \,,$$

where m and c are the mass and the specific heat capacity of the considered material. Hence, the distribution of temperature is described by the *heat equation*

$$\frac{\partial T}{\partial t} = \frac{k}{mc} \nabla^2 T \,. \tag{2-48}$$

Note that the heat equation (2-48) without heat sources or drains has exactly the same form as the Schrödinger equation (2-37) for a free particle. Nevertheless, the resulting dynamics is completely different. Due to the *second law of thermodynamics*, heat only spreads; hence, heat can accumulate only if time is reversed. Therefore, the heat equation is not time-reversal invariant, *i.e.* there exists a distinct direction of time. In the case of the Schrödinger equation, time comes with an imaginary coefficient which prevents this. That is, in QM time always appears in form of the combination $\mathrm{i}t$. Therefore, it is possible to describe the time-reversal operation by a non-linear operator as discussed above.

Just like QM, other classical wave phenomena are also time-reversal invariant, however, for quite a different reason. Classical

waves are described by a wave equation

$$\frac{\partial^2 u}{\partial t^2} = c^2 \nabla^2 u \tag{2-49}$$

with a scalar field u and a constant c. Unlike the heat equation (2-48), Eq. (2-49) contains a second-order time derivative. Hence, a wave equation is *per se* invariant under the time-reversal transformation $t \to -t$.

Last but not least, it should be mentioned that time-reversal symmetry is closely related to the *black hole information paradox*. Black holes are immensely massive objects which can yet be characterised by just a handful of parameters: mass, charge, and spin. Further, because of the *principle of locality*,[36] no information can escape a black hole by means of radiation. Therefore, all information about particles falling into a black hole are "erased". This breaks time-reversal symmetry and thus the unitarity of time evolution in QM discussed in Section 2-4 b). In fact, because of this, QM demands a conservation of quantum information. Such and similar seemingly incompatibilities between general relativity and QM indicate that both of these theories are themselves not fundamental, but that they emerge from another yet unknown theory;[37] though, this is still a topic of current debate [46; 47].

[36] Nothing can move faster than light, including information.

[37] At the present time, *string theory* is in consideration for such a fundamental theory.

2-5 Supersymmetry

In Section 2-3 some fundamental symmetries of the geometry of spacetime were discussed. That is, the discrete symmetries involved space, time and spacetime reflections. Moreover, also symmetries between particles and antiparticles were mentioned.

Now, yet another type of symmetry should be considered which involves the two fundamental types of particles: bosons and fermions. Bosons are particles with integer spin governed by Bose–Einstein statistics. Fermions, on the other hand, possess half-integer spins and can be described by Fermi–Dirac statistics. While fermions are the type of elementary particles forming matter, bosons are the exchange particles of all interactions. Apart from

gravitation, a complete description of bosons, fermions, and their interactions is provided by the *standard model*.

However, the properties of bosons and fermions are so vastly different that one might not expect any symmetries between those particles in the first place. Nevertheless, by allowing conversions between bosons and fermions, a symmetry concept called supersymmetry (SUSY) arises in which every boson possesses a fermionic partner particle[38] and *vice versa*. Although SUSY provides a beautiful mathematical description beyond the standard model, so far there is no experimental evidence that it provides a more correct or accurate description of nature than the standard model.

[38] The partners have equal masses if the SUSY is exact; if it is broken, though, the masses may differ.

In the following, a brief introduction to the theory of SUSY is provided along with an overview of the properties important for this thesis. While there are many books on this subject, the discussions in this thesis follow Ref. [48].

a) A simple supersymmetric model

A supersymmetric system must contain both bosons and fermions. One of the simplest supersymmetric systems therefore consists of the *bosonic* and *fermionic* harmonic oscillators.

The Bose oscillator

The *harmonic oscillator* is well-known and provides a model for many physical phenomena. Although not common, the term *Bose oscillator* is used here to exaggerate its role in the SUSY oscillator. The Hamiltonian of the Bose oscillator reads

$$\mathcal{H}_{\mathrm{B}} = \frac{\hat{p}^2}{2} + \frac{\omega^2 \hat{x}^2}{2}\,, \tag{2-50}$$

where $\hat{x}$ and $\hat{p}$ satisfy the fundamental commutator relations[39]

[39] *cf.* Eq. (B-5)

$$[\hat{x}, \hat{p}] = \mathrm{i}\,,$$
$$[\hat{x}, \hat{x}] = [\hat{p}, \hat{p}] = 0\,.$$

With the creation and annihilation operators

$$\hat{b}^{\pm} = \frac{1}{\sqrt{2\omega}}(\omega\hat{x} \mp \mathrm{i}\hat{p})\,, \tag{2-51}$$

the Hamiltonian (2-50) can be written as

$$\mathcal{H}_{\mathrm{B}} = \omega\left(\hat{b}^{+}\hat{b}^{-} + \frac{1}{2}\right). \tag{2-52}$$

The creation and annihilation operators (2-51) are adjoint to each other and satisfy the commutator relations

$$\left[\hat{b}^{-}, \hat{b}^{+}\right] = 1\,,$$
$$\left[\hat{b}^{\pm}, \hat{b}^{\pm}\right] = 0\,.$$

They can be used to ascent and descent the hierarchy of the occupation number states,[40]

$$\hat{b}^{+}|n_{\mathrm{B}}\rangle = \sqrt{n_{\mathrm{B}}+1}\,|n_{\mathrm{B}}+1\rangle\,, \tag{2-53}$$
$$\hat{b}^{-}|n_{\mathrm{B}}\rangle = \sqrt{n_{\mathrm{B}}}\,|n_{\mathrm{B}}-1\rangle\,. \tag{2-54}$$

[40] They form a basis since Eq. (2-50) commutes with the occupation number operator $\hat{n}_{\mathrm{B}} = \hat{b}^{+}\hat{b}^{-}$.

Because there exists a ground state with energy $E_0 = \omega/2$, which is unoccupied, the annihilation operator per definition must satisfy $\hat{b}^{-}|0\rangle = 0$.

The Fermi oscillator

The *Fermi oscillator* is the fermionic equivalent of the Bose oscillator. Its Hamiltonian reads [48]

$$\mathcal{H}_{\mathrm{F}} = \mathrm{i}\omega\hat{\xi}\,\hat{\pi} \tag{2-55}$$

with the fermionic operators $\hat{\xi}$ and $\hat{\pi}$ satisfying the anti-commutator relations

$$\left\{\hat{\xi}, \hat{\pi}\right\} = 0\,,$$
$$\left\{\hat{\xi}, \hat{\xi}\right\} = \{\hat{\pi}, \hat{\pi}\} = 1\,,$$

where $\{A, B\} = AB + BA$. In analogy to Eq. (2-51), one can construct the fermionic creation and annihilation operators

$$\hat{f}^{\pm} = \frac{1}{\sqrt{2}}\left(\hat{\xi} \mp \mathrm{i}\,\hat{\pi}\right), \tag{2-56}$$

which again are adjoint to each other and satisfy

$$\begin{aligned} \left[\hat{f}^{-}, \hat{f}^{+}\right] &= 1\,, \\ \left[\hat{f}^{\pm}, \hat{f}^{\pm}\right] &= 0\,. \end{aligned} \tag{2-57}$$

Using Eq. (2-56), the Hamiltonian (2-55) can be written as

$$\mathcal{H}_{\mathrm{F}} = \omega\left(\hat{f}^{+}\hat{f}^{-} - \frac{1}{2}\right). \tag{2-58}$$

In contrast to the Bose oscillator (2-52), the Fermi oscillator (2-58) possesses a negative ground state energy $E_0 = -\omega/2$.

Due to the *Pauli exclusion principle*, multiple occupations of fermionic states are not allowed. Hence, the creation and annihilation operators (2-56) act on the fermionic occupation number states as follows,[41]

[41] *cf.* the two relations (2-53) and (2-54)

$$\begin{aligned} \hat{f}^{+}|0\rangle &= |1\rangle\,, \\ \hat{f}^{-}|1\rangle &= |0\rangle\,, \\ \hat{f}^{+}|1\rangle &= 0\,, \qquad (2\text{-}59) \\ \hat{f}^{-}|0\rangle &= 0\,. \qquad (2\text{-}60) \end{aligned}$$

Because of the properties (2-59) and (2-60), the fermionic creation and annihilation operators are nilpotent,

$$\left(\hat{f}^{\pm}\right)^2 = 0\,,$$

which is already encoded in the anti-commutator relations (2-57). By choosing the fermionic states to be the standard Euclidean basis states, *i.e.*

$$|0\rangle = \begin{pmatrix} 1 \\ 0 \end{pmatrix},$$

$$|1\rangle = \begin{pmatrix} 0 \\ 1 \end{pmatrix},$$

the fermionic creation and annihilation operators (2-56) are given by the following 2×2 matrices,

$$\hat{f}^{+} = \begin{pmatrix} 0 & 0 \\ 1 & 0 \end{pmatrix}, \tag{2-61}$$

$$\hat{f}^{-} = \begin{pmatrix} 0 & 1 \\ 0 & 0 \end{pmatrix}. \tag{2-62}$$

The supersymmetric oscillator

By combining the Bose oscillator (2-52) with the Fermi oscillator (2-58), one obtains a model which contains both bosons and fermions. The states of this model can be described by $|n_{\mathrm{B}}, n_{\mathrm{F}}\rangle = |n_{\mathrm{B}}\rangle\,|n_{\mathrm{F}}\rangle$, where $n_{\mathrm{F}} = 0, 1$. Because of n_{F}, one can distinguish two types of states:

1) bosonic states $|\underline{n}\rangle \equiv |n, 0\rangle$,

2) fermionic states $|\bar{n}\rangle \equiv |n, 1\rangle$.

SUSY creates a relationship between them by transforming bosonic states into fermionic states and *vice versa*. Hence, one can define *superoperators*[42] with the following properties,

[42] *i.e.* the generators of SUSY

$$\begin{aligned} Q^{+}|\underline{n}\rangle &= |\overline{n-1}\rangle\,, \\ Q^{-}|\bar{n}\rangle &= |\underline{n+1}\rangle\,, \\ Q^{+}|\bar{n}\rangle &= 0\,, \qquad (2\text{-}63) \\ Q^{-}|\underline{n}\rangle &= 0\,. \qquad (2\text{-}64) \end{aligned}$$

The superoperator Q^{+} "creates" a fermionic state by transforming a boson into a fermion; accordingly, Q^{-} "annihilates" a fermionic state by transforming a fermion into a boson. Therefore, the superoperators can be expressed with the bosonic and fermionic creation and annihilation operators as $Q^{\pm} = \hat{b}^{\mp}\hat{f}^{\pm}$, which immediately shows that they are also adjoint to each other. Since the

fermionic operators $\hat{f}^{\pm}$ are nilpotent, the superoperators $Q^{\pm}$ also possess this property encoded in Eqs. (2-63) and (2-64).

A physical system is called *supersymmetric* if its Hamiltonian $\mathcal{H}_S$ commutes with the superoperators,

$$\left[\mathcal{H}_S, Q^{\pm}\right] = 0\,. \tag{2-65}$$

In physical terms this condition means that all transformations defined by the superoperators $Q^{\pm}$ conserve the energy of the system. With Eqs. (2-63) and (2-64) one finds that a Hamiltonian satisfying Eq. (2-65) can be written as

$$\mathcal{H}_S = \omega\left\{Q^+, Q^-\right\}. \tag{2-66}$$

The prefactor is chosen such that the SUSY oscillator Hamiltonian $\mathcal{H}_S = \mathcal{H}_B + \mathcal{H}_F$ is obtained.

Equations (2-65) and (2-66) form a SUSY algebra, for which the superoperators $Q^{\pm}$ act as generators [48]. However, in contrast to an ordinary Lie algebra as discussed in Section 2-1 b), there occur two types of operators in a SUSY algebra:

1) Bosonic operators, like the Hamiltonian (2-66), do not change the statistics of the state, *i.e.* there is no transformation from bosons into fermions and *vice versa*.

2) Fermionic operators, like the superoperators (2-63) and (2-64), change the statistics of a state from bosonic to fermionic and *vice versa*.

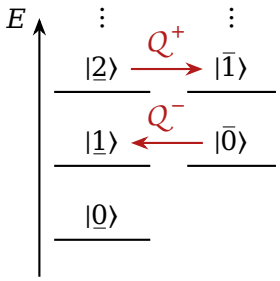

Figure 2-7: The spectrum of the SUSY oscillator

Since the superoperators are nilpotent, *i.e.* $(Q^{\pm})^2 = 0$, the Hamiltonian (2-66) can be written as

$$\mathcal{H}_S = \left(Q^+ + Q^-\right)^2.$$

Due to $(Q^+ + Q^-)$ being Hermitian, the eigenvalues of $\mathcal{H}_S$ must be positive. Further, because $Q^{\pm}$ conserve the energy, the spectrum is two-fold degenerate for $E > 0$. However, the ground state with $E = 0$ is unique and thus non-degenerate [48]. The spectrum of the SUSY oscillator is illustrated in Fig. 2-7.

b) Superpotentials

In Section 2-5 a) the simple SUSY oscillator was discussed. Now, SUSY should be generalised to other types of potentials. With Eqs. (2-61) and (2-62) the Hamiltonian (2-66) can be written solely in terms of the bosonic creation and annihilation operators,

$$\mathcal{H}_{\mathrm{S}} = \begin{pmatrix} \hat{b}^{+}\hat{b}^{-} & 0 \\ 0 & \hat{b}^{-}\hat{b}^{+} \end{pmatrix} = \frac{1}{2}\left\{\hat{b}^{-}, \hat{b}^{+}\right\}\mathbb{1} - \frac{1}{2}\left[\hat{b}^{-}, \hat{b}^{+}\right]\sigma_3 \,, \tag{2-67}$$

which, in general, acts on mixed states[43] $|\psi\rangle = (|\underline{n}\rangle, |\overline{m}\rangle)^{\mathsf{T}}$. Here, the oscillator parameter is set to $\omega = 1$ because other potentials in general depend on different parameters. Instead of Eq. (2-51), the generalised bosonic operators

$$\hat{b}^{\pm} = \frac{1}{\sqrt{2}}\left(W(\hat{x}) \mp \mathrm{i}\hat{p}\right) \tag{2-68}$$

are introduced, which are first-order differential operators. They contain the *superpotential*[44] W. If W is real, $\hat{b}^{+}$ and $\hat{b}^{-}$ are adjoint to each other. With $W(\hat{x}) = \omega\hat{x}$ the harmonic oscillator (2-50) is obtained.

It is worth mentioning here that every Hamiltonian can be written as a product of two linear differential operators [49]. Further, a unique ground state exists for such supersymmetric systems because of the boundary conditions imposed on the superpotential W due to the normalisability of the wave function. A more detailed discussion of the SUSY ground state can be found in Ref. [48].

Assuming that the superpotential can be written as a power series, the operators (2-68) satisfy

$$\left\{\hat{b}^{-}, \hat{b}^{+}\right\} = \hat{p}^2 + W^2(\hat{x}) \,,$$
$$\left[\hat{b}^{-}, \hat{b}^{+}\right] = \frac{\mathrm{d}W}{\mathrm{d}\hat{x}} \,.$$

Hence, the Hamiltonian (2-67) can be written as

$$\mathcal{H}_{\mathrm{S}} = \begin{pmatrix} \mathcal{H}_{-} & 0 \\ 0 & \mathcal{H}_{+} \end{pmatrix}, \tag{2-69}$$

[43] *i.e.* linear combinations of the bosonic and fermionic states

[44] Note that this is not an actual potential energy.

in which the Hamiltonians $\mathcal{H}_\pm$ contain the SUSY potentials

$$V_\pm(\hat{x}) = \frac{1}{2}\left(W^2(\hat{x}) \pm \frac{\mathrm{d}W}{\mathrm{d}\hat{x}}\right). \tag{2-70}$$

Note that $\mathcal{H}_+$ and $\mathcal{H}_-$ solely act on fermionic and bosonic states, respectively. Note also that the roles of $\hat{b}^\pm$ are inverted between $\mathcal{H}^+$ and $\mathcal{H}^-$; *i.e.* "annihilation" for $\mathcal{H}^-$ means "creation" for $\mathcal{H}^+$ and *vice versa*.

c) Spontaneous symmetry breaking

As discussed in Section 2-5 a), the SUSY oscillator possesses a non-degenerate ground state with $E = 0$. This case is called *exact supersymmetry* and it is shown in Fig. 2-8. On the one hand, there exists a bosonic ground state[45] $|\underline{0}\rangle$ if $\mathcal{H}_-|\underline{0}\rangle = 0$, *i.e.* $|\underline{0}\rangle$ is annihilated by $\hat{b}^-$ and thus

[45] States are now labelled by their energies.

$$Q^+|\underline{0}\rangle = 0\,. \tag{2-71}$$

On the other hand, there may also exist a fermionic ground state $|\bar{0}\rangle$ of $\mathcal{H}_+$ — also called a *fermionic zero mode* [50] — which is annihilated by $\hat{b}^+$, so that

$$Q^-|\bar{0}\rangle = 0\,. \tag{2-72}$$

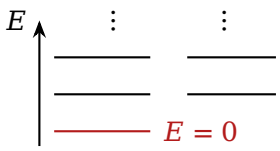

Figure 2-8: Exactly supersymmetric spectrum

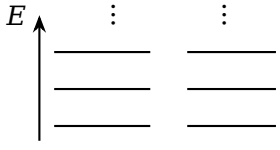

Figure 2-9: Broken-supersymmetric spectrum

SUSY can be *broken spontaneously*, which means that the ground state is no longer supersymmetric; that is, no ground state satisfying either Eq. (2-71) or Eq. (2-72) exists. However, the other features of supersymmetric systems are preserved, even though the SUSY is broken. In particular, this means that the eigenvalues are still two-fold degenerate. The spectrum of a broken-supersymmetric system is shown in Fig. 2-9, which corresponds to Fig. 2-8 without the ground state $|\underline{0}\rangle$.

Whether the SUSY is *exact* or *broken* is determined completely by the asymptotic behaviour of the superpotential W. By defining $W_\pm = \lim_{x\to\pm\infty} W(x)$, one finds that the SUSY is

— exact if the signs of W_+ and W_- are different,

— broken if the signs of W_+ and W_- are equal.

This is an important property of the superpotentials, which is used extensively in Section 5-2.

d) Quantum mechanics from supersymmetry

To conclude this discussion, a practical example of SUSY is considered. SUSY can be used to construct a Hamiltonian from a given ground state wave function ψ_0. Because of Eq. (2-70), a suitable Hamiltonian is given by[46]

$$\mathcal{H} = \frac{1}{2}\left(\hat{p}^2 + W^2(\hat{x}) - \frac{\mathrm{d}W}{\mathrm{d}\hat{x}}\right). \tag{2-73}$$

[46] Only the negative sign is considered in this example.

The aim is to find the superpotential W for which the Hamiltonian (2-73) possesses the ground state ψ_0 with energy $E_0 = 0$. With the Schrödinger equation (2-39) and the identifications from Appendix B one finds

$$\frac{\psi_0''}{\psi_0} = \left(\frac{\psi_0'}{\psi_0}\right)^2 + \frac{\mathrm{d}}{\mathrm{d}\hat{x}}\left(\frac{\psi_0'}{\psi_0}\right) = W^2(\hat{x}) - \frac{\mathrm{d}W}{\mathrm{d}\hat{x}},$$

where the primes indicate derivatives. The simplest solution reads

$$W(\hat{x}) = -\frac{\psi_0'}{\psi_0} = -\frac{\mathrm{d}}{\mathrm{d}\hat{x}} \ln \psi_0 . \tag{2-74}$$

If the ground state wave function is, for example, a Gaussian function,

$$\psi_0(\hat{x}) = \left(\frac{\omega}{\pi}\right)^{1/4} \mathrm{e}^{-\omega\hat{x}^2/2},$$

then the superpotential (2-74) reads $W(\hat{x}) = \omega\hat{x}$. The corresponding Hamiltonian (2-73) then has the well-known form

$$\mathcal{H} = \frac{1}{2}\left(\hat{p}^2 + \omega^2\hat{x}^2 - \omega\right)$$

which describes a harmonic oscillator (2-50) shifted by ω, so that its ground state energy is zero.

Part I

Quantum Systems

I think I can safely say that nobody understands quantum mechanics.

Richard Feynman

—The Character of Physical Law

Introduction to the first part

3

Pray continue. Your narrative promises to be a most interesting one.

Sherlock Holmes

—The Adventure of the Copper Beaches

Quantum mechanics (QM) is based on the premise that every physical observable corresponds to a Hermitian operator whose eigenvalues are real [52; 53]. Therefore, a Hermitian Hamiltonian is suitable to describe the energy of a quantum system and, moreover, leads to a unitary time-evolution which conserves the norm. However, *Stone's theorem* uniquely connects a Hermitian operator to a one-parameter family of unitary operators [54], thus implying that unitary dynamics truly requires a Hermitian Hamiltonian. This simple and self-consistent concept lays the foundation of QM,[I] which certainly is one of the most successful theories — if not even *the* most successful theory to date — in physics.

[I] *cf.* Fig. 3-1

Of course, all of this is well-known for almost a century now, but there are caveats, though. QM only describes *closed* quantum systems, *i.e.* systems which are isolated from any exchange of energy or matter. In principle, this is not an issue because the system could simply be chosen large enough so that all of these interactions are described *explicitly*. In practice, however, large numbers of degrees of freedom may be unfeasible or even impossible to treat explicitly. This can be avoided by considering *open quantum systems* with lesser complexity, where the interaction with an environment, which represents a large part of the system, is described in an *effective* way. As a consequence, the overall probability is no longer conserved, which means that such systems cannot be described by Hermitian operators anymore. This is not so much of an issue, tough: While the form of the Schrödinger

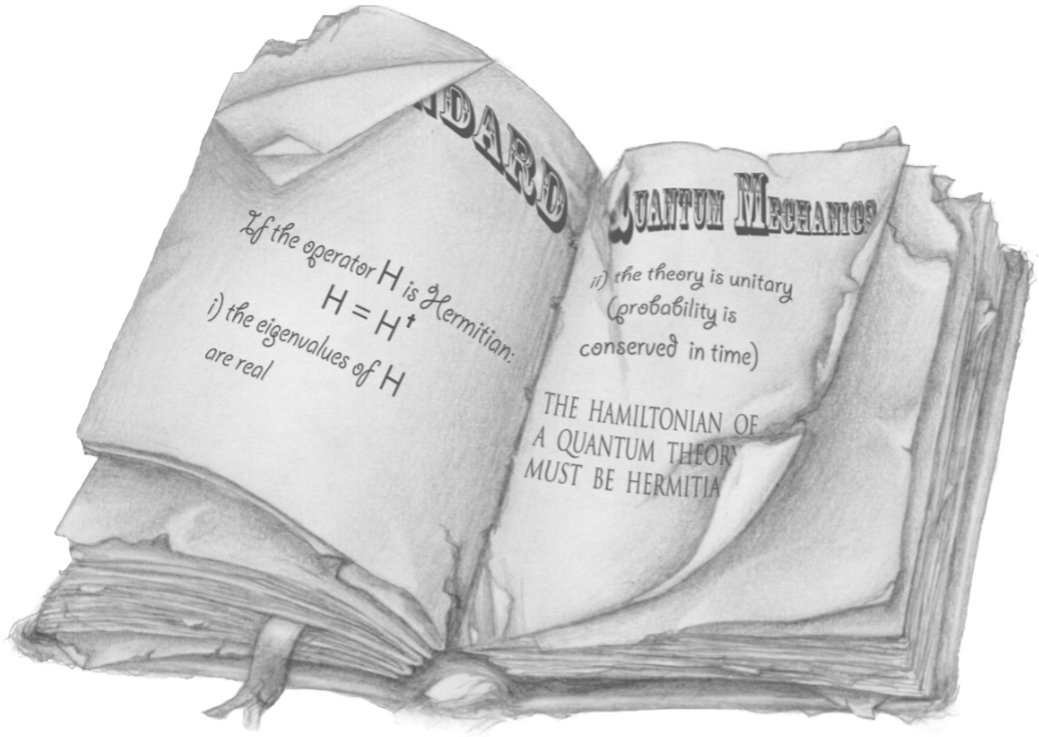

Figure 3-1: The foundations of standard QM are elegant and simple; yet, whole books can be written about them. The illustration is taken from Ref. [51].

equation (2-38) follows from fundamental properties of spacetime,[2] the properties of the Hamiltonian — in particular its Hermiticity — are not determined *per se*. Hence, the Hermiticity of the Hamiltonian can be considered to be a sufficient mathematical constraint, but it is not necessarily required.

[2] *cf.* Section 2-2 c)

This line of though leads to non-Hermitian quantum mechanics (NHQM), *i.e.* the non-Hermitian generalisation of QM. In NHQM the energies and other observables in general are complex quantities and thus the probability densities are no longer conserved. Whether or not a non-Hermitian Hamiltonian describes a physical system ultimately depends on the existence of a physically meaningful interpretation of the additional imaginary parts of both the Hamiltonian and the energies. This is quite similar to the occurrence of a *complex refractive index* in optics,[3] which is used for the mathematical description of the opacity of a material. Such and similar effects apparently are unwanted, though, they can also enrich physics [56]. Therefore, the first part of this thesis is dedicated to the identification and description of physical systems in NHQM, which correspond to a "natural complex extension of the Hermiticity condition" [57].

[3] *e.g.* see Ref. [55]

After a general introduction to NHQM in Chapter 4, symmetries of non-Hermitian Hamiltonians are discussed in Chapter 5 and methods are provided to symmetrise systems or make them symmetric.[4] These concepts are at the heart of this thesis and form the foundation for the discussions on linear and non-linear quantum systems in Chapters 6 and 7, which range from simple matrix models to experimentally realisable multi-well potentials. Last but not least, a brief overview about experimental methods to realise such systems is given in Chapter 8, which concludes the first part of this thesis.

[4] This distinction will become clear in Section 5-3.

While the mathematical concepts introduced in the following are rather simple and straightforward, they may still be hard to grasp from a physical point of view. Hence, one should keep in mind what Richard Feynman said in the 6-th part of his lecture series *The Character of Physical Law*: "I think that I can safely say that nobody understands quantum mechanics. Now, if you appreciate this and don't take the lecture too seriously that you really have to understand in terms of some model what I'm going to describe and just relax and enjoy, I'm going to tell you what nature behaves like and if you simply admit that maybe she behaves like this, you will find her a delightful, entrancing thing. So that's the way to look at the lectures, not to try to understand. Well, you have to understand the english of course." With these words the journey into the non-Hermitian quantum world may begin.

Hon-Hermitian quantum mechanics

4

In QM all physical operators are required to be Hermitian, so that their eigenvalues are real. However, apart from this there are no physical or mathematical constraints which disallow the use of non-Hermitian operators. In fact, non-Hermitian operators have been used in physics since the emergence of QM to solve certain problems which are either not solvable within the framework of ordinary QM or only so with great difficulty [58]. The eigenvalues of a non-Hermitian operator are not guaranteed to be real, although they still can be. However, also complex quantities are not much of an issue, as long as a suitable physical interpretation is at hand.

In the following, a short introduction to the theory behind non-Hermitian quantum mechanics (NHQM) is given. The focus lies on the basics which are required in the further course of this thesis. A more thoroughful and comprehensive introduction to NHQM is given in Ref. [58]. Note that for the sake of simplicity, the following discussions in general refer to operators with non-degenerate discrete spectra. However, the assumption of a discrete spectrum does in fact not cause a loss of generality: By using a *box quantisation condition*[I] the continuous part of the spectrum becomes a discrete quasi-continuum. If the box size is increased to infinity, this quasi-continuum becomes increasingly dense and finally continuous.

[I] *i.e.* the wave function has to be zero at some border

4-1 Crash course on Hermitian quantum mechanics

The basics of the "usual" Hermitian QM are quite simple and can be summarised in just a few sentences: The objects of QM are

physical states of a Hilbert space, say $|\psi\rangle$, $|\phi\rangle$. Any Hilbert space defines an inner product $\langle\psi|\phi\rangle$ with the property

$$\langle\phi|\psi\rangle^* = \langle\psi|\phi\rangle \,. \tag{4-1}$$

Acting on the physical states are operators O which are characterised by the matrix elements $\langle\phi|O|\psi\rangle$.[2] The *adjoint* operator $O^\dagger$ is defined by

[2] *cf.* Appendix B-2

$$\left\langle O^\dagger\phi\middle|\psi\right\rangle = \langle\phi|O\psi\rangle \,.$$

The most important properties in QM relating an operator to its adjoint are *Hermiticity*,

$$\mathcal{H}^\dagger = \mathcal{H} \,, \tag{4-2}$$

which ensures that the eigenvalues of the operator are real and *unitarity*,

$$\mathcal{U}^\dagger\mathcal{U} = \mathbb{1} = \mathcal{U}\mathcal{U}^\dagger \,, \tag{4-3}$$

which ensures that the operator does not change the inner product.

Hermitian matrices can always be diagonalised.[3] This ensures that an orthogonal set of eigenstates exists, which can be used as a basis. The basis states can then be normalised using the inner product of QM. Further, the eigenvalues of a Hermitian operator are guaranteed to be real because

[3] This is called the *spectral theorem*.

$$E_n\langle\psi_m|\psi_n\rangle = \langle\psi_m|\mathcal{H}\psi_n\rangle = \langle\mathcal{H}\psi_n|\psi_m\rangle^* = \langle\psi_n|\mathcal{H}\psi_m\rangle^* \,,$$

where the property (4-1) of the inner product is used. Hence, $E_n = E_n^*$ if the states are orthonormal with $\langle\psi_n|\psi_m\rangle = \delta_{nm}$.

In Hermitian QM the Hamiltonian occurring in the Schrödinger equation (2-39) must be Hermitian by definition, to guarantee that the energies are real. However, it should be noted that Hermiticity is just a sufficient condition for the reality of the eigenvalues, but not necessary. This is one of the very foundations on which this thesis relies.

Some further notes on the mathematical foundations of QM are summarised in Appendix B.

4-2 Physical interpretation of non-Hermitian Hamiltonians

As the name already suggests, operators in NHQM — the Hamiltonian in particular — are non-Hermitian in general, so that their eigenvalues are not necessarily real. However, because the reality of observables like the energy was the motivation for introducing the Hermiticity condition in the first place, one should ask whether scenarios with complex energies can be physically meaningful or not. Despite the fact that there are various different routes to obtain non-Hermitian Hamiltonians [58], in the following, only cases involving a complex potential are considered, *i.e.* their Hamiltonian can always be written as

$$\mathcal{H} = \mathcal{H}_{\mathrm{H}} + \mathrm{i}V_{\mathrm{i}}\,, \tag{4-4}$$

where V_{i} is real and

$$\mathcal{H}_{\mathrm{H}} = -\frac{1}{2}\nabla^2 + V_1$$

is a Hermitian Hamiltonian with the real potential V_1.

a) Complex potentials

The effects of a complex potential $V = V_1 + \mathrm{i}V_{\mathrm{i}}$ can be understood by considering the *probability density* $\rho = \langle\psi|\psi\rangle$. Its time-derivative reads

$$\frac{\mathrm{d}\rho}{\mathrm{d}t} = \frac{1}{2\mathrm{i}}\Big(\langle\nabla^2\psi|\psi\rangle - \langle\psi|\nabla^2\psi\rangle\Big) - \mathrm{i}\Big(V - V^*\Big)\rho$$

using the Hamiltonian (4-4). With the definition of the *probability current*

$$j = \frac{1}{2\mathrm{i}}(\langle\psi|\nabla\psi\rangle - \langle\nabla\psi|\psi\rangle) \tag{4-5}$$

one finds the *continuity equation*

$$\frac{\mathrm{d}\rho}{\mathrm{d}t} + \nabla j = 2V_\mathrm{i}\rho\,. \tag{4-6}$$

For $V_\mathrm{i} = 0$, Eq. (4-6) corresponds to the usual continuity equation of QM in which the probability density ρ is conserved. Hence, an imaginary potential acts as source and drain of the probability density.

b) Complex energies

As in Hermitian QM, the expectation values of operators in NHQM are given by

$$E_n = \frac{\langle\psi_n|\mathcal{H}|\psi_n\rangle}{\langle\psi_n|\psi_n\rangle}\,,$$

where $E_n \in \mathbb{C}$ if $\mathcal{H}$ is non-Hermitian. Complex energy eigenvalues mean that the corresponding states are not stationary in time, even though they are solutions of the time-independent Schrödinger equation (2-39). That is, the norm of a state reads

$$\langle\psi_n(t)|\psi_n(t)\rangle = \mathrm{e}^{2\,\mathrm{Im}\,E_n t}\,\langle\psi_n(0)|\psi_n(0)\rangle\,,$$

i.e. the norm increases exponentially if the imaginary part of the energy is positive and decreases if the imaginary part is negative. The norm is conserved in time if and only if the energy eigenvalues are real.

So the question arises, how can complex observables like the energy be understood physically? In fact, there already exists an analogy in optical systems, which was already mentioned in Chapter 3: The refractive index is a real physical quantity which describes the phase velocity of electromagnetic waves travelling

through a medium. However, by adding an *imaginary part*[4] the effects of absorption can conveniently be taken into account. This leads to an *effective description* of the phenomenon of absorption within the usual formalism of ED. Hence, the imaginary part of an eigenvalue can be considered as the result of an effective description of an *open quantum system*.[5]

[4] *cf.* Ref. [55]

[5] *cf.* Section 4-6

Further, if complex eigenvalues occur explicitly in complex-conjugate pairs, they can be related physically by emission and absorption phenomena [59; 60]. Consider an isolated quantum system with energy eigenvalues E_n. If the system is prepared in an eigenstate, it will remain in that eigenstate for all times. However, if the system is prepared in a superposition of two states, there will be *Rabi oscillations* between those two states with the frequency[6] $\omega_{nm} = (E_n - E_m)$. If the system is coupled to a laser field, one would find that ω_{nm} is in the absorption spectrum, while $\omega_{mn} = -\omega_{nm}$ is in the emission spectrum. Therefore, the imaginary parts of the energy eigenvalues of a non-Hermitian quantum system can be symmetric as well. Such energy eigenvalues can even be conserved in time, even though the norm of the corresponding states is not conserved [61; 62]; by using both states with complex-conjugate energy eigenvalues, a time-independent norm can be constructed, for which the growing and decaying components balance each other.

[6] Reminder: $\hbar = 1$

4-3 Bi-orthogonal basis

In ordinary QM there is only one orthogonal set of basis states associated with a Hermitian operator.[7] However, the orthogonality of the states is merely a consequence of the Hermiticity of the operator. Consider the time-independent Schrödinger equation (2-39) for two different energy eigenvalues $E_n \neq E_m$ and multiply each of them by the state corresponding to the respective other energy eigenvalue,

[7] *cf.* Section 4-1

$$\langle \psi_m | \mathcal{H} | \psi_n \rangle = E_n \langle \psi_m | \psi_n \rangle \,, \tag{4-7}$$

$$\langle \psi_m | \mathcal{H}^\dagger | \psi_n \rangle = E_m^* \langle \psi_m | \psi_n \rangle \,, \tag{4-8}$$

where a complex conjugation and the properties of the inner product were applied to the second equation. By subtracting both equations one finds

$$\left(E_n - E_m^*\right) \langle \psi_m | \psi_n \rangle = \langle \psi_m | \mathcal{H} - \mathcal{H}^\dagger | \psi_n \rangle \,. \tag{4-9}$$

For a Hermitian operator the right-hand side vanishes, so that $\langle \psi_m | \psi_n \rangle = 0$ for $E_n \neq E_m$ since the eigenvalues are real. Though, for non-Hermitian operators the right-hand side is in general non-zero and the non-degenerate eigenstates are not orthogonal.

To get a glimpse on what is going on here, one has to change the point of view: Eqs. (4-7) and (4-8) are, in fact, representations of the *left-hand* and *right-hand eigenvalue equations*. In contrast to Hermitian QM, the left-hand and right-hand eigenvectors do not coincide in NHQM. Consider the left-hand and right-hand eigenvalue equations[8] for a non-degenerate eigenvalue E_n,

[8] see Appendix A for notes on the notation

$$\mathcal{H} \, |\psi_n\rangle = E_n \, |\psi_n\rangle \,, \tag{4-10}$$

$$\left\langle \psi^n \right| \mathcal{H} = \left\langle \psi^n \right| E_n \,. \tag{4-11}$$

Equation (4-11) corresponds to the right-hand eigenvalue equation

$$\mathcal{H}^\dagger \left|\psi^n\right\rangle = E_n^* \left|\psi^n\right\rangle \tag{4-12}$$

which is the adjoint equation of Eq. (4-10). For a Hermitian Hamiltonian with $\mathcal{H} = \mathcal{H}^\dagger$, which has real eigenvalues, a comparison of Eqs. (4-10) and (4-12) shows that $|\psi^n\rangle = |\psi_n\rangle$. Thus, Eqs. (4-10) and (4-11) are actually the same equation. In NHQM, where $\mathcal{H}^\dagger \neq \mathcal{H}$, Eqs. (4-10) and (4-11) are truly distinct. Therefore, E_n and E_n^* can, in general, be considered as right-hand eigenvalues of two different Hamiltonians $\mathcal{H}$ and $\mathcal{H}^\dagger$ with the corresponding eigenstates $|\psi^n\rangle \neq |\psi_n\rangle$. Although left-hand and right-hand eigenstates form no orthogonal sets on their own, surprisingly, they are orthogonal to each other in most cases. To see this, one can multiply the n-th right-hand eigenvalue equation (4-10) by $\langle \psi^m |$ and the m-th left-hand eigenvalue equation (4-11) by $|\psi_n\rangle$ and subtract the results,

$$\left(E_n - E_m\right) \left\langle \psi^m | \psi_n \right\rangle = 0 \,. \tag{4-13}$$

In contrast to Eq. (4-9), where inner products between two right-hand eigenstates were considered, one finds that $\langle \psi^m | \psi_n \rangle = 0$ for $E_n \neq E_m$, which shows that left-hand and right-hand eigenstates are indeed orthogonal to each other; they form a *bi-orthogonal basis* [58; 63–65].

However, Eq. (4-13) does not allow for the opposite conclusion, *i.e.* for $E_n = E_m$ it is not guaranteed that $\langle \psi^m | \psi_n \rangle \neq 0$. Even if the spectrum is non-degenerate, there exists the possibility that the left-hand and right-hand eigenstates associated with the same eigenvalue are orthogonal, *i.e.* $\langle \psi^n | \psi_n \rangle = 0$. This phenomenon is called *self-orthogonality* and it occurs at so-called exceptional points (EPs), which will briefly be discussed in Section 4-3 a). Apart from the EPs, the states $\{|\psi^m\rangle, |\psi_m\rangle\}$ form a bi-orthogonal basis for every diagonalisable operator $\mathcal{H}$ [66–68] with[9]

[9] assuming that the system is not in the vicinity of an EP

$$\left\langle \psi^m | \psi_n \right\rangle = \delta_{nm} \tag{4-14}$$

and the closure relation

$$\sum_n |\psi_n\rangle\langle\psi^n| = \mathbb{1}\,. \tag{4-15}$$

Using a bi-orthogonal basis, the Hamiltonian can be written as

$$\mathcal{H} = \sum_{n,m} |\psi_m\rangle\langle\psi^m|\,\mathcal{H}\,|\psi_n\rangle\langle\psi^n| = \sum_n E_n\,|\psi_n\rangle\langle\psi^n|\,, \tag{4-16}$$

where the properties (4-14) and (4-15) were used. By a suitable transformation, the Hamiltonian can be diagonalised,

$$\mathcal{S}_\mathrm{L}^\mathsf{T}\,\mathcal{H}\,\mathcal{S}_\mathrm{R} = \mathcal{H}_\mathrm{diag} = \begin{pmatrix} E_1 & & \\ & \ddots & \\ & & E_N \end{pmatrix},$$

where

$$\mathcal{S}_\mathrm{L} = \left(|\psi^1\rangle \cdots |\psi^N\rangle\right), \tag{4-17}$$

$$\mathcal{S}_\mathrm{R} = \left(|\psi_1\rangle \cdots |\psi_N\rangle\right). \tag{4-18}$$

Because of the closure relation (4-15), one finds that $\mathcal{S}_\mathrm{R}\mathcal{S}_\mathrm{L}^\mathsf{T} = \mathbb{1}$, *i.e.* $\mathcal{S}_\mathrm{R}$ is the left inverse of $\mathcal{S}_\mathrm{L}^\mathsf{T}$, which is in turn the right inverse of $\mathcal{S}_\mathrm{R}$. Thus,

$$\mathcal{H} = \mathcal{S}_\mathrm{R}\mathcal{H}_\mathrm{diag}\mathcal{S}_\mathrm{L}^\mathsf{T} \tag{4-19}$$

is equal to Eq. (4-16).

Equation (4-14) is called the *bi-orthogonal product* in the following, though, it is also commonly known as the *c-product* [58] in NHQM,

$$(\psi_m|\psi_n) = \left\langle \psi^m|\psi_n\right\rangle , \tag{4-20}$$

which implies that $|\cdot) = |\underline{\cdot}\rangle$ and $(\cdot| = \langle\underline{\cdot}|$ using the notation introduced in Appendix A. The corresponding closure relation (4-15) can be written as

$$\sum_n |\psi_n)(\psi_n| = \mathbb{1} .$$

The concept of *bi-orthogonality* is central in NHQM; in fact, they are tied together so closely that even a comprehensive *bi-orthogonal quantum theory* can be formulated [65]. While, at first glance, it seems as if a bi-orthogonal basis could be used in almost the same manner as any other basis, bi-orthogonal states may possess the undesirable yet interesting property of self-orthogonality.

a) Self-orthogonality

Consider a non-Hermitian matrix of the form

$$\mathcal{H}(\lambda) = \mathcal{H}_0 + \lambda V , \tag{4-21}$$

where $\mathcal{H}_0$ and V are Hermitian matrices which do not commute, *i.e.* $[\mathcal{H}_0, V] \neq 0$, and λ is a control parameter. For $\lambda \in \mathbb{C}$ the matrix (4-21) is non-Hermitian,[10] so that there exists a set of bi-orthogonal eigenstates $\{|\psi^n(\lambda)\rangle , |\psi_n(\lambda)\rangle\}$ satisfying Eqs. (4-14) and (4-15). However, if there exists at least one critical value $\lambda = \lambda_\mathrm{c}$

[10] *cf.* Eq. (4-4)

for which [69]

$$\left\langle \psi^n(\lambda_c) | \psi_n(\lambda_c) \right\rangle = 0\,, \tag{4-22}$$

then the state $\psi_n(\lambda_c)$ is *self-orthogonal* [58].

The term "self"-orthogonality is somewhat misleading, though. At λ_c two eigenstates of $\mathcal{H}$ coalesce, so that two "different" left-hand and right-hand eigenstates are orthogonal in the sense of Eq. (4-14). However, this phenomenon is accompanied by a simultaneous coalescence of the corresponding eigenvalues. While degeneracy of the eigenvalues also occurs in Hermitian QM, the coalescence of both eigenvalues and eigenstates is exclusive to NHQM. This forms a singularity in the parameter space, at which the spectrum becomes incomplete and the bi-orthogonal basis is defective; hence, the Hamiltonian $\mathcal{H}(\lambda_c)$ is not diagonalisable [70]. Because of this and due to the exceptional topological properties of the complex energy surface in their regions, such points are commonly called exceptional points (EPs), *e.g.* see Refs. [58; 71–74].

At an EP a symmetry is *spontaneously broken* and there occur *bifurcations* in the energy eigenvalues. The topology of two complex energy eigenvalues in the vicinity of an EP is illustrated in Fig. 4-1. Each energy eigenvalue is bound to a different *Riemann surface*, respectively. However, the Riemann surfaces are crossing, which causes an exceptional behaviour: If the system parameters are varied adiabatically in such a manner that the energy eigenvalues are moving around the EP, they will switch their positions in the process. That is, it requires two complete iterations of this variation to restore the initial order of the energy eigenvalues [75]. EPs with this property are said to be of *second order*; of *third order* if three iterations are required, *etc*. Further, EPs exhibit a property similar to chirality [71; 76].

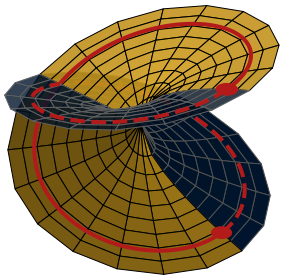

Figure 4-1: Topology around a second-order EP

This unusual behaviour can be illustrated with a simple example. For this, consider the Hamiltonian (4-21), where $\mathcal{H}_0 = \sigma_3$ and $V = \sigma_1$ are given by Pauli matrices,[11] *i.e.*

[11] *cf.* Eq. (2-19)

$$\mathcal{H} = \begin{pmatrix} 1 & \lambda \\ \lambda & -1 \end{pmatrix}. \tag{4-23}$$

The eigenvalues of this matrix are readily obtained and read

$$E_{\pm}(\lambda) = \pm\sqrt{1+\lambda^2} \tag{4-24}$$

with the corresponding right-hand eigenstates

$$|\psi_{\pm}\rangle = \begin{pmatrix} -\lambda \\ 1 - E_{\pm}(\lambda) \end{pmatrix}. \tag{4-25}$$

[12] *i.e.* the Hamiltonian (4-23) is non-Hermitian

Obviously, both Eqs. (4-24) and (4-25) coincide for[12] $\lambda_{\pm} = \pm\mathrm{i}$; hence, there exist two EPs. With the parametrisation

$$\lambda(\varphi) = \mathrm{i} + \rho\exp(\mathrm{i}\varphi)\,,$$

where $\rho \ll |E_+ - E_-|$ and $\varphi \in [0, 2\pi]$, the EP at λ_+ can be encircled. The eigenvalues (4-24) then read

$$E_{\pm}(\varphi) = \pm\sqrt{\rho}\,\mathrm{e}^{\frac{\mathrm{i}\varphi}{2}}\sqrt{2\mathrm{i}+\rho\,\mathrm{e}^{\mathrm{i}\varphi}} \approx \pm\sqrt{2\mathrm{i}\rho}\,\mathrm{e}^{\frac{\mathrm{i}\varphi}{2}}$$

and can be written as

$$E_+ = \sqrt{2\rho}\,\mathrm{e}^{\frac{\mathrm{i}}{2}\left(\varphi+\frac{\pi}{2}\right)}\,, \tag{4-26}$$

$$E_- = \sqrt{2\rho}\,\mathrm{e}^{\frac{\mathrm{i}}{2}\left(\varphi+\frac{5\pi}{2}\right)}\,. \tag{4-27}$$

After a complete encircling, *i.e.* $\varphi = 1, \ldots, 2\pi$, the eigenvalues (4-26) and (4-27) switch places; only after a second encircling the initial eigenvalues are restored. This corresponds exactly to the scenario shown in Fig. 4-1.

The phenomenon of self-orthogonality is rather common in NHQM and it occurs if there exists no similarity transformation which reduces a non-Hermitian matrix to a *Jordan normal form*. It is not restricted to certain types of non-Hermitian Hamiltonians and also occurs in other fields of physics [72]. Despite the fact that EPs occur only at particular parameter values, they are not a rare phenomenon either. Moreover, in contrast to QM, the eigenvalues which are involved in an EP can possess the same symmetry; usually, eigenvalues with the same symmetry do not cross but form an *avoided crossing*[13] instead.

[13] *cf.* Appendix D

b) Normalisation

So far it has been shown that left-hand and right-hand eigenstates form a bi-orthogonal basis. Though, strictly speaking, this means that Eq. (4-13) only yields

$$\langle \psi^m | \psi_{n\neq m} \rangle = 0 \,.$$

But Eq. (4-14) holds only for a *bi-orthonormal* basis, *i.e.* the basis states must be properly normalised. Hence, it is worthwhile to take a closer look onto normalisation procedures in NHQM.

Consider an $N \times N$ non-Hermitian Hamiltonian $\mathcal{H}$ with N linearly independent eigenstates $\{\psi_n : n = 1, \dots, N\}$ of the right-hand Schrödinger equation (4-10). If the eigenstates are not yet normalised, Eq. (4-14) must be replaced by

$$\langle \psi^m | \psi_n \rangle = N_n \delta_{nm} \,, \tag{4-28}$$

where $N_n = \langle \psi^n | \psi_n \rangle \neq 0$. Though, this is possible only if the system is in a parameter region far away from an EP; otherwise, some of the states become almost self-orthogonal, which makes them non-normalisable. The Hamiltonian can be written in the form (4-19), where the states in Eqs. (4-17) and (4-18) are not normalised. To normalise them, one may try to multiply each of them by a suitable complex number,

$$|\hat{\psi}_n\rangle = R_n |\psi_n\rangle \,,$$
$$\langle \hat{\psi}^n | = \langle \psi^n | L_n \,,$$

so that $L_n R_n = N_n$.

By using the Euler representations of the complex numbers[14] one finds

$$|L_n| \cdot |R_n| = |N_n| \,, \tag{4-29}$$
$$\lambda_n + \rho_n = \varphi_n \,, \tag{4-30}$$

where λ_n, ρ_n, and φ_n are the phases of L_n, R_n, and N_n, respectively. Equations (4-29) and (4-30) apparently yield only two degrees of

[14] The bi-orthogonal product is complex due to the missing complex conjugation.

freedom for every pair of bi-orthogonal eigenstates, *i.e.* one for the absolute values of the normalisation factors and one for their phases. However, there is a third degree of freedom, since the global sign of the phase — the global ± phase — can be chosen arbitrarily.

At an EP, however, some states cannot be normalised properly using Eq. (4-28) due to $N_n = 0$. Though, an EP is a singularity and even for a small perturbation of the system parameters the property of self-orthogonality vanishes. Yet, in the vicinity of an EP the value $N_n \approx 0$ is still quite small. In principle, this renders the states normalisable, but in practice the division of the nearly self-orthogonal state $|\psi_n\rangle$ by the small number $\sqrt{N_n}$ causes the components of the wave functions to become extremely large, as the Hermitian inner product shows,

$$\langle \psi_n | \psi_n \rangle \propto \frac{1}{N_n} \,. \tag{4-31}$$

Yet, the Hermitian inner product (4-31) can still be used to re-normalise the states, *i.e.*

$$|\tilde{\psi}_n\rangle = \frac{1}{\sqrt{\langle \psi_n | \psi_n \rangle}} |\psi_n\rangle \,,$$

so that $\langle \tilde{\psi}_n | \tilde{\psi}_n \rangle = 1$ and $\langle \tilde{\psi}^n | \tilde{\psi}_n \rangle \neq 1$; then, the re-normalised eigenstate $|\tilde{\psi}_n\rangle$ is of the order $O(1)$, in principle. This re-normalisation is useful if, for example, a specific algorithm or library for non-Hermitian eigenvalue problems yields eigenstates which for mathematical reasons are normalised with respect to the bi-orthogonal product (4-28); yet, because of physical motivations[15] the eigenstates must be normalised with respect to the Hermitian inner product.

[15] *cf.* Section 4-6 a)

However, the numerical division of large numbers is problematic and can potentially cause a loss of precision, which leads to a decrease in the number of significant digits using standard techniques. Although a numerical calculation will never take place exactly at an EP due to round-off errors, N_n can still be as small as machine precision. Hence, it is discouraged to use the Hermitian norm (4-31) in the vicinity of EPs.

4-4 The metric operator

As discussed in Section 4-3 b), the modified inner product (4-20) can be used to normalise bi-orthogonal states in NHQM. Actually, Eq. (4-20) defines a kind of an inner product for states $|\psi_n\rangle$ and $|\psi_m\rangle$ of the Hilbert space,

$$(\psi_m|\psi_n) = \langle\eta\psi_m|\psi_n\rangle \,, \tag{4-32}$$

where η is a *metric operator* with the property

$$\eta\,|\psi_m\rangle = |\psi^m\rangle \,.$$

For a bi-orthonormal basis the metric operator η must be Hermitian because

$$\langle\psi^m|\psi_n\rangle = \langle\eta\psi_m|\psi_n\rangle = \delta_{nm} = \langle\psi_m|\eta\psi_n\rangle = \langle\psi_m|\psi^n\rangle \,.$$

In this case the bi-orthogonal norm is real, but not necessarily positive definite, as the discussion on self-orthogonality in Section 4-3 a) shows;[16] though, it is still positive semi-definite. The concept of *indefinite metrics* is not new both in physics [77; 78] and mathematics [79; 80]. Such an indefinite metric gives rise to a Krein space [81; 82], in which, for example, non-Hermitian operators with real spectra are self-adjoint.[17]

[16] *cf.* Eq. (4-22) in particular

[17] *cf.* Section 4-4 a)

In contrast, under the assumption that the inner product (4-32) is positive definite,[18] a complete quantum theory can be built upon this metric in pretty much the same manner as the ordinary quantum theory (*e.g.* see Refs. [83–86]). Such a non-Hermitian quantum theory possesses, among other features, a unitary time evolution [87] and a suitable variational principle can be found [84]. As noted in Ref. [85], the metric operator η has to be bounded because the Hilbert space defined by Eq. (4-32) must be norm complete.

[18] This might be the case far away from any EPs.

One should also note that the definition of the Hermitian adjoint with respect to the bi-orthogonal product (4-32) must be changed accordingly. With the usual definition of the Hermitian adjoint[19]

[19] *cf.* Appendix B-3

one finds

$$\langle \psi^m | \mathcal{H} \psi_n \rangle = \langle \psi_m | \eta \mathcal{H} \psi_n \rangle \overset{!}{=} \left\langle \mathcal{H}^\sharp \psi^m \middle| \psi_n \right\rangle = \left\langle \psi_m \middle| \left(\mathcal{H}^\sharp\right)^\dagger \eta \psi_n \right\rangle ,$$

which yields the definition of the *bi-adjoint*

$$\mathcal{H}^\sharp = \eta^{-1} \mathcal{H}^\dagger \eta \tag{4-33}$$

for a Hermitian metric operator η.

a) Quasi-Hermiticity

[20] *cf.* Eq. (4-2)

Hamiltonians with the property[20] $\mathcal{H}^\sharp = \mathcal{H}$ possess real spectra with respect to the bi-orthogonal product (4-32),

$$E_n = \langle \psi^m | \mathcal{H} \psi_n \rangle = \left\langle \psi^n \middle| \mathcal{H}^\sharp \psi_m \right\rangle^* = \langle \psi^n | \mathcal{H} \psi_m \rangle^* = E_m^* \delta_{nm} ,$$

i.e. $E_n = E_n^*$ analogously to the Hermitian spectra in Section 4-1. Therefore, such operators are called *quasi-Hermitian* [84].

b) Quasi-Unitarity

Obviously, the time evolution generated by a general non-Hermitian Hamiltonian $\mathcal{H}$ is not unitary because

$$\mathcal{U}^\dagger = \left(\mathrm{e}^{-\mathrm{i}\mathcal{H}t}\right)^\dagger = \mathrm{e}^{\mathrm{i}\mathcal{H}^\dagger t} \neq \mathcal{U}^{-1} .$$

However, the bi-orthogonal product (4-32) of two time-dependent states reads

$$\mathrm{i}\frac{\mathrm{d}}{\mathrm{d}t} \langle \psi^m(t) | \psi_n(t) \rangle = \langle \psi^m(t) | \mathcal{H} - \mathcal{H}^\sharp | \psi_n(t) \rangle ,$$

i.e. it is invariant under the time evolution generated by a quasi-Hermitian Hamiltonian $\mathcal{H}$ if $\langle \psi(t) | \eta | \psi(t) \rangle$ is a conserved quantity.

The time-evolution operator $\mathcal{U}$ defined by a quasi-Hermitian Hamiltonian $\mathcal{H}$ has the property[21]

[21] *cf.* Eq. (4-3)

$$\mathcal{U}^{\#} = \mathcal{U}^{-1}\,,$$

and is thus said to be *quasi-unitary* [87; 88].

4-5 Complex symmetric Hamiltonians

In Section 4-2 the physical interpretation of non-Hermitian quantum systems has already been discussed, particularly for quantum systems which are non-Hermitian due to a complex external potential.[22] The Hamiltonians of such systems belong to the particular class of *complex symmetric Hamiltonians*.

[22] *cf.* Section 4-2 a)

Consider a generic Hamiltonian as defined in Eq. (2-39),

$$\mathcal{H} = \frac{\hat{p}^2}{2} + V(\hat{x})\,, \tag{4-34}$$

where $V(\hat{x})$ is a complex-valued function of the real positions $\hat{x}$. The *adjoint* of the Hamiltonian (4-34) reads

$$\mathcal{H}^\dagger = \frac{\left(\hat{p}^\dagger\right)^2}{2} + V^*(\hat{x}) = \frac{\hat{p}^2}{2} + V^*(\hat{x})\,,$$

where the Hermiticity of the momentum operator $\hat{p}^\dagger = \hat{p}$ was used. For $V(\hat{x}) \in \mathbb{R}$ the Hamiltonian is Hermitian, $\mathcal{H}^\dagger = \mathcal{H}$, which is the usual case in QM. However, for $V(\hat{x}) \in \mathbb{C}$ the Hamiltonian satisfies

$$\mathcal{H}^\dagger = \mathcal{H}^* \tag{4-35}$$

instead. This is because[23] $\hat{p}^* = -\hat{p}$, *i.e.* $\hat{p}^2$ is invariant under complex conjugations. Note that Eq. (4-35) is equivalent to the condition $\mathcal{H} = \mathcal{H}^\mathsf{T}$, *i.e.* $V = V^\mathsf{T}$.

[23] *cf.* Appendix B

The property (4-35) of being complex symmetric holds for all "physical" Hamiltonians in NHQM, which are described by a complex potential. In fact, all Hamiltonians which are considered in this thesis are complex symmetric, even though they are non-Hermitian. Another example for such a Hamiltonian is given by Eq. (4-21) with

$\lambda \in \mathbb{C}$. For $\lambda \in \mathbb{R}$ the Hamiltonian (4-21) is Hermitian, which is a special case of a complex symmetric Hamiltonian.

a) Complex symmetric matrix models

Since all physical quantum systems with a complex potential can be described by a complex symmetric Hamiltonian in their infinite-dimensional position-space representation, this property must be preserved in any finite-dimensional approximation, especially, because any non-Hermitian matrix can be written in a complex symmetric form [89]. Moreover, if a Hamiltonian becomes non-Hermitian due to an effective description, there is no physical motivation for writing such a Hamiltonian in a non-symmetric form.

A simple consideration shows that this is of no concern. If a quantum systems is discretised with dimension N, *e.g.* by some approximation,[24] the states $|\psi_n\rangle$ become vectors with complex coefficients $\psi_n^{(k)}$ for $k = 1, \dots, N$. Then, the potential term of the Hamiltonian (4-34) cannot affect the property (4-35) because it only corresponds to the diagonal of the Hamiltonian matrix, *i.e.* $V(x)\psi_n^{(k)} \propto \psi_n^{(k)}$. On the other hand, the kinetic part of Eq. (4-34) corresponds to a second-order derivative with respect to the position x and can be approximated by a finite difference, *i.e.*

$$\hat{p}^2 \psi_n^{(k)} \propto (\psi_n^{(k+1)} - \psi_n^{(k)}) + (\psi_n^{(k-1)} - \psi_n^{(k)}) ;$$

hence, the kinetic part provides off-diagonal matrix elements of the Hamiltonian matrix, which must satisfy $H_{kl} = H_{lk}$ for all combinations of $k, l = 1, \dots, N$. However, since $\hat{p}$ is Hermitian, any physically suitable approximation must also yield a Hermitian matrix for the kinetic part, which satisfies Eq. (4-35).

[24] *cf.* Appendix E

b) Bi-orthogonal basis for complex symmetric Hamiltonians

For complex symmetric Hamiltonians the set of bi-orthogonal states is complete [63; 90]. Hence, there exists a complete bi-orthogonal basis for all discrete, non-Hermitian quantum systems.

By looking at Eqs. (4-10) and (4-12), it is easy to see that the left-hand and right-hand eigenstates of a complex symmetric Hamiltonian are related by the complex conjugation,

$$|\psi^m\rangle = |\psi_m^*\rangle \ . \tag{4-36}$$

The corresponding inner product (4-20) is given by [73]

$$(\psi_m|\psi_n) = \langle\psi_m^*|\psi_n\rangle \ .$$

This immediately implies that

$$(\psi_m| = \langle\psi_m^*| = |\psi_m^*\rangle^\dagger = |\psi_m\rangle^\mathsf{T} = |\psi_m)^\mathsf{T} \ ,$$

i.e. the states are just transposed and not Hermitian adjoint to each other; hence, they share the symmetry of the Hamiltonian.

As discussed in Section 4-3 b), in principle, there are three degrees of freedom when normalising a pair of bi-orthogonal eigenstates. In order to preserve the symmetry (4-36) of the states for complex symmetric Hamiltonians, there remains only one degree of freedom, which is the global ± phase.

4-6 Open quantum systems

Although often considered in QM, in reality there exist no closed quantum systems.[25] Any experiment is — much to the dismay of any experimentalist — coupled to an uncontrollable environment, which will perturb the system, eventually causing completely different dynamics. However, the explicit treatment of the environment is often unfeasible. Moreover, even if solutions to a microscopic

[25] maybe with the exception of the whole universe itself

description of the quantum systems and its environment could be derived, there would occur a vast amount of information of which the major part corresponds to the environment and is uninteresting. Instead, NHQM allows for the treatment of *open quantum systems* which involve only a small number of relevant variables.

According to QM any quantum system can be described by a Hermitian Hamiltonian of the form [91]

$$\mathcal{H} = \mathcal{H}_{\text{sys}} \otimes \mathbb{1}_{\text{env}} + \mathbb{1}_{\text{sys}} \otimes \mathcal{H}_{\text{env}} + V_{\text{int}}\,, \tag{4-37}$$

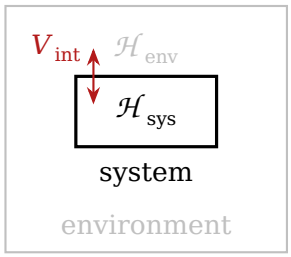

Figure 4-2: A system and its environment

where $\mathcal{H}_{\text{sys}}$ and $\mathcal{H}_{\text{env}}$ are the Hamiltonians for the localised system and the infinite environment, respectively, and V_{int} describes the interactions between them. This scenario is illustrated in Fig. 4-2. Here, $\mathcal{H}_{\text{sys}}$ possesses discrete eigenvalues which are perturbed by the continuous spectrum of the environment.

It is often difficult — if not impossible — to treat such systems either analytically or even numerically. Therefore, one often must resort to the theory of *open quantum systems*,

$$\mathcal{H}_{\text{eff}} = \mathcal{H}_{\text{sys}} + \tilde{V}_{\text{int}}\,. \tag{4-38}$$

Such Hamiltonians can, for example, be derived by tracing out the environmental degrees of freedom [91] or by using projection-operator methods [92; 93]. They are described effectively by a complex potential $\tilde{V}_{\text{int}}$ [63], which governs the interactions with the environment, though, the environment is no longer explicitly treated. In contrast to Eq. (4-37), the resulting Hamiltonian (4-38) is non-Hermitian due to $\tilde{V}_{\text{int}}$ and can be written in a complex symmetric form[26] [89]. Hence, NHQM allows for an *effective description* of open quantum systems (*e.g.* see Ref. [94]). Typically, the considered system is much smaller than the environment, which actually would be infinitely large. Hence, the effective treatment of the system corresponds to a substantial simplification of the problem. If the interaction term vanishes, Eq. (4-38) becomes Hermitian and describes the idealised case of an isolated quantum system.

[26] *cf.* Section 4-5

In open quantum systems one may still determine the solutions of the time-independent Schrödinger equation (2-39). However,

due to the non-Hermiticity of the system, the eigenvalues become complex, so that the norm of the states are changing in time as discussed in Section 4-3; this corresponds to the *gain and loss* of probability. Due to the presence of gain and loss, open quantum systems in general are not *time-reversal invariant*. That is, in contrast to QM, there exists a distinguished direction of time [60]. Hence, the solutions cannot *a priori* be considered as "stationary" states. Nevertheless, the calculation of *steady states* is of particular interest, which is a core topic in this thesis.

If the potential $\tilde{V}_{\text{int}}$ is small enough, though, it can be considered as a perturbation of the Hermitian Hamiltonian. It is interesting to investigate under which circumstances the real spectrum remains real under a non-Hermitian perturbation. The answer depends on whether or not the eigenstates of the perturbed quantum system form a *Riesz basis* [95; 96]. That is, a set of states $\{|\xi_n\rangle\}$ is a Riesz basis for the Hamiltonian if and only if there exists a bounded invertible operator O such that $|\xi_n\rangle = O\,|\psi_n\rangle$, where $\{|\psi_n\rangle\}$ form an orthogonal basis.[27]

[27] This also holds for a bi-orthogonal basis [95].

a) Choice of the inner product

While left-hand and right-hand eigenstates coincide in Hermitian QM and thus form an orthogonal basis, in NHQM neither the left-hand nor the right-hand eigenstates can form a basis on their own. Therefore, the Hermitian inner product[28] of two right-hand or two left-hand states cannot be interpreted in the same manner as in Hermitian QM. There exist two possible approaches to deal with this, which correspond to different interpretations:

[28] *cf.* Section 4-1

1) The bi-orthogonal product (4-32) can be used as an inner product, which preserves some of the mathematical properties of QM. However, by introducing a new *metric*, a new quantum theory is defined in which the left-hand and right-hand eigenstates of the eigenvalues of the Hamiltonian form a bi-orthogonal basis. In the course, one defines a new Hilbert space in which quasi-Hermitian Hamiltonians are effectively Hermitian. The motivation for the bi-orthogonal product is mainly of mathematical nature, as it

allows for an elegant mathematical description of NHQM, similar to the usual Hermitian QM.

2) The usual inner product between left-hand and right-hand states, respectively, is still valid if the non-Hermiticity is considered as a pure consequence of boundary conditions, *i.e.* they effectively describe open quantum systems with non-unitary evolutions[29] as described in Section 4-4 b). In this scenario, only the effective Hamiltonian (4-38) is non-Hermitian, while the whole system is still Hermitian and described by Eq. (4-37).

[29] *cf.* the concluding remarks in Ref. [97]

Both of these choices for the inner product can be interpreted as *analytical continuations* of the inner product of Hermitian QM into the non-Hermitian domain. However, in the remainder of this thesis, non-Hermiticity is always considered to be a result of an effectively described open quantum system.

Symmetry and Symmetrisation

5

Chapter 2 already gives a short overview of symmetry in physics. Further, in Section 2-4 the concept of symmetry in QM is discussed. In the following, this discussion is continued and extended to NHQM using the foundations laid in Chapter 4. In the course of this chapter, the concepts of $\mathcal{PT}$-symmetric[1] and SUSY[2] QM are shortly summarised. Then, symmetrisation is introduced as a tool in NHQM and its relations to exact symmetries are discussed.

Note that, for the sake of simplicity and clarity, from now on the eigenstates are labelled by their eigenvalues in contrast to Chapter 4. While the introduction of the bi-orthogonal basis in the previous chapter profited from the index notation of the states, *e.g.* $|\psi_n\rangle$, the discussions in this chapter become much clearer without it; that is, in the following, $|\overline{E}\rangle$ and $|\underline{E}\rangle$ denote the left-hand and right-hand eigenstates corresponding to the eigenvalue E.

[1] *cf.* Section 2-2 a)

[2] *cf.* Section 2-5

5-1 $\mathcal{PT}$-symmetric quantum systems

Spacetime inversion was already introduced in Section 2-2 a), as it emerges from the structure of the Lorentz group. Remember also that, according to Eq. (2-18), the generators of real spacetime are invariant to spacetime inversions described by $\mathcal{CPT}$; this corresponds to the $\mathcal{PT}$ operator in the absence of charges. *$\mathcal{PT}$ symmetry*, however, is no fundamental symmetry on its own because charge conjugation is neither;[3] *i.e.* $\mathcal{PT}$ cannot be a fundamental symmetry because of the $\mathcal{CPT}$ theorem. However, if a complex spacetime $\mathbb{C}^{(1,3)}$ is considered in the absence of charges, one finds that the corresponding Lorentz group consists only of two disconnected components [1]:

[3] Otherwise, the overall amount of matter and anti-matter in the universe should be symmetric.

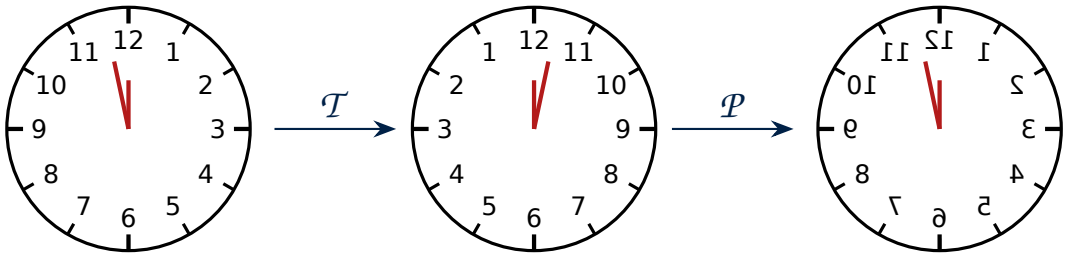

Figure 5-1: The *Doomsday Clock* [98] is an example of a $\mathcal{PT}$-symmetric system. If the direction of time is reversed, space must also be reflected to return the system to its initial state.

1) The proper Lorentz group and the $\mathcal{PT}$ component, both with the property $\det \Lambda > 0$.

2) The $\mathcal{P}$ and the $\mathcal{T}$ components, with the property $\det \Lambda < 0$.

In this sense the concept of $\mathcal{PT}$ symmetry emerges naturally in complex extensions of theories in real spacetime. For fermions and charged particles, though, $\mathcal{CPT}$ is still the fundamental symmetry.[4]

[4] *cf.* Section 2-3 b)

In real spacetime $\mathcal{PT}$ symmetry is also worthwhile to consider, which holds for NHQM in particular. In fact, the interest in non-Hermitian Hamiltonians rapidly increased after Carl Bender and Stefan Boettcher introduced the concept of $\mathcal{PT}$-symmetric QM in 1998 [1; 99]. The Hamiltonian of such a quantum system must satisfy Eq. (2-40) with the $\mathcal{PT}$ operator, *i.e.*

$$[\mathcal{PT}, \mathcal{H}] = 0\,, \tag{5-1}$$

so that $\mathcal{PT}$ transformations conserve the energy.[5] Here, the actions of the linear *parity operator* $\mathcal{P}$ and the anti-linear *time-reversal operator* $\mathcal{T}$ are defined as[6]

[5] *cf Section 2-5 a)*

[6] *cf.* Section 2-4

$$\begin{aligned} \mathcal{P}: &\quad \hat{p} \to -\hat{p}\,, \quad \hat{x} \to -\hat{x}\,, \\ \mathcal{T}: &\quad \hat{p} \to -\hat{p}\,, \quad \mathrm{i} \to -\mathrm{i}\,. \end{aligned}$$

Since both operators reverse the momentum, their combination must preserve it,

$$\mathcal{PT}: \quad \hat{x} \to -\hat{x}\,, \quad \mathrm{i} \to -\mathrm{i}\,. \tag{5-2}$$

All of these operators are involutory, *i.e.* $\mathcal{P}^2 = \mathcal{T}^2 = (\mathcal{PT})^2 = \mathbb{1}$. Of course, the $\mathcal{PT}$ operator is also anti-linear, such that its action involves a complex conjugation which represents time reversal.

Thus, $\mathcal{PT}$ essentially is the operation of spacetime reflection, which is illustrated in Fig. 5-1.

In the case of a complex symmetric Hamiltonian of the form (4-34) with a complex external potential,[7] the condition (5-1) reduces to

[7] *cf.* Sections 4-5 and 4-6

$$[\mathcal{PT}, V(\hat{x})] = 0\,, \tag{5-3}$$

because the kinetic part of the Hamiltonian is invariant under the transformation (5-2). Hence, a complex potential $V(\hat{x})$ is $\mathcal{PT}$-symmetric if it satisfies the condition $V^*(-\hat{x}) = V(\hat{x})$; in other words, the real part of the potential must be a *symmetric* function and the imaginary part must be an *anti-symmetric* function in space.

$\mathcal{PT}$-symmetric quantum systems possess some outstanding properties. By applying the $\mathcal{PT}$ operator to the Schrödinger eigenvalue equation (2-39) one finds

$$\mathcal{PT}\mathcal{H}\,|E\rangle = \mathcal{H}\mathcal{PT}\,|E\rangle \overset{!}{=} E^*\mathcal{PT}\,|E\rangle\,,$$

where Eq. (5-1) and the non-linearity of the $\mathcal{PT}$ operator were used. One can conclude that for every eigenstate $|E\rangle$ which is a solution of a $\mathcal{PT}$-symmetric Hamiltonian with eigenvalue E, $\mathcal{PT}\,|E\rangle$ is also a solution with eigenvalue E^*. The eigenvalues of a $\mathcal{PT}$-symmetric Hamiltonian thus always occur in complex-conjugate pairs. If the eigenstates obey the same symmetry as the Hamiltonian, that is $\mathcal{PT}\,|E\rangle = |E\rangle$, the eigenvalues must even be real. This is called *exact* or *unbroken* $\mathcal{PT}$ *symmetry* and, together with its simplicity, is the reason for the success and popularity of $\mathcal{PT}$ symmetry in NHQM. In regions with complex-conjugate eigenvalues, though, the $\mathcal{PT}$ symmetry is said to be *broken*.

In $\mathcal{PT}$-symmetric QM the parity operator $\mathcal{P}$ defines an indefinite norm as discussed in Section 4-4 [100; 101]. Yet, also a positive norm can be constructed for a $\mathcal{PT}$-symmetric, non-Hermitian quantum system if the $\mathcal{PT}$ symmetry is unbroken. In this case there exists another linear operator $\mathcal{C}$ which commutes both with $\mathcal{PT}$ and the Hamiltonian $\mathcal{H}$, *i.e.* it is a *hidden symmetry* of the system [57; 102–104]. Like $\mathcal{P}$ and $\mathcal{T}$, the operator $\mathcal{C}$ is also involutory and

is thus called "charge conjugation"; therefore, $\mathcal{PT}$-symmetric QM always obeys the "$\mathcal{CPT}$ theorem".[8] Moreover, $\eta = \mathcal{CP}$ is a metric operator of the type discussed in Section 4-4.

[8] *cf.* Section 2-3 b)

$\mathcal{PT}$ symmetry is well established nowadays and several books were already published on the subject, *e.g.* see Refs. [1; 74; 105]. It is applicable to all domains of physics, ranging from classical and wave-mechanical systems over QM to quantum field theories.[9] Since its first observation in optical wave guides [106], $\mathcal{PT}$ symmetry was also observed experimentally, among other fields, in mechanical [1; 107], electrical [108; 109], and only recently in quantum systems [110–113]. Of particular interest is also the study of EPs in $\mathcal{PT}$-symmetric open quantum systems [114–117], since they are an exclusive feature of non-Hermitian systems as discussed in Section 4-3 a). In recent years advances were made towards technical applications in superconducting wires [118; 119], $\mathcal{PT}$ lasers [120; 121], synthetic materials [122; 123], NMR spectroscopy [124], and also in WPT [125; 126]; the latter will further be discussed in the second part of this thesis. There is even a proposal for using a $\mathcal{PT}$-symmetric Hamiltonian to approach the Riemann hypothesis [127; 128].

[9] see Ref. [1] and references therein

Yet in QM, $\mathcal{PT}$ symmetry is just a special case of the broader class of anti-unitary symmetries allowed by Wigner's theorem.[10] In spite of its simplicity, $\mathcal{PT}$ symmetry requires for specific potentials with symmetric real parts and anti-symmetric imaginary parts as discussed above. In Section 5-3 a method for finding systems with looser requirements but similar spectral properties is introduced and compared to anti-unitary symmetries and $\mathcal{PT}$ symmetry in particular.

[10] *cf.* Section 2-4 a)

5-2 Non-Hermitian supersymmetric quantum systems

In Section 2-5 SUSY was introduced as a symmetry between bosons and fermions. In principle, though, SUSY requires only for two different types of states which can be related. As discussed in

Section 4-3, in any non-Hermitian quantum system there exist right-hand and left-hand eigenstates corresponding to the same energy eigenvalues. This closely resembles the broken-supersymmetric spectrum shown in Fig. 2-9. Hence, one may already assume that left-hand and right-hand states can be related using a non-Hermitian SUSY Hamiltonian of the form (2-69) with a suitable superpotential W.

In the following, the application of SUSY to NHQM is investigated. For the sake of simplicity, a specific type of complex, $\mathcal{PT}$-symmetric but broken-supersymmetric potential is considered to demonstrate the concept. Nevertheless, the discussions apply analogously to non-$\mathcal{PT}$-symmetric potentials as well.

a) Complex superpotentials

Consider a superpotential of the specific form

$$W(x) = \omega \hat{x}^n$$

with $n \geq 1$. Because of Eq. (2-70), this superpotential generates the potentials

$$V_{\pm}(\hat{x}) = \frac{\omega^2}{2}\hat{x}^{2n} \pm \frac{n\omega}{2}\hat{x}^{n-1}$$

which for $n = 1$ both correspond to the potential of a *harmonic oscillator*. From Section 2-5 c) it is known that the SUSY is broken if n is even. Hence, the simplest non-trivial, broken-supersymmetric potentials read

$$V_{\pm}(\hat{x}) = \frac{\omega^2}{2}\hat{x}^4 \pm \omega\hat{x}\,,$$

which are real for $\omega \in \mathbb{R}$. However, by choosing $\omega = \mathrm{i}$ the potentials become complex, *i.e.*

$$V_{\pm}(\hat{x}) = -\frac{(\mathrm{i}\hat{x})^4}{2} \pm \mathrm{i}\hat{x}\,. \tag{5-4}$$

Since $\mathrm{i}\hat{x}$ is invariant under $\mathcal{PT}$, the potentials (5-4) are $\mathcal{PT}$-symmetric, meaning that they describe balanced gain and loss. Therefore, the corresponding Hamiltonians

$$\mathcal{H}^{\pm} = \frac{1}{2}\left(\hat{p}^2 - \hat{x}^4\right) \pm \mathrm{i}\hat{x}$$

possess either real or complex-conjugate eigenvalues. Note that $\mathcal{H}^{+}$ and $\mathcal{H}^{-}$ are still adjoint to each other, even though the potentials correspond to non-Hermitian quantum systems.

Now, one can introduce the generalised "creation" and "annihilation" operators (2-68)

$$\hat{b}^{\pm} = \frac{\mathrm{i}}{\sqrt{2}}\left(\hat{x}^2 \mp \hat{p}\right) = -\left(\hat{b}^{\pm}\right)^{\dagger} \tag{5-5}$$

which can be used to write the Hamiltonians $\mathcal{H}^{\pm}$ in the form (2-67). However, in contrast to cases with real potentials, the operators (5-5) are non-Hermitian and *not* adjoint to each other; instead, they are *anti-adjoint*[11] to themselves. From Eqs. (2-67) and (2-69) it is known that

[11] *i.e.* adjoint with the opposite sign

$$\mathcal{H}_{\pm} = \hat{b}^{\mp}\hat{b}^{\pm}\,. \tag{5-6}$$

Since the representation of $\mathcal{H}^{-}$ resembles the harmonic oscillator (2-52) with its energy shifted by $\omega/2$, one may introduce the following notation:

$$\begin{aligned} \mathcal{H} &\equiv \mathcal{H}^{-}\,, \\ (\mathcal{H})^{\dagger} &\equiv \mathcal{H}^{+}\,. \end{aligned}$$

Hence, the states which correspond to $\mathcal{H}^{-}$ are considered to be right-hand eigenstates defined by

$$\mathcal{H}\,|\underline{E}\rangle = E\,|\underline{E}\rangle\,, \tag{5-7}$$

while the states which correspond to $\mathcal{H}^{+}$ are interpreted as left-hand eigenstates defined by

$$\langle\overline{E}|\,\mathcal{H} = \langle\overline{E}|\,E\,. \tag{5-8}$$

Since $\mathcal{H}$ is complex symmetric, the left-hand and right-hand eigenstates are simply related by a complex conjugation,

$$|\overline{E}\rangle = |\underline{E^*}\rangle \ .$$

Because $\mathcal{H}$ and $\mathcal{H}^\dagger$ are directly related by the broken SUSY, their spectra are completely identical. Moreover, from Eq. (5-8) it follows that the spectrum of $\mathcal{H}^\dagger$ is complex-conjugate to the spectrum of $\mathcal{H}$, *i.e.*

$$\mathcal{H}^\dagger|\overline{E}\rangle = E^*|\overline{E}\rangle \ . \tag{5-9}$$

Hence, the eigenvalues E can either only be real or occur in complex-conjugate pairs. These are the same spectral properties which the $\mathcal{PT}$-symmetric systems in Section 5-1 possess.

Imaginary *vs.* complex superpotentials

As mentioned above, the operators (5-5) are not adjoint to each other. This is a result of the bi-orthogonality of the basis in NHQM. Nevertheless, they are still related by being *anti-adjoint* to each other, which is a consequence of the specific form of the superpotential $W(\hat{x}) = \mathrm{i}\hat{x}^2 = -W^*(\hat{x})$, *i.e.* it is purely imaginary. In this case, one can introduce another set of operators $\hat{d}^\pm = -\hat{b}^\mp$ to represent the Hamiltonians (5-6),

$$\mathcal{H}^+ = \hat{d}^+\hat{d}^- \ ,$$
$$\mathcal{H}^- = \hat{d}^-\hat{d}^+ \ .$$

However, if the superpotential is complex, an independent set of "creation" and "annihilation" operators

$$\hat{d}^\pm = \frac{1}{\sqrt{2}}\Big(W^*(\hat{x}) \mp \mathrm{i}\hat{p}\Big)$$

formed by W^* exists, which corresponds to another pair of Hamiltonians $\widetilde{\mathcal{H}}^\pm$ being adjoint to $\mathcal{H}^\mp$. That is, while an imaginary superpotential only connects a Hamiltonian $\mathcal{H}$ to its adjoint, a complex superpotential connects two different Hamiltonians and

their adjoints.[12] This represents a significant difference from the Hermitian case with a real superpotential and leads to a theory which cannot provide balanced gain and loss in the sense that the eigenvalues are either only real or pairwise complex-conjugate.[13] This becomes clear in the further course of this thesis. For now, it is simply assumed that the superpotentials are purely imaginary and thus satisfy Eq. (5-5).

[12] Note that the potential energy is complex in both cases.

[13] *cf.* Ref. [129]

Symmetrisation operators

In Section 2-5 a) the superoperators were introduced as the generators of SUSY. The dominant feature of the superoperators is that they transform the different types of states with the same energy into each other. The operators (5-5) possess similar properties, though, they are not symmetry generators:

1) With Eqs. (5-6) and (5-7) one finds that

$$\mathcal{H}^\dagger\left(\hat{b}^-|\underline{E}\rangle\right) = \hat{b}^-\hat{b}^+\hat{b}^-|\underline{E}\rangle = \hat{b}^+\mathcal{H}|\underline{E}\rangle = E\left(\hat{b}^-|\underline{E}\rangle\right), \tag{5-10}$$

where $|\underline{E}\rangle$ is a right-hand eigenstate of $\mathcal{H}$ with energy eigenvalue E. Hence, $\hat{b}^-|\underline{E}\rangle$ is a left-hand eigenstate of $\mathcal{H}$ with eigenvalue E^*,

$$\langle\underline{E}|\left(\hat{b}^+\right)^\dagger\mathcal{H} = \langle\underline{E}|\left(\hat{b}^+\right)^\dagger E^*.$$

2) Analogously, with Eqs. (5-6) and (5-9) one finds that

$$\mathcal{H}\left(\hat{b}^+|\overline{E}\rangle\right) = \hat{b}^+\hat{b}^-\hat{b}^+|\overline{E}\rangle = \hat{b}^+\mathcal{H}^\dagger|\overline{E}\rangle = E^*\left(\hat{b}^+|\overline{E}\rangle\right), \tag{5-11}$$

i.e. $\hat{b}^+|\overline{E}\rangle$ is a right-hand eigenstate of $\mathcal{H}$ with energy eigenvalue E^* if $|\overline{E}\rangle$ is a left-hand eigenstate of $\mathcal{H}$ with energy eigenvalue E.

In the course of this calculation, an important property of the operators $\hat{b}^\pm$ is found, which follows directly from the definition of the Hamiltonians (5-6):

$$\hat{b}^-\mathcal{H} = \hat{b}^-\hat{b}^+\hat{b}^- = \mathcal{H}^\dagger\hat{b}^-, \tag{5-12}$$

$$\hat{b}^+\mathcal{H}^\dagger = \hat{b}^+\hat{b}^-\hat{b}^+ = \mathcal{H}\hat{b}^+ \,. \tag{5-13}$$

The relations (5-12) and (5-13) replace the commutator relations (2-65) for the superoperators. Therefore, $\hat{b}^\pm$ are not symmetry operators but *symmetrisation operators*: In the following, a *right-hand symmetrisation operator* $\underline{S}$ is defined by

$$\mathcal{H}\underline{S} = \underline{S}\mathcal{H}^\dagger \tag{5-14}$$

and a *left-hand symmetrisation operator* $\overline{S}$ is defined by

$$\overline{S}\mathcal{H} = \mathcal{H}^\dagger\overline{S} \,. \tag{5-15}$$

The general concept of symmetrisation is further investigated in Section 5-3. Nevertheless, it is reasonable to change the notation here already, *i.e.* $\hat{b}^+ \to \underline{S}$ and $\hat{b}^- \to \overline{S}$.

Equations (5-10) and (5-11) show that $\underline{S}$ transforms left-hand eigenstates into right-hand eigenstates and $\overline{S}$ does the opposite.[14] However, the resulting states are no longer normalised. To understand this, there are two different cases to consider:

[14] $\overline{S}$ is not necessarily the inverse of $\underline{S}$; this is discussed in Section 5-3 in detail.

1) If the energy E is real, then the symmetrisation operators transform between eigenstates with the same energy $E = E^*$,

$$\overline{S}\,|\underline{E}\rangle = \overline{\alpha}\,|\overline{E}\rangle \,, \tag{5-16}$$
$$\underline{S}\,|\overline{E}\rangle = \underline{\alpha}\,|\underline{E}\rangle \,. \tag{5-17}$$

   Hence,

$$|\underline{E}\rangle \overset{!}{=} \frac{1}{\underline{\alpha}}\underline{S}\left(\frac{1}{\overline{\alpha}}\overline{S}\,|\underline{E}\rangle\right) = \frac{1}{\underline{\alpha}\,\overline{\alpha}}\mathcal{H}\,|\underline{E}\rangle = \frac{E}{\underline{\alpha}\,\overline{\alpha}}\,|\underline{E}\rangle \,,$$

   which can be satisfied by the choice $\underline{\alpha} = \overline{\alpha} = \sqrt{E}$.

2) If the energy E is complex instead, the symmetrisation operators transform between eigenstates with complex-conjugate energies E and E^*,

$$\overline{S}\,|\underline{E}\rangle = \overline{\alpha}\,\left|\overline{E^*}\right\rangle \,, \tag{5-18}$$
$$\underline{S}\,|\overline{E}\rangle = \underline{\alpha}\,\left|\underline{E^*}\right\rangle \,, \tag{5-19}$$

$$\overline{S}\left|\underline{E^*}\right\rangle = \overline{\beta}\,|\overline{E}\rangle\,, \tag{5-20}$$

$$\underline{S}\left|\overline{E^*}\right\rangle = \underline{\beta}\,|\underline{E}\rangle\,. \tag{5-21}$$

Analogously to the case of a real energy one finds $\overline{\alpha} = \underline{\beta} = \sqrt{E}$ and $\underline{\alpha} = \overline{\beta} = \sqrt{E^*}$.

Note that these results are consistent with respect to both the bi-orthogonal and the Hermitian norm, which were discussed in Section 4-6 a). That is, consider a given norm

$$\langle\cdot|\underline{E}\rangle = 1\,,$$

where $\langle\cdot|$ can be taken either by a left-hand or a right-hand eigenstate. The energy expectation value can now be calculated using the same norm,

$$\langle\cdot|\mathcal{H}|\underline{E}\rangle = \langle\cdot|\underline{S}\,\overline{S}|\underline{E}\rangle = \sqrt{E}\left\langle\cdot\middle|\underline{S}\middle|\overline{E^*}\right\rangle = E\,\langle\cdot|\underline{E}\rangle\,.$$

Scattering states

SUSY does not only relate bound states of $\mathcal{H}$ and $\mathcal{H}^\dagger$ corresponding to discrete energy eigenvalues, but also scattering states which form a continuum. In the limit of continuous energies the difference between *exact* and *broken* SUSY vanishes, so that the relations (5-18) to (5-21) hold in both cases. Further, spectral singularities may appear in this continuum if the superpotential is complex [130–132].

Scattering states occur if a spatially extended potential remains finite for $x \to \infty$ or $x \to -\infty$, *i.e.*

$$\lim_{x\to\pm\infty} \frac{\mathrm{d}V}{\mathrm{d}x} \stackrel{!}{=} 0\,.$$

With Eq. (2-70) one finds the trivial condition

$$\lim_{x\to\pm\infty} \frac{\mathrm{d}W}{\mathrm{d}x} = \frac{\mathrm{d}}{\mathrm{d}x} \lim_{x\to\pm\infty} W(x) \equiv \frac{\mathrm{d}}{\mathrm{d}x} W_\pm(x) \stackrel{!}{=} 0$$

for the superpotential W. Hence, at least one of the asymptotic values $W_\pm$ must be finite.

SUSY also relates the transmissive and reflective properties of the potentials. Without giving the calculations,[15] one may find that

[15] *cf.* Ref. [48]

— the reflection probabilities are equal, *i.e.* $|R_+|^2 = |R_-|^2$,

— in the special case of $W_+ = W_-$ also the transmission probabilities are equal, *i.e.* $|T_+|^2 = |T_-|^2$.

Therefore, by starting with a given potential which possesses some specific properties,[16] SUSY allows for finding other non-trivial potentials with the same properties.

[16] *e.g.* totally reflective or completely reflectionless potentials

b) Supersymmetric chains

Section 5-2 a) shows that if a non-Hermitian Hamiltonian $\mathcal{H}$ and its adjoint $\mathcal{H}^\dagger$ are related by broken SUSY directly, then the symmetrisation operators satisfying Eqs. (5-14) and (5-15) are first-order *differential operators*. However, also higher-order differential operators are suitable choices [129]. This can be understood by introducing *SUSY chains*. For simplicity, it is assumed that the spectrum is entirely real. However, the same line of argument can be applied to Hamiltonians with complex eigenvalues.

Consider a Hamiltonian

$$\mathcal{H}_1 = \hat{b}_1^+ \hat{b}_1^-$$

with the ground state energy $E_0^{(1)} = 0$ and an entirely real spectrum. The bosonic operators

$$\hat{b}_1^\pm = \frac{1}{\sqrt{2}}(W_1(\hat{x}) \mp \mathrm{i}\hat{p})$$

are defined by the superpotential W_1. The SUSY partner of $\mathcal{H}_1$ is given by

$$\mathcal{H}_2 = \hat{b}_1^- \hat{b}_1^+ .$$

If the SUSY is exact, then the operators $\hat{b}_1^\pm$ connect states with different "occupation numbers",[17]

[17] One can still think of the states as being labelled by a number in increasing order.

$$\left|E_n^{(2)}\right\rangle = \frac{\hat{b}_1^- \left|E_{n+1}^{(1)}\right\rangle}{\sqrt{E_{n+1}^{(1)}}}\,, \qquad \left|E_{n+1}^{(1)}\right\rangle = \frac{\hat{b}_1^+ \left|E_n^{(2)}\right\rangle}{\sqrt{E_{n+1}^{(1)}}}\,.$$

Apart from the ground state $E_0^{(1)}$, each energy level occurs in both the spectrum of $\mathcal{H}_1$ and $\mathcal{H}_2$, respectively, *i.e.* $E_{n+1}^{(1)} = E_n^{(2)}$.

This procedure can now be repeated: By introducing another Hamiltonian

$$\mathcal{H}_3 = \hat{b}_3^+ \hat{b}_3^-$$

with

$$\hat{b}_3^\pm = \frac{1}{\sqrt{2}}(W_3(\hat{x}) \mp \mathrm{i}\hat{p})\,,$$

one can again construct an exact SUSY partner. However, by requiring that the SUSY partner of $\mathcal{H}_3$ is equal to $\mathcal{H}_2$, *i.e.*

$$\mathcal{H}_2 \stackrel{!}{=} \hat{b}_3^- \hat{b}_3^+\,,$$

the Hamiltonians $\mathcal{H}_1$ and $\mathcal{H}_3$ can be connected; $\mathcal{H}_1$, $\mathcal{H}_2$, and $\mathcal{H}_3$ then form a SUSY chain. Instead of the trivial choice $\hat{b}_3^\pm = \hat{b}_1^\pm$, one can also chose $\hat{b}_3^\pm = (\hat{b}_1^\mp)^\dagger$, which corresponds to the requirement $\mathcal{H}_3 = \mathcal{H}_1^\dagger$. In this case, the eigenstates of $\mathcal{H}_1$ and $\mathcal{H}_3$ are related by

$$\left|E_n^{(3)}\right\rangle = \frac{\hat{b}_3^+ \hat{b}_1^- \left|E_n^{(1)}\right\rangle}{\sqrt{E_n^{(1)} E_n^{(3)}}}\,, \qquad \left|E_n^{(1)}\right\rangle = \frac{\hat{b}_1^+ \hat{b}_3^- \left|E_n^{(3)}\right\rangle}{\sqrt{E_n^{(1)} E_n^{(3)}}}\,.$$

The spectra of the operators $\mathcal{H}_1$ and $\mathcal{H}_3 = \mathcal{H}_1^\dagger$ are complex-conjugate to each other, *i.e.* $E_n^3 = (E_n^1)^*$. By using the same notation as in the previous section, that is $|\underline{E}\rangle \equiv |E_n^{(1)}\rangle$ and $|\overline{E^*}\rangle \equiv |E_n^{(3)}\rangle$, one obtains

$$|\underline{E}\rangle = \frac{\hat{b}_1^+ \left(\hat{b}_1^+\right)^\dagger \left|\overline{E^*}\right\rangle}{|E|}\,, \qquad |\overline{E^*}\rangle = \frac{\left(\hat{b}_1^-\right)^\dagger \hat{b}_1^- \,|\underline{E}\rangle}{|E|}\,.$$

This corresponds to Eqs. (5-18) and (5-21) with the *second-order differential* symmetrisation operators

$$\underline{S} = \hat{b}_1^+ \left(\hat{b}_1^+\right)^\dagger ,$$
$$\overline{S} = \left(\hat{b}_1^-\right)^\dagger \hat{b}_1^- .$$

SUSY chains can, in principle, be created with an arbitrary number of intermediate Hamiltonians. If the number of Hamiltonians involved is odd, then the chain is linked only by *exact* SUSY. However, if the number of Hamiltonians is even, the central connection must be *broken-supersymmetric* instead. The spectra of an even and an odd SUSY chain are illustrated in Figs. 5-2 and 5-3.

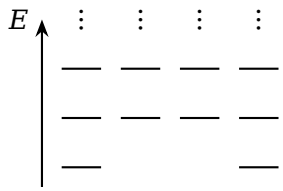

Figure 5-2: An even SUSY chain

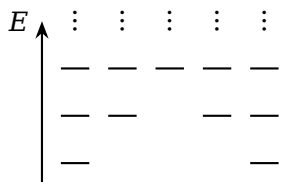

Figure 5-3: An odd SUSY chain

5-3 Symmetrisation

The concept of $\mathcal{PT}$ symmetry discussed in Section 5-1 is intriguingly powerful, yet simple and versatile in applications. It must be noted, however, that in 1992, already several years before its introduction, Scholtz, Geyer, and Hahne published a paper on *quasi-Hermitian Hamiltonians in NHQM* [84]. Quasi-Hermiticity does not rely on the strict symmetry conditions posed upon the potentials, which $\mathcal{PT}$ symmetry requires, but allows for the occurrence of real eigenvalues in asymmetric potentials and even in cases with either pure gain or loss [129]. The latter was observed experimentally a while ago in anti-$\mathcal{PT}$-symmetric systems [133; 134]. Similar to $\mathcal{PT}$ symmetry, the applicability of quasi-Hermitian QM is broad and ranges from scattering problems [63; 135; 136] to constant-intensity waves [137; 138], which were recently realised experimentally with pressure waves [139]. Quasi-Hermiticity can also be used to define a generalised entropy functional for non-Hermitian quantum systems [59; 140].

There are other types of non-$\mathcal{PT}$-symmetric systems with similar properties. Anti-$\mathcal{PT}$ symmetry was, for example, observed for coupled atomic spin waves [141], in electric circuits [142], and in diffusive systems [143]. Another type of non-$\mathcal{PT}$-symmetric

potentials is based on the connection between the Zakharov–Shabat spectral problem and the Schrödinger eigenvalue problem [129; 139; 144–148], which, for example, allows for the construction of *unidirectionally invisible* asymmetric potentials [138]. Such *Wadati-type potentials* correspond to a specific form of complex potentials,

$$V(x) = w^2(x) + \mathrm{i}\frac{\partial w}{\partial x}\,, \tag{5-22}$$

where $w(x)$ is an arbitrary real function defining the whole system. In fact, the occurrence of a potential of the form (5-22) can directly be related to the SUSY potentials (2-70).

The characteristic feature of such non-$\mathcal{PT}$-symmetric potentials clearly is their lack of any obvious symmetries or any requirements thereof. Hence they can be applied to situations where gain or loss are either uncontrolled or even uncontrollable. This could be useful for quantum transport in chain potentials with gain and loss. Such systems were recently discussed in the context of $\mathcal{PT}$-symmetric quantum dot chains [149]. However, the realisation of stable $\mathcal{PT}$-symmetric potentials is demanding and small perturbations will immediately break the symmetry. A first step towards applications using BECs with asymmetric potentials has been made by Lunt *et al*. [150], who reported on the formation of a steady ground state in a non-$\mathcal{PT}$-symmetric two-mode BEC with balanced gain and loss. Due to the non-linear properties of the condensate, the system is stable with respect to small asymmetries in gain and loss. However, their approach seems phenomenological and gives the impression that the occurrence of steady states is coincidental.

Basically, there are two possible approaches to ensure that the spectrum of an operator is complex-conjugate to itself — that is the statement of Wigner's theorem [35; 151] — which are discussed in the following. However, it should be emphasised once again that, for the sake of simplicity and clarity, the spectra considered are assumed to be discrete and non-degenerate. The case with degeneracy is, for example, described in Ref. [152].

a) The presence of an anti-unitary symmetry

Consider a non-Hermitian operator $\mathcal{H}$ and the corresponding *right-hand* eigenvalue equation

$$\mathcal{H}\,|\underline{E}\rangle = E\,|\underline{E}\rangle\,, \tag{5-23}$$

where E are the complex eigenvalues of $\mathcal{H}$ corresponding to the right-hand eigenstates $|\underline{E}\rangle$. By introducing an *anti-linear*[18] operator $\mathcal{A}$, one finds a right-hand eigenvalue equation $\mathcal{H}\,|\underline{E}'\rangle = E^*\,|\underline{E}'\rangle$ with $|\underline{E}'\rangle = \mathcal{A}\,|\underline{E}\rangle$ if[19]

[18] *cf.* Eq. (2-42)

[19] *cf.* Section 2-4

$$[\mathcal{A}, \mathcal{H}] = 0\,. \tag{5-24}$$

Therefore, if $E \in \mathbb{C}$ is in the spectrum of $\mathcal{H}$ so is E^*; the eigenvalues arise in complex-conjugate pairs. Note that this is particularly true for real eigenvalues [153] which can be considered as their own complex conjugates.

An eigenvalue E of $\mathcal{H}$ is real if the corresponding eigenstate is invariant under the action of the anti-linear symmetry, *i.e.*

$$\mathcal{A}\,|\underline{E}\rangle = |\underline{E}\rangle\,, \tag{5-25}$$

in which case the symmetry is called *exact* [83]. To see this, consider the eigenvalue equation (5-23); by applying $\mathcal{A}$ and using Eq. (5-24) one finds

$$\mathcal{A}\mathcal{H}\,|\underline{E}\rangle = \mathcal{H}\,\mathcal{A}\,|\underline{E}\rangle = E^*\,\mathcal{A}\,|\underline{E}\rangle = \mathcal{A}E\,|\underline{E}\rangle\,,$$

so that the reality of E follows from Eq. (5-25).

Now, consider the most simple anti-linear operator $\mathcal{A} = \mathcal{K}$ introduced in Section 2-4. In this case, Eq. (5-24) requires that $\mathcal{H}^* = \mathcal{H}$ and thus that $\mathcal{H}$ is real. More general cases are obtained by combining the complex-conjugation operator with another linear operator, *i.e.* $\mathcal{A} = O\mathcal{K}$, so that Eq. (5-24) reads

$$O[\mathcal{K}, \mathcal{H}] + [O, \mathcal{H}]\mathcal{K} = 0\,.$$

For real Hamiltonians the first commutator vanishes, which means that O must be a *unitary symmetry* of $\mathcal{H}$. For complex Hamiltonians, though, both terms must be non-zero. The commutator (5-24) can then be written as

$$\mathcal{H}O = O\mathcal{H}^* . \tag{5-26}$$

In physical terms, *anti-unitary symmetries* can always be related to a time-reversal invariance [63], as the time-reversal operator is anti-linear. Some widely known examples for such anti-unitary symmetries are the already discussed parity-time symmetry with $\mathcal{A} = \mathcal{PT}$ and the charge-parity-time symmetry with $\mathcal{A} = \mathcal{CPT}$.

b) The concept of symmetrisation

Instead of Eq. (5-23) one can also consider its adjoint equation. The complex conjugate of E then appears naturally on the right-hand side and one may introduce a *linear* operator $\overline{S}$ in such a way that

$$\langle \underline{E}| \mathcal{H}^\dagger \overline{S}^\dagger = \langle \underline{E}| \overline{S}^\dagger E^* . \tag{5-27}$$

Requiring that the operator $\overline{S}$ satisfies the relation (5-15), a *left-hand* eigenvalue equation is found,

$$\langle \overline{E}| \mathcal{H} = \langle \overline{E}| E^* ,$$

where $|\overline{E}\rangle = \overline{S}\,|\underline{E}\rangle \neq 0$ is a left-hand eigenstate which must not necessarily be normalised. Since the Hamiltonian considered is not Hermitian, its eigenbasis is bi-orthogonal as discussed in Section 4-3. This means that the left-hand and right-hand eigenstates which correspond to the same eigenvalue do not coincide, as it would be the case for Hermitian operators.

Equation (5-15) shows that the combination of $\mathcal{H}$ and $\overline{S}$ is Hermitian if and only if $\overline{S}$ is Hermitian. However, Eq. (5-15) always allows for the Hermitian choice $(\overline{S} + \overline{S}^\dagger)/2$ in finite-dimensional Hilbert spaces[20] [129; 155]. A Hamiltonian satisfying Eq. (5-15) is thus called *symmetrised* [140; 156; 157] with respect to the

[20] In infinite-dimensional Hilbert spaces the symmetrisation operators need not to be Hermitian [152; 154]; though, they can be considered to be Hermitian in the sense of Eq. (4-33).

left-hand symmetrisation operator $\overline{S}$ defined by Eq. (5-15). This corresponds to the method proposed by Jean Gaston Darboux [158; 159], which relates the spectra of the Hamiltonians $\mathcal{H}$ and $\mathcal{H}^\dagger$.

The left-hand symmetrisation operator $\overline{S}$ is a metric operator.[21] A relation similar to Eq. (5-15) was found while discussing the Lorentz group in Section 2-2 a). In Eq. (5-15) the operator $\overline{S}$ plays the same role as the metric operator η of spacetime in Eq. (2-13). At the same time, the left-hand symmetrisation operator can also be understood as a symmetry of $\mathcal{H}$ within a superoperator framework [151]. It transforms a right-hand eigenstate of $\mathcal{H}$ into a left-hand eigenstate with the complex-conjugate eigenvalue as discussed in Section 5-2 a).

[21] *cf.* Section 4-4

Analogously to the left-hand symmetrisation operator, the right-hand symmetrisation operator $\underline{S}$ satisfies Eq. (5-14) via the left-hand eigenvalue equation

$$\mathcal{H}^\dagger |\overline{E}\rangle = E^* |\overline{E}\rangle \,.$$

The operator $\underline{S}$ transforms left-hand eigenstates into right-hand eigenstates — that is $\underline{S}\,|\overline{E}\rangle = |\underline{E}\rangle$ — thus complementing $\overline{S}$.

The symmetrisation operators play the same role as the creation and annihilation operators (5-13) and (5-14). Further, the combination $\underline{S}\overline{S}$ commutes with $\mathcal{H}$ by definition,

$$\underline{S}\overline{S}\mathcal{H} = \underline{S}\mathcal{H}^\dagger\overline{S} = \mathcal{H}\underline{S}\overline{S} \,. \tag{5-28}$$

Therefore, $\underline{S}\overline{S}$ and $\mathcal{H}$ share the same eigenbasis. However, $\mathcal{H}$ and $\underline{S}\overline{S}$ are not necessarily equal,[22] as it is typically the case in SUSY QM discussed in Section 5-2. Yet, $\underline{S}\overline{S}$ is diagonal with respect to the bi-orthogonal product (4-32); hence, with a suitable choice of the symmetrisation operators, the eigenvalues of $\underline{S}\overline{S}$ are unity.

[22] This is of particular importance for more general cases which are discussed in Section 5-4.

If $\overline{S}$ is invertible, then a Hamiltonian is, if at all, always symmetrisable from both sides due to

$$\underline{S} \propto \overline{S}^{-1} \,. \tag{5-29}$$

In this case, Eq. (5-28) is equivalent to both Eqs. (5-14) and (5-15) and can be written as

$$\underline{S}\mathcal{H}^{\dagger}\overline{S} = \mathcal{H}\,, \tag{5-30}$$

which corresponds to Eq. (4-33) and is thus a modification of the Hermiticity condition (4-2). An operator satisfying Eq. (5-28) is called either quasi-Hermitian [84; 160], $\overline{S}$-Hermitian [81; 161; 162], pseudo-Hermitian [83; 163–165], crypto-Hermitian [166–168], or simply generalised Hermitian [169]. The various names that were coined and used for the properties (5-14), (5-15) and (5-30) throughout history depend on the properties of the respective metric operators as described in Ref. [154]. To avoid confusion, this thesis will stick consequently to the term "symmetrisation", which simultaneously is considered as a less restrictive concept in its own right [157], as it is not necessary for the operators $\overline{S}$ and $\underline{S}$ to be invertible [129; 154].

Further, it should be emphasised that symmetrisation must not be understood as a generalisation or extension of QM; *e.g.* see Refs. [57; 86], where the inner product is redefined by Eq. (4-32). Here, NHQM is understood as an effective description of open quantum systems as discussed in Section 4-6. Hence, the Hermitian inner product of QM must be used to obtain physical quantities. In this interpretation the left-hand and right-hand states are just parts of some larger orthogonal states describing a Hermitian system which contains also the environment;[23] thus, they do not form a basis on their own, respectively. Equations (5-14) and (5-15) are then considered as properties of a given open quantum system, where $\overline{S}$ and $\underline{S}$ are constructed and utilised specifically for the given Hamiltonian [84]. Therefore, symmetrisation represents a *tool* rather than a *theory*.

[23] *cf.* Eq. (4-37)

As discussed in Section 4-3 a), the only exception for not using the Hermitian inner product has to be made for EPs, where the left-hand and right-hand states become self-orthogonal. Hence, for numerical calculations in the vicinity of an EPs the states should be normalised using the bi-orthogonal product (4-32) instead.

c) The characteristic polynomial

For finite-dimensional Hilbert spaces there exists another important property of symmetric and symmetrised systems, which is essential for the calculations in Chapter 6.

Consider the characteristic equation for the Schrödinger eigenvalue problem (2-39),

$$\det(\mathcal{H} - E\mathbb{1}) = 0\,.$$

With the cyclic property of the determinant, $\det(AB) = \det A \det B$ for square matrices A and B, one can easily show that[24]

$$\begin{aligned}\det(\mathcal{H} - E\mathbb{1})^* &= \det\left(\mathcal{H}^* - E^*\mathbb{1}\right)\\ &= \det\left(\mathcal{K}\mathcal{H}\mathcal{K}^{-1} - E^*\mathbb{1}\right)\det\left(\mathcal{U}\mathcal{U}^{-1}\right)\\ &= \det\left(\mathcal{U}\mathcal{K}\mathcal{H}\mathcal{K}^{-1}\mathcal{U}^{-1} - \mathcal{U}E^*\mathcal{U}^{-1}\right)\\ &= \det\left(\mathcal{H} - E^*\mathbb{1}\right)\end{aligned} \tag{5-31}$$

[24] Note that the identity $\det(\mathcal{U}\mathcal{U}^{-1}) = 1$ is inserted in the third step.

for any Hamiltonian $\mathcal{H}$ satisfying Eq. (5-24) with an anti-unitary operator $\mathcal{A} = \mathcal{U}\mathcal{K}$, *i.e.* $\mathcal{U}$ is unitary and $\mathcal{K}$ is the anti-linear complex-conjugation operator. That is, the complex conjugation acts only on the eigenvalues E, which shows that the coefficients of the characteristic polynomial are real.

A similar consideration can be made for symmetrised systems, where

$$\det(\mathcal{H} - E\mathbb{1})\det\left(\overline{S}\underline{S}\right) = \det\left(\overline{S}\mathcal{H}\underline{S} - \overline{S}E\underline{S}\right) = \det\left(\mathcal{H}^\dagger - E\overline{S}\underline{S}\right) \tag{5-32}$$

holds for any Hamiltonian $\mathcal{H}$ satisfying Eq. (5-14) or Eq. (5-15) with the symmetrisation operators $\overline{S}$ and $\underline{S}$; if they are invertible and satisfy $\overline{S}\underline{S} = \mathbb{1}$, then Eq. (5-32) is equivalent to the characteristic polynomial. Further, since $\det(A^\mathsf{T}) = \det A$ for all square matrices A, Eq. (5-32) corresponds to the same result as Eq. (5-31). Therefore, the coefficients of the characteristic polynomial are also real for a completely symmetrised system.

Due to the *fundamental theorem of algebra*, the spectra of operators with real characteristic polynomials consist only of complex-

conjugate pairs. In contrast to the symmetrisation conditions (5-14) and (5-15), which are merely sufficient conditions [129], the reality of the coefficients of the characteristic polynomial is a necessary condition to obtain a complex-conjugate spectrum [1; 170], as it ensures that the kernel of the symmetrisation operators are empty, thus guaranteeing their invertibility. The consequences of non-invertible symmetrisation operators with non-empty kernels are discussed in Section 5-4.

Note that real eigenvalues of a completely symmetric or symmetrised Hamiltonian are robust with respect to small perturbations under the assumption that the spectrum is non-degenerate [73]. The reason for this is quite simple: A real eigenvalue can become complex if and only if it bifurcates into a complex-conjugate pair, which is not possible if the spectrum is non-degenerate. Moreover, real eigenvalues also remain real under perturbations which leave the Hamiltonian quasi-Hermitian[25] [171]. Nevertheless, both the presence of an anti-linear symmetry, *i.e.* Eq. (5-24), and the properties (5-14) and (5-15) of a symmetrised system are insufficient to guarantee the completeness of the eigenstates [154].

[25] *cf.* Section 4-4 a)

d) Relation between anti-unitary symmetries and symmetrisation

The concepts of anti-unitary symmetries satisfying Eq. (5-24) and symmetrisation governed by Eqs. (5-14) and (5-15) seem to be contradictory. While Eq. (5-24) requires an anti-linear operator and relates the spectrum of $\mathcal{H}$ to its complex-conjugate spectrum, Eqs. (5-14) and (5-15) require a set of linear operators and relate the spectra of $\mathcal{H}$ and $\underline{S}\mathcal{H}^\dagger\overline{S}$. Because of Eqs. (5-31) and (5-32), the spectra of $\mathcal{H}$ and $\mathcal{H}^\dagger$ coincide, so that every symmetric Hamiltonian is symmetrisable if the symmetrisation operators are invertible and *vice versa*. Hence, the question arises whether there exist any further relations between symmetric and symmetrised Hamiltonians.

First, note that Eq. (5-26) closely resembles Eq. (5-15). In fact, for *complex symmetric* Hamiltonians, where $\mathcal{H}^\dagger = \mathcal{H}^*$, both equations coincide with $O^\dagger = \overline{S}$. To find a corresponding relation

for general Hamiltonians, one might recall that the combination of two anti-linear operators is again linear. Therefore, $\overline{S} = \overline{\mathcal{T}}\,\mathcal{A}$ with some anti-linear operator $\overline{\mathcal{T}}$. Equation (5-15) then yields

$$\overline{S}\mathcal{H} = \overline{\mathcal{T}}\,\mathcal{A}\mathcal{H} = \overline{\mathcal{T}}\,\mathcal{H}\,\mathcal{A} = \mathcal{H}^\dagger\overline{S}$$

under the assumption that Eq. (5-24) holds. The last equality can only be true if

$$\overline{\mathcal{T}}\,\mathcal{H} \stackrel{!}{=} \mathcal{H}^\dagger\overline{\mathcal{T}}\,. \tag{5-33}$$

In general, there is no universal anti-linear operator $\overline{\mathcal{T}}$ which satisfies Eq. (5-33) for arbitrary operators $\mathcal{H}$ because $\overline{\mathcal{T}}$ ought to be the operator for Hermitian conjugation. The reason why there cannot be such an operator can be ascribed to the fact that Hermitian conjugation requires the transpose of an operator. However, the action of transposition depends on the basis and is therefore no physical operation; thus, it cannot be expressed by a linear operator. If such an operator is assumed to exist, however, then it would be the symmetry connected with Hermiticity, *i.e.*

$$\left[\overline{\mathcal{T}}, \mathcal{H}\right] = 0$$

if $\mathcal{H}^\dagger = \mathcal{H}$.

For the specific case of a complex symmetric Hamiltonian, a complex conjugation is sufficient to satisfy Eq. (5-33), *i.e.* the complex-conjugation operator $\overline{\mathcal{T}} = \mathcal{K}$ is the desired anti-linear operator. In general cases, though, $\overline{\mathcal{T}}$ must be constructed for the Hamiltonian $\mathcal{H}$ specifically. To do so, one might exploit the fact that a non-Hermitian Hamiltonian possesses a bi-orthogonal basis.[26] Therefore, one can express the anti-linear operator in the form

[26] *cf.* Section 4-3

$$\overline{\mathcal{T}} = \sum_E |\overline{E}\rangle\mathcal{K}\langle\overline{E}| \tag{5-34}$$

which satisfies the relation Eq. (5-33).

For the sake of completeness, a corresponding anti-linear right-hand operator

$$\underline{\mathcal{T}} = \sum_E |\underline{E}\rangle \mathcal{K} \langle \underline{E}| \tag{5-35}$$

can be defined, which satisfies $\mathcal{H}\underline{\mathcal{T}} = \underline{\mathcal{T}}\mathcal{H}^\dagger$, so that $\underline{S} = \mathcal{A}\underline{\mathcal{T}}$ satisfies Eq. (5-14).

These discussions show that the symmetrisation of a Hamiltonian is equivalent to generalised $\mathcal{PT}$ symmetry with some linear operator $\mathcal{P}$ and some anti-linear operator $\mathcal{T}$ [100; 101; 172], where $\mathcal{P}$ and $\mathcal{T}$ are not necessarily the parity and the time-reversal operators as in Section 5-1. However, this requires $\overline{S}$ and $\underline{S}$ to be unitary; only then, $\mathcal{A}$ can be anti-unitary and is thus an actual symmetry according to *Wigner's theorem*.[27] Further, if $\mathcal{A}$ is involutory, then the operators (5-34) and (5-35) are inverse to each other because of Eq. (5-29). In fact, due to their Hermiticity, unitary symmetrisation operators also ought to be involutory.[28] Because of Eq. (5-29), this would also imply the equality of the left-hand and right-hand symmetrisation operators. The unitarity of such a metric operator — or the property of being an involution, respectively — is not really surprising, though, as it describes a discrete symmetry of the system in this case. For such an operator the set $\{\overline{S}, \mathbb{1}\}$ forms the cyclic group $\mathbb{Z}_2$ and $\overline{S}$ could thus be considered as a generalisation of the parity operator $\mathcal{P}$. However, while this argumentation remains rather abstract, the conditions imposed on such an operator are quite specific; though, the question if and if so under which conditions such unitary symmetrisation operators may in general exist is not further discussed within the scope of this thesis. This argument is, however, taken up again for the specific case of symmetric potentials in Section 5-3 e).

[27] *cf.* Appendix C

[28] Operators possessing two of the three properties of being Hermitian, unitary, or involutory also possess the third.

Last but not least, it should be noted that the symmetrisation conditions (5-14) and (5-15) also hold for arbitrary functions of $\mathcal{H}$. This is, for example, because

$$\overline{S}\mathcal{H}^2 = \mathcal{H}^\dagger \overline{S} \mathcal{H} = \left(\mathcal{H}^\dagger\right)^2 \overline{S},$$

and thus

$$\overline{S}\mathcal{H}^n = \left(\mathcal{H}^\dagger\right)^n \overline{S} \tag{5-36}$$

for $n \in \mathbb{N}$. As any function of $\mathcal{H}$ can be expanded into a Taylor series, Eq. (5-36) ensures that every order of this expansion is symmetrisable.

e) Symmetrisation operators

Real spectrum

Due to the property of transforming between left-hand and right-hand eigenstates, the symmetrisation operators can simply be written in terms of projection operators (*e.g.* see Refs. [83; 152]). If the spectrum of $\mathcal{H}$ is real, then a suitable choice of symmetrisation operators is given by

$$\overline{S} = \sum_E \overline{p}_E \, |\overline{E}\rangle\langle\overline{E}| \,, \tag{5-37}$$

$$\underline{S} = \sum_E \underline{p}_E \, |\underline{E}\rangle\langle\underline{E}| \,, \tag{5-38}$$

where the coefficients $\overline{p}_E$ and $\underline{p}_E$ are assumed to be constant.

The operators in Eqs. (5-37) and (5-38) can both be positive definite, *i.e.* $\overline{p}_E > 0$ and $\underline{p}_E > 0$, and simultaneously possess unit traces, *i.e.* $\sum_E \overline{p}_E = 1 = \sum_E \underline{p}_E$. Thus, in a mathematical sense, Eqs. (5-37) and (5-38) are "density operators"[29] which are associated with the ensembles $\{\overline{p}_E, |\overline{E}\rangle\}$ and $\{\underline{p}_E, |\underline{E}\rangle\}$. The corresponding time evolutions are governed by

[29] *e.g.* see Ref. [173]

$$\mathrm{i}\frac{\mathrm{d}\overline{S}}{\mathrm{d}t} = \left[\mathcal{H}^\dagger \overline{S} - \overline{S}\mathcal{H}\right], \tag{5-39}$$

$$\mathrm{i}\frac{\mathrm{d}\underline{S}}{\mathrm{d}t} = \left[\mathcal{H}\underline{S} - \underline{S}\mathcal{H}^\dagger\right] \tag{5-40}$$

which can be considered as *generalised* von Neumann equations. If the Hamiltonian is left-hand and right-hand symmetrised by the symmetrisation operators (5-37) and (5-38), then Eqs. (5-39)

and (5-40) vanish due to the symmetrisation conditions (5-14) and (5-15), respectively, so that $|\overline{S}|^2$ and $|\underline{S}|^2$ are conserved.

Another possible choice of the coefficients in Eqs. (5-37) and (5-38) is given by $\overline{p}_E = \underline{p}_E = \sqrt{p_E}$, where $p_E \geq 0$ and $\sum_E p_E = 1$. Then,

$$\underline{S}\overline{S} = \sum_E p_E \, |\underline{E}\rangle\langle\overline{E}| \tag{5-41}$$

is also a "density operator" with respect to the bi-orthogonal product (4-32). Its time evolution is governed by the von Neumann equation

$$\mathrm{i}\frac{\mathrm{d}\underline{S}\overline{S}}{\mathrm{d}t} = \left[\mathcal{H}, \underline{S}\overline{S}\right],$$

i.e. $|\underline{S}\overline{S}|^2$ is also conserved if the Hamiltonian is symmetrised because of Eq. (5-28).

All of these choices are generalisations of the Hermitian case, in which left-hand and right-hand eigenstates coincide, depending only on the inner product one relies on. For a Hermitian system either the operators (5-37) and (5-38) or the operator (5-41) correspond to the usual definition of the density operator, whereas the respective other choice must be considered unphysical due to the coefficients being either squares or square roots of the probability coefficients, respectively. However, whether or not any of these operators is, in the end, physically meaningful solely depends on the probabilities and their interpretations. Since the Hermitian inner product with respect to the right-hand states is considered to be physical in this thesis, $\overline{S}$ defined by Eq. (5-37) can be considered as the distinguished extension of the usual density operator from QM, which is diagonal with respect to the right-hand eigenstates. Further, it corresponds to a mixed state reflecting the incomplete knowledge about the state of the non-Hermitian open quantum system.[30]

[30] *cf.* Section 4-6

Although the classification as density operators may be of some mathematical interest, from a physical point of view the choices $\overline{p}_E = \underline{p}_E = \sqrt{E}$ with the energies E of the corresponding states seem to be more natural. In particular, because they are in agreement with Eqs. (5-16) and (5-17) known from supersymmetric

non-Hermitian quantum systems. However, in contrast to supersymmetric systems, in general $\underline{S}\overline{S} \neq \mathcal{H}$. Hence, it might also be reasonable to use the principle of *Occam's razor* according to which the simplest solution might also be the best. Here, the simplest solution corresponds to the case without any prefactors, *i.e.* $\overline{p}_E = \underline{p}_E = 1$, so that Eqs. (5-16) and (5-17) are reduced to

$$\overline{S}\,|\underline{E}\rangle = |\overline{E}\rangle\,,$$
$$\underline{S}\,|\overline{E}\rangle = |\underline{E}\rangle\,.$$

This convention is used in the remaining thesis and can also be found in the majority of the mathematical literature on quasi-Hermiticity.[31]

[31] *e.g.* see Ref. [86] for an overview

By considering the time derivative of the expectation value of $\overline{S}$ with respect to a right-hand state, that is

$$\mathrm{i}\frac{\mathrm{d}}{\mathrm{d}t}\langle\underline{E}|\overline{S}|\underline{E}\rangle = \langle\underline{E}|\overline{S}\mathcal{H} - \mathcal{H}^\dagger\overline{S}|\underline{E}\rangle + \mathrm{i}\langle\underline{E}|\frac{\mathrm{d}\overline{S}}{\mathrm{d}t}|\underline{E}\rangle\,, \tag{5-42}$$

one finds that $\langle\underline{E}|\overline{S}|\underline{E}\rangle$ is a conserved quantity if Eq. (5-15) holds.[32] The statement (5-42) holds in general [83] and is thus also applicable if the spectrum is not entirely real.

[32] *cf.* Eq. (5-39)

Finally, it should be noted that symmetrisation operators are not unique [87; 174]. In fact, one can construct an infinite number of symmetrisation operators for one and the same Hamiltonian [175]. The specific choice of the symmetrisation operators is, however, not important, as long as the Hamiltonian and the boundary conditions are the same. Since any operators of the form (5-37) and (5-38) satisfy Eqs. (5-14) and (5-15), which are necessary for the properties of $\mathcal{H}$, different choices of the coefficients can be considered as different gauges.

Complex spectrum

If the spectrum is not entirely real, then the complex eigenvalues must arise in complex-conjugate pairs, as long as the Hamiltonian is symmetrised. The corresponding symmetrisation operators are generalisations of the operators (5-37) and (5-38) [152; 174],

$$\overline{S} = \sum_{E_0} |\overline{E_0}\rangle\langle\overline{E_0}| + \sum_{E_\pm} \left(|\overline{E_+}\rangle\langle\overline{E_-}| + |\overline{E_-}\rangle\langle\overline{E_+}|\right), \tag{5-43}$$

$$\underline{S} = \sum_{E_0} |\underline{E_0}\rangle\langle\underline{E_0}| + \sum_{E_\pm} \left(|\underline{E_+}\rangle\langle\underline{E_-}| + |\underline{E_-}\rangle\langle\underline{E_+}|\right), \tag{5-44}$$

where E_0 and $E_\pm$ run over all real and complex-conjugate energies, respectively.[33] Their evolution is still governed by Eqs. (5-39) and (5-40). The terms corresponding to the complex part of the spectrum are non-diagonal and traceless; hence, $\overline{S}$ and $\underline{S}$ are indefinite. For this reason, there occur states of the Hamiltonian with negative norm, which must to be considered unphysical [84] and may be excluded by *superselection rules* [176]. Nevertheless, the occurrence of symmetric pairs of complex eigenvalues can be considered physical in general, as they can be understood as emission and absorption phenomena [59].

[33] The coefficients of the dyadic products are dropped according to the discussions before.

Symmetric potentials

One may assume that there exists an operator $\mathcal{P}$ with the property

$$\mathcal{P}^2 |E\rangle = \mathrm{e}^{\mathrm{i}\varphi_n} |E\rangle \,, \tag{5-45}$$

where $|E\rangle$ can be any eigenstate of a bi-orthogonal basis. Equation (5-45) defines a parity operator which can be chosen such that $\mathcal{P}^2 = \mathbb{1}$, *i.e.* $\mathcal{P}$ is involutory. One could now conclude that $\underline{S}\overline{S} = \mathcal{P}^2$ and thus

$$\mathcal{P} = \overline{S} = \underline{S} = \mathcal{P}^{-1} \,. \tag{5-46}$$

This is in agreement with Eq. (5-28) and does not imply that the Hamiltonian $\mathcal{H}$ must commute with $\mathcal{P}$.

Equation (5-46) seems to be a distinguished extension of the Hermitian case, where the symmetrisation operators (5-37) and (5-38) also coincide due to the lack of bi-orthogonality. Yet, in a non-Hermitian quantum system there does not in general exist such a pair of symmetrisation operators obeying $\overline{S} = \underline{S}$. One may however find a system in which the states obey $\mathcal{P}|\underline{E}\rangle \propto |\overline{E}\rangle$, *i.e.* the left-hand side equals a left-hand eigenstate up to a phase factor. In this

case, the parity operator $\mathcal{P}$ is expected to satisfy both Eqs. (5-14) and (5-15). In combination with an anti-linear operator $\mathcal{T}$, this corresponds to $\mathcal{PT}$ symmetry. As discussed in Section 5-1, a $\mathcal{PT}$-symmetric Hamiltonian must possess a real symmetric and an anti-symmetric imaginary potential, which causes the symmetry in the states assumed above and also ensures that the spectrum is complex-conjugate.

An interesting aspect of this discussion is that the parity operator $\mathcal{P}$ defined by Eq. (5-46) is independent of the eigenstates of the Hamiltonian; this certainly is not the case for the symmetrisation operators defined by Eqs. (5-43) and (5-44). Therefore, $\mathcal{PT}$ symmetry seems to be a distinguished choice and is thus applicable to almost every kind of physical system. Nevertheless, the requirement of exactly symmetric potentials can be demanding, especially in the presence of perturbations in experiments.[34]

[34] *cf.* Chapter 8

Another example, in which symmetrisation operators are independent of the eigenstates, is given by the differential operators discussed in Section 5-2 b). Similar to the $\mathcal{PT}$-symmetric case, they allow for complex-conjugate spectra but with arbitrary complex potentials. However, such potentials do not always allow for a physical interpretation[35] and the corresponding symmetrisation operators are unbound.

[35] *cf.* Section 5-5

As stated in Section 5-3, this discussion again clearly shows that symmetrisation should not be thought of as a general theory, but as a concept which is applied to specific physical systems; that is, the symmetrisation operators defined in Eqs. (5-43) and (5-44) are constructed specifically for a particular Hamiltonian.

5-4 Semi-symmetrisation

Until now, only such cases were considered in which the symmetrisation operators are invertible, *i.e.* the corresponding metric is positive semi-definite. In the following, however, the symmetrisation operators are non-invertible. Nevertheless, the results discussed in Section 5-3 remain valid because the invertibility of the symmetrisation operators was not a requirement.[36]

[36] in contrast to quasi-Hermiticity, *cf.* Section 4-4 a)

A similar scenario is described by Nixon and Yang in Ref. [129], however, with the distinction that their symmetrisation operators are required to be *differential operators*; this imposes additional assumptions on the system, which can be understood with SUSY chains.[37] Symmetrisation, in contrast, does not require the specific type of potential (5-22) proposed by Wadati in Ref. [144], which is not physical in all types of systems. To make this clear, a discussion on different types of complex potentials follows in Section 5-5.

[37] *cf.* Section 5-2 b)

Now, consider a left-hand symmetrisation operator $\overline{S}$ with zero determinant, *i.e.* $\det \overline{S} = 0$. Clearly, there is no inverse of $\overline{S}$ and its kernel is non-empty. Nevertheless, it is still possible to satisfy Eq. (5-15) if one demands that the elements in the kernel of $\overline{S}$ are exclusively right-hand eigenstates $|\underline{E}\rangle$ of $\mathcal{H}$. For these states, Eq. (5-27) holds trivially as[38] $\overline{S}\,|\underline{E}\rangle = 0$. However, the corresponding eigenvalues are neither real nor part of a complex-conjugate pair; they form isolated complex resonances in the spectrum of $\mathcal{H}$.

[38] *cf.* Eq. (5-43)

Since Eq. (5-28) still holds, $\underline{S}\overline{S}$ can be considered as an identity with respect to those right-hand eigenstates of $\mathcal{H}$ which are not in the kernel of $\overline{S}$. In contrast, it acts as an "annihilation operator" for states from the kernel of $\overline{S}$. Although $\underline{S}$ is not the inverse of $\overline{S}$, they are *semi-inverse*. The semi-inverse B of A is defined by the condition $ABA = A$ [177], *i.e.*

$$\overline{S}\underline{S}\overline{S}\,|\underline{E}\rangle = \overline{S}\underline{S}\left|\overline{E^*}\right\rangle = \overline{S}\,|\underline{E}\rangle \ .$$

Hence, such a system is called *semi-symmetrised*.

Semi-symmetrised operators possess the properties of symmetrised operators on a subspace spanned by eigenstates of the Hamiltonian which are not in the kernels of the symmetrisation operators. The dimension of this subspace is given by rank $\overline{S}$. With respect to the definition (5-43), it is obvious that for any left-hand eigenstate excluded from the sums, the corresponding right-hand eigenstate — because of bi-orthogonality — must be part of the kernel of the left-hand symmetrisation operator. The same applies to the definition (5-44) of the right-hand symmetrisation operator. Since the rank of the symmetrisation operators can take any value between 1 and the full rank, any operator with a discrete number of real eigenvalues can be considered as semi-symmetrised,[39] even

[39] That is, if all the requirements from Section 5-3 are satisfied.

if the spectrum is not entirely discrete. For this reason, one can apply symmetrisation to a specific subspace, for example obtained by means of some approximation,[40] without the need to care for the entirety of the spectrum. A specific example of a physical system that is solely semi-symmetrisable is given by the two-mode system with balanced gain and loss for generalised complex potentials, which is discussed in Section 6-1 c).

[40] *cf.* Section 6-4

An illustrative example

To conclude this section, the previous discussions on semi-symmetrisation are illustrated with an example of a non-invertible symmetrisation operator $\overline{S}$ for the non-Hermitian matrix

$$\mathcal{H} = \begin{pmatrix} 3 & 0 & 0 \\ \mathrm{i} & 1 & 0 \\ 0 & 0 & \mathrm{i} \end{pmatrix}. \tag{5-47}$$

The eigenvalues of the matrix (5-47) and their corresponding non-normalised right-hand eigenvectors read

$$E_1 = 3\,, \quad |\underline{E_1}\rangle = (2, \mathrm{i}, 0)^{\mathsf{T}}\,, \tag{5-48}$$

$$E_2 = 1\,, \quad |\underline{E_2}\rangle = (0, 1, 0)^{\mathsf{T}}\,, \tag{5-49}$$

$$E_3 = \mathrm{i}\,, \quad |\underline{E_3}\rangle = (0, 0, 1)^{\mathsf{T}}\,. \tag{5-50}$$

A suitable left-hand symmetrisation operator is given by

$$\overline{S} = \begin{pmatrix} 1 & \mathrm{i} & 0 \\ -\mathrm{i} & 2 & 0 \\ 0 & 0 & 0 \end{pmatrix}, \tag{5-51}$$

so that Eq. (5-15) is satisfied,

$$\overline{S}\mathcal{H} = \begin{pmatrix} 2 & \mathrm{i} & 0 \\ -\mathrm{i} & 2 & 0 \\ 0 & 0 & 0 \end{pmatrix} = \mathcal{H}^{\dagger}\overline{S}\,.$$

Note that the matrix (5-51) is not invertible because $\det \overline{S} = 0$.

Obviously, not all eigenvectors in Eqs. (5-48) to (5-50) are orthogonal with respect to the ordinary inner product. The eigenvectors of the real eigenvalues are, however, orthogonal with respect to the modified inner product

$$\left\langle E_2 \middle| \overline{S} E_1 \right\rangle = \frac{1}{2} \begin{pmatrix} 0 \\ 1 \\ 0 \end{pmatrix} \cdot \begin{pmatrix} 1 \\ 0 \\ 0 \end{pmatrix} = 0 \,,$$

whereas $\langle E_2 | E_1 \rangle = \mathrm{i}$. The eigenvector $|E_3\rangle$ of the complex eigenvalue is in the kernel of $\overline{S}$, *i.e.* $\overline{S}\,|E_3\rangle = 0$, so that the original eigenvalue equation

$$\mathcal{H}\,\overline{S}\,|E_3\rangle = E_3^* \overline{S}\,|E_3\rangle$$

holds trivially.

The corresponding right-hand symmetrisation operator can be found similarly,

$$\overline{S} = \begin{pmatrix} 2 & -\mathrm{i} & 0 \\ \mathrm{i} & 1 & 0 \\ 0 & 0 & 0 \end{pmatrix}, \tag{5-52}$$

so that Eq. (5-14) is satisfied,

$$\mathcal{H}\,\underline{S} = \begin{pmatrix} 6 & -3\mathrm{i} & 0 \\ 3\mathrm{i} & 2 & 0 \\ 0 & 0 & 0 \end{pmatrix} = \mathcal{H}^\dagger \overline{S} \,,$$

and

$$\overline{S}\,\underline{S} = \begin{pmatrix} 1 & 0 & 0 \\ 0 & 1 & 0 \\ 0 & 0 & 0 \end{pmatrix}. \tag{5-53}$$

It is easy to check that the matrices (5-51) and (5-52) transform between the left-hand and right-hand eigenvectors of the real eigenvalues, respectively.

Note that the choices for the matrices $\overline{S}$ and $\underline{S}$ are not unique and not all of them are semi-inverses as in Eq. (5-53). For example,

the matrix

$$\overline{S}' = \begin{pmatrix} 1 & -\mathrm{i} & 0 \\ \mathrm{i} & -2 & 0 \\ 0 & 0 & 0 \end{pmatrix},$$

also satisfies Eq. (5-15), but it is not semi-inverse to Eq. (5-52).

5-5 Physical complex potentials

In Sections 5-2 to 5-4 different concepts for obtaining complex-conjugate — physical — spectra in non-Hermitian quantum systems were discussed. Apart from the mathematical considerations, it is important to consider the types of potentials which can be treated with these concepts. $\mathcal{PT}$ symmetry, for example, allows for arbitrary real and imaginary potentials, as long as they are real symmetric and imaginary anti-symmetric [178].

The Wadati-type potentials of the form (5-22), on the other hand, do not require such symmetries. However, they do not always allow for a physical interpretation, which makes them unsuitable for describing real, open physical systems via complex potentials. An example of a system which yields a physical interpretation of such potentials is given by the pressure waves in Ref. [139]. Yet, in the case of BECs which are localised in distinct potential wells,[41] a differential imaginary potential cannot be interpreted directly. This is because for BECs the imaginary part of the potential describes in and out-coupling of particles; thus, a Wadati-type potential would

[41] *e.g.* see Ref. [179]

1) describe in and out-coupling of particles in the same well,

2) require gain and loss to depend locally on the changes of the real potential.

Both of these reasons make such potentials hard to interpret physically and they can also hardly be realised in a quantum system.[42]

[42] *cf.* Ref. [180] and references therein

In this thesis the focus lies on open quantum systems described by Hamiltonians with complex multi-well potentials, which effectively represent gain and loss in each well, respectively. In general,

such systems correspond to discrete matrix models, *i.e.* the operators are represented by finite-dimensional matrices.[43] Further, the Hamiltonians of such models are *complex symmetric*, *i.e.* $\mathcal{H}^{\mathsf{T}} = \mathcal{H}$, thus being real apart from their diagonal. This involves no loss of generality, since any matrix can be transformed into a complex symmetric form [89] and the set of bi-orthogonal states of a complex symmetric matrix is complete.[44]

[43] *cf.* Appendix E

[44] *cf.* Section 4-5 b)

For such systems Eq. (5-24) coincides with the Hermiticity condition if $\mathcal{A} = \mathcal{K}$ because

$$[\mathcal{H}, \mathcal{K}] = \left[\mathcal{H} - \mathcal{H}^*\right]\mathcal{K} = \left[\mathcal{H} - \mathcal{H}^\dagger\right]\mathcal{K} = 0\,.$$

Thus, any anti-unitary symmetry with $\mathcal{A} \propto \mathcal{K}$ can be considered as a generalisation of Hermiticity.[45]

[45] *cf.* Section 5-3 d)

Another interesting property arises for symmetrisation in the context of complex potentials. If one considers Eq. (5-15) as a property of a given system with an imaginary potential, then Eq. (5-14) is a property of the same system with the negative imaginary potential. In other words, if the system is symmetrised from both sides simultaneously, then there exist two suitable gain-loss distributions, each corresponding to one symmetrisation operator. The inversion of gain and loss corresponds to time reversal, so that

$$\mathcal{H} = \mathcal{T}\mathcal{H}^\dagger\mathcal{T} = \mathcal{H}^{\mathsf{T}} \tag{5-54}$$

with the involutory time-reversal operator $\mathcal{T}$. By plugging this into Eq. (5-15) and comparing the result to Eq. (5-14), one finds

$$\underline{S} = \mathcal{T}\bar{S}\mathcal{T} = \bar{S}^*\,. \tag{5-55}$$

This is a consequence of the dual character of $\mathcal{H}$ and $\mathcal{H}^\dagger$, which in the case of complex symmetric Hamiltonians is defined with respect to the complex conjugate rather than the Hermitian adjoint. An interesting discussion on this duality can be found in Ref. [151], where it is shown that the left-hand eigenstates of a quantum system evolve backwards in time compared to the right-hand eigenstates and *vice versa*.

Note that the properties (5-54) and (5-55) are consistent with both choices of the inner product discussed in Section 4-6 a). Further, Eq. (5-55) can also be extracted from the general definitions (5-18) to (5-21).

a) Numerical calculation of symmetrisation operators

While Eqs. (5-14) and (5-15) can be solved analytically in simple cases,[46] they are either hard or even unfeasible to treat in larger and more complicated systems; it may even be entirely impossible in non-linear quantum systems.[47] Hence, it is reasonable to resort to numerical calculations. To solve Eqs. (5-14) and (5-15) numerically, it is useful to rewrite them as a matrix equation of the form $C \cdot s = 0$, where s contains all components of the respective symmetrisation operator and C is a coefficient matrix. In the following, the coefficient matrices for discrete left-hand and right-hand symmetrisation operators are derived.

[46] *cf.* Chapter 6

[47] *cf.* Chapter 7

For a quantum system described by a discrete matrix Hamiltonian $\mathcal{H} \in \mathbb{C}^{N\times N}$, the left-hand symmetrisation condition (5-15) can be written as

$$\begin{pmatrix} \sum_n \left[\mathcal{H}_{n1}\overline{S}_{1n} - \mathcal{H}_{n1}^*\overline{S}_{n1}\right] & \cdots & \sum_n \left[\mathcal{H}_{nN}\overline{S}_{1n} - \mathcal{H}_{n1}^*\overline{S}_{nN}\right] \\ \vdots & \ddots & \vdots \\ \sum_n \left[\mathcal{H}_{n1}\overline{S}_{Nn} - \mathcal{H}_{nN}^*\overline{S}_{n1}\right] & \cdots & \sum_n \left[\mathcal{H}_{nN}\overline{S}_{Nn} - \mathcal{H}_{nN}^*\overline{S}_{nN}\right] \end{pmatrix} = 0 \tag{5-56}$$

with $n = 0, \ldots, N-1$. Equation (5-56) can be understood as the N^2 determining equations for the matrix elements of the left-hand symmetrisation operator $\overline{S}$. They can also be written as the matrix equation

$$\overline{C} \cdot \overline{s} = 0\,, \tag{5-57}$$

where $\overline{s}_{Nk+l} = \overline{S}_{kl}$ is the vector of all elements of $\overline{S}$ and

$$\overline{C}_{Nl+k,Nl+n} = \mathcal{H}_{nk}\,, \tag{5-58}$$

$$\overline{C}_{Nl+k,Nn+k} = -\mathcal{H}_{nl}^* \tag{5-59}$$

with $k, l = 0, \ldots, N-1$; hence, for $n = (Nl-k)/(N-1)$ the coefficient reads

$$\overline{C}_{Nl+k,Nn+k} = \mathcal{H}_{nk} - \mathcal{H}^*_{kl} \,.$$

Analogously, by using Eq. (5-14) one finds

$$\underline{C} \cdot \underline{s} = 0 \,, \tag{5-60}$$

where $\underline{s}_{Nk+l} = \underline{S}_{kl}$ contains the matrix elements of the right-hand symmetrisation operator. The elements of the corresponding coefficient matrix are then given by

$$\underline{C}_{Nl+k,Nn+k} = \mathcal{H}_{ln} \,, \tag{5-61}$$

$$\underline{C}_{Nl+k,Nl+n} = -\mathcal{H}^*_{kn} \,. \tag{5-62}$$

The coefficient matrices can easily be obtained numerically by initiating a pair of zero matrices followed by looping over the indices n, k, and l and adding Eqs. (5-58) and (5-59) and Eqs. (5-61) and (5-62) to the respective matrix elements. To check whether a Hamiltonian is symmetrisable or not, it is sufficient to calculate the determinant of the coefficient matrix of the symmetrisation operator; Eqs. (5-57) and (5-60) yield solutions only if $\det \overline{S} = 0$ and $\det \underline{S} = 0$, respectively. In these cases, Eqs. (5-57) and (5-60) can be solved by numerical algorithms provided, for example, by the ARPACK library [181; 182].

Linear systems

6

In the following, the concept of symmetrisation discussed in Section 5-3 is applied to complex multi-mode potentials, where the imaginary part describes gain and loss in each well, respectively, as shown in Fig. 6-1. Hence, the Schrödinger equation (2-39) must be solved for linear but non-Hermitian discrete Hamiltonians, for which the foundations were laid in Chapter 4; this specifically means that the corresponding Hilbert spaces are finite-dimensional. Further, extended potentials, which in general correspond to infinite-dimensional Hilbert spaces, are briefly considered in Section 6-4. The generalisation of symmetrisation to non-linear non-Hermitian systems is discussed in Chapter 7.

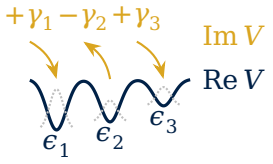

Figure 6-1: A multi-well potential with gain and loss

6-1 Two-mode systems

The most simple discrete, open quantum systems are given by non-Hermitian two-mode matrix models. In such systems the eigenvalues and eigenstates of the Hamiltonian can easily be calculated explicitly. Therefore, a two-mode matrix model provides a suitable basis to start investigating the occurrence of balanced gain and loss in open quantum systems.

Two-mode systems are well studied both for $\mathcal{PT}$-symmetric potentials [106; 183–187] and recently also for potentials with arbitrary gain and loss [188; 189]. The most general symmetrisation operator for two-dimensional systems is also known already [88; 155]. In the following, the two-mode system is discussed yet again but with respect to symmetrisation. Though, a short overview of the $\mathcal{PT}$-symmetric two-mode model is inevitable in this context.

In contrast to the — in general infinite-dimensional — matrix representations discussed in Appendix B-2, the matrix models considered here correspond to the finite-dimensional *tight-binding approximation*[I] of the Schrödinger equation in a complex multi-

[I] *cf.* Appendix E

well potential as shown in Fig. 6-1 [190–192]. Such a matrix model can, for example, also be understood as the mean-field limit of a many-body system,[2] which is a suitable approximation even in the presence of a complex potential [183; 194; 195].

[2] *e.g.* see [193]

a) $\mathcal{PT}$-symmetric two-mode model

Probably the simplest $\mathcal{PT}$-symmetric Hamiltonian is given by

$$\mathcal{H} = \begin{pmatrix} i\gamma & -J \\ -J & -i\gamma \end{pmatrix} \tag{6-1}$$

which describes an open two-mode system of the form shown in Fig. 6-1. The two modes are coupled by the parameter J, which in the following serves as a unit for the energies.[3] The gain-loss parameter γ corresponds to an anti-symmetric imaginary potential which effectively describes interactions of the two-mode system with an environment.

[3] It could thus effectively be eliminated by the choice $J = 1$.

It is immediately clear that the Hamiltonian (6-1) satisfies the condition (5-1) for $\mathcal{PT}$ symmetry, where $\mathcal{P}$ corresponds to the transposition with respect to the second diagonal and $\mathcal{T}$ is just a complex conjugation. The eigenvalues are readily obtained,

$$\frac{E_\pm}{J} = \pm\sqrt{1 - \left(\frac{\gamma}{J}\right)^2}\,. \tag{6-2}$$

For $|\gamma| < J$ the square root yields real values, so the $\mathcal{PT}$ symmetry is *exact*. In this region the gain at the in-coupling mode, the loss at the out-coupling mode, and the current between them are *balanced*. However, for $|\gamma/J| > 1$ the eigenvalues become complex-conjugate, which indicates that the $\mathcal{PT}$ symmetry is now *broken*. This characteristic scenario is shown in Fig. 6-2 and illustrates all features of $\mathcal{PT}$-symmetric spectra in a compact manner.

Figure 6-2 is an example of a *spontaneous symmetry breaking*. The physical reason behind it is that the two-mode system is unable to maintain the current[4] which is required to keep the two modes in balance. That is, the energy eigenvalues become complex and thus the norms of their corresponding states are no longer conserved

[4] Depending on the system, this can be either an exchange of energy or matter.

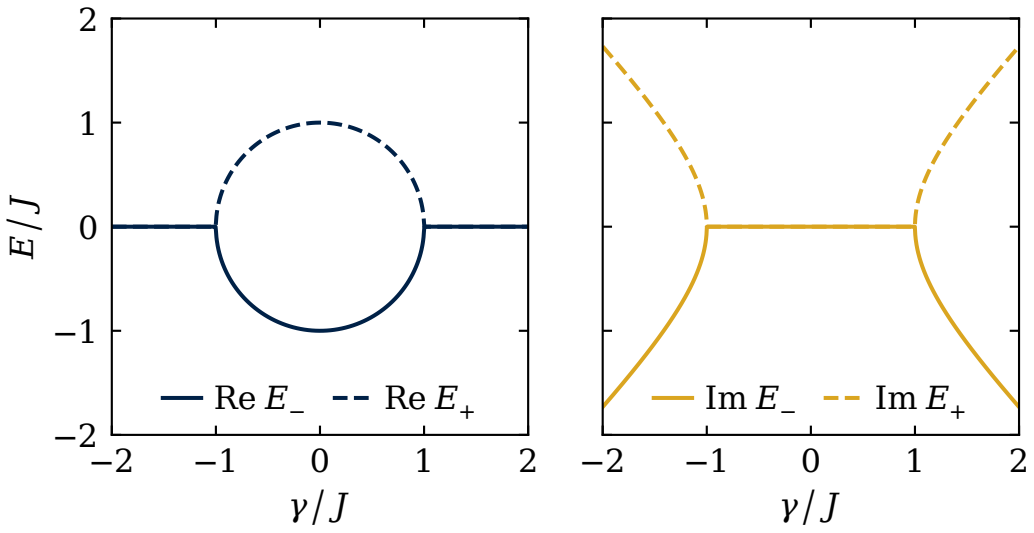

Figure 6-2: Eigenvalues of the $\mathcal{PT}$-symmetric two-mode model (6-1) as a function of the gain-loss parameter γ. If the gain-loss strength is small enough the two-mode model is exactly $\mathcal{PT}$-symmetric, *i.e.* the eigenvalues are real. If the interaction with the environment increases the $\mathcal{PT}$ symmetry is broken and the eigenvalues become complex-conjugate.

in time; that is, the modes are no longer time-reversal invariant. The $\mathcal{PT}$-symmetric and the broken $\mathcal{PT}$-symmetric solutions form a *tangent bifurcation*, *i.e.* they are connected by a *branch point* created by the complex square root function (6-2) at $|\gamma/J| = 1$. This corresponds to an EP of *second order* as introduced in Section 4-3 a); in fact, the topology shown in Fig. 4-1 is exactly that of the square root function in the complex plane.

The normalised time-independent eigenstates which correspond to the solutions (6-2) for $|\gamma/J| \leq 1$ read

$$\psi_{\pm}(0) = \frac{1}{\sqrt{2}} \begin{pmatrix} \mathrm{e}^{\mathrm{i}\varphi} \\ \mathrm{e}^{-\mathrm{i}\varphi} \end{pmatrix}, \tag{6-3}$$

where

$$\varphi = -\frac{1}{2} \arcsin\left(\frac{\gamma}{J}\right). \tag{6-4}$$

As long as the eigenvalues $E_{\pm}$ are real, the time-dependent eigenstates

$$\psi_{\pm}(t) = \psi_{\pm}(0)\, \mathrm{e}^{-\mathrm{i}E_{\pm}t}$$

are steady states and their norms are conserved. Moreover, the norms of the single modes are always balanced in the $\mathcal{PT}$-symmetric regime, *i.e.* $|\psi_{\pm}^{(1)}|^2 = |\psi_{\pm}^{(2)}|^2$. Though, if the energy eigenvalues

become complex, their imaginary parts cause the norms to increase or decrease in time.

Note that the solutions (6-3) can also be extended into the broken $\mathcal{PT}$-symmetric regime [179]. Although real values of the phase (6-4) no longer exist for $|\gamma/J| > 1$, the arcus sine function can be extended into the complex plane via

$$\arcsin(\hat{\gamma}) = -\mathrm{i}\ln\left(\mathrm{i}\hat{\gamma} \pm \sqrt{1-\hat{\gamma}^2}\right) = \frac{\pi}{2} - \mathrm{i}\ln\left(\hat{\gamma} \pm \sqrt{\hat{\gamma}^2-1}\right),$$

where $\hat{\gamma} = \gamma/J \in \mathbb{R}$ is the "normalised" gain-loss parameter. Then, the components of Eq. (6-3) read

$$\psi_{\pm}^{(1)}(0) = \sqrt{\hat{\gamma} \pm \sqrt{\hat{\gamma}^2-1}}\frac{\mathrm{e}^{-\mathrm{i}\frac{\pi}{4}}}{\sqrt{2}},$$
$$\psi_{\pm}^{(2)}(0) = \sqrt{\hat{\gamma} \mp \sqrt{\hat{\gamma}^2-1}}\frac{\mathrm{e}^{\mathrm{i}\frac{\pi}{4}}}{\sqrt{2}},$$

i.e. the norms of the time-independent states are modified.

b) Steady states in non-Hermitian two-mode systems

[5] *cf.* Eq. (6-1)

Now, consider the more general[5] matrix Hamiltonian

(6-5)
$$\mathcal{H} = \begin{pmatrix} \epsilon + \mathrm{i}\gamma(1+\delta) & -J \\ -J & -\epsilon - \mathrm{i}\gamma(1-\delta) \end{pmatrix},$$

which is complex symmetric for $J \in \mathbb{R}$. Due to the gauge freedom of the energy, the three real parameters — the on-site potential parameter ϵ, the gain-loss parameter γ, and the asymmetry parameter δ — are sufficient to describe any two-dimensional, complex symmetric matrix Hamiltonian. The parameter δ causes the potential to be asymmetric, *i.e.* for $\delta = 0$ the diagonal of Eq. (6-5) is anti-symmetric, while for $\delta \neq 0$ the imaginary part becomes asymmetric.

The characteristic polynomial of the Hamiltonian (6-5) reads

(6-6)
$$\det(\mathcal{H} - E\mathbb{1}) = E^2 + \mathrm{i}2\gamma\delta E - J^2 - \gamma^2\delta^2 - (\epsilon + \mathrm{i}\gamma)^2 \stackrel{!}{=} 0\,.$$

To determine whether there exist any steady states, one may start by assuming that Eq. (6-6) yields a real solution $E \in \mathbb{R}$. Then, Eq. (6-6) can be divided into its real and imaginary parts,

$$E^2 - \left[J^2 + \epsilon^2 - \gamma^2\left(1 - \delta^2\right)\right] = 0\,, \tag{6-7}$$

$$\gamma(\epsilon - \delta E) = 0\,. \tag{6-8}$$

Equation (6-7) yields two non-trivial real solutions if the term in the square brackets is positive. This is always the case if $|\gamma|$ is small enough in comparison with the transition strength J and the on-site potential parameter $|\epsilon|$. Physically, this means that the interactions between the two-mode system and its environment must be sufficiently weak. However, Eq. (6-8) must also be satisfied. In fact, Eq. (6-8) completely determines the type of the system.

To give an example, for $\gamma = 0$ the Hamiltonian (6-5) is Hermitian, so its eigenvalues are necessarily real. In this case, Eq. (6-7) yields two real solutions and Eq. (6-8) holds independently. For $\gamma \neq 0$, however, the Hamiltonian (6-5) is non-Hermitian. Yet, in this case there also exists a distinguished type of system: With $\delta = 0$ the potential is anti-symmetric and Eq. (6-8) requires either ϵ or γ to be zero as well. For $\epsilon = 0$ the real potential vanishes,[6] so that the Hamiltonian corresponds to Eq. (6-5), which is $\mathcal{PT}$-symmetric, and possesses two real solutions if $|\gamma/J| < 1$ as discussed in Section 6-1 a).

[6] *i.e.* the two sites become equivalent energetically

If all three parameters ϵ, γ, and δ are non-zero, the potential is always asymmetric and Eq. (6-8) yields only one solution. Therefore, there exists at most one stationary state of the Hamiltonian (6-5) with a real eigenvalue E. Thus, two stationary states can occur only in the trivial Hermitian case or if the system is $\mathcal{PT}$-symmetric. Therefore, the spectrum of the $\mathcal{PT}$-symmetric two-mode model is discussed in Section 6-1 a) for reference.

Note, however, that this behaviour is not restricted to discrete systems. If the two-mode model is replaced by a continuous system with a double-delta potential as in Appendix F, one finds that the number of steady states in an asymmetric extended potential is also limited in contrast to the $\mathcal{PT}$-symmetric case [185], for example. This can be seen by inspecting Eqs. (F-7) and (F-8): The left-hand

sides are independent of the distance a between the two delta peaks, while the right-hand sides are not. Therefore, a real-valued solution can exist only if a specific relation between ϵ_1, ϵ_2, γ_1, γ_2, and a is satisfied, where a takes the role of the coupling parameter J. The discussion on symmetrisation in spatially extended systems is continued in Section 6-4.

c) Two-mode models with arbitrary gain and loss

Although Sections 6-1 a) and 6-1 b) show that a non-$\mathcal{PT}$-symmetric Hamiltonian can possess only a single real eigenvalue, it is nevertheless worthwhile to explore the concept of symmetrisation introduced in Chapter 5 in this context; in particular, this provides an excellent application for semi-symmetrisation.

While the form (6-5) of a non-Hermitian two-mode Hamiltonian is suitable to describe perturbations from the $\mathcal{PT}$-symmetric Hamiltonian (6-1) with the parameter δ, in the following, the generic form

$$\mathcal{H} = \begin{pmatrix} \epsilon_1 + \mathrm{i}\gamma_1 & -J \\ -J & \epsilon_2 + \mathrm{i}\gamma_2 \end{pmatrix} \tag{6-9}$$

with $\epsilon_1 = \epsilon$, $\epsilon_2 = -\epsilon$, $\gamma_1 = \gamma(1+\delta)$, and $\gamma_2 = -\gamma(1-\delta)$ is used. Hence, the parameters ϵ_1 and ϵ_2 are not independent and only their difference is physically meaningful.

The reality of the characteristic polynomial of the Hamiltonian (6-9) allows for checking efficiently whether the Hamiltonian is symmetrisable or not. This evaluation yields the two conditions

$$\gamma_1 + \gamma_2 = 0\,, \tag{6-10}$$

$$\epsilon_1\gamma_2 + \gamma_1\epsilon_2 = 0\,. \tag{6-11}$$

Of these, Eq. (6-10) is satisfied only for an anti-symmetric imaginary potential and thus by a $\mathcal{PT}$-symmetric Hamiltonian. Since the reality of the characteristic polynomial is a sufficient condition for a real or complex-conjugate spectrum,[7] one can conclude that there are no asymmetric potentials with entirely real spectra, which is in

[7] *cf.* Section 5-3 c)

agreement with the results of Section 6-1 b). The symmetrisation condition (5-15), however, is not a sufficient condition; thus, it might be possible to obtain a system with at least some real eigenvalues, that is. Therefore, the symmetrisation or semi-symmetrisation of the Hamiltonian (6-9) is investigated in the following.

In two-dimensional spaces the symmetrisation operator may conveniently be written in terms of the Pauli matrices (2-19) via

$$\overline{S} = \sum_{n=0}^{3} \overline{S}_{\mathrm{n}} \sigma_{\mathrm{n}} \,, \tag{6-12}$$

where $\sigma_0 = \mathbb{1}$ and $\overline{S}_{\mathrm{n}} \in \mathbb{R}$, so that $\overline{S}$ is Hermitian. With Eqs. (6-9) and (6-12) the symmetrisation condition (5-15) yields

$$\begin{pmatrix} \gamma_1 + \gamma_2 & 0 & 0 & \gamma_1 - \gamma_2 \\ 0 & \gamma_1 + \gamma_2 & \epsilon_1 - \epsilon_2 & 0 \\ 0 & -(\epsilon_1 - \epsilon_2) & \gamma_1 + \gamma_2 & -2J \\ \gamma_1 - \gamma_2 & 0 & 2J & \gamma_1 + \gamma_2 \end{pmatrix} \begin{pmatrix} \overline{S}_0 \\ \overline{S}_1 \\ \overline{S}_2 \\ \overline{S}_3 \end{pmatrix} = 0 \,. \tag{6-13}$$

A solution for this equation exists only if the determinant of the coefficient matrix vanishes, *i.e.*

$$(\gamma_1 + \gamma_2)^2 \Big[(\gamma_1 + \gamma_2)^2 - (\gamma_1 - \gamma_2)^2 + 4J^2 \Big] + (\epsilon_1 - \epsilon_2)^2 \Big[(\gamma_1 + \gamma_2)^2 - (\gamma_1 - \gamma_2)^2 \Big] = 0 \,. \tag{6-14}$$

For a symmetric potential with $\epsilon_1 = \epsilon_2$ and $\gamma_1 = -\gamma_2 = \gamma$ both terms in Eq. (6-14) vanish identically. Then, the solution of Eq. (6-13) is given by the left-hand symmetrisation operator

$$\overline{S} = \begin{pmatrix} \overline{S}_0 & \overline{S}_1 - \mathrm{i} \frac{\gamma}{J} \overline{S}_0 \\ \overline{S}_1 + \mathrm{i} \frac{\gamma}{J} \overline{S}_0 & \overline{S}_0 \end{pmatrix}, \tag{6-15}$$

which has the two degrees of freedom $\overline{S}_0$ and $\overline{S}_1$. The corresponding right-hand symmetrisation operator can simply be obtained by changing the sign of γ, as this corresponds to the adjoint Hamiltonian. Hence, $\underline{S} = (\overline{S})^\dagger$. For $\overline{S}_0 = 0$ and $\overline{S}_1 = 1$ the parity operator $\mathcal{P}$ is retrieved.

For $J \neq 0$ there is no other choice of parameters for which the first term in Eq. (6-14) vanishes. However, by choosing

$$\epsilon_1 - \epsilon_2 = \pm(\gamma_1 + \gamma_2)\sqrt{-\frac{J^2}{\gamma_1\gamma_2} - 1} \tag{6-16}$$

with $-J^2 < \gamma_1\gamma_2 < 0$, the condition (6-14) is satisfied. The lower bound of the product $\gamma_1\gamma_2$ stems from the fact that — under the assumption that only either γ_1 or γ_2 is non-zero — Eq. (6-14) can be satisfied if and only if the modes are decoupled, *i.e.* $J = 0$, or if there is no gain or loss at all, *i.e.* $\gamma_1 = \gamma_2 = 0$, which contradicts the assumption. The upper bound is required for the expression under the square root to be negative, so that the difference of the on-site potential parameters is a real quantity. Hence, a symmetrised operator of the form (6-9) always requires the presence of both gain and loss. This appears to be intuitive, particularly if one recalls that real energies describe stationary states in open quantum systems. However, as shown in Ref. [129], there exist potentials in unbound systems which do not require gain at all; this is hard to grasp from a physical point of view.

From a mathematical point of view, there is, in principle, an infinite number of systems which can satisfy the relation (6-16), as it only requires a specific difference in the on-site potential parameters. Due to the possibility to freely gauge the energy scale, though, just two physically distinct situations have to be considered. They correspond to a system $\mathcal{H}$ with parameters ϵ_1 and ϵ_2 set according to Eq. (6-16) and its time-reversed counterpart $\mathcal{H}^\dagger$. In the following, a system is considered to evolve forwards in time if particles or energy in the system move from left to right; consequently, if the particles are moving from right to left, the system evolves backwards in time.

By plugging Eq. (6-16) into Eq. (6-13), the corresponding symmetrisation operator can be calculated, which in matrix form reads

$$\overline{S} = \begin{pmatrix} -\frac{J}{\gamma_1} & -\mathrm{i} \mp \sqrt{-\frac{J^2}{\gamma_1\gamma_2} - 1} \\ \mathrm{i} \mp \sqrt{-\frac{J^2}{\gamma_1\gamma_2} - 1} & \frac{J}{\gamma_2} \end{pmatrix} \overline{S}_2 \,.$$

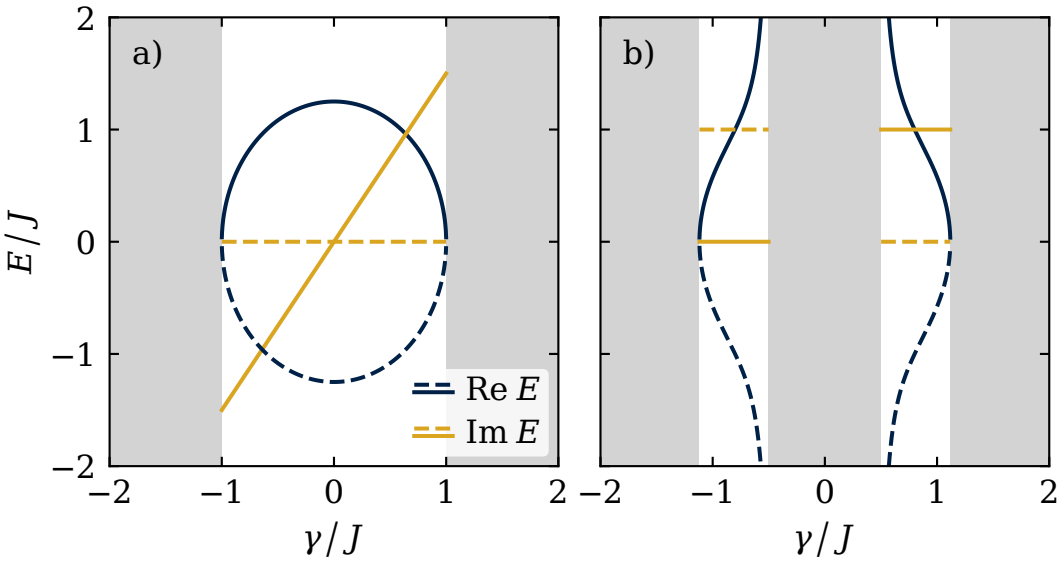

Figure 6-3: Real and imaginary parts of the eigenvalues (6-17) for Eq. (6-16) with $\epsilon_1 \geq \epsilon_2$. The different parametrisations are given a) by Eq. (6-18) and b) by Eq. (6-20). There exists one real and one complex solution, respectively, as long as the Hamiltonian can be symmetrised; the shaded regions indicate where this is no longer possible.

In contrast to Eq. (6-15), this symmetrisation operator possesses only one single degree of freedom $\bar{S}_2$. Further, it is non-invertible as $\det \bar{S} = 0$ hold independently of the choice of $\bar{S}_2$. Hence, $\operatorname{rank} \bar{S} = 1$, which immediately implies that there must exist one real eigenvalue E. By shifting the energy scale suitably, this real eigenvalue can take the form $E = 0$, so that its existence is determined by $\det \mathcal{H} = 0$; the solutions of this condition are given by Eq. (6-16). The situation can thus be stated as follows: There are two physically distinct systems with $\epsilon_1 > \epsilon_2$ and $\epsilon_1 < \epsilon_2$, respectively, which satisfy Eq. (6-16). For both these systems there exist two imaginary potentials[8] $\gamma_1 > \gamma_2$ and $\gamma_1 < \gamma_2$, respectively, so that each system has one real eigenvalue. Semi-symmetrisation thus connects the four Hamiltonians $\mathcal{H}_+$, $\mathcal{H}_-$, $\mathcal{H}_+^\dagger$, and $\mathcal{H}_-^\dagger$, where the index refers to the sign in Eq. (6-16).

[8] The corresponding systems evolve forwards and backwards in time, respectively.

The general solutions for the eigenvalues of the two-mode system are given by

$$E_\pm = \frac{1}{2}\left[(\epsilon_1 + \epsilon_2) + \mathrm{i}(\gamma_1 + \gamma_2) \pm \sqrt{[(\epsilon_1 - \epsilon_2) + \mathrm{i}(\gamma_1 - \gamma_2)]^2 + 4J^2}\right]. \tag{6-17}$$

These solutions E_+ and E_- are plotted in Fig. 6-3 for different parametrisations of gain and loss. Figure 6-3 a) shows a system with asymmetric gain and loss parametrised by

$$\gamma_1 = 2\gamma\,, \quad \gamma_2 = -\frac{\gamma}{2}\,. \tag{6-18}$$

The on-site potential parameters are chosen symmetrically via

$$\epsilon_1 = -\epsilon_2 = \frac{\Delta\epsilon}{2}\,, \tag{6-19}$$

where $\Delta\epsilon$ corresponds to the difference (6-16); thus, $\epsilon_1 + \epsilon_2 = 0$ in Eq. (6-17). As discussed above, there is an ambiguity in the sign of $\Delta\epsilon$. In the following, this freedom is used to choose the sign such that $\epsilon_1 \geq \epsilon_2$. For $|\gamma/J| < 1$ the spectrum resembles the $\mathcal{PT}$-symmetric case shown in Fig. 6-2, but with the imaginary part of E_+ rotated about the origin at $\gamma = 0$, while E_- remains entirely real. The real parts of E_+ and E_- are still symmetric but they no longer form a unit circle; instead, they appear elliptic.[9] In the domain $|\gamma/J| > 1$ there exist no symmetrised solutions at all, since Eq. (6-16) becomes imaginary and cannot be used to determine the on-site potential parameters anymore. Last but not least, there are no EPs at $|\gamma/J| = \pm 1$, *i.e.* no bifurcations occur as in the $\mathcal{PT}$-symmetric case because the imaginary part of E_+ is non-zero for $\gamma \neq 0$.

[9] Precisely they are stretched by a factor of 1.25 at $\gamma = 0$.

In Fig. 6-3 a) another parametrisation of asymmetric gain and loss is shown, which is given by

$$\gamma_1 = \gamma + \frac{1}{2}\,, \qquad \gamma_2 = -\gamma + \frac{1}{2} \tag{6-20}$$

with Eq. (6-19), so that $\gamma_1 + \gamma_2 = 1$. The corresponding solutions are again deformed in comparison with the $\mathcal{PT}$-symmetric case in Fig. 6-2. However, there no longer exist solutions on the interval $-1/2 \leq \gamma/J \leq 1/2$, in which the gain-loss parameters (6-20) possess the same sign; *i.e.* for $\gamma < 0$ there is only gain and for $\gamma > 0$ there is only loss. For $|\gamma/J| > 1$ there are no solutions either, due to the same reasons discussed above. In the remaining parameter regions there are solutions with either $\operatorname{Im} E_+ = 0$ for $\gamma < 0$ or $\operatorname{Im} E_- = 0$ for $\gamma > 0$. The offset of the respective other imaginary parts are given by $\mathrm{i}(\gamma_1 + \gamma_2)$, which vanishes only in the Hermitian and $\mathcal{PT}$-symmetric cases. Further, the real parts of the energy eigenvalues diverge at $\gamma = \pm J/2$. By approaching the regions where only either gain or loss occurs, the parameters γ_1 and γ_2 become increasingly unsuitable for sustaining the properties imposed onto the system by symmetrisation. This is reflected by the divergence of the term

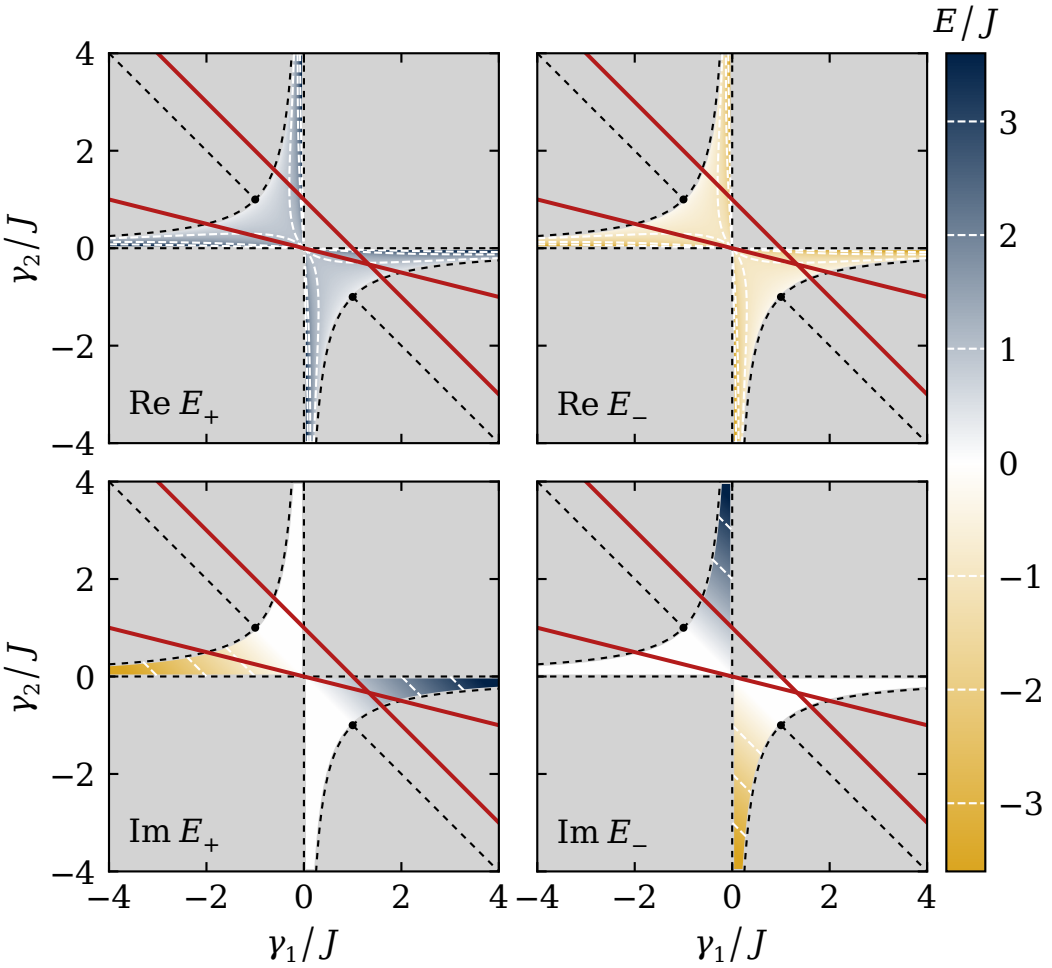

Figure 6-4: Real and imaginary parts of the eigenvalues (6-17) as functions of γ_1 and γ_2, where $\epsilon_1 \geq \epsilon_2$ are determined by Eq. (6-16). The two solid lines represent the two parametrisations used in Fig. 6-3. Further, black dashed lines indicate the regions in which the system is symmetrised and white dashed lines indicate contours of the eigenvalues. The other case with $\epsilon_1 \leq \epsilon_2$ looks identical but with the imaginary parts exchanged.

(6-16) at $\gamma = \pm J/2$ due to

$$\gamma_1 \gamma_2 = \frac{1}{4} - \gamma^2$$

and the subsequent divergences of $\operatorname{Re} E_+$ and $\operatorname{Re} E_-$.

Figure 6-4 shows the real and imaginary parts of the energy eigenvalues (6-17) as functions of the gain-loss parameters. The areas in which real solutions of Eq. (6-16) exist are enclosed by hyperbolas and the axes in the second and forth quadrants, respectively. In the first and third quadrants there exist no solutions at all, as these regions correspond to pure gain or loss. The $\mathcal{PT}$-symmetric two mode system[10] is retained by $\gamma_1 = \gamma_2$, which corresponds to the off-diagonal; both eigenvalues $E_\pm$ are real and $\Delta\epsilon = 0$.

The slices in the (γ_1, γ_2) space, which correspond to the parametrisations (6-18) and (6-20), are shown by the two solid lines in Fig. 6-4. The imaginary parts of E_+ and E_- are growing linearly

[10] *cf.* Section 6-1 a)

along directions parallel to the diagonal. Hence, the imaginary part is shifted constantly by slicing parallel to the off-diagonal and one obtains a, as it were, rotated imaginary part by slicing along any other direction through the origin. Since both real parts diverge towards the axes, the energy eigenvalues may be arbitrarily large by rotating the slice around the origin.

It is worth mentioning that similar theoretical results were found previously for a BEC in a two-well potential [150]. By balancing asymmetries in gain and loss with an asymmetric trapping potential, the formation of a real ground state is possible. This is in agreement with semi-symmetrisation as discussed in Section 5-4. Lunt *et al*. also discuss a two-mode system with asymmetric gain and loss but with a symmetric trapping potential [150]. This corresponds to $\epsilon_1 = \epsilon_2 = 0$ and

$$\gamma_1 = \pm J\sqrt{\frac{1+a}{1-a}}, \qquad \gamma_2 = \mp J\sqrt{\frac{1-a}{1+a}},$$

where $a \in \mathbb{R}$ is a free parameter. This Hamiltonian also yields a single real eigenvalue, yet it is not semi-symmetrisable because of Eq. (6-16). This again shows that semi-symmetrisation is neither necessary nor sufficient for the occurrence of real eigenvalues.

d) Bi-complex continuation

In contrast to the $\mathcal{PT}$-symmetric solutions shown in Fig. 6-2, symmetrisation cannot yield suitable parameters in all parameter regions; in particular, Eq. (6-16) does not yield real numbers in the shaded regions shown in Figs. 6-3 and 6-4. While the physical explanation — *i.e*. such systems become unable to maintain balanced gain and loss — is perfectly fine, yet the solutions shown in Fig. 6-3 evoke the impression that they could easily be extended. Hence, rather out of mathematical curiosity than of physical necessity, an *analytical continuation* of the problem is considered, in which the otherwise real on-site parameters ϵ_1 and ϵ_2 of the complex Hamiltonian (6-9) are allowed to become complex themselves. To keep them distinct from the proper imaginary part, which describes gain and loss, they

are extended into an additional complex plane; the Hamiltonian thus becomes *bi-complex*.

Analytical continuations are often used in non-linear NHQM to make a Hamiltonian analytic [196], so that the overall number of states at each point in the parameter space remains constant. This is, for example, completely analogous to the argumentation in Chapter 4, where the number of solutions with real energies is not preserved;[11] only by considering also complex energies, the number of solutions remains the same. However, analytical continuation can also be applied in the context of symmetrisation in linear NHQM [197]. Here, a new imaginary unit j is introduced with respect to which Eq. (6-16) is allowed to become complex. Extending the real coefficients of a complex number into another complex plane creates a *bi-complex number*.[12] In contrast to the more famous quaternions [199], bi-complex numbers are commutative with respect to multiplications. Yet, bi-complex numbers possess zero divisors, so that they do not form a *division algebra*; though, this property allows for the introduction of an *idempotent basis*[13] with elements e_+ and e_-. The fundamentals of QM — the Schrödinger equation and the Hilbert space — can also be generalised using bi-complex numbers [200; 201]. Appendix G gives a short introduction on bi-complex numbers and the idempotent basis.

[11] *cf.* Fig. 6-2

[12] *e.g.* see Ref. [198]

[13] *cf.* Appendix G-1

Using the idempotent representation,[14] the Hamiltonian (6-9) with $\epsilon_k \to \epsilon_k + \mathrm{j}\epsilon_k'$ can be written as

[14] *cf.* Appendix G-1

$$\mathcal{H} = \mathcal{H}_+ \mathrm{e}_+ + \mathcal{H}_- \mathrm{e}_-$$

with

$$\mathcal{H}_\pm = \begin{pmatrix} \epsilon_1 + \mathrm{i}\left(\gamma_1 \mp \epsilon_1'\right) & -J \\ -J & \epsilon_2 + \mathrm{i}\left(\gamma_2 \mp \epsilon_2'\right) \end{pmatrix}. \tag{6-21}$$

Since the bi-complex numbers e_+ and e_- act like a basis, the Hamiltonians (6-21) define two distinct eigenvalue equations, which makes solving the bi-complex model straightforward.

The bi-complex extension of the parametrisation (6-18) used in Fig. 6-3 a) is shown in Fig. 6-5. For increasing interactions with the environment, the difference (6-16) becomes bi-complex

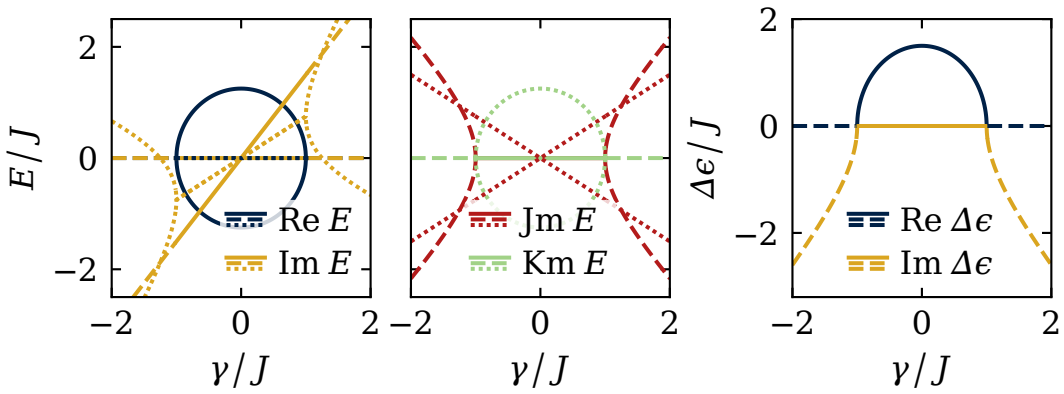

Figure 6-5: The bi-complex extensions (dashed) of the complex solutions (solid) shown in Fig. 6-3 a). There occur two additional, all bi-complex solutions (dotted).

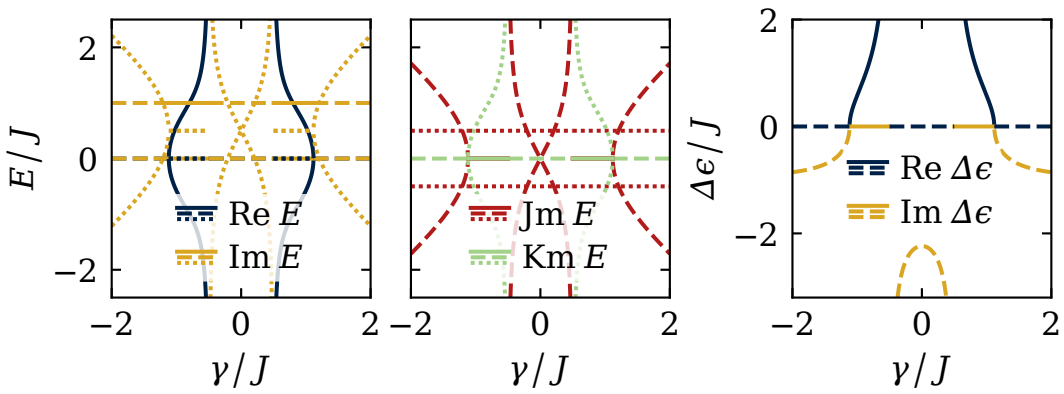

Figure 6-6: Bi-complex extensions of the solutions shown in Fig. 6-3 b) in analogy to Fig. 6-5. However, the bi-complex numbers seem to not contain all solutions for $-1/2 \leq \gamma/J \leq 1/2$.

with respect to j at $\gamma = \pm J$. Simultaneously, a pair of bi-complex eigenvalue solutions arises, which extend the complex solutions. Moreover, an additional pair of solutions occurs, which always are truly bi-complex.

Analogously, the parametrisation (6-20) used in Fig. 6-3 b) can be extended, which is shown in Fig. 6-6. If γ is large enough, the situation is equivalent to the discussions above. For $\gamma = \pm J/2$, though, the additional bi-complex solutions are not continuous; this might be an indication that bi-complex numbers are not sufficient to describe all solutions in Fig. 6-6, just like complex numbers are not sufficient to describe all solutions in Fig. 6-3. However, since this concerns only the "unphysical" states, another analytical continuation is unnecessary.

The bi-complex solutions which extend the stationary states shown in Fig. 6-3 possess an additional, non-zero imaginary part with respect to the complex number j, so that the energy eigenvalue is given by a bi-complex number $E_k + \mathrm{j}E_k'$ for $k = 1, 2$, where $E_k, E_k' \in \mathbb{R}$. Using Eq. (G-9), the time evolution then yields the

idempotent representation

$$\begin{aligned} \mathrm{e}^{\mathrm{i}E_k t} &= \mathrm{e}^{\mathrm{i}(E_k+E'_k)t}\mathrm{e}_+ + \mathrm{e}^{\mathrm{i}(E_k-E'_k)t}\mathrm{e}_- \\ &= \mathrm{e}^{\mathrm{i}E_k t}\left(\cos E'_k t - \mathrm{j}\sin E'_k t\right). \end{aligned}$$

This clearly shows that such states can still be considered as stationary, as there occurs no exponential increase or decrease in their norm.

6-2 Few-mode models

Although few-mode systems with up to four dimensions can, in principle, be treated analytically in the same way described in Section 6-1, the number of equations grows quadratically, which is not feasible. However, by demanding the reality of the characteristic polynomial,[15] the number of equations grows only linearly; this allows for the analytical investigation of a three-dimensional model in the following. Since the reality of the characteristic polynomial is sufficient, completely symmetrised systems occur.

[15] *cf.* Section 5-3 c)

The Hamiltonian of the three-mode model possesses the same structure as the Hamiltonian (6-9),

$$\mathcal{H} = \begin{pmatrix} \epsilon_1 + \mathrm{i}\gamma_1 & -J & 0 \\ -J & \epsilon_2 + \mathrm{i}\gamma_2 & -J \\ 0 & -J & \epsilon_3 + \mathrm{i}\gamma_3 \end{pmatrix}. \tag{6-22}$$

An evaluation of the imaginary parts of the coefficients of the characteristic polynomial yields

$$\gamma_1 + \gamma_2 + \gamma_3 = 0\,, \tag{6-23}$$

$$\epsilon_1\gamma_2 + \gamma_1\epsilon_2 + \epsilon_2\gamma_3 + \gamma_2\epsilon_3 + \epsilon_1\gamma_3 + \gamma_1\epsilon_3 = 0\,, \tag{6-24}$$

$$\gamma_1\epsilon_2\epsilon_3 + \epsilon_1\gamma_2\epsilon_3 + \epsilon_1\epsilon_2\gamma_3 + \gamma_1\gamma_2\gamma_3 - J^2(\gamma_1 + \gamma_3) = 0\,. \tag{6-25}$$

Equation (6-23) shows — as already stated in Ref. [202] — that the sum of all gain and loss terms must vanish. This stems from the condition that the trace of the Hamiltonian must be real, which cor-

responds to the highest-order non-trivial coefficient of the characteristic polynomial,[16] and appears to be a necessary consequence[17] of balanced gain and loss. However, as shown in the two-dimensional case, there exist stationary solutions with real energies even if Eq. (6-10) is not satisfied. Hence, balanced gain and loss has to be considered per state, meaning that one also has to consider the absolute square $|\psi_k|^2$ of the components of the wave function in each well. Thus, balanced gain and loss means

[16] *cf.* Eq. (6-10)

[17] *e.g.* see Ref. [129]

$$\sum_k \gamma_k |\psi_k|^2 = 0\,. \tag{6-26}$$

It is easy to find the trivial solutions of Eqs. (6-23) to (6-25), which are given by the Hermitian potential with $\gamma_1 = \gamma_2 = \gamma_3 = 0$ and the $\mathcal{PT}$-symmetric potential with $\gamma_1 = -\gamma_3$, $\gamma_2 = 0$, and $\epsilon_1 = \epsilon_3$, where ϵ_2 can be chosen arbitrarily. However, if either only γ_1 or γ_3 is zero, Eq. (6-25) cannot be satisfied for $J \neq 0$. The other solutions of Eqs. (6-23) to (6-25) are given by

$$\gamma_1 = -(\epsilon_2 - \epsilon_3)\gamma_0\,, \tag{6-27}$$
$$\gamma_2 = (\epsilon_1 - \epsilon_3)\gamma_0\,, \tag{6-28}$$
$$\gamma_3 = -(\epsilon_1 - \epsilon_2)\gamma_0\,, \tag{6-29}$$

where

$$\gamma_0 = \pm\sqrt{\frac{\Delta\epsilon_{12}^3 + \Delta\epsilon_{23}^3 - \Delta\epsilon_{13}^3 + 3J^2\Delta\epsilon_{13}}{3\Delta\epsilon_{12}\Delta\epsilon_{23}\Delta\epsilon_{13}}} \tag{6-30}$$

with $\Delta\epsilon_{kl} = \epsilon_k - \epsilon_l \neq 0$.

Of course, the solutions (6-27) to (6-29) again depend only on the difference of the on-site potential parameters.[18] Further, these solutions exist only if the term under the square root in Eq. (6-30) is positive. By assuming that $\Delta\epsilon_{12}\Delta\epsilon_{23} > 0$, one finds

[18] *cf.* Eq. (6-16)

$$\Delta\epsilon_{12}\Delta\epsilon_{23} \leq J^2\,.$$

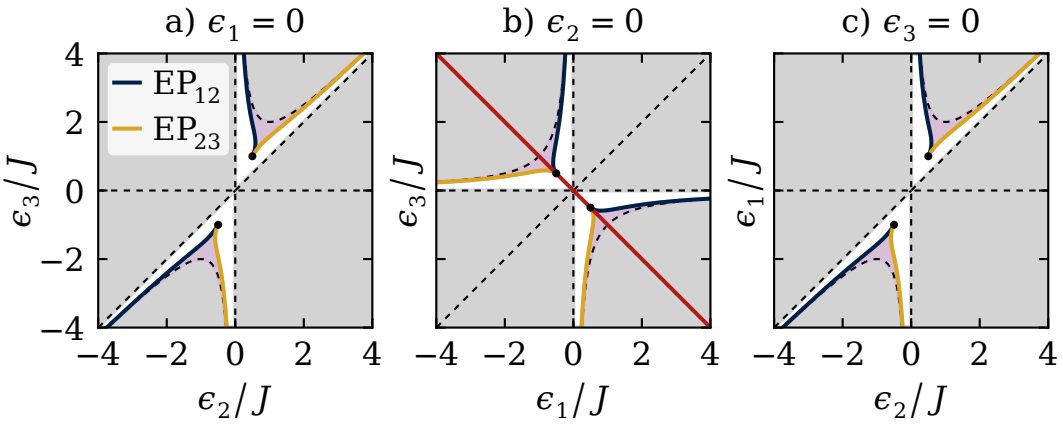

Figure 6-7: Slices along the coordinate planes in the on-site potential parameter space. In the blue shaded regions all of the three solutions are real. The solid line in b) indicates the parametrisation used in Fig. 6-9.

For $\Delta\epsilon_{12}\Delta\epsilon_{23} < 0$ there exist no solutions at all. Hence, $\Delta\epsilon_{12}$ and $\Delta\epsilon_{23}$ must either both be positive or negative, which yields

$$\epsilon_1 \lesseqgtr \epsilon_2 \lesseqgtr \epsilon_3 \,,$$

i.e. there are two possible gain-loss distributions with

$$\gamma_1 \gtreqless 0 \,, \quad \gamma_2 \lesseqgtr 0 \,, \quad \gamma_3 \gtreqless 0 \,.$$

The regions in the $(\epsilon_1, \epsilon_2, \epsilon_3)$ parameter space, in which solutions occur, are shown in Fig. 6-7 for slices along the coordinate planes; they are symmetric in the sense that ϵ_1 and ϵ_3 are completely interchangeable. As in the two-dimensional case, an anti-symmetric imaginary potential, *i.e.* $\gamma_1 = -\gamma_2$ and $\gamma_2 = 0$, is required by a symmetric real potential with $\epsilon_1 = \epsilon_3$ and arbitrary ϵ_2. The spectrum for a symmetric real potential looks similar to the spectrum of the $\mathcal{PT}$-symmetric two-mode system in Fig. 6-2, but with an additional state which has zero energy everywhere. In contrast to the two-dimensional case, where the $\mathcal{PT}$-symmetric potentials are special cases of symmetrised systems,[19] $\mathcal{PT}$-symmetric[20] and symmetrised systems are completely exclusive for non-trivial choices of the parameters as shown in Fig. 6-7. That is, they coincide only if $\epsilon_1 = \epsilon_2 = \epsilon_3 = 0$.

Since all three states can potentially be real now, EPs occur in the spectrum where at least two states coalesce; this phenomenon was introduced and discussed in Section 4-3 a). The two independent, second-order EPs between the ground state and the first excited state, and the first and second excited states, respectively, are

[19] *cf.* Fig. 6-4

[20] They correspond to the zero lines of ϵ_3 and ϵ_1 in Figs. 6-7 a) and 6-7 c) and the diagonal in Fig. 6-7 b), respectively.

shown in Fig. 6-7. They correspond to tangent bifurcations, where two stationary states coalesce and give birth to a pair of states with complex-conjugate energies. The trajectories of these EPs in the coordinate planes meet in the vicinity of the origin and create the characteristic form of a cusp; hence, such a bifurcation scenario is called a *cusp catastrophe* [203]. The cusp points are again EPs but of *third order*, *i.e.* the coalescence of three states in a pitchfork bifurcation [204–207]. The corresponding real energy surfaces form a fold, which is illustrated in Fig. 6-8. In Ref. [207] it is shown that such cusp catastrophes also occur in $\mathcal{PT}$-symmetric BECs.

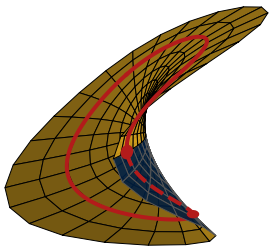

Figure 6-8: Topology around a cusp catastrophe

Note that there is a strong resemblance between Fig. 6-7 b) and the area in Fig. 6-4, despite the fact that completely different parameter spaces are shown. This is because the on-site potential parameters and the gain-loss parameters differ only by an imaginary unit on entering the Schrödinger equation. Hence, real and imaginary parts of the potential are connected in a certain way. This is most obvious in $\mathcal{PT}$-symmetric systems, where the real potential is symmetric — this corresponds to the diagonal in Fig. 6-7 b) — and the imaginary potential is anti-symmetric. However, this relation also holds *vice versa*, *i.e.* if the imaginary potential is symmetric and the real potential is anti-symmetric. As an example, the anti-symmetric real potential $\epsilon_1 = -\epsilon_3$ and $\epsilon_2 = 0$ can be considered, which corresponds to the off-diagonal in Fig. 6-7 b). Note that this type of potentials is partially embedded into the region of the symmetrisable Hamiltonians in the same way as the $\mathcal{PT}$-symmetric potentials are in Fig. 6-4. The corresponding spectrum is shown in Fig. 6-9 as a function of the on-site potential parameter ϵ_1, and the corresponding imaginary potential is chosen according to Eqs. (6-27) to (6-30). Remarkably, the imaginary potential is always symmetric with $\gamma_1 = \gamma_3$. Such potentials are called anti-$\mathcal{PT}$-symmetric [133; 134] since they satisfy[21]

$$\{\mathcal{PT}, V\} = 0\,,$$

where the curly braces indicate the anti-commutator. $\mathcal{PT}$ and anti-$\mathcal{PT}$ symmetry are two special cases which show that symmetrised systems indeed bear certain symmetries, even though they may not always be obvious.

[21] *cf.* Eq. (5-3)

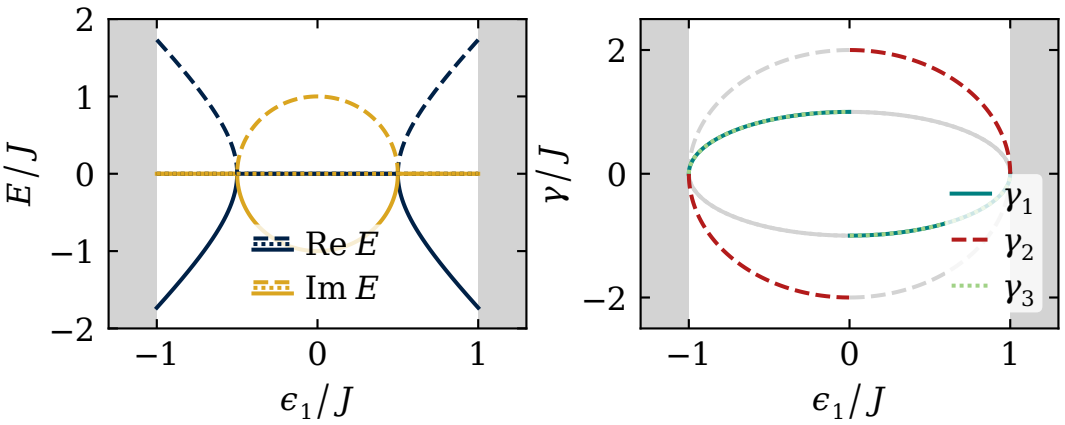

Figure 6-9: Solutions of the three-mode system for an anti-symmetric potential with $\epsilon_2 = 0$ and $\epsilon_1 = -\epsilon_3$, *i.e.* this corresponds to the solid line in Fig. 6-7 b). Suitable gain-loss parameters are determined by Eqs. (6-27) to (6-29) for $\gamma_0 > 0$. The same spectrum can be obtained with $\gamma_0 < 0$, being indicated by grey lines.

Apart from $\mathcal{PT}$ and anti-$\mathcal{PT}$-symmetric configurations, there again exist also completely asymmetric potentials which still lead to symmetrised Hamiltonians. This holds, in particular, also for semi-symmetrised Hamiltonians. In principle, one can find potentials with any number of real or complex-conjugate energies up to the number of sites. However, there is no straightforward way of constructing such semi-symmetrised Hamiltonians in multi-well potentials. Even in a three-mode system it is already feasible — though, for three dimensions not yet essential — to resort to numerical methods for calculating the potential parameters using a variational approach. In the next section, though, a special class of multi-mode systems is introduced which yield interesting properties for an arbitrary number of potential wells.

6-3 Transport chains

One might observe that for $\epsilon_2 = \gamma_2 = 0$ Eqs. (6-23) and (6-24) of the three-mode system reduce to Eqs. (6-10) and (6-11) of the two-mode system in the (ϵ_1, ϵ_3) space. This holds, in fact, for any multi-mode systems of dimension n with "empty" inner sites, *i.e.*

$$\epsilon_k = \gamma_k = 0 \tag{6-31}$$

for $k = 2, \ldots, n-1$.

Eq. (6-25) and the respective conditions in a general multi-mode system can only be satisfied with $\gamma_1 = -\gamma_3$ for $J \neq 0$. By dropping

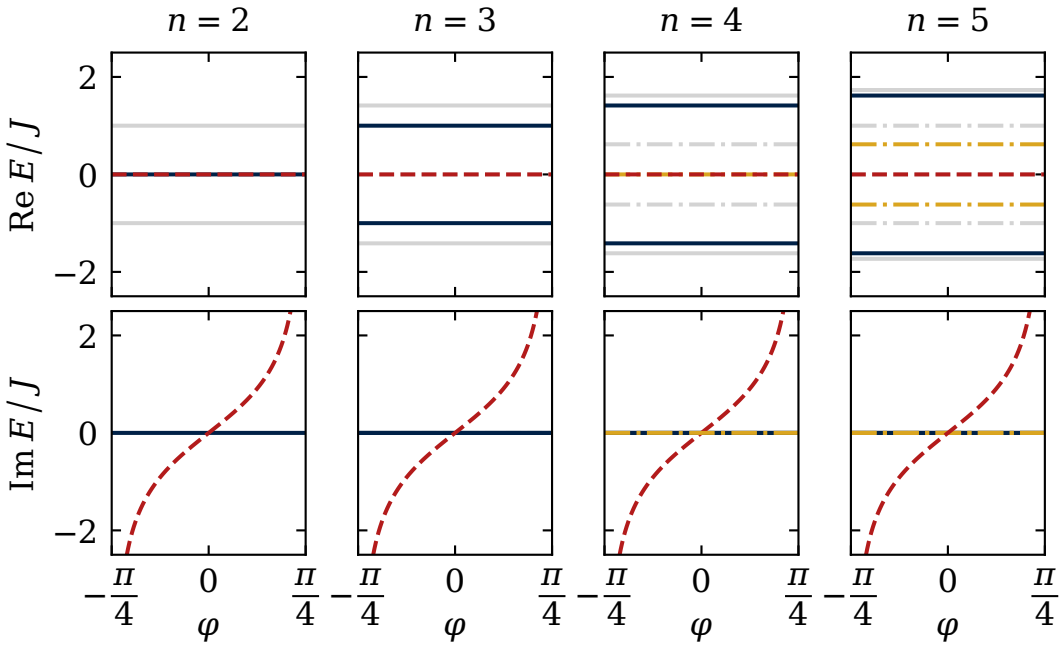

Figure 6-10: Spectra of chain potentials with n sites varied along the hyperbolic edge in the fourth quadrant in Fig. 6-4 via the angle φ. In all cases the spectra are real with the exception of a purely imaginary eigenvalue, respectively. For comparison, the spectra of the corresponding isolated n-mode systems are shown in grey.

Eq. (6-25), though, the analytic solutions of the two-mode system can be used to determine the parameters in the outer sites. The investigation of the two-mode system already showed that the dropping of some of the sufficient conditions may lead to semi-symmetrised systems; hence, this approach appears to be plausible.

The parameters of the outer sites are chosen according to the solutions of the two-mode system in Section 6-1 c) as

$$\epsilon_1 = \epsilon_n = 0 \tag{6-32}$$

and

$$\frac{\gamma_1}{J} = \sqrt{\cot\left(\frac{\pi}{4} - \varphi\right)}, \tag{6-33}$$

$$\frac{\gamma_n}{J} = -\sqrt{\tan\left(\frac{\pi}{4} - \varphi\right)}, \tag{6-34}$$

which corresponds to the hyperbola along which the term under the square root in Eq. (6-16) vanishes for non-symmetric imaginary potentials in Fig. 6-4. Equations (6-33) and (6-34) are parametrised by the angle $\varphi \in [-\pi/4, \pi/4]$ in the fourth quadrant.

The complex spectra of such systems with up to $n = 5$ wells are shown in Fig. 6-10. A comparison with the spectrum of the two-mode system in Fig. 6-10 shows that, by using the analytical

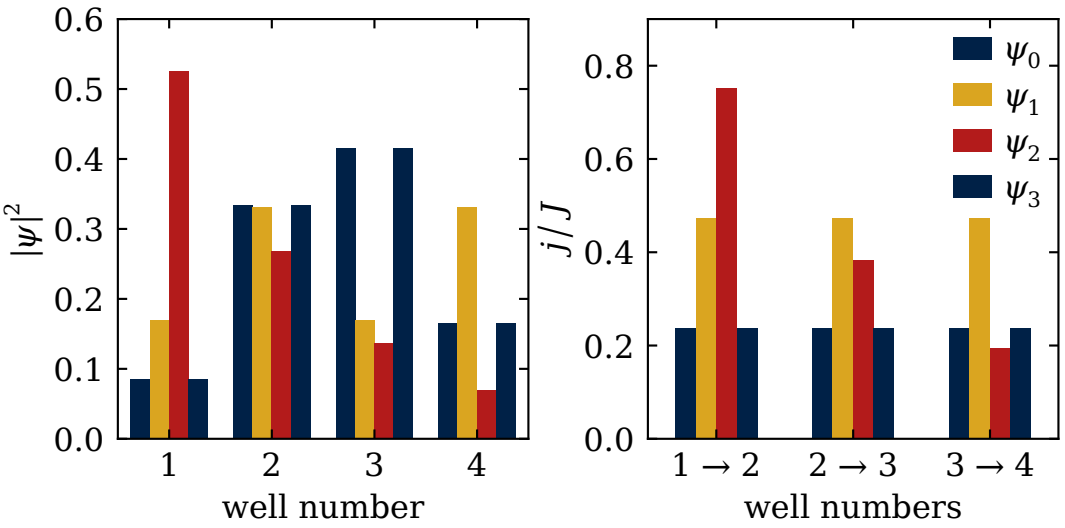

Figure 6-11: Occupations $|\psi|^2$ of and the currents j between the sites of the four-mode system shown in Fig. 6-10 at the angle $\varphi = \pi/10$.

solutions of the two-mode systems, the multi-mode systems "inherit" some of its properties. In all systems the same purely imaginary energy eigenvalue occurs, which crosses the real axis only for a $\mathcal{PT}$-symmetric potential at $\varphi = 0$. This is, in fact, exactly where the EP in Fig. 6-4 occurs. Surprisingly, the remaining $n-1$ states possess entirely real energies with their real parts being distributed symmetrically around $E = 0$. This is because an empty subsystem supports any currents imposed on it by the parameters in the outer wells. For comparison, the spectra of isolated n-well systems[22] along the same parametrisations are shown. This reveals that the real subspectrum of a semi-symmetrised n-well system equals the spectrum of the isolated $(n-1)$-well system with the addition of the complex eigenvalue. This is, however, only the case if gain and loss are balanced.[23] In general, for arbitrary gain-loss parameters the spectrum becomes complex.

[22] *i.e.* $\gamma_1 = \gamma_n = 0$

[23] *cf.* Eq. (6-26)

One might assume that this behaviour stems from the fact that the open transport chain can effectively be separated into an open two-mode system and an isolated potential chain. However, this would imply that the eigenstates are, for example, dominant only in the outer sites with eigenvalues which are similar to the two-mode system. Figures 6-11 and 6-13 show the occupations $|\psi_k|^2$ and the currents j_{kl} between adjacent sites $l = k \pm 1$, which are defined by Eq. (4-5),

$$j_{kl} = -\mathrm{i}J\left(\psi_k^*\psi_l - \psi_k\psi_l^*\right),$$

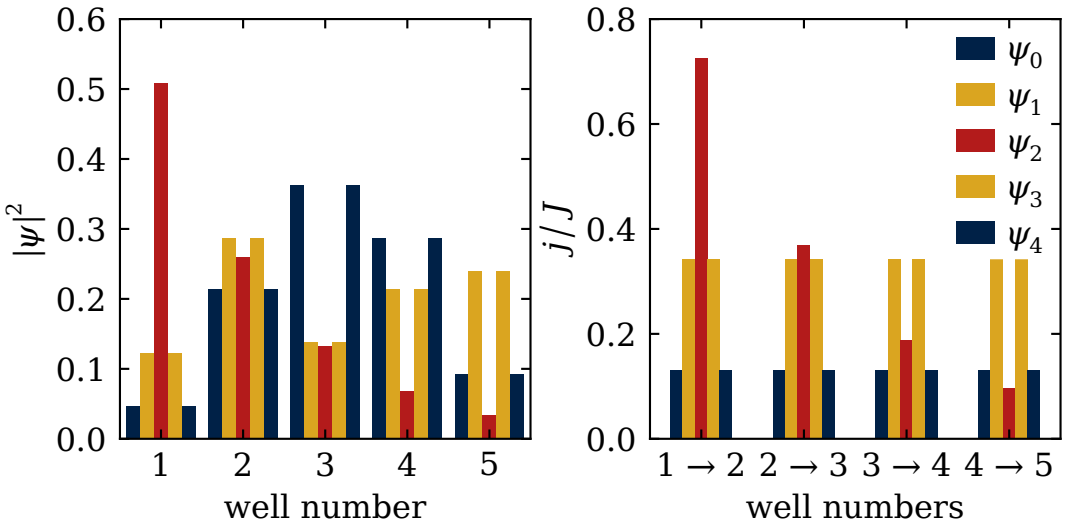

Figure 6-13: Occupations $|\psi|^2$ of and the currents j between the sites of the five-mode system shown in Fig. 6-10 at the angle $\varphi = \pi/10$.

of the four and five-mode transport chains. It is apparent that the solutions in Fig. 6-10 must be genuine solutions of the multi-well potential, as the states indicate no obvious distinction between the outer and the inner sites of the system.

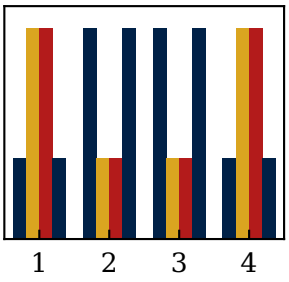

Figure 6-12: Occupations in an isolated four-mode system

For comparison, the occupations of the isolated four and five-mode potentials are shown in Figs. 6-12 and 6-14. While the discrete wave functions of the isolated multi-mode systems are truly symmetric, only some states of the open transport chains are symmetric; in fact, this seems to occur only for an odd overall number of sites as in Fig. 6-13. The reason, of course, is the presence of gain and loss which introduces a distinct direction — *i.e.* that of the probability current — into the system. Further, there is a clear difference between the stationary states with real eigenvalues, for which the currents between all wells are equal, and the state of the isolated complex eigenvalue which will change in time. For the latter the initial occupations are also always exponentially distributed along the potential chains.

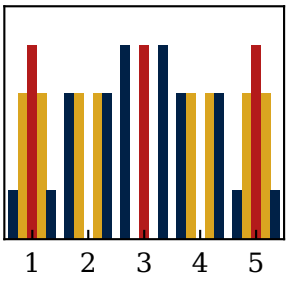

Figure 6-14: Occupations in an isolated five-mode system

6-4 Continuous model

Last but not least, the concept of symmetrisation should also briefly be discussed in the context of spatially extended quantum systems with infinite-dimensional Hilbert spaces.

As noted in Ref. [86], there exists an important difference between finite and infinite-dimensional Hilbert spaces: In contrast to finite-dimensional Hilbert spaces, where one can define a basis independently of the inner product, the definition of a basis in an infinite-dimensional Hilbert space relies on the definition of the inner product explicitly; in particular, the requirement of a *separable*[24] Hilbert space makes use of the norm. Moreover, while a comprehensive bi-complex quantum theory can in principle be defined in such cases, yet several issues occur in going from finite to infinite-dimensional systems [65]. For example, it is not guaranteed, that there exists a complete set of bi-orthogonal basis states for a non-Hermitian quantum system [64]. Another example is the occurrence of unbounded operators.[25] Suppose there is an unbounded metric operator η, which is not everywhere defined, *i.e.* the domain of η is smaller than the Hilbert space. If $|\psi\rangle$ is in the domain of η and $|\psi'\rangle$ is not, then $\langle\psi'|\eta\psi\rangle$ is well defined, while $\langle\eta\psi'|\psi\rangle$ is not; hence, $\langle\overline{\psi'}|\underline{\psi}\rangle \neq \langle\overline{\psi}|\underline{\psi'}\rangle^*$, which violates a fundamental assumption about the inner product [85].

Space is big. You just won't believe how vastly, hugely, mind-bogglingly big it is. I mean, you may think it's a long way down the road to the chemist's, but that's just peanuts to space.

Douglas Adams

[24] *i.e.* there exists a dense, finite or countable infinite subset of the Hilbert space

[25] *cf.* Appendix B-1

Despite all these potential issues, it is known already that concepts like $\mathcal{PT}$-symmetry[26] or the Wadati-type potentials (5-22), which were discussed at the beginning of Section 5-3, can successfully be applied to spatially extended quantum systems, *e.g.* see Refs. [61; 138; 207; 208]. The reason for this, as discussed in Section 5-3 e), mainly lies in the fact that they are connected to operators which are independent of the basis of the system to which they are applied, so that most of the concerns above are negligible.

[26] *cf.* Section 5-1

In Section 6-1 b) a first step towards symmetrisation in a spatially extended system has been made by using a double-delta potential. The discussion in Appendix F shows that the absence of two stationary solutions is not restricted to the two-dimensional matrix model, but it is rather a consequence of the limited number of degrees of freedom. That is, delta potentials can be considered as a type of system in between discrete and spatially extended systems.

In the following, complex *Gaussian potentials* are considered, which — under the assumption that the potential wells are deep enough — in the *mean-field approximation* correspond to the finite-

[27] *e.g.* see [192; 209]

dimensional matrix models with complex potentials[27] as discussed before. Hence, only a finite subspace of the infinite-dimensional Hilbert space is considered and thus the issues related to the completeness of the basis in its entirety or the domains of unbound operators should mostly be irrelevant. The physical interpretation of such potentials corresponds exactly to the one for multi-well potentials shown in Fig. 6-1.

Gaussian potentials

To derive the corresponding matrix model of a spatially extended quantum system, usually some kind of *tight-binding approximation* is used; for this, a strongly localised set of orthogonal functions like the *Wannier functions* are required (*e.g.* see Ref. [210] for an overview of the *Bose–Hubbard model*, from which one can derive a low-dimensional matrix approximation [193]). Such functions are, however, often complicated and involve impractical control parameters. For this reason, it is of interest to use simpler sets of localised functions, though, they are not orthogonal in most cases. Because of their properties, Gaussian functions are an obvious choice, as their form is determined by a simple set of parameters.[28]

[28] *cf.* Chapter 8

In the following, a Gaussian multi-well potential of the form

$$V(x) = \sum_{k=1}^{n} (\varepsilon_k + \mathrm{i}\,\gamma_k) \exp\left(-\frac{(x - x_k)^2}{2\sigma_k^2}\right). \tag{6-35}$$

is considered, where ε_k and γ_k are, in analogy to the matrix model, the real and imaginary part of the complex on-site potential. Since the potential (6-35) is spatially extended, each potential well at position x_k has a non-zero width σ_k; hence, the potential barrier between two adjacent wells — which is, roughly speaking, described by J^{-1} in the matrix model — is determined by the distance $(x_k - x_l)$ and the widths σ_k and σ_l for $l = k \pm 1$.

The connection between matrix models of the form (6-9) and (6-22) and their corresponding Gaussian potentials of the form (6-35) is derived in Appendix E. Yet, the relations between the Gaussian potential parameters and the parameters of a matrix model

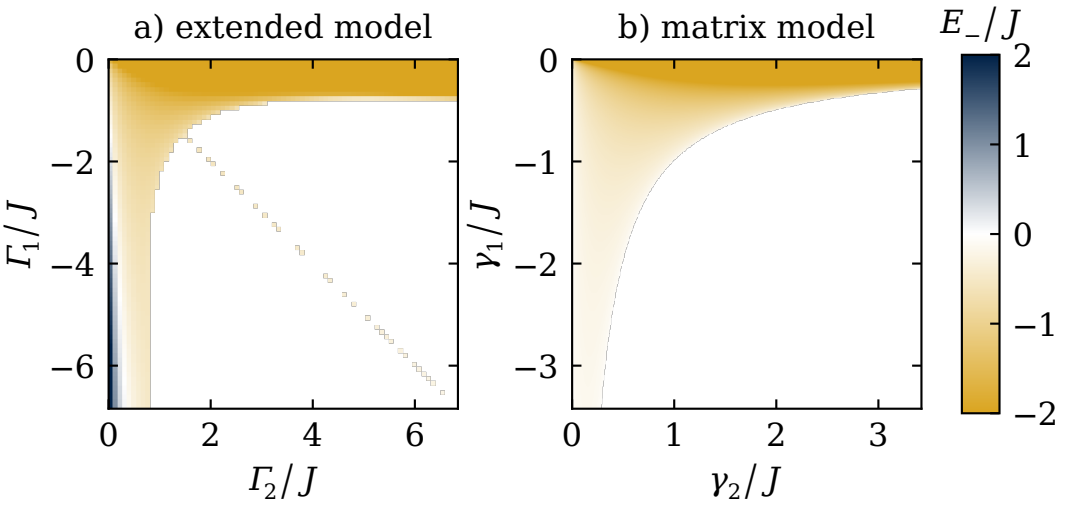

Figure 6-15: Ground state energy for a) the Gaussian double-well potential (6-35) described by the parameters $\sigma_1 = \sigma_2 = 1$, $x_1 = -x_2 = -1.5$, and $V_1 = -3$ and b) its corresponding matrix model. The data is taken from Ref. [180] and adapted in such a way that the matrix model corresponds to $J = 1$ and $\epsilon_1 = 0$.

are not shown explicitly, as this would definitely exceed the scope of this thesis; see Refs. [180; 192; 209; 211; 212] and references therein for more details on this topic. Instead, a short and rather qualitative discussion of the results described in Ref. [180] should be sufficient to conclude this chapter.

Figure 6-15 shows a comparison between a spatially extended Gaussian double-well potential and its matrix model as discussed in Section 6-1 c). In contrast to Ref. [180], all quantities are normalised with respect to the coupling parameter J and the energy scales are shifted by ϵ_1, which corresponds to the choice $\epsilon_1 = 0$ in the matrix model. The spatially extended solutions are obtained by means of numerical variation with the condition that the discrete matrix approximation of the double well corresponds to a symmetrised two-mode matrix model, for which the solutions are known analytically.[29] This has to be done at every point in the parameter space, so that only a low-resolution image as in Fig. 6-15 a) can be produced within a reasonable amount of time. Nevertheless, a comparison with the analytical matrix model in Fig. 6-15 b) shows that, apart from a real ground state energy, the qualitative features of the symmetrised matrix model are preserved in the extended system. That is, there exists only one real ground state, a phenomenon which is known already from the double-delta potential discussed in Appendix F. Further, the domain in which the real ground state exists is also enclosed by some hyperbolic function, even though it approaches the axes a lot more gentle than the hyperbolas in

[29] *i.e.* Eq. (6-17) with Eq. (6-16)

Fig. 6-15 b); yet, because of physical constraints, it is still to be expected that no such systems exists for $\Gamma_k \to \infty$. It should further be noted that Fig. 6-15 also shows the $\mathcal{PT}$-symmetric potentials along the off-diagonal with $\Gamma_1 = -\Gamma_2$.

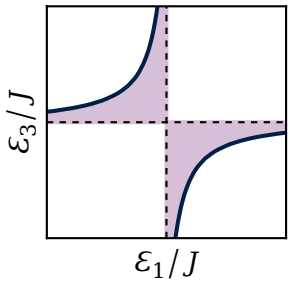

Figure 6-16: Extended three-mode model taken from Ref. [180]

One might notice that the symmetric structure with respect to the off-diagonal seen in Fig. 6-4 is missing in Fig. 6-15 b). The reason for this is two-fold: First, the parameters in Fig. 6-15 b) are chosen such that the ground state E_- is always real, which corresponds to the signs of the on-site potential parameters in Eq. (6-16). Second, in Ref. [180] the system was adjusted with a focus on the extended potential in Fig. 6-15 a); that is, also the parameters of the matrix model were changed to more suitable but non-trivial values.

In principle, this method should be applicable to any multi-well system, provided that the calculations do not exceed the computational power on hand. However, a three-well potential raises the difficulty and the calculation time already severely because of the involvement of a higher-dimensional optimisation procedure. Thus, potentials with an even higher number of wells are unfeasible to treat, at least with the same method, that is. Hence, in Fig. 6-16 only the domain is shown[30] in which real solutions of a triple-well Gaussian potential of the form (6-35) with $\sigma_1 = \sigma_2 = \sigma_3 = 1/\sqrt{2}$, $x_1 = -x_3 = -3$, and $V_2 = -2$ occur. Again, the qualitative behaviour of the extended potential and the matrix model shown in Fig. 6-7 b) are in good agreement. In Ref. [180] it is further shown that this qualitative agreement extends also to the eigenvalues and states, as should be expected if the matrix approximation is well defined.

[30] *i.e.* only the edges have to be found

These examples show that the concept of semi-symmetrisation can also be applied in the case of specific, spatially extended potentials of the form (6-35). While the Hilbert space in principle is infinite-dimensional in these cases, only a finite subspace of energies and states is considered; this can always be interpreted as a semi-symmetrised system for which the kernels of the symmetrisation operators contain an infinite number of states. Nevertheless, the Gaussian potentials discussed in this section correspond to complex potentials and thus allow for a suitable physical inter-

pretation. In particular, such potentials are suited quite well for a potential experimental realisation as discussed in Chapter 8.

Non-linear systems

7

So far, only linear quantum systems were considered. However, in many applications a non-linear variation of the Schrödinger equation (2-38) arises, which is often simply called the non-linear Schrödinger equation (NLSE) [213]. The corresponding time-independent eigenvalue problem then reads

$$\left(\frac{p^2}{2} + V + f(\psi)\right)|\psi\rangle = E\,|\psi\rangle\ , \tag{7-1}$$

where f is a non-linear functional of the wave function ψ. Thus, the Hamiltonian $\mathcal{H}(\psi)$ of such a non-linear system depends explicitly on its solution $|\psi\rangle$. In the case of

$$f(\psi) \propto |\psi|^2 = \langle\psi|\psi\rangle\ , \tag{7-2}$$

Eq. (7-1) is called the Gross–Pitaevskii equation (GPE) [214; 215], which describes a Bose–Einstein condensate (BEC) with contact interactions in optical potentials [179; 183; 192; 208; 216]. However, there is also a wide range of other systems described by a GPE [217; 218], such as light in paraxial approximation with a Kerr non-linearity [216; 219; 220], polarons [221–223], excitons [224], the propagation of radio waves in the ionosphere [225], or even the contraction of proteins [226].

There occur several mathematical obstacles regarding the NLSE (7-1). For one, there exists no basis[1] for non-linear quantum systems. This is because, technically speaking, every state of a non-linear system defines its own Hamiltonian. The only connection between these different systems is that their Hamiltonians arise from the non-linear form $\mathcal{H}(\psi)$ for a specific solution. Thus, there exists no mathematically rigorous, general framework for the treatment of non-linear NHQM. This makes an analytical treatment quite difficult, even for simple discrete systems. Hence, in most of these cases one must resort to numerical investigations.[2]

[1] This refers likewise to orthogonal and bi-orthogonal bases.

[2] *e.g.* see Ref. [150]

Further, there exist multiple sources for instabilities. Due to the superposition principle in linear QM, perturbations of a stationary state can only be caused by other eigenstates of the Hamiltonian. Hence, stationary solutions can only be considered stable if the imaginary parts of the eigenvalues of the other states are all negative; such states will decay exponentially and thus do not perturb the stationary state. If, on the other hand, one or more of the remaining states have an eigenvalue with positive imaginary part, this state and also its influence is amplified indefinitely, eventually leading to the destruction of the stationary state. This can be considered as a dynamical effect, as it requires the system to evolve in time. In non-linear systems, however, the stationary states themselves can also be unstable at the initial time. This is a general property of non-linear systems and it is discussed in detail in Section 7-2.

Nevertheless, the investigation of non-linear quantum systems also yields unique and highly practical properties. Remember that the existence of stationary solutions in the symmetrised systems discussed in Chapter 6 largely depends on precise choices of the parameters relative to each other.[3] If only one parameter is perturbed, the stationary solutions might vanish. This property is highly undesirable, particularly in experimental situations, where the accuracy of the parameters strongly depends on the experimental setup and the amount of control the experimentalist has over the system and its environment. This issue can be overcome by adding a non-linear part of the form (7-2) to the Hamiltonian of the system [150]. Therefore, this chapter is dedicated to the numerical investigation of stationary states in non-linear multi-mode systems and their stability properties.

[3] *i.e.* Eq. (6-16) and Eqs. (6-27) to (6-29)

7-1 Non-linear eigenvalue problems

A general, non-linear n-mode system with a non-linear term of the form (7-2) is described by the n-dimensional, tridiagonal matrix

$$\mathcal{H} = \begin{pmatrix} \epsilon_1 + \mathrm{i}\gamma_1 + g|\psi_1|^2 & -J & & \\ -J & \ddots & \ddots & \\ & \ddots & \ddots & -J \\ & & -J & \epsilon_n + \mathrm{i}\gamma_n + g|\psi_n|^2 \end{pmatrix} \tag{7-3}$$

which, for example, represents the mean-field description of a BEC in a one-dimensional optical lattice of length n, where the non-linear terms describe contact interactions. Equation (7-3) has the following parameters:[4]

[4] *cf.* Chapter 6

— The n real potential parameters ϵ_1, ..., ϵ_n provide only $n - 1$ degrees of freedom because of the gauge freedom of the energy.

— The n imaginary potential parameters γ_1, ..., γ_n, on the other hand, are all independent.

— The coupling constant J determines the exchange between neighbouring sites and can be set to $J = 1$ by a suitable choice of the energy unit.

— The strength g of the state-dependent non-linear part depends on properties of the system under consideration. Hence, it is assumed that g is given and that it is equal at each site.

In a linear quantum system[5] these parameters are sufficient to describe the linear Hamiltonian completely. However, for $g \neq 0$ the Hamiltonian (7-3) depends on its own state vector. Hence, in addition to the control parameters described above, one also has to consider the system parameters:

[5] *i.e.* $g = 0$

— The wave function is described by $2n$ real parameters. However, due to the freedom of the global phase, this yields only $(2n - 1)$ degrees of freedom.

— Because the energy in Eq. (7-1) is complex, there are another 2 degrees of freedom.

Assuming that all control parameters are given, the Schrödinger eigenvalue problem (2-39) is well determined, since it yields $(2n+1)$ conditions, including the normalisation of the wave function.

The fact that the Hamiltonian depends on its state vector also means that, technically speaking, each such non-linear matrix has only *one* solution. This immediately implies that there exists no bi-orthogonal basis for a non-linear quantum system. Thus, the eigenvectors and eigenvalues of a state-dependent Hamiltonian matrix cannot be obtained by ordinary algorithms for diagonalisation. Therefore, the following section is dedicated to the numerical procedures used in this thesis for finding solutions to non-linear systems.

a) Solving non-linear eigenvalue problems

"The Answer to the Great Question... Of Life, the Universe and Everything... Is... Forty-two," said Deep Thought, with infinite majesty and calm.

Douglas Adams

A time-dependent NLSE can in general be solved using the inverse scattering transform, where it appears as the compatibility condition of a Zakharov–Shabat system [227]. However, this thesis is mainly concerned in obtaining the solutions of the discrete GPE (7-1) and similar non-linear matrix eigenvalue problems which are not time-dependent but explicitly eigenvector-dependent. Such equations frequently occur in electronic structure calculations [228; 229] and, of course, for contact interactions in BECs [230]. However, most methods for solving non-linear eigenvalue problems either only work for a specific type of equations or are developed in the context of Hermitian QM. For these reasons, only purely numerical and also rather general methods are considered in the following.

Self-consistent field iteration

Note that the state-dependent matrix (7-24) yields an ordinary linear matrix after the insertion of the state; thus, it possesses n "solutions"[6] which can be calculated by usual means. If the inserted

[6] they are not necessarily solutions of the non-linear problem

state ψ_i is a solution of the non-linear eigenvalue problem, though, then it must also be one of the n solutions of the linear matrix, *i.e.* $\psi_o \overset{!}{=} \psi_\mathrm{i}$ for $o \in [0, n]$. However, if ψ_i is not a solution, it will differ from all resulting states ψ_o.

Under the assumption that the inserted state is already close to an actual solution, an iterative algorithm can be constructed if a suitable state $\psi_\mathrm{i}^{(k+1)}$ for the next iteration is chosen among the n eigenvectors resulting in the k-th step. This can be done with the condition $\max_o \langle \psi_\mathrm{i}^{(k)} | \psi_o^{(k)} \rangle$, which is satisfied by the eigenvector ψ_o being most similar to the inserted state ψ_i. Thus, the evolution of a specific state under the non-linear matrix may be traced. When the changes between the states in two consecutive steps is mall enough, this state can, within numerical limits, considered to be the solution of the non-linear eigenvalue problem. This approach is called a *self-consistent field iteration*, which is both intuitive and widely used, *e.g.* see Refs. [229; 231] and references therein.

The advantages of this approach clearly lie in its simplicity and in the fact that there are just simple operations involved which are numerically inexpensive. Thus, a self-consistent field iteration yields rather short run-times and scales quite well. If and if so under which circumstances the state vector converges is hard to determine beforehand, though, and these factors largely depend on the quality of the initial choice of the state; this may be chosen randomly or can simply be guessed. However, if the non-linear terms are small in comparison with the other matrix elements, then the solutions of the corresponding linear problem with $\psi_\mathrm{i}^{(0)} = 0$ can provide suitable approximations for the solutions of the non-linear problem.

Enumerative optimisation

While the self-consistent field iteration approach is motivated by physical considerations and works particularly well if the non-linearity occurs as a perturbation of the linear eigenvalue problem, it heavily relies on the initial choice of the inserted state. If the heuristic approach of using the solutions of the linear problem fails, one is forced to resort to guesswork, which may even in the

simplest cases be unfeasible. Moreover, with this approach the number of initial guesses is limited to the dimension n of the linear eigenvalue problem, whereas there may exist more solutions for the non-linear eigenvalue problem.

Both of these reasons above make it necessary to have a joker in one's sleeve, so to speak. Numerically, the last resort always is the *numerical variation*, which essentially means to solve an equation via a root search algorithm. This approach is applicable in almost any situation, although convergence is not guaranteed either and, in general, depends on the complexity of the problem and again also on the initially guessed solution.

The issue with the initial guess may be resolved by an *enumerative optimisation*, which combines a root search algorithm with the enumerative approach to use all different combinations of initial parameters from a specific subspace of the parameter space. If the grid points in the parameter space are chosen densely enough, chances are good that all solutions in this region are found. Moreover, since most root search algorithms are implemented with some heuristic of their own, they can also explore regions outside of the initial parameter region and retrieve solutions in its surroundings.

While the enumerative optimisation approach is, in principle, limited only by the computational hardware at hand, calculations may take long amounts of time depending on the grid size and density. They also scale rather poorly with the dimensionality of the problem and can become increasingly error-prone due to the complexity of the multi-dimensional parameter landscape. Therefore, such numerical variational approaches are considered as brute-force methods, which might not be fast but should still work practically in all situations.

7-2 Stability of stationary solutions

In contrast to linear systems, the stability of states is not *a priori* clear. This becomes apparent by considering the most simple type of a non-linear system, that is a one-dimensional quadratic

potential. Figures 7-1 and 7-2 show the two fundamentally different types of quadratic potentials, *i.e.* they possess a stable and an unstable equilibrium point, respectively. *Stable* means that the system remains close to its equilibrium state if it is perturbed; *unstable* means the opposite and in most cases the system actually deviates exponentially from its equilibrium after a perturbation. From a physical point of view such unstable equilibria must not be considered as stationary solutions at all, since they mathematically represent singularities.[7] Such an equilibrium is never observable in nature or in a lab, since there exist uncertainty relations which prevent both their preparation and their preservation.

[7] Here, the term "singularity" is used in a system-theoretic context and means a singular point at which a small perturbation causes the system to change its behaviour completely.

Yet, unstable equilibria are still of mathematical interest: In classical double-well potentials there exist two stable equilibria — one in each well, respectively — and one unstable equilibrium on top of the potential barrier separating the two wells. In fact, the unstable equilibrium represents the threshold for transitions between the two wells; that is, if a particle which is located in one well possesses enough energy to reach the unstable equilibrium, then it can transition into the other well. This occurs, for example, in the *Kramers escape problem* [232], which belongs to the field of *transition state theory*, *e.g.* see [233; 234].

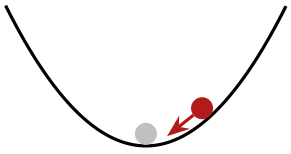

Figure 7-1: Stable

The situation in non-linear and potentially multi-dimensional systems is in general more complex and there may exist multiple equilibrium points. To determine if a certain equilibrium is either stable or unstable, it is, in principle, sufficient to study the response of the system with respect to small perturbations, *i.e.* its *linear stability*. However, linear stability does not imply that the system is also stable with respect to stronger perturbations; it only shows that the system is stable for sufficiently small perturbations. In general, linear stability is a weaker form of stability as it also covers *metastable equilibria* that are linearly stable but otherwise unstable.

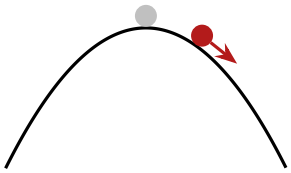

Figure 7-2: Unstable

In the first part of this section, linear stability is considered for general dynamical systems. To give an example, these results are then applied explicitly to the two-mode matrix model introduced in Section 6-1 b). It is shown that this corresponds to the Bogoliubov–de Gennes equations (BdGE) — a linear system of equations which

can be used to determine the linear stability of solutions of the GPE [150; 235].

a) Linear stability in dynamical systems

A general, dynamic system can be described by its equations of motion

$$\dot{\mathbf{z}} = \mathbf{d}(\mathbf{z})\,, \tag{7-4}$$

where $\mathbf{z} \in \mathbb{C}^N$. A fixed point solution $\mathbf{z}_0$ satisfies $\dot{\mathbf{z}}_0 = \mathbf{d}(\mathbf{z}_0) = 0$. To determine its stability, a perturbation can be introduced, so that

$$\mathbf{z}(t) = \mathbf{z}_0 + \delta\mathbf{z}(t) \tag{7-5}$$

with $|\delta\mathbf{z}_i| \ll 1$. The equations of motion (7-4) in the proximity of the fixed point then read

$$\mathbf{d}(\mathbf{z}) = \underbrace{\mathbf{d}(\mathbf{z}_0)}_{=0} + \delta\mathbf{z}\,\frac{\partial \mathbf{d}}{\partial \mathbf{z}}\bigg|_{\mathbf{z}_0} + O\left(\delta\mathbf{z}^2\right) = \frac{\mathrm{d}}{\mathrm{d}t}\delta\mathbf{z}\,.$$

This yields a differential equation,

$$\frac{\mathrm{d}}{\mathrm{d}t}\delta\mathbf{z} = J_d\,\delta\mathbf{z}\,, \tag{7-6}$$

which describes the dynamics of the perturbation with the Jacobian matrix

$$[J_d]_{kl} = \frac{\partial d_k}{\partial z_l}\bigg|_{\mathbf{z}_0} \tag{7-7}$$

evaluated at the fixed point. The solution of Eq. (7-6) is given by

$$\delta\mathbf{z}(t) = \mathrm{e}^{J_d t}\,\delta\mathbf{z}(0)\,,$$

where $\delta\mathbf{z}(0)$ is the perturbation at time $t = 0$. If the perturbations $\delta\mathbf{z}_k(0)$ are chosen as eigenvectors of the Jacobian matrix J_d, then the corresponding eigenvalues j_k determine whether the system is

stable or unstable under such a perturbation, *i.e.*

$$\delta \mathbf{z}_k(t) = \mathrm{e}^{j_k t}\, \delta \mathbf{z}_k(0)\,. \tag{7-8}$$

That is, if $\operatorname{Re} j_k > 0$, then the perturbation $\delta \mathbf{z}_k(0)$ is amplified exponentially, which means that $\mathbf{z}_0$ is unstable. For $\operatorname{Re} j_k < 0$ the perturbation is damped off and the system returns to its stable equilibrium state $\mathbf{z}_0$. The imaginary parts $\operatorname{Im} j_k$, on the other hand, merely describe oscillations around the fixed point, which makes them unimportant for a stability analysis. Changes of stability can be connected to bifurcations[8] which occur in NHQM at EPs as discussed in Section 4-3 a); though, they may also occur at non-exceptional points.[9]

[8] *e.g.* see Fig. 7-3

[9] *cf.* Section 7-4 b)

b) Linear stability of non-linear quantum systems

In principle, the linearisation of a non-linear quantum system described by Eq. (7-1) is straightforward and leads to an equation similar to Eq. (7-8): With an ansatz of the form $\psi(t) = \psi_0 + \delta\psi(t)$, where ψ_0 again describes a fixed point solution,

$$\mathrm{i}\frac{\mathrm{d}\psi_0}{\mathrm{d}t} = (\mathcal{H} - \mu\mathbb{1})\psi_0 = 0\,.$$

Here, the energy has to be shifted by the eigenvalue μ because a fixed point solution must not evolve in time, *i.e.* it corresponds to the eigenvalue $\mu = 0$. However, care has to be taken due to the appearance of the absolute square $|\delta\psi|^2$ of the wave function; it is not holomorphic for $\delta\psi \neq 0$, *i.e.*

$$\begin{aligned}
\frac{\partial \operatorname{Re}|\delta\psi_k|^2}{\partial \operatorname{Re}(\delta\psi_k)} &= 2\operatorname{Re}(\delta\psi_k) \neq 0 = \frac{\partial \operatorname{Im}|\delta\psi_k|^2}{\partial \operatorname{Im}(\delta\psi_k)}\,,\\
\frac{\partial \operatorname{Re}|\delta\psi_k|^2}{\partial \operatorname{Im}(\delta\psi_k)} &= 2\operatorname{Im}(\delta\psi_k) \neq 0 = \frac{\partial \operatorname{Im}|\delta\psi_k|^2}{\partial \operatorname{Re}(\delta\psi_k)}\,.
\end{aligned}$$

Hence, the complex derivatives required for the calculation of the Jacobian matrix (7-7) are not well defined.

To solve this issue there are basically two possible approaches:

1) The N-dimensional complex wave function can be described by up to $2N$ real parameters[10] $\mathbf{z}$, *i.e.* $\psi(\mathbf{z})$. Then, the absolute square, being a real function of the parameters, is differentiable with respect to z_k, respectively. The ansatz (7-5) corresponds to a perturbation of the wave function

$$\delta\psi(t) = \psi(\mathbf{z}_0 + \delta\mathbf{z}(t)) - \psi(\mathbf{z}_0) \approx \delta\mathbf{z}(t)\, \frac{\partial\psi}{\partial\mathbf{z}}\bigg|_{\mathbf{z}_0}$$

in linear order. This approach is particularly suited if the wave function is already parametrised by a set of real quantities.

2) By distinguishing between left-hand and right-hand wave functions explicitly, the absolute square can be considered to be a linear function,

$$|\psi_k|^2 = \overline{\psi}_k \underline{\psi}_k \,, \tag{7-9}$$

where $\overline{\psi}_k \equiv \psi_k^*$ and $\underline{\psi}_k \equiv \psi_k$ are the left-hand and right-hand wave functions, respectively, which differ only by a complex conjugation for complex symmetric matrices. In this case, Eq. (7-9) is complex differentiable with respect to both $\overline{\psi}_k$ and $\underline{\psi}_k$, *i.e.* they are considered to be independent.

[10] Due to the global phase and the norm, the degrees of freedom of the wave function can be reduced at least to $2N-2$.

In the following, the second option is considered. The equations of motion for $\underline{\psi}$ and $\overline{\psi}$ are given by

$$\mathrm{i}\dot{\underline{\psi}} = \left[\mathcal{H}\left(\underline{\psi}, \overline{\psi}\right) - \mu\mathbb{1}\right]\underline{\psi} \,, \tag{7-10}$$

$$\mathrm{i}\dot{\overline{\psi}} = -\left[\mathcal{H}^*\left(\underline{\psi}, \overline{\psi}\right) - \mu^*\mathbb{1}\right]\overline{\psi} \,, \tag{7-11}$$

where Eq. (7-11) is merely the complex conjugate of Eq. (7-10). However, if the Hamiltonian is complex symmetric, *i.e.* $\mathcal{H}^* = \mathcal{H}^\dagger$, Eq. (7-11) corresponds, in fact, to the correct left-hand eigenvalue equation. Hence, $\underline{\psi}$ and $\overline{\psi}$ can be considered as independent quantities corresponding to the different Hamiltonians

$$\widetilde{\mathcal{H}}\left(\underline{\psi}, \overline{\psi}\right) \equiv \mathcal{H}\left(\underline{\psi}, \overline{\psi}\right) - \mu\mathbb{1} \,,$$

$$-\widetilde{\mathcal{H}}^*\left(\underline{\psi},\overline{\psi}\right) \equiv -\mathcal{H}^*\left(\underline{\psi},\overline{\psi}\right) + \mu^* \mathbb{1}\,. \tag{7-12}$$

The minus sign in Eq. (7-12) is not only important because it makes the Hamiltonians distinct, but also because it provides the correct time evolution for left-hand wave functions with respect to the ordinary Schrödinger equation; hence, from this "perspective" the left-hand wave functions evolve backwards in time.

The corresponding left-hand and right-hand wave functions can now be combined into a single vector $\phi \equiv (\underline{\psi},\overline{\psi})^{\mathsf{T}}$, for which the "Schrödinger equation" reads

$$\mathrm{i}\dot{\phi} = \begin{pmatrix} \widetilde{\mathcal{H}}(\phi) & 0 \\ 0 & -\widetilde{\mathcal{H}}^*(\phi) \end{pmatrix} \phi \equiv h(\phi)\,. \tag{7-13}$$

A stationary solution ϕ_0 then satisfies $\mathrm{i}\dot{\phi}_0 = h(\phi_0) = 0$. A perturbation of ϕ_0 evolves in time according to

$$\delta\phi(t) = \mathrm{e}^{-\mathrm{i}J(\phi_0)t}\delta\phi(0)\,, \tag{7-14}$$

where

$$J_{kl}(\phi_0) = \left.\frac{\partial h_k}{\partial \phi_l}\right|_{\phi_0}\,. \tag{7-15}$$

By again assuming that the initial perturbations $\delta\phi(0)$ are eigenstates of the Jacobian matrix (7-15), the problem reduces to the eigenvalue problem

$$J_h(\phi_0)\delta\phi_k = \omega_k \delta\phi_k\,. \tag{7-16}$$

Perturbations are damped off if $\operatorname{Im}\omega_k < 0$, *i.e.* ϕ_0 is stable if this condition holds for all eigenvalues ω_k of J.

Some remarks about Eqs. (7-14) and (7-15) are listed below:

1) $\delta\phi$ corresponds to a simultaneous perturbation of the left-hand and right-hand stationary states.

2) In a linear system the state can only be perturbed by another state solution of the Schrödinger equation due to the superposition principle. Hence, one can easily show that the stability

eigenvalues ω_k of Eq. (7-16) are given by the energy differences between the stationary state under consideration and the perturbing state. This immediately shows that a linear system is stable if all eigenvalues are real, *i.e.* perturbations with other eigenstates will just cause oscillations of the system around the stationary solution.

3) In contrast to Eq. (7-8), an additional imaginary unit appears in the exponential function. This is because the Jacobian matrix (7-15) corresponds to the Schrödinger-type equation (7-13) instead of the classical type of equations of motion $\dot{\phi} = -\mathrm{i}h(\phi)$ discussed in Section 7-2 a). Therefore, the imaginary parts of the eigenvalues now determine the stability of the states. This definition seems to be more natural for quantum systems and leads to the BdGE as shown in Section 7-2 c).

4) It is not surprising that not all components of the Jacobian matrix (7-15) are independent. In fact, only half of its components have to be calculated. One may write Eq. (7-13) in the form $h(\phi) = (\underline{h}, \bar{h})^\mathsf{T}$. Then

$$\frac{\partial \underline{h}_k}{\partial \underline{\psi}_l} = -\frac{\partial \bar{h}_k^*}{\partial \underline{\psi}_l} = -\left(\frac{\partial \bar{h}_k}{\partial \bar{\psi}_l}\right)^*,$$
$$\frac{\partial \underline{h}_k}{\partial \bar{\psi}_l} = -\frac{\partial \bar{h}_k^*}{\partial \bar{\psi}_l} = -\left(\frac{\partial \bar{h}_k}{\partial \underline{\psi}_l}\right)^*.$$

[11] *cf.* Eq. (7-19)

Therefore, the Jacobian matrix has the form[11]

$$J_h = \begin{pmatrix} A & B \\ -B^* & -A^* \end{pmatrix}. \tag{7-17}$$

Nevertheless, all eigenvalues of J_h have to be calculated, since Eq. (7-17) is not symmetric *per se*.

5) The numerical calculation of the Jacobian matrix (7-15) is straightforward: The derivatives of $h_k(\phi_1, \ldots, \phi_N)$ can be well approximated by the finite difference

$$\frac{\partial h_k}{\partial \phi_l} = \frac{h_k(\ldots, \phi_l + \Delta, \ldots) - h_k(\ldots, \phi_l - \Delta, \ldots)}{2\Delta} + O\left(\Delta^2\right),$$

which can readily be obtained from the Taylor expansions of $h_k(\dots, \phi_l + \Delta, \dots)$ and $h_k(\dots, \phi_l - \Delta, \dots)$ around ϕ_l. The parameter $\Delta \ll 1$ represents a small change in the variable ϕ_l. For $\Delta \to 0$ the derivative of $h_k(\phi)$ can be obtained exactly. However, any computer can only provide a finite precision. Moreover, calculations with very small numbers introduce not only rounding errors, but can also lead to a reduction of the number of significant digits due to cancellation. Hence, care has to be taken in choosing the value of Δ, which must not be too large nor too small.

c) Linear stability of the two-mode model

As an example, the linear stability analysis is now applied to a nonlinear, state-dependent two-mode matrix model. For the Hamiltonian (7-3) with $n = 2$ one finds

$$h(\underline{\psi}, \overline{\psi}) = \begin{pmatrix} (\epsilon_1 + \mathrm{i}\gamma_1 + g\underline{\psi}_1\overline{\psi}_1 - \mu)\underline{\psi}_1 - J\underline{\psi}_2 \\ (\epsilon_2 + \mathrm{i}\gamma_2 + g\underline{\psi}_2\overline{\psi}_2 - \mu)\underline{\psi}_2 - J\underline{\psi}_1 \\ -(\epsilon_1 - \mathrm{i}\gamma_1 + g\overline{\psi}_1\underline{\psi}_1 - \mu^*)\overline{\psi}_1 + J\overline{\psi}_2 \\ -(\epsilon_2 - \mathrm{i}\gamma_2 + g\overline{\psi}_2\underline{\psi}_2 - \mu^*)\overline{\psi}_2 + J\overline{\psi}_1 \end{pmatrix}$$

and its Jacobian matrix

$$J_h = \begin{pmatrix} \epsilon_1+\mathrm{i}\gamma_1+2g\underline{\psi}_1\overline{\psi}_1-\mu & -J & g\underline{\psi}_1^2 & 0 \\ -J & \epsilon_2+\mathrm{i}\gamma_2+2g\underline{\psi}_2\overline{\psi}_2-\mu & 0 & g\underline{\psi}_2^2 \\ -g\overline{\psi}_1^2 & 0 & -\epsilon_1+\mathrm{i}\gamma_1-2g\underline{\psi}_1\overline{\psi}_1+\mu^* & J \\ 0 & -g\overline{\psi}_2^2 & J & -\epsilon_2+\mathrm{i}\gamma_2-2g\underline{\psi}_2\overline{\psi}_2+\mu^* \end{pmatrix}\Bigg|_{\substack{\underline{\psi}=\underline{\psi}_0 \\ \overline{\psi}=\overline{\psi}_0}}, \tag{7-18}$$

where $\epsilon_1 = -\epsilon_2 = \epsilon$, $\gamma_1 = \gamma(1 + \delta)$, and $\gamma_2 = -\gamma(1 - \delta)$.

Equation (7-16) with Eq. (7-18) corresponds to the Bogoliubov–de Gennes equations (BdGE) for the two-mode matrix model. This becomes clear if Eqs. (7-16) and (7-18) are rewritten in the form

$$\begin{pmatrix} \mathcal{H}_0(\underline{\psi}_0, \overline{\psi}_0) - \mu\mathbb{1} & \Delta(\underline{\psi}_0) \\ -\Delta^*(\overline{\psi}_0) & -\mathcal{H}_0^*(\underline{\psi}_0, \overline{\psi}_0) + \mu^*\mathbb{1} \end{pmatrix} \begin{pmatrix} \delta\underline{\psi} \\ \delta\overline{\psi} \end{pmatrix} = \omega \begin{pmatrix} \delta\underline{\psi} \\ \delta\overline{\psi} \end{pmatrix}, \tag{7-19}$$

where $\mathcal{H}_0(\underline{\psi}_0, \overline{\psi}_0)$ is the Hamiltonian (6-5) with twice the non-linear coupling strength, that is $g \to 2g$, evaluated at the stationary solution and

$$\Delta\left(\underline{\psi}_0\right) \equiv \begin{pmatrix} g\underline{\psi}_1^2 & 0 \\ 0 & g\underline{\psi}_2^2 \end{pmatrix}\Bigg|_{\underline{\psi}=\underline{\psi}_0} ,$$

$$\Delta^*\left(\overline{\psi}_0\right) \equiv \begin{pmatrix} g\overline{\psi}_1^2 & 0 \\ 0 & g\overline{\psi}_2^2 \end{pmatrix}\Bigg|_{\overline{\psi}=\overline{\psi}_0} .$$

Equation (7-19) describes a linear system of coupled equations for $\delta\underline{\psi}$ and $\delta\overline{\psi}$,

$$(\mu + \omega)\delta\underline{\psi} = \mathcal{H}_0\left(\underline{\psi}_0, \overline{\psi}_0\right)\delta\underline{\psi} + \Delta\left(\underline{\psi}_0\right)\delta\overline{\psi} , \tag{7-20}$$

$$\left(\mu^* - \omega\right)\delta\overline{\psi} = \mathcal{H}_0^*\left(\underline{\psi}_0, \overline{\psi}_0\right)\delta\overline{\psi} + \Delta^*\left(\overline{\psi}_0\right)\delta\underline{\psi} , \tag{7-21}$$

which can be obtained from the "ordinary" right-hand GPE with the ansatz

$$\psi(t) = \mathrm{e}^{-\mathrm{i}\mu t}\left(\psi_0 + \lambda\psi_\mathrm{p}(t)\right) , \tag{7-22}$$

where ψ_0 is the fixed point solution and $\delta\psi = \lambda\psi_\mathrm{p}(t)$ with $\lambda \in \mathbb{R}$ is a small perturbation, *i.e.* $|\lambda| \ll 1$. Instead of shifting the energy suitably as before, so that the unitary time evolution vanishes, the ansatz (7-22) includes the correct time evolution.

A suitable ansatz for the perturbation is given by

$$\psi_\mathrm{p}(t) = \delta\underline{\psi}\,\mathrm{e}^{-\mathrm{i}\omega t} + \delta\overline{\psi}^*\,\mathrm{e}^{\mathrm{i}\omega^* t} , \tag{7-23}$$

which resembles the general solutions for a wave equation or an oscillator equation. Again, $\delta\underline{\psi}$ and $\delta\overline{\psi}$ are considered to be independent, simultaneous perturbations of the left-hand and right-hand stationary states. After plugging Eqs. (7-22) and (7-23) into the GPE, a comparison of the coefficients of $\exp(-\mathrm{i}\omega t)$ and its complex conjugate can be performed. This yields the BdGE (7-20) and (7-21) in linear order of λ.

The ansatz (7-23) also reveals a symmetry of the BdGE (7-20) and (7-21): The replacements $\delta\underline{\psi} \to \delta\overline{\psi}^*$ and $\delta\overline{\psi}^* \to \delta\underline{\psi}$ immediately

show that for every stability eigenvalue ω with $(\delta\underline{\psi}, \delta\overline{\psi})^\mathsf{T}$, also $-\omega^*$ is a solution with $(\delta\underline{\psi}^*, \delta\overline{\psi}^*)^\mathsf{T}$; that is, the real part of the spectrum is symmetric. However, the linear stability is governed only by the imaginary parts of the eigenvalues, which are two-fold degenerate.

7-3 Symmetrisation in non-linear systems

The concept of symmetrisation in linear quantum systems was already introduced in Chapter 5. Now, one could simply try to apply this concept to non-linear systems of the form

$$\mathcal{H} = \mathcal{H}_\mathrm{lin} + f(\psi)\,, \tag{7-24}$$

where $f(\psi)$ is given by Eq. (7-2) and $\mathcal{H}_\mathrm{lin}$ is a linear, complex symmetric Hamiltonian. Yet, also the resulting Hamiltonian (7-24) is still complex symmetric, *i.e.* Eq. (5-54) holds. In particular, this means that left-hand and right-hand eigenstates are complex-conjugate, which in turn again implies the property (5-55) for the symmetrisation operators.

In analogy to Ref. [208], where a BEC in a $\mathcal{PT}$-symmetric double-well potential is considered, the existence of symmetrisation operators in non-linear systems can be considered by symmetrising Eq. (7-24) via the condition (5-15) while assuming that the linear part is always symmetrised; this yields

$$\overline{S} f(\psi) = f^\dagger\big(\overline{S}\psi\big)\overline{S}\,. \tag{7-25}$$

However, as discussed in Section 7-1, a non-linear quantum system has neither an orthogonal nor a bi-orthogonal basis anymore. This is because only one eigenstate can be considered to be a solution of the matrix obtained by using the very same state. Thus, every state defines its own Hamiltonian matrix and one cannot *a priori* expect to find the same symmetrisation operators for multiple — let alone all — states, as it is possible in linear systems. Instead, one finds that Eqs. (5-14) and (5-15) can still be satisfied,

but there exists a pair of symmetrisation operators $\overline{S}$ and $\underline{S}$ for every single state with real energy eigenvalue. This corresponds to symmetrised linear systems with $\operatorname{rank}\overline{S} = \operatorname{rank}\underline{S} = 1$. Though, terms such as "rank" and "kernel" are no longer well defined because the states do not form a basis in non-linear systems. It may thus seem preposterous to consider symmetrisation for non-linear systems, as most of the information contained in the symmetrisation operators is redundant. Nevertheless, such systems formally are semi-symmetrised and the evaluation of the symmetrisation operators may still yield some physical insight as discussed below.

This does not only hold for states with real energy eigenvalues, but also for complex-conjugate pairs, as such states share the same symmetrisation operators for a non-linear system of the form (7-24) with $f(\psi) \propto |\psi|^2$. This is because the absolute square is invariant under complex conjugation,

$$\langle\psi|\psi\rangle = \langle\psi|\psi\rangle^* = \langle\psi^*|\psi^*\rangle\,,$$

i.e. the states $|\psi\rangle$ and $|\psi^*\rangle$, which correspond to complex-conjugate energy eigenvalues for a complex symmetric system, share the same non-linear Hamiltonian. Hence, for every eigenstate $|\psi\rangle$, for which the non-linear functional f satisfies the relation (7-25), the corresponding eigenvalue should still be real or there should exist another eigenstate corresponding to the complex-conjugate energy eigenvalue which shares the same set of symmetrisation operators.

Because $f(\psi) = \langle\psi|\psi\rangle$ is both scalar and real, Eq. (7-25) reduces to $f(\overline{S}\psi) = f(\psi)$, *i.e.* the non-linear functional must be invariant under the insertion of the left-hand symmetrisation operator; an equivalent condition can be obtained for the right-hand symmetrisation operator. Hence, symmetrisation operators are required to be unitary[12] in the non-linear case. However, since symmetrisation operators are also necessarily Hermitian, they are in fact involutory. Hence, the symmetrisation operators must be part of the cyclic group $\mathbb{Z}_2$ in general, which corresponds to generalisations of the parity operator (5-46). The corresponding symmetries are anti-linear like $\mathcal{PT}$ symmetry and its generalisations as discussed in Chapter 5. It should be noted that these considerations do not only hold for the specific non-linear functional (7-2), but for all

[12] *cf.* Section 5-3 d)

functionals f being invariant under a change of the global phase of the wave function ψ.

In contrast to an actual symmetry like $\mathcal{PT}$ symmetry, though, the separation of the linear and the non-linear parts represents a special case. That is, a symmetry may involve the same operator in both the linear and non-linear system. Symmetrisation, however, involves completely different symmetrisation operators which depend explicitly on the state solutions. Yet, the full non-linear problem obtained by plugging Eq. (7-24) into the symmetrisation conditions (5-14) and (5-15) cannot be solved by analytical means. Though, it can still be solved by the method described in Section 5-5 a), if suitable control parameters are known for which the Hamiltonian possesses at least one real or two complex-conjugate energy eigenvalues. While this method is used and further discussed in the following sections, one could also attempt to solve the complete problem involving the Schrödinger eigenvalue equation (2-39) and at least one of the symmetrisation conditions Eqs. (5-14) and (5-15). This requires at least an $(n+1)^2$-dimensional root search for an n-mode system, assuming that all control parameters are known already. For every additional control parameter an additional condition has to be postulated, the nature of which is, however, not *a priori* clear. For example, if one of the potential parameters is free, one could require that one of the symmetrisation operators is normalised, *i.e.* $\operatorname{tr}\bar{S} = 1$.

Symmetrisation is now discussed explicitly in the context of non-linear two-mode systems. In this case, $\mathcal{H}_{\text{lin}}$ is given by the Hamiltonian (6-9) combined with

$$f(\psi) = \begin{pmatrix} g|\psi_1|^2 & 0 \\ 0 & g|\psi_2|^2 \end{pmatrix}, \tag{7-26}$$

where the non-linearity parameter g is considered to be equal in both modes.

Under the assumption that Eq. (5-15) still holds for the linear part, *i.e.* $\bar{S}\mathcal{H}_{\text{lin}} = \mathcal{H}_{\text{lin}}^{\dagger}\bar{S}$, the non-linear part has to satisfy the symmetrisation condition separately as discussed in Section 7-3.

The left-hand side of this equation yields

$$\bar{S}\mathcal{H}\,|\underline{\psi}\rangle = \frac{g\kappa}{2}\begin{pmatrix}\bar{S}_{11} & -\bar{S}_{12}\\ \bar{S}_{21} & -\bar{S}_{22}\end{pmatrix}, \tag{7-27}$$

where $\kappa = |\psi_1|^2 - |\psi_1|^2$ is the imbalance between the two sites. Note that the wave function is included explicitly, since the non-linear term κ depends on the state on which the operators act. This is in particular important when the right-hand side is evaluated, which yields

$$\mathcal{H}\bar{S}\,|\underline{\psi}\rangle = \frac{g\kappa_S}{2}\begin{pmatrix}\bar{S}_{11} & -\bar{S}_{12}\\ \bar{S}_{21} & -\bar{S}_{22}\end{pmatrix} \tag{7-28}$$

with

$$\kappa_S = \left|\left(\bar{S}\psi\right)_1\right|^2 - \left|\left(\bar{S}\psi\right)_2\right|^2.$$

The only difference between Eqs. (7-27) and (7-28) is in the non-linear terms κ and κ_S. Therefore, the non-linear part of the Hamiltonian can satisfy Eq. (5-15) if and only if $\kappa = \kappa_S$. To satisfy this condition, there exist two different scenarios:

1) For $\kappa = \kappa_S = 0$ one must require that $|\psi_1|^2 = |\psi_2|^2$, *i.e.* both sites are equally occupied, which has to be preserved by $\bar{S}$. The equal occupation of the sites in a non-Hermitian two-mode system is a characteristic property of $\mathcal{PT}$ symmetry. Hence, one can conclude that $\bar{S}$ is either equal to the parity operator $\mathcal{P}$ or is a generalisation of it.

2) For $\kappa = \kappa_S \neq 0$ one would demand that $|(\bar{S}\psi)_k| = |\psi_k|$ for $k = 1, 2$. This case has already been described in Section 7-3 and requires an involutory symmetrisation operator. While this is still compatible with $\mathcal{PT}$ symmetry, it also allows for unequal occupations of the two sites.

7-4 Non-linear two-mode model

A general, non-linear two-mode model is described by the linear Hamiltonian (6-9) combined with the non-linear term (7-26). However, this can be written in a more symmetric form by using Eq. (6-5) instead [150] and by applying the non-linear energy shift [186]

$$\delta E = -\frac{g}{2}\left(|\psi_1|^2 + |\psi_2|^2\right). \tag{7-29}$$

The Hamiltonian of the non-linear two-mode model then reads

$$\mathcal{H}(\psi) = \begin{pmatrix} \epsilon + \mathrm{i}\gamma(1+\delta) + \frac{g}{2}\left(|\psi_1|^2 - |\psi_2|^2\right) & -J \\ -J & -\epsilon - \mathrm{i}\gamma(1-\delta) - \frac{g}{2}\left(|\psi_1|^2 - |\psi_2|^2\right) \end{pmatrix}. \tag{7-30}$$

The energy shift (7-29) affects only the real part of the spectrum which is now distributed "symmetrically"[13] around $E = 0$. Another advantage of Eq. (7-30) again is that the parameter δ naturally describes perturbations of the $\mathcal{PT}$-symmetric system for $\epsilon = 0$, as already discussed in Section 6-1 c) for the linear model. Further, the real potential can be described completely by one parameter ϵ due to the gauge freedom of the energy. This freedom is used once again to make the real potential anti-symmetric, *i.e.* $\epsilon_1 = -\epsilon_2$.

[13] Only in the $\mathcal{PT}$-symmetric case the real part of the spectrum is exactly symmetric.

a) Non-linear $\mathcal{PT}$-symmetric two-mode model

The $\mathcal{PT}$-symmetric two-mode model is obtained from Eq. (7-30) with $\epsilon = \delta = 0$ and can be solved analytically [186]. However, this provides a suitable opportunity to test the implementation of the numerical methods discussed in Section 7-1 a).

The numerically obtained complex eigenvalues of the non-linear, $\mathcal{PT}$-symmetric two-mode system are shown in Fig. 7-3 for different values of the non-linearity parameter g. This immediately reveal some fundamental differences between linear and non-linear systems: While there exist only two solutions of the eigenvalue problem (2-39) in a linear two-mode system, in the $\mathcal{PT}$-symmetric, non-linear two-mode system there exist up to four solutions of the

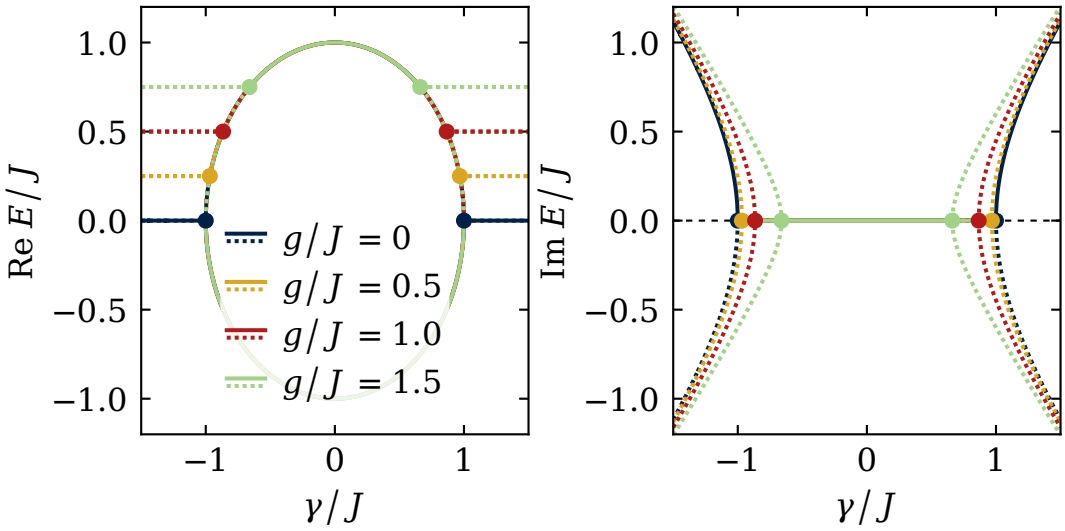

Figure 7-3: Real and imaginary parts of the eigenvalues of the two-mode model (7-30) with $\epsilon = 0$ and $\delta = 0$. The energies are real for $\gamma \leq |\gamma_c|$, where $|\gamma_c|$ decreases for increasing values of the non-linearity strength. Here, solid and dotted lines indicate stable and unstable states, respectively.

form

$$\psi = \begin{pmatrix} \sqrt{\frac{1+\kappa}{2}}\, e^{-i\varphi} \\ \sqrt{\frac{1-\kappa}{2}}\, e^{i\varphi} \end{pmatrix} \tag{7-31}$$

with the imbalance κ introduced in Section 7-3 and a phase φ. Two of these solutions are real and exist for $|\gamma/J| \leq 1$. They represent balanced gain and loss and require $\kappa = 0$, so that both wells are equally occupied; this corresponds to *exact $\mathcal{PT}$ symmetry*. However, for $\gamma^2 \geq J^2 - g^2/4$, two complex solutions with $\kappa \neq 0$ exist, which are complex-conjugate to each other. These are the *broken $\mathcal{PT}$-symmetric* solutions which overlap with the $\mathcal{PT}$-symmetric solutions for $g \neq 0$, so that four solutions occur simultaneously. It is worth emphasising that the absolute value of γ, at which complex solutions arise, decreases with the strength of the non-linearity parameter g; a similar property becomes quite important in Section 7-4 b).

Next, the stability of the states must be considered because the system is both non-Hermitian and non-linear. Hence, there exist two mechanisms for instability:

1) As discussed in Section 7-2, there exist both linearly stable and unstable stationary states in non-linear systems.

2) Because there occur complex energy eigenvalues, the probability density of the states can change in time, which is also considered

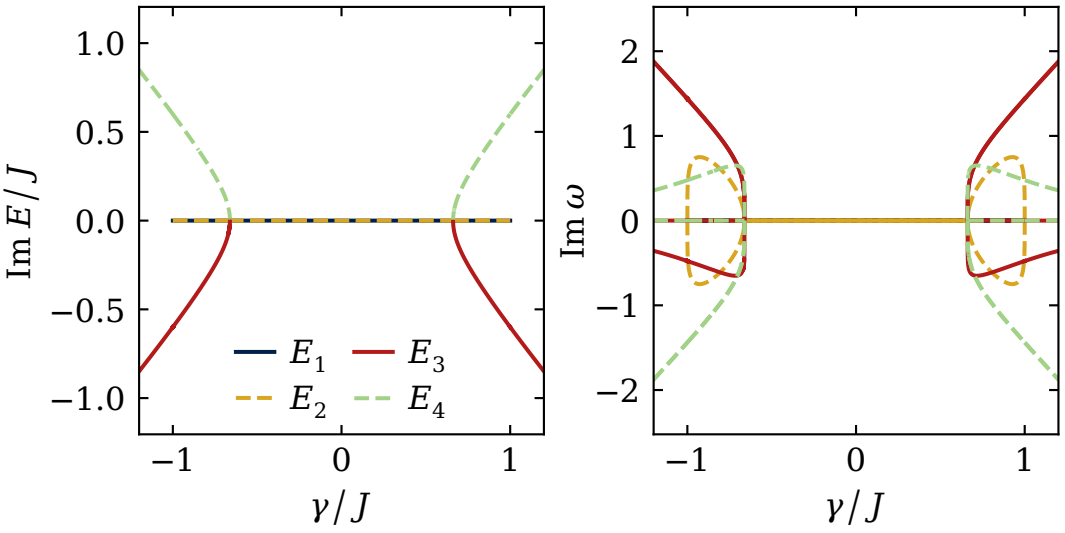

Figure 7-4: Stability eigenvalues for the solutions of the non-linear $\mathcal{PT}$-symmetric two-mode model with $g = 1.5J$ as shown in Fig. 7-3. For reference, the corresponding imaginary parts of the energy eigenvalues are shown using different colours.

as being unstable with respect to stationarity. Additionally, an ever growing state may also perturb other states in the system, which can directly be observed in linear QM. This additional effect is of particular importance in Sections 7-4 b) and 7-5.

The stability of the states in Fig. 7-3 is indicated by solid and dotted lines which represent stable and unstable states, respectively. Note that in contrast to the stability matrix from Ref. [186], the Jacobian matrix (7-18) is used to determine the stability of the states. The stability eigenvalues, which correspond to the different states, are shown in Fig. 7-4 for the strong non-linear case with $g = 1.5J$. Due to the symmetry of the wave function, the stability eigenvalues can occur only in complex-conjugate pairs for an exactly $\mathcal{PT}$-symmetric system.

As mentioned in Section 7-2 b), in a linear system all states are stable in the range in which only real energies occur. However, this property also holds for non-linear $\mathcal{PT}$-symmetric systems. Stability changes occur only when the additional states appear, which is indicated by the positive imaginary parts of the stability eigenvalues in Fig. 7-4. In particular, this means that one of the real states becomes unstable due to the occurrence of other states with complex energy eigenvalues.

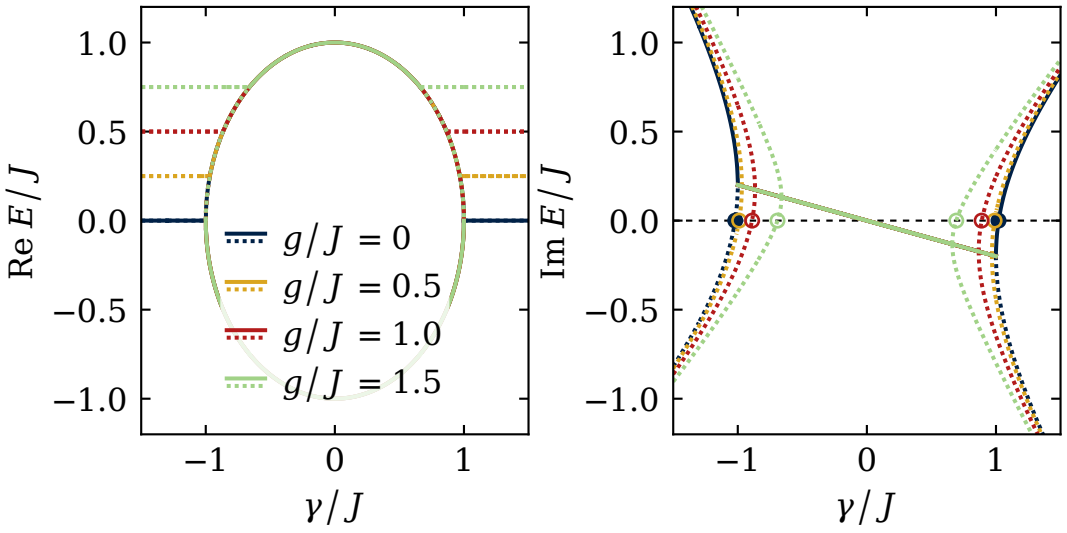

Figure 7-5: Real and imaginary parts of the eigenvalues of the asymmetric two-mode model (7-30) with the parameters $\epsilon = 0$, $\delta = -0.2J$. The real part is the same as in Fig. 7-3, but the imaginary part is shifted. For specific values of γ the formerly broken $\mathcal{PT}$-symmetric states become real as indicated by the circles.

b) Two-mode models with arbitrary gain and loss

If at least one of the parameters ϵ or δ of the two-mode model (7-30) are chosen to be non-zero, the potential is rendered non-$\mathcal{PT}$-symmetric. For example, if $\delta \neq 0$, the imaginary potential becomes asymmetric, while the real potential remains symmetric. Hence, the properties of a $\mathcal{PT}$-symmetric system are lost, even though real eigenvalues may still occur for suitable choices of γ. In Ref. [150] the authors demonstrate how an asymmetric imaginary part causes a linear shift in the imaginary part of the energy eigenvalues, which means that the formerly broken $\mathcal{PT}$-symmetric states become real at some point as shown in Fig. 7-5. It should be emphasised, though, that this does not coincide with the EPs at which the additional solutions bifurcate, as can clearly be seen in the imaginary part.

The discussions of symmetrised linear systems in Chapter 5 show that an asymmetric imaginary potential requires for an asymmetric real part. This means that such a system is not symmetrised, even if real solutions occur when either the real or imaginary part of the potential is symmetric and the other is not. For a non-linear system this can be shown numerically by calculating[14] the parameter values of γ at which one state becomes real. To check whether there exists a pair of symmetrisation operators, the determinant of the coefficient matrices given in Eqs. (5-58), (5-59), (5-61) and (5-62) must vanish, which is not the case for the stationary solutions

[14] *e.g.* via the *bisection method*

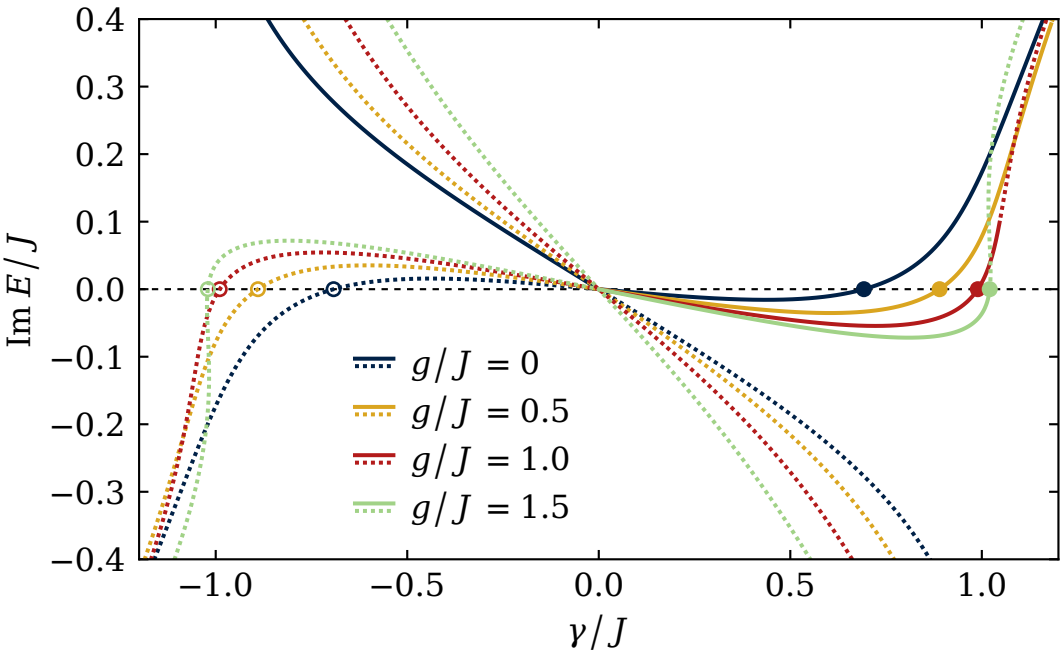

Figure 7-6: Imaginary parts of the energy eigenvalues for a completely asymmetric system due to $\epsilon = -0.15\,J$ and with $\delta = -0.2\,J$ for different values of the non-linearity strength g. The solid lines again indicate stable states, while the dotted lines are unstable.

shown in Fig. 7-5. Moreover, the usability of these stationary states is limited because they are unstable.

Figure 7-6 shows the imaginary parts of the eigenvalues for a completely asymmetric system for different values of the non-linearity parameter g. The very same system has already been investigated by Lunt *et al.* in Ref. [150] and serves as a preliminary example. The system parameters are chosen such that stable real states — indicated by the zero-crossings of the imaginary parts drawn in solid lines — occur at specific values of the gain-loss parameter γ. For larger values of g there occur bifurcations in the imaginary part of the spectrum.

The real solutions for $\gamma > 0$ eventually become unstable if the value of g is large enough. This is because there occurs a stability change in the corresponding state if the gain-loss parameter γ becomes too large.[15] This seems strange at first because stability changes usually occur at EPs; however, this must not necessarily be the case [187; 236]. The stability eigenvalues for both states with $g = 1.5\,J$ are shown in Fig. 7-7. While one state remains unstable for all parameters γ in the considered interval,[16] the state considered in Fig. 7-6 is stable within a certain interval with positive values of γ until one of its stability eigenvalues becomes

[15] This value decreases for an increasingly non-linear system.

[16] One can see that this state may however become stable at some point for $\gamma \ll 0$.

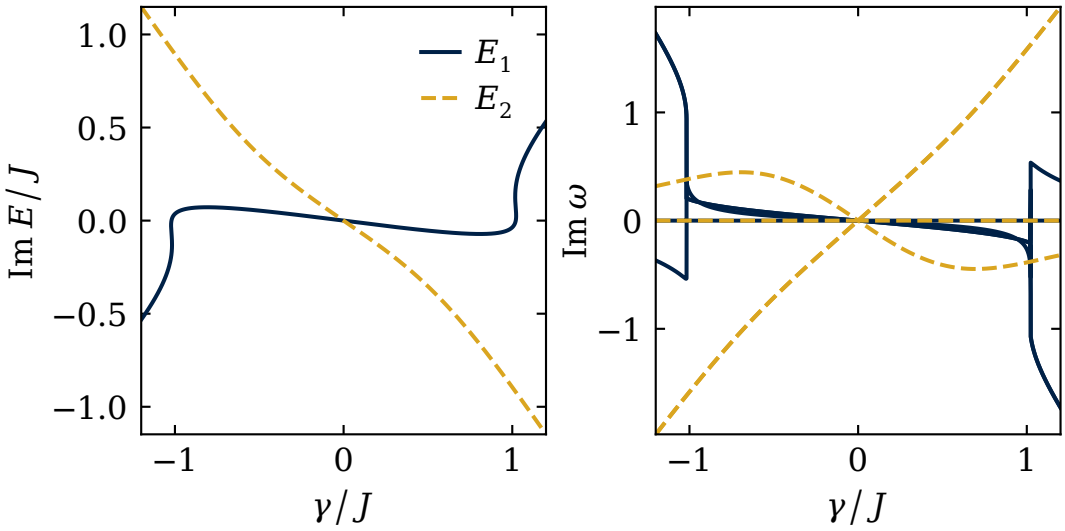

Figure 7-7: Stability eigenvalues ω for the solutions of the non-linear, asymmetric two-mode model for $g = 1.5J$. While the state with energy E_2 is unstable in the whole interval due to the imaginary parts of the stability eigenvalues, there exists a range with $\gamma > 0$ for which the state with energy E_1 is stable.

complex. The stability eigenvalues for the remaining states can also be found in Ref. [150].

The location of the stable real solutions γ_s is of particular interest because it depends on the value of the non-linearity parameter, *i.e.* γ_s increases with g. At the same time, the wave function decays for values $\gamma < \gamma_s$ and grows for $\gamma > \gamma_s$. However, because the wave function enters the Hamiltonian via the non-linear terms Eq. (7-2), a change in the norm of the state has the same effect as a change in the parameter g. That is, if the parameter γ in Eq. (7-30) increases, for example, then the norm of the wave function starts to grow, which shifts the value γ_s of the stable real state towards higher values, so that the system becomes stationary and stable once again; the same applies to a decrease of γ. Hence, the two-mode model possesses a *self-stabilising* mechanism via its non-linear part [150].

This property is particularly suitable for experimental situations. Under the assumption that the remaining system parameters are setup within a certain — not necessarily high — precision,[17] the value of γ, in contrast, has to be tuned quite precisely — possibly up to several digits of significance — to bring a linear system into a stationary state. This is because in asymmetric systems the real energy solutions do not occur in extended regions sharing the same parameters, as opposed to $\mathcal{PT}$-symmetric systems.[18] However, in a non-linear system the parameter γ could be tuned to a value in

[17] Except for in the vicinity of an EP, the qualitative behaviour should not change for small changes in the system parameters.

[18] To make gain and loss exactly symmetric is a challenge on its own.

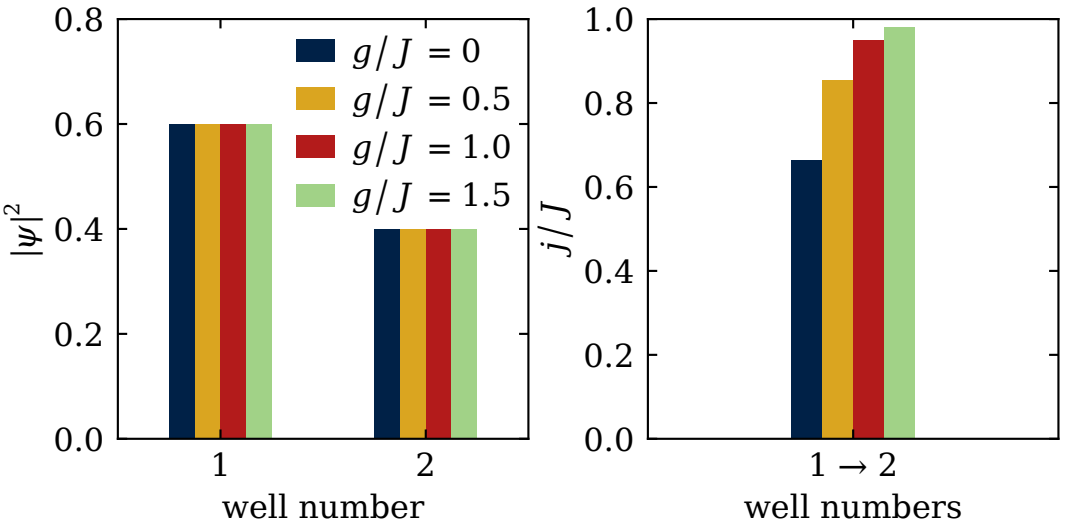

Figure 7-8: Occupations and the current at the stable stationary states of the non-linear two-mode system shown in Fig. 7-6. The ratio of the occupations remains constant, while the current increases with γ to compensate the increasing gain and loss.

the proximity of γ_s for fixed system parameters. From then on, the non-linear system can stabilise itself.

Figure 7-8 illustrates the occupations $|\psi_k|^2$ at each site $k = 1, 2$ of the two-mode model as well as the current j between the two sites at the stable stationary solutions in Fig. 7-6, at which the imaginary part of the eigenvalues vanish. It is remarkable that the occupations of the two states are distributed symmetrically around[19] $|\psi|^2 = 1/2$ and that their ratio remains constant for different values of the gain-loss parameter γ. Actually, this is quite similar to the $\mathcal{PT}$-symmetric two-mode system, in which the two states (7-31) are also symmetrically distributed and their ratio is given by $|\psi_1|^2/|\psi_2|^2 = (1+\kappa)/(1-\kappa)$ with the occupation imbalance $\kappa \neq 0$; it makes sense that the asymmetric potential also corresponds to an asymmetric initial occupation instead of a symmetric one as for the $\mathcal{PT}$-symmetric solutions. Thus, the real energy solutions can be considered to possess both properties of exact and broken $\mathcal{PT}$ symmetry simultaneously.

The current between the two sites of the non-linear two-mode model shown in Fig. 7-8 is, of course, also stationary. However, in contrast to the occupations, it changes with γ. This is a consequence of the increased gain and loss and is necessary to ensure that the system remains stationary. The capability of a system to accommodate a suitable current is essential for its ability of balancing the applied gain and loss.

[19] This stems from the fact that the states are normalised to 1.

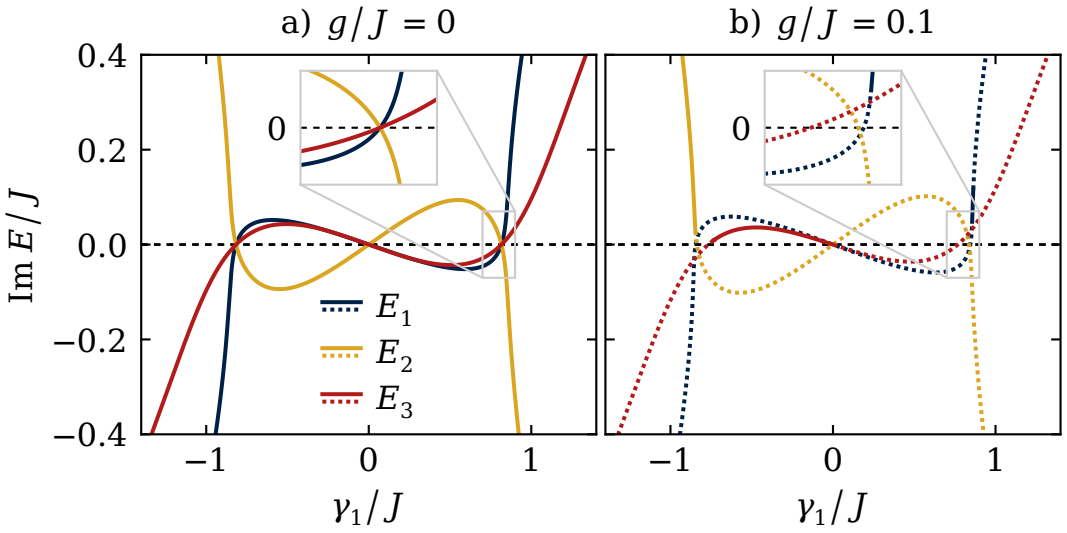

Figure 7-9: While a) three real eigenvalues coincide in the linear three-mode system, b) real solutions occur only individually at different values of γ_1 in the non-linear case. The gain-loss parameters γ_2 and γ_3 are chosen according to Eqs. (7-33) and (7-34).

7-5 Non-linear three-mode model

In analogy to Chapter 6, also non-linear systems with additional wells can be considered. However, the challenges which arise in non-linear systems and which were discussed in Section 7-1 provide increasing difficulties for larger non-linear multi-well systems and the numerical effort also increases with the system size. Nevertheless, the solutions of a non-linear three-mode model can still be obtained and a brief discussion of some of its features now follows. In Section 11-4 also larger non-linear multi-mode systems are considered in the context of resonator chains.

The discrete Hamiltonian for a triple-well potential is given by Eq. (7-3) with $n = 3$, *i.e.*

$$\mathcal{H} = \begin{pmatrix} \epsilon_1 + \mathrm{i}\gamma_1 + g|\psi_1|^2 & -J & 0 \\ -J & \epsilon_2 + \mathrm{i}\gamma_2 + g|\psi_2|^2 & -J \\ 0 & -J & \epsilon_3 + \mathrm{i}\gamma_3 + g|\psi_3|^2 \end{pmatrix}, \tag{7-32}$$

which corresponds to the linear three-mode Hamiltonian (6-22). The eigenvalues of the non-linear matrix (7-32) can be calculated as before with the methods described in Section 7-1 a). In contrast to the non-linear two-mode systems discussed in Section 7-4 b), it is not *a priori* clear whether there occur multiple stationary states simultaneously or not.

Figure 7-9 shows the spectrum of the linear three-mode model with $g = 0$ in comparison with the spectrum of a non-linearly perturbed system with $g = 0.1\,J$. The parameters are chosen as $\epsilon_1 = -0.6\,J$, $\epsilon_2 = 0$, and $\epsilon_3 = J$ as well as

$$\gamma_2 = -1.6\gamma_1\,, \tag{7-33}$$

$$\gamma_3 = 0.6\gamma_1 \tag{7-34}$$

parametrised by γ_1. While three real solutions coincide at the value $\gamma_1 \approx 0.81\,J$ as in the linear case shown in Fig. 7-9 a) — a fully symmetrised system — the non-linear terms cause a distribution of the individual eigenvalues to different parameter values as shown in Fig. 7-9 b). Hence, to find multiple real solutions simultaneously, the parameters must again be chosen quite specifically, which may be achieved with the non-linear symmetrisation conditions discussed in Section 7-3. Moreover, the states shown in Fig. 7-9 are rendered unstable even in the case of the rather modest non-linearity strength used here. This is caused to some extend by the larger number of different parameter choices, *i.e.* there exist more possibilities to use adverse combinations of parameters. However, the complexity of the system also increases and there exist two currents in the system which are responsible for compensating the gain and loss at each site, respectively, as discussed in Section 7-4 b). The three-mode system can thus be considered as being more fragile than the two-mode model, as the system now has to maintain two currents instead of one, which doubles the possibilities for failures.

As discussed before, the parameters of the non-linear three-mode model have to be chosen precisely to obtain multiple stationary states at once. This is illustrated in Fig. 7-10 for a slightly different system with an anti-symmetric real potential described by the parameters $\epsilon_1 = -\epsilon_3 = 0.6\,J$ and $\epsilon_2 = 0$. While $\gamma_2 = -0.5\,J$ remains unchanged, the order of the real solutions with respect to γ_1 changes between $\gamma_3 = 0.3\,J$ in Fig. 7-10 a) and $\gamma_3 = 0.4\,J$ in Fig. 7-10 b). More precisely, the trajectory of the eigenvalue E_1 crosses the real solution of E_3 at $\gamma_1 \approx 0.36\,J$ and $\gamma_3 \approx 0.37\,J$. While this shows that multiple stationary states can occur simultaneously just as in the linear case, one also finds that the solutions are again

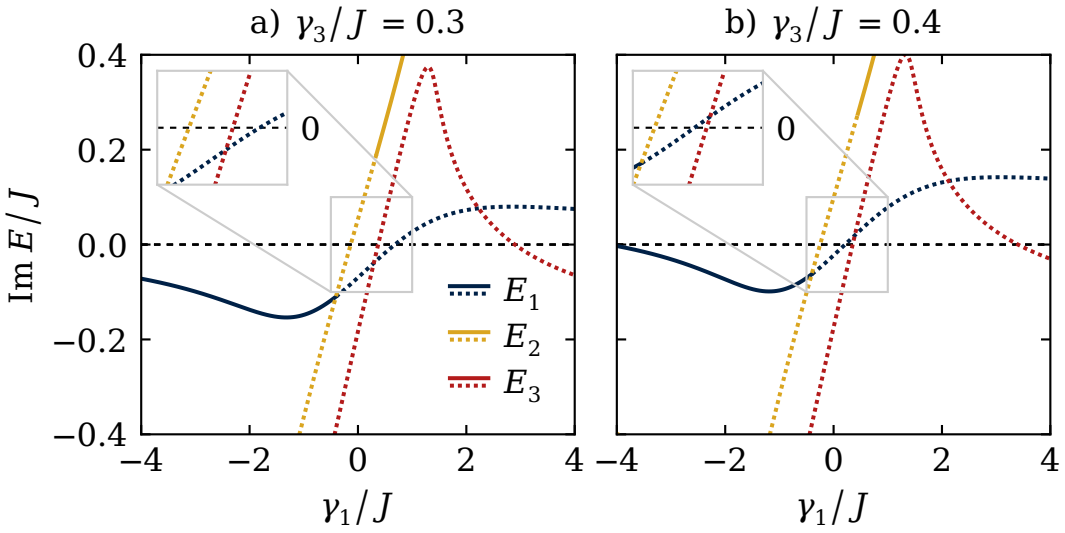

Figure 7-10: Imaginary parts of the solutions of the asymmetric three-mode model with $g = 0.1J$ and $\gamma_2 = -0.5J$. The real solutions of E_1 and E_3 must coincide at some value of γ_3 between a) and b).

unstable because there are other states which are exponentially growing and thus destabilise the system. Therefore, such solutions cannot be considered as being stationary.

The non-linear three-mode model (7-32) possesses also stable stationary solutions as shown in Fig. 7-11; here, the onsite-potential parameters are chosen as $\epsilon_1 = 0.1$, $\epsilon_2 = 0$, and $\epsilon_3 = -0.6$ and the gain-loss parameters are now parametrised by γ_3 via

$$\gamma_1 = -\gamma_2 = 0.6\gamma_3\,. \tag{7-35}$$

There are extended regions in which stable states occur, even in cases with larger values of the non-linearity parameter g. In fact, there exists at least one stable state for every value $\gamma_3 < 0$; yet, because the corresponding eigenvalues are complex in most of the cases, they are not of physical interest. There also occur stationary solutions; however, for $g \neq 0$ they are only stable for $\gamma_3 > 0$. Just as for the two-mode model, the position of the stationary states with respect to the gain-loss parameter[20] γ_3 depends on the non-linearity strength g. Because the state is growing for stronger gain and loss and decaying otherwise, the three-mode system shows the same self-stabilising mechanism as the two-mode system shown in Fig. 7-6.

[20] Because of the parametrisation (7-35), the parameter γ_3 is a measure of the overall gain and loss.

The similarities between the two scenarios in the two-mode model shown in Fig. 7-6 and in the three-mode model shown in Fig. 7-11 are astonishing. Just as in the two-mode model, stable

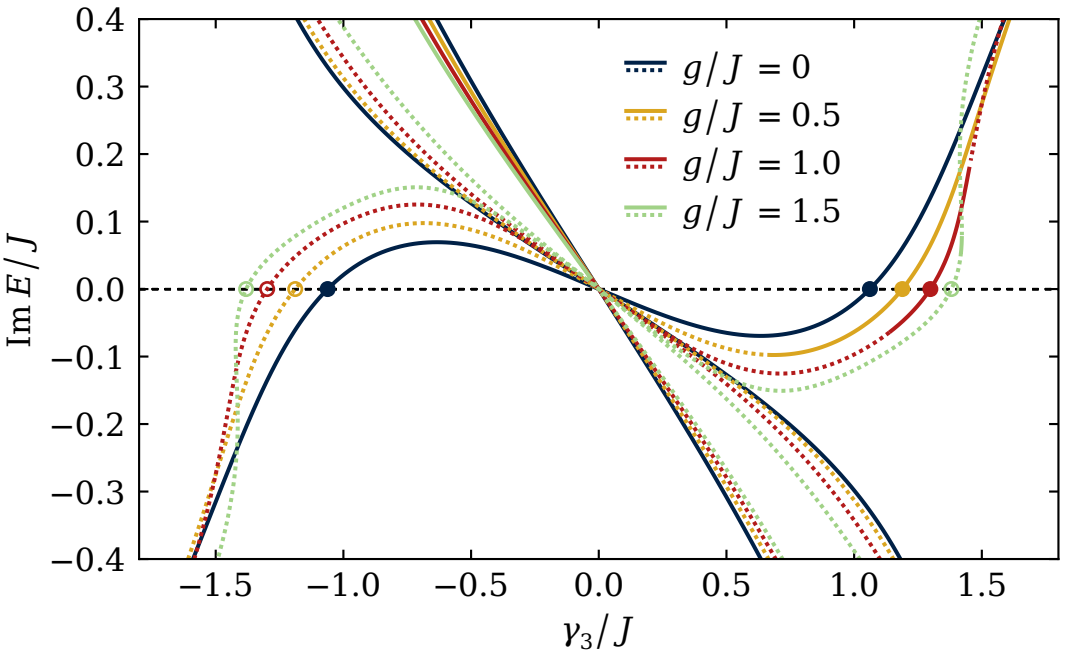

Figure 7-11: Imaginary parts of the solutions of the asymmetric three-mode model. Solid lines indicate the stable regions for γ_3, in which also stable stationary states occur for different values of the non-linearity strength g. If g becomes large enough, though, the stationary solutions become unstable.

real solutions occur where all other energy eigenvalues possess negative imaginary parts, *i.e.* other states will decay exponentially and thus cannot lead to perturbations of the stationary states. The reason for this striking resemblance can be understood with Fig. 7-12: The occupation of and the current to the third site are rather small in comparison with the other two sites. Hence, the first two two sites act similar to a two-mode system. This can also be seen by comparing their occupations and current shown in Fig. 7-11 to those of the two-mode model in Fig. 7-8. Yet, there are

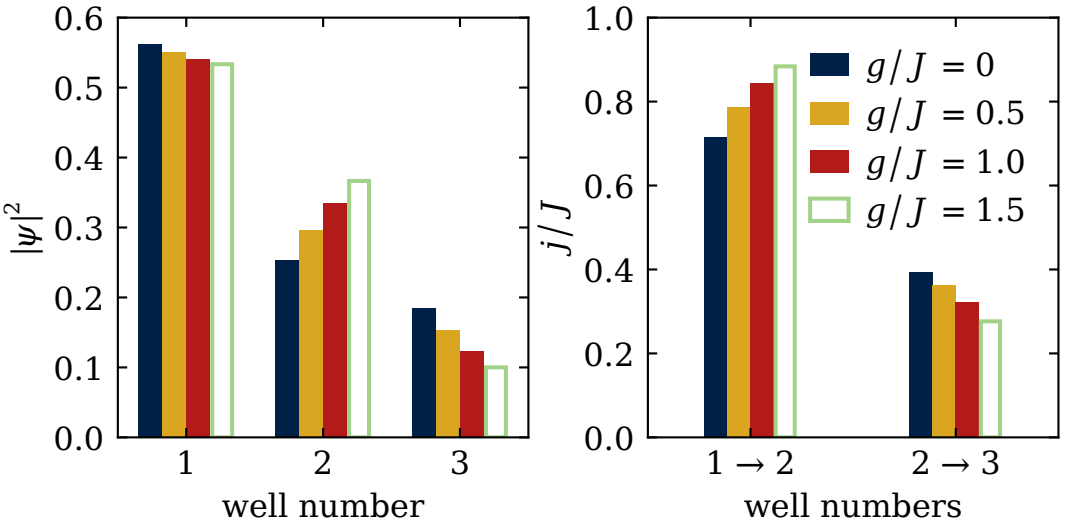

Figure 7-12: Occupations and currents at the stable stationary solutions of the three-mode system in Fig. 7-11. For the stronger non-linearities the first two wells isolate themselves from the third well because both its occupation and current decrease.

clear differences, like the fact that the occupations are changing with the non-linearity strength g. This is because the presence of the third well causes a perturbation the “two-well system”. Thus, Figs. 7-11 and 7-12 show genuine solutions of the asymmetric three-mode model, but with similar properties as a non-linear two-mode system.

The discussions above show that stationary states still occur even if the system under consideration are non-linear and non-symmetric. Although these states are isolated for the most part, meaning that the remaining states are non-stationary, they exhibit remarkable properties which enable the system to become self-stabilising. This property is particularly beneficial for real, physical scenarios like actual experiments or technical applications, an example of which is considered in Chapter 8.

Experimental realisation 8

Last but not least, it should briefly be discussed how the symmetric and symmetrised quantum systems introduced in Chapters 6 and 7 can be realised experimentally. For this, the literature concerning $\mathcal{PT}$-symmetric systems is considered, as it should in most cases be possible to disturb the potentials asymmetrically in such a way that the system becomes symmetrised.

The first experimental realisations of $\mathcal{PT}$ symmetry succeeded in optical systems [106; 184; 237–241], but it was later also observed, among other fields, in mechanical [1; 107] and electrical [108; 109] systems. However, since the very first experimental demonstration in optical wave guides in 2009 [106], it took a whole decade to realise $\mathcal{PT}$ symmetry in multi-mode spin systems [110–112], *i.e.* in actual quantum systems. The three-mode spin systems in Refs. [110; 112] are equivalent to an effective two-mode system in which both modes are coupled to the same reservoir mode; this corresponds to *passive* $\mathcal{PT}$ symmetry, *i.e.* the system exhibits only absolute losses but can be mapped to an effective system with relative gain and loss. The four-mode spin system in Ref. [111], on the other hand, is realised via an NV centre in diamond, which corresponds to a two-mode system in which each of the two modes is coupled to its own reservoir mode;[I] *i.e.* this is a genuine effective quantum system with gain and loss.

[I] Since the reservoir modes are also coupled, this can be considered as two interacting two-mode systems, *cf.* Ref. [242].

8-1 $\mathcal{PT}$-symmetric double well

One of the first proposals for the realisation of $\mathcal{PT}$ symmetry actually was made even ealier by Klaiman *et al.* [237]. They considered a BEC in a laser generated optical double-well potential [243; 244] to be an appropriate candidate to realise $\mathcal{PT}$ symmetry in a genuine quantum system with gain and loss, for which the experimental techniques had already been developed [245; 246]; gain and loss

[2] *cf.* Section 4-2

of particles in BECs also correspond to imaginary potentials[2] [247]. BECs are well suited to bring the quantum behaviour of matter from the microscopic world into macroscopic scales, which allows for direct observations of quantum effects. The low temperatures required for the formation of BECs of actual particles, which typically are in the vicinity of the absolute zero [248], can be created by laser cooling methods. The experimental techniques are so advanced and robust nowadays that a BEC of Rubidium atoms could recently even be created on the International Space Station in earth's orbit [249]; the micro-gravity environment enhances the stability of the condensate, which allows for weaker trapping potentials. Moreover, by using quasi-particles, a BEC can also be realised at room temperature [250–252], which could make such experiments even more accessible.

Another advantage of this approach lies in its simplicity and flexibility. That is, optical multi-well potentials can easily be created by using counter-propagating laser beams [253; 254] or by "painting" them in the time average with a rapidly moving laser beam [255]; the latter method allows not only for the creation of dynamical — *i.e.* time-dependent — potentials, but also for arbitrary asymmetric potentials as considered in this thesis. Afterwards, a BEC can be loaded into the optical potential [256]. Because they are created via lasers, optical multi-well potentials allow for a large amount of control and precision, both of which are required to realise the symmetrised systems discussed in Chapters 6 and 7.

While the $\mathcal{PT}$-symmetric double-well potential is well investigated theoretically [183; 185–187; 194; 195; 207; 208; 257; 258], an experimental realisation has not been accomplished so far. This can be attributed to the fact that the experimental realisation of gain in a specific potential well is rather difficult, as it requires the feeding of atoms from another condensate into the potential well. This can, for example, be achieved via gravity, *i.e.* the atoms "trickle" into the potential well [245; 259]. In contrast, the realisation of loss can simply be achieved by means of a focused electron beam [246; 260; 261] which "knocks" condensate particles out of the potential well. Hence, systems exhibiting just localised loss are easier accessible.

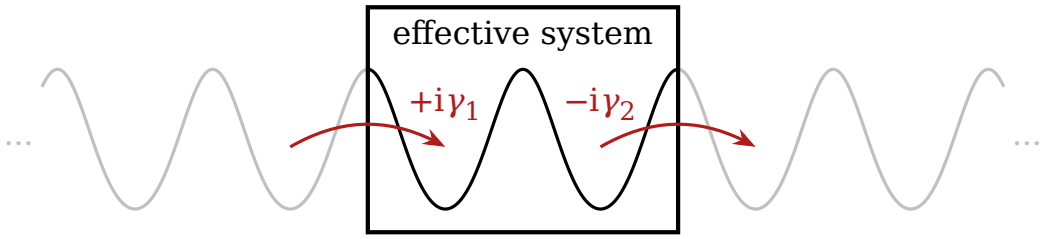

Figure 8-1: An effectively open few-mode subsystem can be embedded into a multi-well potential by suitably engineering the interactions between them.

As shown in Refs. [185; 187; 208], the formalism of $\mathcal{PT}$ symmetry can be applied to non-linear quantum systems which can develop stable, $\mathcal{PT}$-symmetric states [258]. The non-linear term (7-2) in the GPE, which is used for the description of BECs, represents contact interactions between the condensate particles; it can be tuned — and also set to zero — via *Feshbach resonances* [92; 93]. In more recent works the use of bounded and unbounded states [262] or coupling to another BEC [242] were suggested to realise $\mathcal{PT}$-symmetric double-well systems with coherent in and out-coupling of particles. However, both of these methods are also rather difficult to implement experimentally.

8-2 Embedded few-well systems

Since the realisation of real gain is experimentally demanding, one could also resort to cases with effective gain. That is, the interaction between a subsystem and an explicitly modelled environment is tuned such that the subsystem effectively corresponds to an open quantum system.[3] Thus, the environment must explicitly be taken into account — at least to some degree — and the interactions between system and environment have to be engineered minutely. While the overall system is Hermitian, the subsystem is effectively non-Hermitian. In fact, all of the systems described in Refs. [111; 112; 143], which were discussed in the introduction of this chapter, are examples for effective two-mode models.

[3] *cf.* Section 4-6

In the case of optical multi-well potentials, this scenario is illustrated in Fig. 8-1. Here, a subsystem of two wells can be considered as an effective double-well potential, if the tunnelling currents into and out of the subsystem are tuned such that they have the same effect as imaginary gain and loss terms, *e.g.* see Refs. [192;

193; 209; 262–264]. Usually, the environment is considered to be very large, so that it does not change due to the interactions with the system.[4] However, if the parameters of the optical potential are varied in a time-dependent manner based on the current state of the system, a single reservoir well at each side of the system, respectively, is sufficient to simulate an open two-mode system in the mean-field approximation [192; 263] and beyond [193; 264]. Although this approach effectively allows for the realisation of $\mathcal{PT}$ symmetry as long as the the in-coupling reservoir is non-empty,[5] the experimental setup is again rather demanding due to the time-dependent optical potentials.

In Ref. [179] an experiment with a time-independent optical potential is proposed. The basic idea is that only the gain term has to be simulated, while an actual particle loss can easily be created via an electron beam [261]. Hence, the loss term actually removes particles from the system and does not cause any ill effects. However, this again requires a large reservoir and also the precise control over the initial state of the condensate; that is, if the BEC is suitably prepared, an effectively open, embedded few-mode system can be simulated for a finite amount of time until the changes in the in-coupling reservoir becomes noticeable. This is crucial, in particular, for the relative phases of the condensate wave functions between adjacent wells, as they determine the initial currents in the system.[6] Such large optical multi-well potentials are realisable experimentally [265] and effectively show balanced gain and loss; though, they are not *per se* $\mathcal{PT}$-symmetric.

To conclude this discussion, the methods described in this chapter are, in principle, suitable to realise effectively open few-mode quantum systems experimentally. Until now, an actual experimental realisation of such a system still remains a standing goal. While a $\mathcal{PT}$-symmetric scenario appears to be a first logical step towards more general systems with balanced gain and loss — in particular, because $\mathcal{PT}$-symmetric systems are allegedly simpler — the requirement of exact symmetric potentials might even require further experimental rigour. It could thus be beneficial to start with a symmetrised BEC with contact interaction instead as proposed in

[4] This assumption is commonly called the *Markov property* and refers to the memorylessness of the environment.

[5] The effects caused due to the changes in the out-coupling reservoir can be corrected via the time-dependent potential parameters.

[6] *cf.* Eq. (4-5)

Ref. [150], which exploits the self-stabilising mechanism described in Section 7-4 b).

The difficulties described above mostly arise due to the nature of QM; that is, it is far from being trivial to prevent a quantum system from loosing its properties due to *decoherence*. In other — non-quantum — fields the application and realisation of $\mathcal{PT}$ symmetry is simpler.[7] However, also non-$\mathcal{PT}$-symmetric non-Hermitian potentials were realised recently in classical systems via pressure waves [139]. Hence, it might be feasible to find suitable applications of symmetrisation outside of QM, which is the topic of the second part of this thesis.

[7] *cf.* the introduction of this chapter

Part II

Electromagnetic systems

More important than all of this, however, will be the transmission of power, without wires, which will be shown on a scale large enough to carry conviction.

Nikola Tesla

—The Future of the Wireless Art

Introduction to the second part

9

The plot thickens.

Sherlock Holmes
—A Study in Scarlet

The concepts of NHQM and, in particular, $\mathcal{PT}$ symmetry discussed in the first part of this thesis were used for some astounding applications in recent years. Some of them, like the realisation of invisible structures [138; 267–269] or completely efficient wireless power transfer (WPT) [125; 126], could equally belong to the realm of science fiction.

Any sufficiently advanced technology is indistinguishable from magic.

Arthur C. Clark

One of the pioneers of WPT was Nikola Tesla [270–273]. In 1890, Tesla first demonstrated wireless lighting via inductive and capacitive coupling [274]. Later, he continued working on long-range wireless power transmission via high-voltage, high-frequency alternating current [273]. This led him to pursuing his idea of a global WPT — the *world wireless system*[I] — which should transmit both information and power through the earth and the atmosphere [270]; though, this could not be finished due to a series of unfortunate events.[2] Since then, WPT has already become a part of our daily lives, as it is used for charging toothbrushes, mobile phones, or other devices and even more technologies might also make use of WPT in the future.[3]

Essentially, there are two major types of WPT technologies,[4] both of which were used by Tesla already:

1) *Radiative* transmission via a focused[5] microwave beam or a laser is suitable for long-range power transfer [281].

2) *Non-radiative* transmission using either *capacitive* or *inductive* coupling is suitable for short to mid-range power transfer [282].

[I] *cf.* Fig. 9-1

[2] *e.g.* see Ref. [275]

[3] An example is given by wearable medical sensors [276].

[4] *cf.* Refs. [277–280]

[5] Unlike for signals, an omni-directional transmission is unfit for WPT.


TESLA'S TOWER

Amazing Scheme of the Great Inventor to Draw Millions of Volts of Electricity Through the Air From Niagara Falls and Then Feed It Out to Cities, Factories and Private Houses from the Tops of the Towers WITHOUT WIRES.

Figure 9-1: The *Wardenclyffe Tower* [266] was the vision about the possibility to avail energy everywhere without wires. Built in 1901, it stood ~57 m tall until its demolition in 1917.

The efficiency of WPT can be improved by means of resonance and piezoelectric effects [278]. It can be improved even further by using effects of NHQM. For example, the efficiency of autonomous thermal motors can be maximised when they operate in the vicinity of an EP [283], which occur only in non-Hermitian systems. Similarly, the efficiency of stable WPT was observed to be optimal for a $\mathcal{PT}$-symmetric system [125]. Hence, it may be of interest to apply other concepts from NHQM discussed in the first part of this thesis to electrodynamics (ED). Physical states for stable WPT in non-Hermitian systems are discussed in Chapter 11. However, beforehand a suitable description of WPT systems is required.

In contrast to quantum systems, which are described by the Schrödinger equation (2-38) which contains a first-order time derivative, systems in ED are commonly described either by a *wave equation*,

$$\left(\partial_t^2 - c^2\nabla^2\right)u(\hat{x},t) = 0\,,$$

or by an *oscillator equation*,

$$\left(\partial_t^2 + \omega_0^2\right) u(t) = 0\,,$$

both of which contain a second-order time derivative, respectively. A resonant circuit can also be described approximately by a mode equation; though, its derivation is subtle and not well covered in the literature.[6] Hence, Chapter 10 is dedicated to a rather detailed derivation of the multi-mode model of coupled electric resonators.

[6] In fact, Ref. [284] appears to be the only work which contains a rigorous treatment.

10 Coupled electric resonators

An electrical circuit which contains both a capacitor with capacity C as well as an inductor with inductance L acts as an oscillator. This is because capacitors and inductors modify the relation between the current $I(t)$ and the voltage $U(t)$ at a given time t in an electrical system:

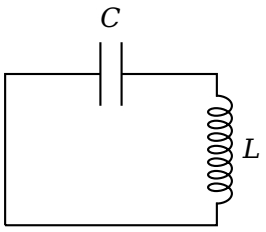

Figure 10-1: A resonant circuit

— A capacitor has to be charged or discharged by the current $I(t)$ over time. Hence, the voltage $U(t)$ follows the changes in the current $I(t)$,

$$\frac{\mathrm{d}U}{\mathrm{d}t} = -\frac{I}{C}\,. \tag{10-1}$$

— The current $I(t)$ in an inductor, on the other hand, creates a magnetic field which counteracts the current and thus delays changes due to it. In this case the current $I(t)$ follows the changes in the voltage $U(t)$,

$$\frac{\mathrm{d}I}{\mathrm{d}t} = \frac{U}{L}\,. \tag{10-2}$$

Such an electrical circuit is shown in Fig. 10-1 and can be described by the second-order differential equation

$$\frac{\mathrm{d}^2U}{\mathrm{d}t^2} + \omega_0^2 U = 0 \tag{10-3}$$

that is obtained by using *Kirchhoff's second law*. Due to the properties described above the energy in such a circuit is alternating between the capacitor and the inductor. Hence, such a system represents an electrical oscillator with resonance frequency $\omega_0 = 1/\sqrt{LC}$, where Eq. (10-3) corresponds to a *harmonic oscillator equation* for the voltage.[I]

[I] A harmonic oscillator equation for the current can analogously be derived with Kirchhoff's first law.

The solutions of Eq. (10-3) are given by

$$U(t) = U(0)\,\mathrm{e}^{\mathrm{i}\omega_0 t}\,, \tag{10-4}$$

which immediately yields[2]

[2] *cf.* Eq. (10-2)

$$I(t) = -\mathrm{i}\omega_0 C U(0)\,\mathrm{e}^{\mathrm{i}\omega_0 t}\,. \tag{10-5}$$

Both solutions are oscillating in time with a relative phase shift of $\arg(-\mathrm{i}) = -\pi/2$.

10-1 Resonator modes

While the description of the system via current and voltage is perfectly fine, it is convenient to combine these quantities [284], *i.e.* $U + \alpha I$ with a yet to be determined constant α. With Eqs. (10-1) and (10-2) one finds

$$\frac{\mathrm{d}}{\mathrm{d}t}\left(U - \frac{L}{\alpha C} I\right) = -\frac{1}{\alpha C}(U + \alpha I)\,,$$

which appears unnecessarily complicated at a first glance. However, for $\alpha^{-2} = -\omega_0^2 C^2$ two uncoupled, first-order differential equations are found,

$$\frac{\mathrm{d}a_\pm}{\mathrm{d}t} = \pm\mathrm{i}\omega_0 a_\pm\,, \tag{10-6}$$

where

$$a_\pm = \sqrt{\frac{C}{2^3}}\left(U \pm \frac{\mathrm{i}I}{\omega_0 C}\right). \tag{10-7}$$

Here, the choice of the prefactor $\sqrt{C/2^3}$ in Eq. (10-7) does not change Eq. (10-6), however, the intention will become clear shortly.

Since the two first-order differential equations (10-6) are equivalent to the second-order differential equation (10-3), the same must also hold for their solutions. With the solutions (10-4) and

(10-5) for the voltage and the current the solutions (10-7) read

$$a_+ = \sqrt{\frac{C}{2}} U(t)\, \mathrm{e}^{\mathrm{i}\omega_0 t}\,, \tag{10-8}$$

$$a_- = 0\,. \tag{10-9}$$

That is, the solution (10-9), which corresponds to the negative frequency in Eq. (10-6), does not yield any information. This does also manifest in the fact that the differential equations (10-6) are not independent but merely complex-conjugates of each other. The positive-frequency solution (10-8), on the other hand, corresponds to the square root of the energy stored in the resonator,[3] *i.e.*

$$|a_+|^2 = \frac{CU^2(0)}{2} = W\,.$$

[3] This is due to the specific prefactor in Eq. (10-7).

Therefore, Eq. (10-6) corresponds to a single-mode system and Eq. (10-8) is thus called the mode amplitude [284]; in the following, the index is dropped, *i.e.* $a \equiv a_+$ with

$$\frac{\mathrm{d}a}{\mathrm{d}t} = \mathrm{i}\omega_0 a\,. \tag{10-10}$$

10-2 Resonators with loss

While a capacitor and an inductor are, in principle, the only requirements for an electric resonator, Fig. 10-1 shows only an idealised circuit. That is, all non-superconducting materials possess a non-zero resistivity[4] ρ which leads to an intrinsic resistance R. Hence, any real circuit will suffer from intrinsic losses. To account for the intrinsic resistance of the wires, an additional resistor may be introduced as shown in Fig. 10-2.

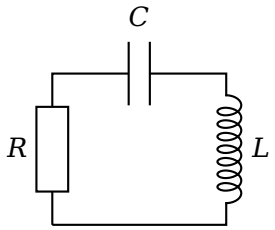

Figure 10-2: Resonant circuit with loss

It is reasonable to assume that the major contribution to the intrinsic resistance of a resonant circuit comes from the inductor. For N wire loops with radii R_w and wire radius ρ_w the intrinsic resistance of a resonator can be estimated by

$$R = 2N\rho\frac{R_\mathrm{w}}{\rho_\mathrm{w}^2}\,, \tag{10-11}$$

[4] Typical metals have a resistivity in the order of $\rho \sim 10^{-8}$ [285].

which depends on the ratio between the length and the cross section of the wire.

The presence of a resistance can be accounted for by introducing a loss term in Eq. (10-10), which is of the same form as the loss terms discussed in Chapters 6 and 7, *i.e.*

$$\frac{\mathrm{d}a}{\mathrm{d}t} = \mathrm{i}\omega_0 a - \gamma a\,, \tag{10-12}$$

where $\gamma = 1/\tau$ is the loss factor which is given by the inverse of the decay rate τ. To obtain an expression for the decay rate, *Kirchhoff's first law* can be considered for the modified circuit shown in Fig. 10-2,

$$\frac{\mathrm{d}^2 I}{\mathrm{d}t^2} + \frac{R}{L}\frac{\mathrm{d}I}{\mathrm{d}t} + \omega_0^2 I = 0\,.$$

With an ansatz of the form $I(t) = I(0)\exp(\mathrm{i}\omega t)$ one finds

$$\mathrm{i}\omega = \pm\mathrm{i}\omega_0\sqrt{1 - \frac{R^2 C}{4L}} - \frac{R}{2L}\,. \tag{10-13}$$

This represents a damped oscillator: The real part of Eq. (10-13) causes the current to decay over time. For $R < 2\sqrt{L/C}$ the first term is imaginary and represents the modified resonance frequency; for $R \geq 2\sqrt{L/C}$, though, there occurs no oscillation at all.

The modification of the resonance frequency in Eq. (10-13) is caused only indirectly by the resistor. Actually, the two first-order differential equations (10-6) are no longer uncoupled in the presence of a resistor, *i.e.* the two mode amplitudes $a_\pm$ are now coupled. However, for $R \ll 2\sqrt{L/C}$, which corresponds to a small loss, the square root can be approximated by its Taylor series, which yields

$$\mathrm{i}\omega = \pm\mathrm{i}\omega_0 - \frac{R}{2L} + O\left(R^2\right) \approx \mathrm{i}\omega_0 - \frac{1}{\tau}\,.$$

This corresponds to the approximation that the single-mode equation (10-10) is modified separately by a loss term with decay rate $\tau = 2L/R$. Hence, the corresponding loss term $\gamma \propto R$ introduced in Eq. (10-12) must be considered as being just an approximation.

10-3 Resonators with gain

So far, the resonant circuits were treated with the implicit assumption that some amount of energy is already stored within them and which causes the existence of a current. However, such circuits are *per se* "empty" and one has to introduce a mechanism to increase the mode energy, or in other words, a mechanism for gain.

A resistor leads to a loss of energy in a resonator due to friction and consequently the emission of heat. A corresponding component for gain should effectively behave exactly like the opposite, which implies that such a component — some kind of power source, for example — acts as if it would possess a negative intrinsic resistance $R < 0$. However, in contrast to the introduction of loss in Section 10-2, it is not quite as simple to relate a corresponding gain term to an actual physical circuit. For this, an ideal resonator is coupled to some device[5] via a *transmission line* in the following, which can be considered as a wave guide. Such a transmission line is illustrated in Fig. 10-3 and introduces some immediate effects:

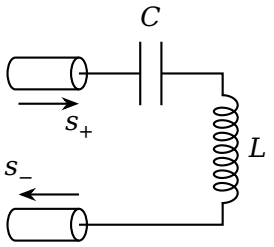

Figure 10-3: Resonant circuit with gain

[5] The actual mechanism is not really important here.

1) Energy can enter the system in form of an incident wave s_+ that excites the mode amplitude and thus increases the energy stored in the resonator. Thus, this actually corresponds to gain.

2) Energy can also leave the system via the leaking wave s_-. This introduces a decay rate similar to a resistor and thus also corresponds to loss.

The loss term due to the leaking wave s_- can be accounted for in the same manner as in Eq. (10-12). The rate of change of the energy in the resonator may thus be written as

$$\frac{\mathrm{d}a}{\mathrm{d}t} = \mathrm{i}\omega_0 a - \gamma a + k s_+ , \tag{10-14}$$

where k describes the coupling between the mode amplitude a and the incident wave s_+. Assuming that the incident wave oscillates at frequency ω, *i.e.*[6] $s_+ \propto \exp(\mathrm{i}\omega t)$, the response of the mode amplitude will occur at the same frequency, *i.e.* $a \propto \exp(\mathrm{i}\omega t)$; hence,

[6] The proportionality constant may be chosen such that $|s_+|^2$ describes the energy carried by the incident wave.

$$a = \frac{k s_+}{\mathrm{i}(\omega - \omega_0) + \gamma} \,. \tag{10-15}$$

The parameters k and γ are, in fact, not independent [284]. To uncover their relation, one might remember that ED is invariant under *time reversal*[7] as discussed in Section 2-3 a). If there is no incident wave s_+, then the circuit will experience only loss and thus corresponds to the same scenario shown in Fig. 10-2. This can also be described by the leaking wave s_- for which

[7] at least for lossless media, that is

$$\frac{\mathrm{d}}{\mathrm{d}t}|a|^2 = -2\gamma|a|^2 = -|s_-|^2$$

holds due to the conservation of the energy. Under time reversal the leaking wave s_- becomes an incident wave s_+', which then drives the system with the frequency $\omega' = \omega_0 - \mathrm{i}\gamma$; *i.e.* the energy grows as $W \propto \exp(2\gamma t)$. Here, the prime indicates quantities associated with the time-reversed solution

$$a' = \frac{k s_+'}{2\gamma} \,, \tag{10-16}$$

which can be obtained with Eq. (10-15). As discussed above, it should be required that Eq. (10-16) corresponds also to the positive frequency. However, since time reversal acts as a complex conjugation, it exchanges the positive and negative frequency components; hence, Eq. (10-16) must be the time-reversed solution of the *negative* mode amplitude a_-. Further, time reversal changes only the direction of a wave in the transmission line but not its amplitude, *i.e.* $|s_+'|^2 = |s_-|^2$. At the initial time $t = 0$ also the mode amplitudes are equal,[8] *i.e.* $|a'|^2 = |a|^2$. Therefore,

[8] For $t > 0$, though, $|a'|^2$ grows, while $|a|^2$ decays.

$$|s_+'|^2 = |s_-|^2 = 2\gamma|a|^2 = 2\gamma|a'|^2$$

at $t = 0$. With Eq. (10-16) one finally finds[9]

[9] In the second step $|a/b| = |a|/|b|$ is used, since the considered system is classical.

$$|k|^2 = 4\gamma^2 \left|\frac{a'}{s_+'}\right|^2 = 4\gamma^2 \frac{|a'|^2}{|s_+'|^2} = 2\gamma \,,$$

i.e. $|k| = \sqrt{2\gamma}$ is the desired relation. Because k and s_+ occur only in combination, their relative phase can be chosen arbitrarily, so

that $k = \sqrt{2\gamma}$ without a loss of generality, *i.e.*

$$a = \frac{\sqrt{2\gamma}\, s_+}{\mathrm{i}(\omega - \omega_0) + \gamma}\,. \tag{10-17}$$

a) The reflection coefficient

The incident wave and the leaking wave introduced by the transmission line in Fig. 10-3 are not independent. That is, the leaking wave can only depend on the incident wave and thus describes its reflection. This can be characterised with the *reflection coefficient* which is defined as the ratio between the incident wave s_+ and the leaking wave s_- in the resonator,[10]

[10] *e.g.* see Ref. [284]

$$\Gamma = \frac{s_-}{s_+} = \sqrt{2\gamma}\frac{a}{s_+} - 1\,. \tag{10-18}$$

With the response to the incident wave (10-17) the reflection coefficient (10-18) can be written as

$$\Gamma = \frac{\gamma - \mathrm{i}(\omega - \omega_0)}{\gamma + \mathrm{i}(\omega - \omega_0)}\,. \tag{10-19}$$

This immediately reveals that $\Gamma = 1$ for $\omega = \omega_0$; in other words, total reflection occurs for resonant in-coupling.

The reflection coefficient (10-19) corresponds to an ideal resonator without intrinsic losses. However, if an intrinsic loss occurs,[11] which is described by γ_0, the response to a resonant incident wave is modified,

[11] *e.g.* because of the intrinsic resistance of the resonator circuit

$$a = \frac{\sqrt{2\gamma}\, s_+}{\gamma + \gamma_0}\,.$$

The reflection coefficient (10-18) then reads

$$\Gamma = \frac{\gamma - \gamma_0}{\gamma + \gamma_0}\,,$$

which vanishes for $\gamma_0 = \gamma$, so that there occurs no reflection at all.

10-4 Inductive coupling

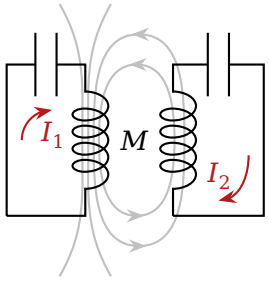

Figure 10-4: Coupled resonant circuits

In addition to the direct excitation of an electric resonator via a transmission line as introduced in Section 10-3, energy can also be transferred into a circuit by means of induction.[12] Consider two resonant circuits as shown in Fig. 10-4. An alternating current I_1 in the primary resonator will create a time-dependent magnetic field which induces an alternating current I_2 in the secondary resonator. The same argument also applies to the current I_2, of course, which in turn affects the primary circuit; thus, the two resonators are coupled.

Inductive coupling can be used for WPT.[13] However, the energy stored in the magnetic field decreases rapidly with distance. This is because the energy depends on the square of the magnetic field strength, *i.e.* $E_B = B^2/2\mu_0$. The magnetic field — which can for example be calculated via the *Biot–Savart law*[14] — decreases as[15] $B \sim d^{-2}$ with the distance d, so that $E_B \sim d^{-4}$.

[12] *cf.* Appendix H-3

[13] *cf.* Chapter 11

[14] *cf.* Eq. (H-7)

[15] Though, this behaviour highly depends on the geometric arrangement.

a) Mutual inductance

The two resonators shown in Fig. 10-4 are coupled due to mutual induction. With *Faraday's induction law* the corresponding coupling constant can be found. Consider the voltage U_2 induced by the magnetic field B_1 of the primary inductor in every closed secondary wire loop with area A_2,

$$U_2 = -\frac{\mathrm{d}}{\mathrm{d}t}(B_1 A_2) = -A_2 \frac{\mathrm{d}B_1}{\mathrm{d}t} = M \frac{\mathrm{d}I_1}{\mathrm{d}t} \,. \tag{10-20}$$

The proportionality constant M is called the *mutual inductance*; it depends solely on the geometric properties of the two inductors and is thus symmetric,[16] *i.e.* $U_1 = M\dot{I}_2$. The mutual inductance can, in general, be calculated via the *Neumann formula*[17] [286; 287]

$$M = \frac{\mu_0}{4\pi} \int_{\partial A_1} \int_{\partial A_2} \frac{\mathrm{d}\mathbf{l}_1 \cdot \mathrm{d}\mathbf{l}_2}{|\mathbf{r}_1 - \mathbf{r}_2|} \,. \tag{10-21}$$

[16] Actually, this is a consequence of the *reciprocity theorem*.

[17] *cf.* Appendix H-1

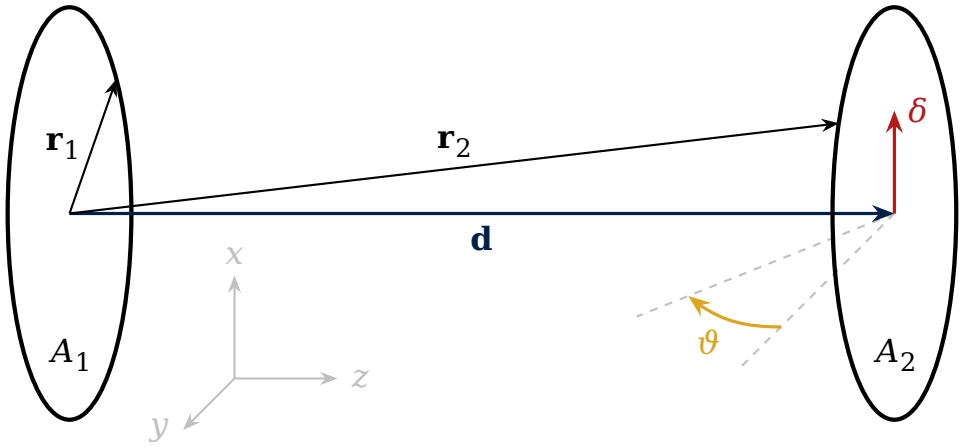

Figure 10-5: Geometry of two coupled, circular wire loops with radii R_1 and R_2, which are separated by the length d in the z direction. An additional misalignment in the x direction and a rotation around the x-axis are described by the parameters δ and ϑ, respectively.

In simple cases — two identical solenoids, for example — the mutual inductance is related to the self-inductances by $M^2 = L_1 L_2$. However, this holds only in idealised systems with perfect magnetic coupling and no flux leakage. In real systems a coupling constant must be introduced,

$$M = \hat{M}\sqrt{L_1 L_2}\,, \tag{10-22}$$

where $\hat{M} = M/\sqrt{L_1 L_2} \leq 1$ is the normalised mutual inductance.

The self-inductances can be calculated in a similar manner as the mutual inductance, which is discussed in Appendix H-3 at the example of a single wire loop. However, a suitable expression can, in principle, also be obtained directly from the mutual inductance of two identical inductors at the distance $d = 0$. Hence, in the case of two circular wire loops with radii $R_1 = R_2$, which are perfectly aligned, one can conclude that

$$L = M\big|_{d=0,R_1=R_2}\,,$$

so that $M/L \leq 1$ as required above. Nevertheless, this calculation is far from being trivial in practice, which is briefly discussed in Appendix H-3.

Instead of a single wire loop, one can also consider multiple wire loops forming a tightly wound coil with a length which is small in comparison to its diameter. That is, the N_1 wire loops of the primary inductor create a magnetic field which induces a current

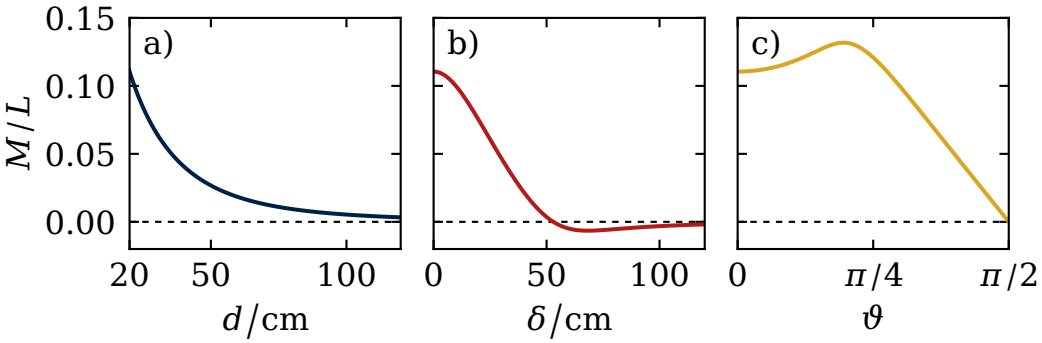

Figure 10-6: Mutual inductance M of two coupled, circular wire loops with equal radii $R_1 = R_2 = 29\,\mathrm{cm}$ for different values of a) the distance d, b) the misalignment δ, and c) the rotation ϑ. In b) and c) the separation is $d = 20\,\mathrm{cm}$.

in the N_2 wire loops of the secondary inductor. Hence,

$$M \propto N_1 N_2\,,$$
$$L_1 \propto N_1^2\,,$$
$$L_2 \propto N_2^2\,.$$

This immediately shows that the normalised mutual inductance $\hat{M}$ is independent of the windings numbers. Further, Eqs. (10-2) and (10-20) yield

$$\frac{U_2}{U_1} = \frac{M}{L_1} \propto \frac{N_2}{N_1}\,,$$

which corresponds to a *transformer equation*, *i.e.* the ratio of the voltages of two coupled inductors depends on the ratio of their winding numbers.

The mutual inductance does not only depend on the geometric properties of the inductors themselves, but also on their geometric arrangement. Thus, factors like their distance,[18] their alignment, and their relative orientation to each other have to be considered; this is illustrated in Fig. 10-5 for two wire loops. The evaluation of the mutual inductance via the Neumann formula (10-21) depending on different geometrical arrangements can be found in Appendix H; the corresponding numerical evaluations of M as a function of the distance and the influence of different forms of misalignment are shown in Fig. 10-6. It should be noted beforehand that the absolute values of the normalised mutual inductances are rather small; however, this will be of importance in the further course of this thesis, as it ensures that the matrix model introduced in

[18] *cf.* Ref. [288]

the upcoming Section 10-5 is a valid approximation.[19] Further, the coupling becomes weaker when the separation increases. This is intuitive because the magnetic field decreases quadratically with distance; the polynomial dependence is readily identifiable in Fig. 10-6 a).

As opposed to this, the influence of misalignments on the inductive coupling for a fixed distance is more complicated. For a parallel displacement, which is shown in Fig. 10-6 b), the absolute strength of the inductive coupling also decreases, although the effect is rather small at first. Further, the mutual inductance becomes even negative at some point. In contrast to the self-inductance, which must be positive by definition,[20] there is no such restriction on the mutual inductance; *i.e.* the direction of the induced current depends entirely on the alignment of the wire loops with respect to the magnetic field lines.

A rotational misalignment is shown in Fig. 10-6 c), where the value $\vartheta = \pi/2$ means that the two wire loops are perpendicular to each other. Surprisingly, small rotations can even increase the inductive coupling. The reason is that the magnetic field strength changes more strongly for smaller distances than it does for larger distances; in other words, the increase in the induced current in the part of the wire which is rotated towards the primary inductor is larger than the respective decrease in the part of the wire which is rotated away. However, eventually the coupling decreases and vanishes if the two inductors are perpendicular to each other.

These brief considerations show that the mutual inductance strongly depends on the geometric properties of the individual inductors as well as their geometric arrangement. To find an ideal arrangement can be difficult, though, real applications are hard to control anyway. Therefore, it is required to develop robust coupled systems that can adapt to different geometric arrangements.[21] Such systems are briefly discussed in Chapter 11.

[19] *cf.* Eq. (10-28)

[20] The direction of the induced current and thus the sign follow *Lenz's law*.

[21] Usually, this would require the active tuning of specific system parameters, *e.g.* see Ref. [289].

b) Coupled modes

The mutual inductance couples two resonators as shown in Fig. 10-4. For this reason, they can also be described according to the *coupled*

mode theory [284; 290; 291] via

$$\frac{\mathrm{d}a_1}{\mathrm{d}t} = \mathrm{i}\omega_1 a_1 + \mathrm{i}\kappa a_2\,, \tag{10-23}$$

$$\frac{\mathrm{d}a_2}{\mathrm{d}t} = \mathrm{i}\omega_2 a_2 + \mathrm{i}\kappa a_1\,, \tag{10-24}$$

where $\omega_1, \omega_2 > 0$ are the resonance frequencies of the two individual resonators, respectively, and κ is a coupling constant which is derived in the following.

Assuming that the current in each oscillator is of the form

$$I_k(t) = \frac{1}{2}\Big(I_k(0)\,\mathrm{e}^{\mathrm{i}\omega_k t} + I_k^*(0)\,\mathrm{e}^{-\mathrm{i}\omega_k t}\Big)\,,$$

then, because of Eq. (10-20), the mean power at an inductor due to the coupling to the other inductor reads

$$\bar{P}_{kl} = \left\langle M\frac{\mathrm{d}I_k}{\mathrm{d}t}I_l(t)\right\rangle = \left\langle P_{kl}^{+} + P_{kl}^{-}\right\rangle$$

with

$$P_{kl}^{+} = \frac{\mathrm{i}\omega_k M}{4}\Big(I_k(0)I_l(0)\,\mathrm{e}^{\mathrm{i}(\omega_k+\omega_l)t} - I_k^*(0)I_l^*(0)\,\mathrm{e}^{-\mathrm{i}(\omega_k+\omega_l)t}\Big)\,, \tag{10-25}$$

$$P_{kl}^{-} = \frac{\mathrm{i}\omega_k M}{4}\Big(I_k(0)I_l^*(0)\,\mathrm{e}^{\mathrm{i}(\omega_k-\omega_l)t} - I_k^*(0)I_l(0)\,\mathrm{e}^{-\mathrm{i}(\omega_k-\omega_l)t}\Big)\,. \tag{10-26}$$

The terms in Eq. (10-25) are oscillating rapidly with the frequency $(\omega_k + \omega_l)$; hence, they can be neglected in the time average[22] when compared to the slowly oscillating terms in Eq. (10-26) with the frequency $(\omega_k - \omega_l)$. Thus,

[22] particularly for the near-resonant case in which $\omega_k \approx \omega_l$

$$\bar{P}_{kl} \approx \frac{\mathrm{i}\omega_k M}{4}\left\langle I_k I_l^* - I_k^* I_l\right\rangle = \frac{\mathrm{i}\omega_l}{2}\frac{M}{\sqrt{L_k L_l}}\left\langle a_k a_l^* - a_k^* a_l\right\rangle\,, \tag{10-27}$$

where $a_k = \mathrm{i}\omega_k L_k I_k\sqrt{C_k/2}$ are the mode amplitudes.

Now, one can assume that the mean rate of change of the energy in a resonator due to the couplings in Eqs. (10-23) and (10-24) is given by the difference of the mutually induced powers which are

described by Eq. (10-27), *i.e.*

$$\left\langle \frac{\mathrm{d}|a_l|^2}{\mathrm{d}t} \right\rangle = \mathrm{i} \left\langle \kappa a_k a_l^* - \kappa^* a_k^* a_l \right\rangle \stackrel{!}{=} \bar{P}_{kl} - \bar{P}_{lk} \,.$$

This assumption yields an explicit expression for the coupling constant,[23]

[23] *cf.* Ref. [280]

$$\kappa = \frac{\omega_k + \omega_l}{2} \hat{M} \,, \tag{10-28}$$

where $\hat{M} = M/\sqrt{L_k L_l}$ is the normalised mutual inductance introduced in Eq. (10-22). Equation (10-28) is real and depends directly on the mean frequency of the two resonators; since $\hat{M}$ is dimensionless, the dimension of the coupling constant is the same as for frequencies, which is in agreement with Eqs. (10-23) and (10-24). Note that the same line of thought holds for the mean rate of change of the energy in the other resonator; this yields the very same coupling constant.[24]

[24] The coupling constants are symmetric, which is an expression of the conservation of energy.

Note that for weak couplings the coupling terms are proportional only to the mode amplitude of the respective other resonator as in Eqs. (10-23) and (10-24). This is because the time evolution of the mode amplitude is only slightly perturbed by the coupling if the coupling constant is weak in comparison with the resonance frequencies. However, the coupling terms are, in general, described by specific functions of the mode amplitudes. Hence, Eqs. (10-23) and (10-24) can be considered as the first-order Taylor approximations of the mode equations.[25]

[25] *cf.* Ref. [290]

10-5 Matrix model for coupled resonators

Coupled electric resonators can be described by the mode equations (10-23) and (10-24), where the coupling constant κ is given by

Eq. (10-28). These equations can be written in the matrix form

$$\frac{\mathrm{d}}{\mathrm{d}t}\begin{pmatrix} a_1 \\ a_2 \end{pmatrix} = \mathrm{i}\begin{pmatrix} \omega_1 & \kappa \\ \kappa & \omega_2 \end{pmatrix}\begin{pmatrix} a_1 \\ a_2 \end{pmatrix}, \tag{10-29}$$

which is mathematically equivalent to the discrete Schrödinger equation (2-38), where a_k represent the wave function and $-\omega_k$ correspond to the potential for $k = 1, 2$.

Gain and loss can also be described by mode equations as discussed in Sections 10-2 and 10-3. However, while a loss term can readily be included into the matrix model (10-29), the mode equation (10-14) with gain explicitly depends on the incident wave. Therefore, gain cannot yet be described by a matrix model in a self-consistent manner.[26]

[26] *i.e.* the mode equations depend only on the mode amplitudes

a) Effective description of gain

It is desirable to describe the effects of a transmission line, which introduces both gain and loss, in an effective manner. This corresponds to the replacement of the gain and loss terms in the mode equation (10-14) by an effective gain term, that is

$$\frac{\mathrm{d}a}{\mathrm{d}t} = \mathrm{i}\bar{\omega}a + \bar{\gamma}a \tag{10-30}$$

being equal to Eq. (10-12) with a negative loss factor if $\bar{\omega} = \omega_0$ is the resonance frequency. A comparison between Eqs. (10-14) and (10-30) yields the condition

$$(\mathrm{i}\omega_0 - \gamma)a + \sqrt{2\gamma}s_+ \stackrel{!}{=} (\mathrm{i}\bar{\omega} - \bar{\gamma})a\,,$$

where the assumption is made that a is a solution of both Eqs. (10-14) and (10-30). This condition can be satisfied with a suitable choice of the incident wave,

$$s_+ = \frac{\mathrm{i}(\bar{\omega} - \omega_0) + (\bar{\gamma} + \gamma)}{\sqrt{2\gamma}}a\,, \tag{10-31}$$

where a can be determined by solving the effective mode equation (10-30).

The combination of Eqs. (10-12), (10-23), (10-24) and (10-30) then yields a matrix model for coupled resonators with gain and loss which is described by the Hamiltonian

$$-\mathrm{i}\mathcal{H} = \begin{pmatrix} \mathrm{i}\bar{\omega}_1 + \bar{\gamma}_1 & \mathrm{i}\kappa \\ \mathrm{i}\kappa & \mathrm{i}\omega_2 - \gamma_2 \end{pmatrix}, \tag{10-32}$$

where $\bar{\omega}_1$ and $\bar{\gamma}_1$ correspond to the effective resonance frequency and the effective gain factor, respectively. The Hamiltonian (10-32) corresponds to the two-mode matrix Hamiltonian (6-5) with the definitions $\epsilon \equiv -\omega \leq 0$ and $J \equiv \kappa > 0$; all parameters are given in dimensions of frequencies.[27] By a suitable choice of the incident wave (10-31) the model parameter $\bar{\omega}_1$ can also correspond to the actual resonance frequency of the physical electric resonator.

[27] That is, one may assign them to the energies $\hbar\omega$.

The matrix model (10-32) possesses the same degrees of freedom in its parameters as its quantum counterpart. Some of these parameters are determined by actual physical components of the circuits:

— The resonance frequency $\omega_2 = 1/\sqrt{L_2 C_2}$ is determined by the properties of the inductor and the capacitor in the secondary circuit.

— The loss factor $\gamma_2 = R_2/2L_2$ is determined primarily by the resistor in the secondary circuit.

In contrast, the effective resonance frequency $\bar{\omega}_1$ and the effective gain factor $\bar{\gamma}_1$ are both determined via Eq. (10-31) by the choice of the incident wave in the primary resonator.[28] They can, in principle, be chosen arbitrarily; due to the gauge freedom of the energy, though, only the difference of the model resonance frequencies $(\bar{\omega}_1 - \omega_2)$ is physically meaningful. Further, the coupling constant (10-28) depends on the real frequencies of the physical circuits, which are determined by the inductances and the capacities; therefore, κ can be chosen independently of the quantities $\bar{\omega}_1$ and ω_2 in the matrix model. For these reasons, a system of two coupled, electric resonators is a suitable platform for implementing

[28] To put it the other way around: The incident waves depend only on the quantities in the primary resonator.

the symmetric and symmetrised systems discussed in Chapter 6. This provides the means for an experimental realisation that is rather simple and robust in comparison with actual quantum systems.[29] Thus, due to their mathematical equivalence, the results of Chapter 6 can, in principle, be transferred with only minor physical restrictions; an example being that the corresponding on-site parameters must be negative.

[29] *cf.* Chapter 8

In the upcoming Chapter 11 the wireless transmission of power is discussed. To allow for stable WPT, at least one stationary state must exist. With the condition[30] $\det \mathcal{H} = 0$ the Hamiltonian (10-32) yields

[30] Due to the gauge freedom of a Hamiltonian, $\omega = 0$ may be chosen as the eigenvalue.

$$\left(\mathrm{i}\bar{\omega}_1 + \bar{\gamma}_1\right)\left(\mathrm{i}\omega_2 - \gamma_2\right) = -\kappa^2 \,. \tag{10-33}$$

A specific set of solutions for the effective parameters $\bar{\omega}_1$ and $\bar{\gamma}_1$, both of which can easily be modified via the incident wave, are given by

$$\bar{\omega}_1 = \frac{\kappa^2}{\omega_2^2 + \gamma_2^2}\omega_2 \,, \qquad \bar{\gamma}_1 = \frac{\kappa^2}{\omega_2^2 + \gamma_2^2}\gamma_2 \,. \tag{10-34}$$

The parameters (10-34) satisfy Eq. (6-16) with $\epsilon \to -\omega$, *i.e.* such systems are semi-symmetrised; of course, this also holds for other solutions of Eq. (10-33). Further, the following relation is found for the ratio of the resonator energies,

$$\frac{|a_2|^2}{|a_1|^2} = \frac{\kappa^2}{\omega_2^2 - \gamma_2^2} \,. \tag{10-35}$$

b) Non-linear in-coupling

Since the parameters in the first mode of the effective matrix model can be chosen arbitrarily, one can also construct non-linear models similar to the ones discussed in Chapter 7. In these cases the relation between the incident wave s_1^+ and the mode a_1 is no longer given by Eq. (10-31), but also becomes non-linear. For example,[31] $\bar{\omega}_1 \to \bar{\omega}_1 + g|a_1|^2$ yields a model with a non-linear imaginary part of strength g. Remember, that this corresponds to a quantum system

[31] *cf.* Ref. [125]

with a non-linear *real* potential, which is consistent with the non-linear quantum systems considered in Chapter 7.

This can easily be generalised to arbitrary complex functions $f(a_1)$ of the in-coupling mode amplitude, *i.e.*

$$f(a_1) = \bar{\omega}_1 + g|a_1|^2 - \mathrm{i}\bar{\gamma}_1 \tag{10-36}$$

corresponds to the example discussed above. The Hamiltonian of the corresponding matrix model reads

$$-\mathrm{i}\mathcal{H} = \begin{pmatrix} \mathrm{i}f(a_1) & \mathrm{i}\kappa \\ \mathrm{i}\kappa & \mathrm{i}\omega_2 - \gamma_2 \end{pmatrix}, \tag{10-37}$$

which can be obtained with the incident wave

$$s_+ = \frac{\mathrm{i}(\mathrm{Re}\, f(a_1) - \omega_1) + (\mathrm{Im}\, f(a_1) + \gamma_1)}{\sqrt{2\gamma_1}} a_1\,, \tag{10-38}$$

where ω_1 and γ_1 are the parameters of the physical in-coupling oscillator. In contrast to the quantum system (7-30), which exhibits non-linear effects in both modes,[32] only the resonators with gain can become non-linear.

[32] *e.g.* due to interactions, *cf.* Chapter 8

The advantage of a non-linear in-coupling of energy lies in the fact that it acts as an implicit control technique for the circuit. That is, the non-linear gain term in Eq. (10-37) can stabilise the system with respect to perturbations of its parameters[33] in a similar fashion as the non-linear terms for the quantum systems discussed in Chapter 7 do. Moreover, this allows for emulating different systems without the need to change the physical components of the resonant circuits. Usually, to change the resonance frequency of a circuit, for example, a *variable capacitor*[34] is required; analogously, changes to the loss factor require a *variable resistor*.[35] With a transmission line both quantities can effectively be changed in the model as described in Section 10-5 a).

[33] *e.g.* see Ref. [125]

[34] *e.g.* see Ref. [292]

[35] For this purpose, a *potentiometer* can be used, for example.

Wireless power transfer

11

The matrix model introduced in Chapter 10 for the description of coupled electric resonators is mathematically equivalent to the matrix models in QM which were considered in the first part of this thesis. Thus, all the results of Chapters 6 and 7 remain valid. However, coupled resonant circuits also allow for technical applications like wireless power transfer (WPT). While it is, in principle, sufficient to tune the system parameters in such a way that stable stationary[I] states occur, additional factors like the *efficiency* of the WPT must necessarily be considered to assess its utility.

[I] Here, the term "stationary" means that the total amount of energy that is stored in a resonator is conserved; it still oscillates between the inductor and the capacitor, of course.

11-1 Wireless power transfer with coupled resonators

As discussed in Section 10-4, two inductively coupled resonators can be used to implement WPT — *e.g.* see Refs. [125; 277–279; 287; 288; 291; 293–296] and references therein — where energy is inserted into the primary circuit and extracted at the secondary circuit.

The properties of such a system can best be described by introducing another transmission line for the extraction of energy from the circuit. The corresponding coupled resonant circuits are shown in Fig. 11-1, where $s_k^\pm$ describe the incident and leaking waves in each resonator, respectively; here, $s_2^+ = 0$ because energy should only be inserted into the primary circuit. The corresponding coupled mode equations read[2]

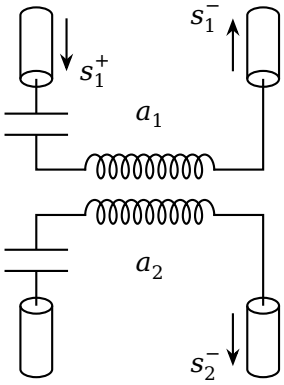

Figure 11-1: Wireless power transmission

[2] *cf.* Eqs. (10-12) and (10-30)

$$\frac{\mathrm{d}a_1}{\mathrm{d}t} = (\mathrm{i}\omega_1 - \gamma_1)a_1 + \mathrm{i}\kappa a_2 + \sqrt{2\gamma_1}s_1^+ , \tag{11-1}$$

$$\frac{\mathrm{d}a_2}{\mathrm{d}t} = (\mathrm{i}\omega_2 - \gamma_2)a_2 + \mathrm{i}\kappa a_1 , \tag{11-2}$$

where ω_1 and γ_1 are the real resonance frequency and the loss factor of the in-coupling resonant circuit. Further, the parameters γ_1 and γ_2 describe the losses due to the leaking waves s_1^- and s_2^- in each resonator, respectively.

For further evaluations it is necessary to find explicit expressions for the leaking waves in terms of the system parameters and the incident wave. For this, consider that Eqs. (11-1) and (11-2) are uncoupled for $\kappa = 0$. From Section 10-3 it is known already that in this case $|s_2^-|^2 = 2\gamma_2|a_2|^2$, *i.e.*

$$s_2^- \equiv \sqrt{2\gamma_2}a_2 \tag{11-3}$$

by choosing the positive sign. Similarly, s_1^- can depend only on s_1^+ and a_1. For a linear system a suitable ansatz is given by

$$s_1^- = c_s s_1^+ + c_a a_1$$

with the complex coefficients c_s and c_a. The relation between the leaking wave and the mode amplitude is known already,[3] *i.e.* $c_a \equiv \sqrt{2\gamma_1}$; here, the phase relation is chosen to be unity, which corresponds to the choice of a specific reference plane at which s_1^- is evaluated [284]. Further, due to energy conservation, the following relation must always hold in the first resonator,

[3] *cf.* Eq. (11-3)

$$\left|s_1^+\right|^2 - \left|s_1^-\right|^2 = \frac{\mathrm{d}}{\mathrm{d}t}|a_1|^2 + 2\gamma_0|a_1|^2\,. \tag{11-4}$$

Here, $|s_1^+|^2 > |s_1^-|^2$ correspond to the in-coming and out-going powers, so that the left-hand side of Eq. (11-4) corresponds to the net power flowing into the resonator. The first term on the right-hand side of Eq. (11-4) describes the built-up rate of the resonator energy, while the second term corresponds to the rate of energy dissipation due to internal losses. In the following, the latter term is neglected under the assumption of an ideal resonator without any internal resistance. A comparison between the left-hand side of Eq. (11-4) and the time-derivative of a_1 evaluated with Eq. (11-1) yields the two conditions $|c_s|^2 = 1$ and $c_s = c_s^* = -1$. Hence,

$$s_1^- = -s_1^+ + \sqrt{2\gamma_1}a_1 \tag{11-5}$$

is the desired expression for the leaking wave in the primary resonator.

Only in the uncoupled case Eqs. (11-3) and (11-5) hold exactly. However, it can still be assumed that they remain approximately valid for weak couplings with small values of κ, if the dynamics of the mode amplitudes described by Eqs. (11-1) and (11-2) is only slightly perturbed.

a) Stationary solutions

Stationary solutions of the coupled resonators can be used to implement WPT in a stable manner; that is, some portion of the energy inserted via the incident wave s_1^+ can be extracted via the leaking wave s_2^-. The stationary solutions of Eqs. (11-1) and (11-2) are given by

$$a_1 = -(\mathrm{i}\omega_2 - \gamma_2)\sqrt{2\gamma_1}\,\alpha\, s_1^+ , \tag{11-6}$$

$$a_2 = \mathrm{i}\kappa\sqrt{2\gamma_1}\,\alpha\, s_1^+ , \tag{11-7}$$

where

$$\alpha = \frac{1}{(\mathrm{i}\omega_1 - \gamma_1)(\mathrm{i}\omega_2 - \gamma_2) + \kappa^2} . \tag{11-8}$$

The stationary solutions (11-6) and (11-7) both depend on the incident wave s_1^+ and so does the leaking wave (11-5) in the primary resonator.

b) Transfer efficiency

The *efficiency* of the WPT is defined as the ratio between the power which is inserted into the primary resonator and the power which is extracted from the secondary resonator,[4]

[4] *e.g.* see Ref. [125]

$$\eta = \frac{|s_2^-|^2}{|s_1^+|^2} = 2\gamma_2 \frac{|a_2|^2}{|s_1^+|^2} . \tag{11-9}$$

The amount of power which is reflected and leaves the system via the leaking wave s_1^- is not taken into account because this energy is neither transferred nor lost.[5]

[5] *cf.* Section 10-3 a)

The efficiency and the reflection coefficient (10-18) are related; the absolute square $|\Gamma|^2$ of the reflection coefficient describes the portion of the power which is reflected by the primary circuit. The efficiency is thus given by $\eta = 1 - |\Gamma|^2$, which describes the portion of the power transferred to the secondary circuit. However, while the reflection coefficient Γ depends only on the primary resonator and thus also exists in the uncoupled case, Eq. (11-9) is a sole consequence of the coupling. For example, the WPT efficiency which corresponds to the stationary solutions (11-6) and (11-7) is given by

$$\eta = 4\gamma_1\gamma_2\kappa^2|\alpha|^2$$

with the constant α defined in Eq. (11-8). The corresponding reflection coefficient can be written as

$$\Gamma = -\alpha\Big[(\mathrm{i}\omega_1 + \gamma_1)(\mathrm{i}\omega_2 - \gamma_2) + \kappa^2\Big].$$

In general, the efficiency (11-9) can also be written independently of the incident wave. That is, for the effective matrix model discussed in Section 10-5 the incident wave can be expressed in terms of the mode amplitude a_1 of the primary resonator via Eq. (10-31). Hence,

$$\eta = \frac{4\gamma_1\gamma_2}{\big(\bar{\omega}_1 - \omega_1\big)^2 + \big(\bar{\gamma}_1 - \gamma_1\big)^2}\,\frac{|a_2|^2}{|a_1|^2}, \tag{11-10}$$

which holds for any system of the form (10-32) with the effective resonance frequency $\bar{\omega}_1$ and the effective gain factor $\bar{\gamma}_1$. The ratio of the resonator energies corresponds to Eq. (10-35), *i.e.*

$$\eta = \frac{4\gamma_1\gamma_2\kappa^2}{\Big[\big(\bar{\omega}_1 - \omega_1\big)^2 + \big(\bar{\gamma}_1 + \gamma_1\big)^2\Big]\,(\omega_2^2 - \gamma_2^2)},$$

which is in agreement with Eqs. (11-6) and (11-7). These expressions can be generalised to non-linear models of the form (10-37) with an arbitrary complex function $f(a_1)$ by setting $\bar{\omega}_1 = \mathrm{Re}\, f(a_1)$ and $\bar{\gamma}_1 = \mathrm{Im}\, f(a_1)$.

11-2 Robust power transfer with $\mathcal{PT}$ symmetry

Consider the matrix model (10-32) with $\bar{\omega}_1 = \omega_2 = \omega_0$. The corresponding eigenvalue equation reads

$$\begin{pmatrix} \mathrm{i}(\omega_0 - \nu) + \bar{\gamma}_1 & \mathrm{i}\kappa \\ \mathrm{i}\kappa & \mathrm{i}(\omega_0 - \nu) - \gamma_2 \end{pmatrix} \begin{pmatrix} a_1 \\ a_2 \end{pmatrix} = 0\,, \tag{11-11}$$

where ν denotes the eigenfrequencies. The stationary solutions are given by

$$\omega_0 - \nu = \frac{\bar{\gamma}_1 - \gamma_2}{2} \left(\mathrm{i} \pm \sqrt{\frac{4\left(\kappa^2 - \bar{\gamma}_1 \gamma_2\right)}{\left(\bar{\gamma}_1 - \gamma_2\right)^2} - 1} \right) \tag{11-12}$$

and the corresponding mode amplitudes must satisfy

$$-\mathrm{i}\kappa a_1 = (\mathrm{i}(\omega_0 - \nu) - \gamma_2) a_2\,. \tag{11-13}$$

For $\bar{\gamma}_1 \approx \gamma_2$ the model becomes $\mathcal{PT}$-symmetric and Eqs. (11-12) and (11-13) yield

$$\frac{|a_1|^2}{|a_2|^2} \approx \frac{1}{\kappa^2} \left| \frac{\bar{\gamma}_1 + \gamma_2}{2} \mp \mathrm{i} \sqrt{\kappa^2 - \bar{\gamma}_1 \gamma_2} \right|^2 ,$$

which is approximately unity for $\kappa^2 > \bar{\gamma}_1 \gamma_2$; as discussed in Section 6-1 a), this corresponds to the region in which the system is *exactly $\mathcal{PT}$-symmetric*. Further, if $\omega_1 \approx \bar{\omega}_1$ and $\gamma_1 \approx \bar{\gamma}_1$, then the WPT efficiency (11-10) reads

$$\eta \approx \frac{|a_2|^2}{|a_1|^2} \approx 1\,, \tag{11-14}$$

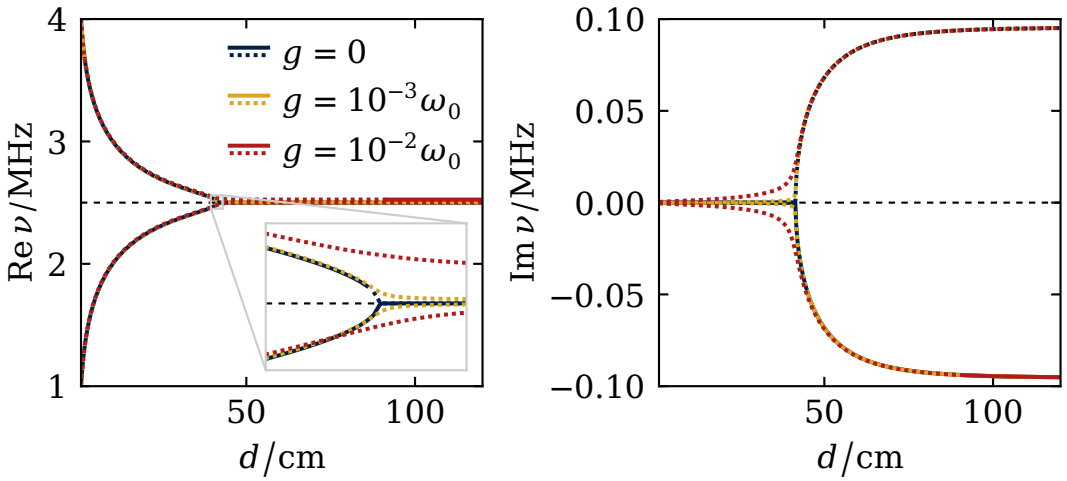

Figure 11-2: Real and imaginary parts of the eigenfrequencies of two $\mathcal{PT}$-symmetric, coupled resonators with the parameters (11-17) and (11-18) and the values given in Table 11-1. The solid and dotted lines indicate stable and unstable states, respectively.

i.e. a $\mathcal{PT}$-symmetric system of coupled resonators exhibits perfect WPT.[6] However, this requires the physical parameters ω_1 and γ_1 of the resonator to be in the same order of magnitude as the effective parameters $\bar{\omega}_1$ and $\bar{\gamma}_1$ of the model. This occurs also for circuits with a *non-linear gain saturation element* [125], which corresponds to[7]

[6] *cf.* Section 10-3 a)

[7] *cf.* Section 10-5 b)

$$f(a_1) = \bar{\omega}_1 - \mathrm{i}\left(\bar{\gamma}_1 + \tilde{g}|a_1|^2\right). \tag{11-15}$$

Figure 11-2 shows the complex eigenfrequencies of the generalised model (10-37) with the non-linear function (10-36) for two resonant circuits coupled via two wire loops that are separated by the distance d as shown in Fig. 10-5. This corresponds to a Schrödinger eigenvalue equation of the form[8]

[8] *cf.* Eq. (11-11)

$$\mathcal{H}\,\mathbf{a} = -\nu\mathbf{a}\,. \tag{11-16}$$

The parameters of some typical electric components — *e.g.* see Ref. [125] — are summarised in Table 11-1, where N is the number of current loops with radius R_w. Further,[9]

[9] Note that the capacities are chosen accordingly.

$$\omega_1 = \bar{\omega}_1 = \omega_2 = \omega_0\,, \tag{11-17}$$

$$\gamma_1 = \bar{\gamma}_1 = -\gamma_2 = \gamma_0\,, \tag{11-18}$$

where $\gamma_0 \approx 95\,\mathrm{kHz}$, which is defined by[10]

[10] *cf.* Section 10-2

$$\gamma_0 = \frac{R}{2L}\,. \tag{11-19}$$

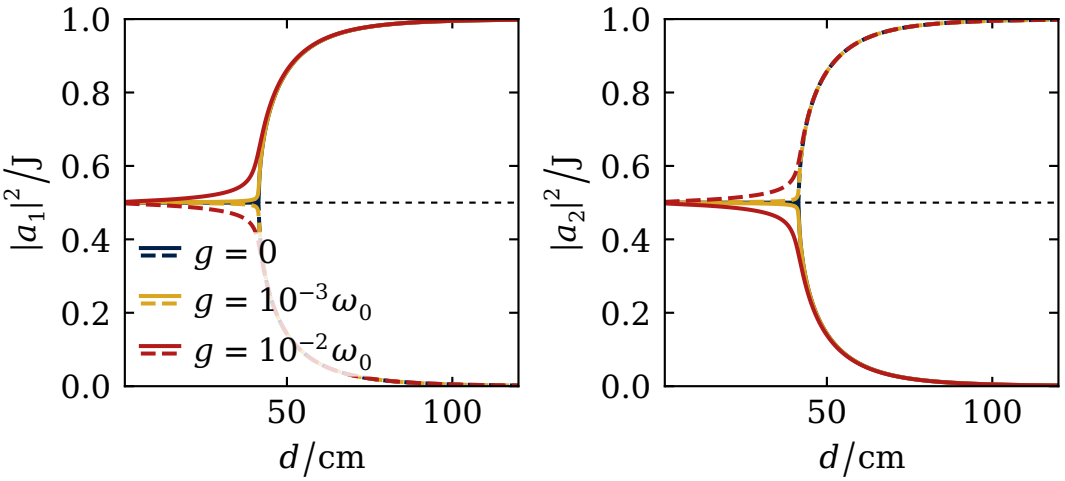

Figure 11-3: The energy in the individual resonators is given by the absolute square of the eigenstates which correspond to Fig. 11-2. The physical states are illustrated with solid lines, unphysical ones with dashed lines.

The coupling constant κ is determined by Eqs. (10-28) and (H-6) and decreases as a function of the distance between the two wire loops as shown in Fig. 10-6 a).

The reason for using the non-linear function (10-36) rather than Eq. (11-15) as in Ref. [125] is that it acts as a perturbation of the effective resonance frequency, which corresponds to the real potential in analogy with the non-linear function (7-2) in Chapter 7.

For the linear case, *i.e.* $g = 0$, the eigenvalues of the coupled electric resonators show a $\mathcal{PT}$-symmetry breaking as it has already been observed in the $\mathcal{PT}$-symmetric two-mode quantum system shown in Fig. 6-2. This is induced by the decrease of the coupling constant κ because the $\mathcal{PT}$ symmetry is *spontaneously broken* at the EP with $\gamma_0/\kappa = 1$. For $g \neq 0$, however, the $\mathcal{PT}$ symmetry is always broken. While the solutions of the non-linear model are quite similar to the solutions of the linear case, as long as the perturbation is small, deviations are apparent for larger values of g. Since the non-linear term occurs only in the primary resonator, the Hamiltonian cannot be $\mathcal{PT}$-symmetric for non-zero mode amplitudes without changing ω_2.

The corresponding resonator energies[11] are shown in Fig. 11-3. The changes due to the non-linear perturbation with strength g are rather subtle, which indicates that the non-linear systems show a similar behaviour as the linear $\mathcal{PT}$-symmetric system. However, it is immediately clear that for larger distances only one of the two solutions is of physical relevance. As energy is inserted only in the primary resonator, the energy of the secondary resonator

Table 11-1: Parameters for the electric components

Param.	Value
ω_0	2.5 MHz
R	400 kΩ
L	2.095 H
N	1000
R_w	29 cm

[11] Reminder: The absolute square of the mode amplitude corresponds to the energy stored in the resonator.

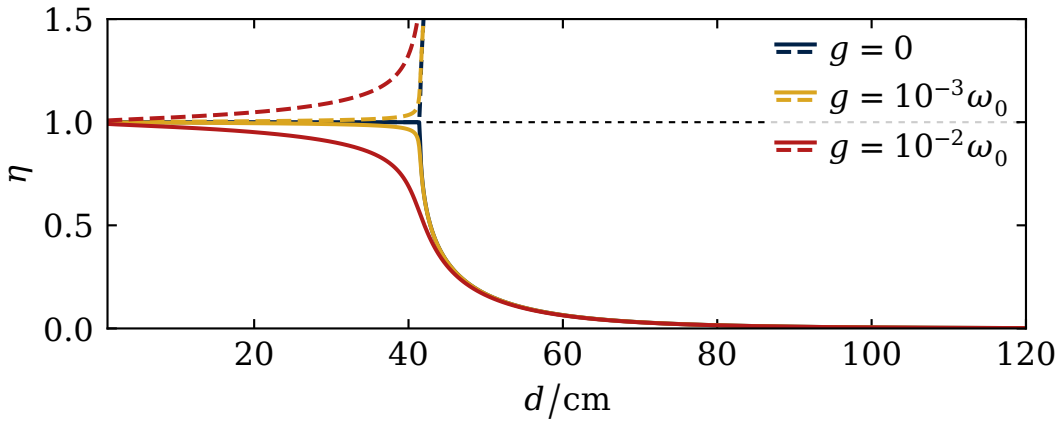

Figure 11-4: WPT efficiency for the solutions in Figs. 11-2 and 11-3. Physical solutions ($\eta \leq 1$) are illustrated with solid lines, unphysical solutions ($\eta > 1$) with dashed lines.

should decrease for weaker couplings; thus, the energy in the primary resonator builds up. The other solution shows the opposite behaviour, so that the energy in the secondary resonator builds up, while the energy in the primary resonator decreases.

The properties described above are common for $\mathcal{PT}$-symmetric quantum systems;[12] that is, there exist solutions in which the eigenfunction increases at the primary site and decreases at the secondary site and *vice versa*. In a system of coupled resonators, though, this leads to unphysical behaviour. This can be seen by calculating the WPT efficiency (11-10) as shown in Fig. 11-4. The efficiency of the physical states with $|a_1|^2 > |a_2|^2$ is always smaller than unity. Instead, the unphysical states with $|a_1|^2 < |a_2|^2$ would allow to extract more energy than the amount that is inserted, thus breaking energy conservation.

[12] *cf.* Section 6-1 a)

Nevertheless, it is remarkable that the physical, $\mathcal{PT}$-symmetric solutions allow for a perfect WPT with maximum efficiency.[13] This holds also for non-linear systems, for which the WPT is almost as efficient if the parameter g is small enough. Though, for $g \neq 0$ the solutions are unstable at smaller distances. This can be seen in Fig. 11-2, where the stable regions are indicated by solid lines, while dotted lines represent the unstable solutions. Thus, $\mathcal{PT}$ symmetry can provide efficient WPT; though, such systems are just marginally stable, since any small non-symmetric perturbation of the system parameters may break the $\mathcal{PT}$ symmetry. Hence, it is of interest whether the self-stabilising behaviour discussed in Section 7-4 b) also occurs for a non-linearity which acts only in the primary resonator.

[13] *cf.* Eq. (11-14)

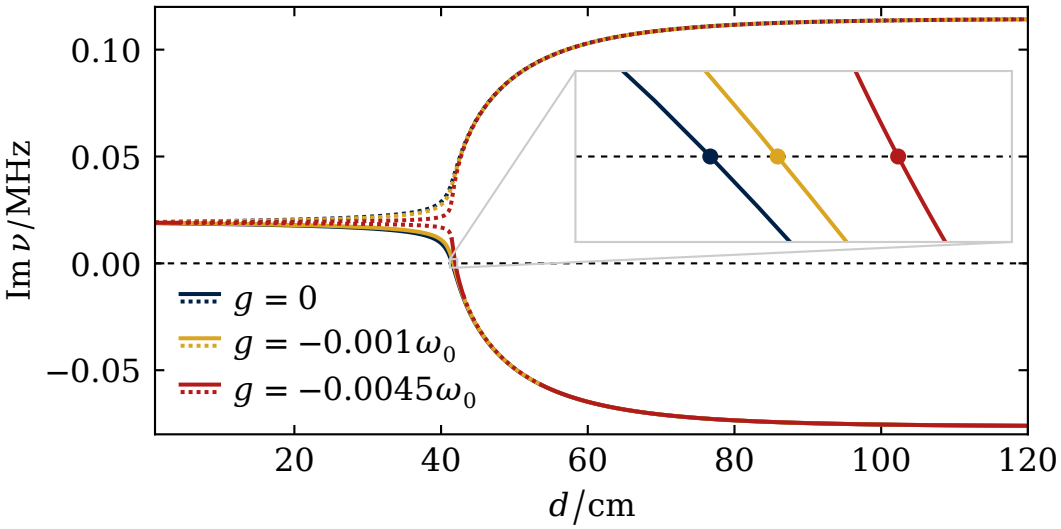

Figure 11-5: The imaginary parts of the eigenfrequencies of two asymmetric, coupled resonators with the parameters (11-20) and (11-21) and the values given in Table 11-2. The solid and dotted lines and the dots indicate the stable, unstable, and stationary states, respectively.

11-3 Non-linear power transfer in asymmetric systems

Similar to the discussions in Section 7-4 b), an asymmetric system of two coupled resonators is investigated. The parameters of the Hamiltonian (10-37) are chosen according to

$$\omega_1 = \omega_0\,, \quad \bar{\omega}_1 = 0.0115\omega_0\,, \quad \omega_2 = 0.0085\omega_0\,, \tag{11-20}$$

$$\gamma_1 = \gamma_0\,, \quad \bar{\gamma}_1 = 0.008\gamma_0\,, \quad \gamma_2 = -0.012\gamma_0\,, \tag{11-21}$$

where $\gamma_0 \approx 9.5\,\mathrm{MHz}$ is given again by Eq. (11-19). The parameters of the electrical components are summarised in Table 11-2. Note that, in contrast to Section 11-2, the physical parameters ω_1 and γ_1 and the model parameters $\bar{\omega}_1$, ω_2, $\bar{\gamma}_1$, and γ_2 in Eqs. (11-20) and (11-21) are not in the same order of magnitude. This is because no such systems with stable stationary solutions were found[14] apart from the $\mathcal{PT}$-symmetric systems discussed in Section 11-2.

Figure 11-5 shows the imaginary parts of the eigenfrequencies of the asymmetric model. Although they look quite similar to the solutions of the $\mathcal{PT}$-symmetric models shown in Fig. 11-2, the imaginary parts are shifted, so that real eigenfrequencies and thus stationary states occur only for larger distances. In contrast to Section 11-2, the non-linearity strength g is chosen to be negative, which in this case yields stable regions in the vicinity

[14] However, this does not mean that there are none.

Table 11-2: Parameters for the electric components

Param.	Value
ω_0	2.5 MHz
R	400 kΩ
L	20.95 mH
N	100
R_w	29 cm

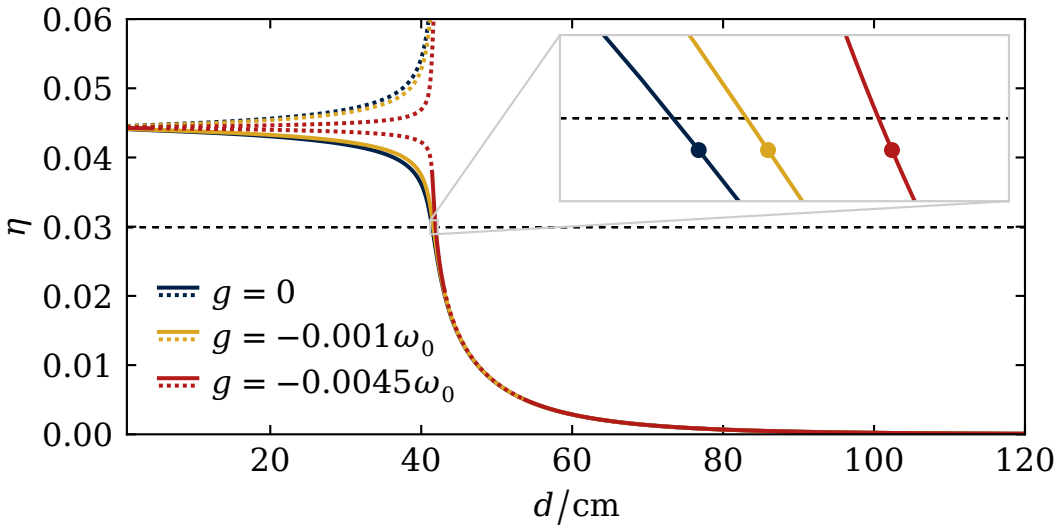

Figure 11-6: WPT efficiency for the solutions in Fig. 11-5. The stationary solutions are illustrated by dots; they appear just below the dashed line which indicates a measure for the optimal efficiency of the model, *i.e.* $\eta = 1$ if ω_1, γ_1 and $\bar{\omega}_1$, $\bar{\gamma}_1$ are in the same order of magnitude.

of the stationary solutions; though, this is only a minor technical detail here, as the parameter g has no physical significance unlike in a quantum system,[15] for example. Unfortunately, these stable regions vanish quickly[16] even for small values of g. Nevertheless, the stationary solutions show the same qualitative behaviour as in Fig. 7-6. This is because the mode amplitude decays for $\mathrm{Im}\,\nu > 0$ and grows for $\mathrm{Im}\,\nu < 0$ due to Eq. (11-16), which has the same effect as decreasing or increasing the parameter g in the model. This again acts as a self-stabilising mechanism — similar as in non-linear quantum systems — with respect to small changes in the separation distance d. The stationary solutions also become unstable if the non-linear terms become too strong. However, the system discussed here seems to be more sensible, so that this occurs already for rather small values of g.

The WPT efficiency can again be calculated via Eq. (11-10), though, this is only relevant exactly at the stationary points. Nevertheless, Fig. 11-6 shows the WPT efficiency for all states in Fig. 11-5. The stationary points are marked, which reveals that the WPT is rather inefficient in comparison with the $\mathcal{PT}$-symmetric solutions in Section 11-2. This is because the efficiency depends on both the system and the model parameters, which in this case are not in the same order of magnitude. If they were,[17] however, the solutions at $\eta \sim 0.03$ would be almost optimal.

[15] *cf.* Chapter 8

[16] A closer inspection reveals that the stable region around the stationary solutions shrinks towards some point near $\mathrm{Im}\,\nu = 0$ in Fig. 11-5.

[17] *e.g.* by increasing the model parameters in Eqs. (11-20) and (11-21) by two orders of magnitude

11-4 Resonator chains

Last but not least, the considerations about WPT in Section 11-1 for two coupled resonators with gain and loss, as shown in Fig. 11-1, can be generalised to resonator chains, at least as long as gain and loss occur only in the outer-most circuits, that is. An example of a chain with n resonators is shown in Fig. 11-7.

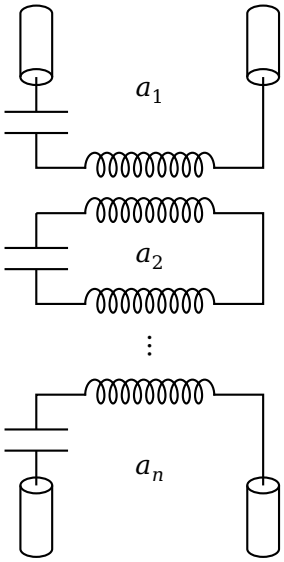

Figure 11-7: Chain of resonant circuits

In Section 6-3 the concept of transport chains was introduced as a special linear type of multi-mode systems with stationary states. For transport chains in QM the parameters are chosen according to Eqs. (6-31) to (6-34). However, Eqs. (6-31) and (6-32) would require the resonance frequencies ω_k of the resonators to be zero. While this is possible for the effective resonance frequency $\bar{\omega}_1$ in the primary resonator, it certainly is not for the physical resonance frequencies determined by $\omega_k = 1/\sqrt{L_k C_k}$. Instead, all resonance frequencies are chosen to be non-zero but equal, *i.e.*

$$\omega_k = \omega_0 = \bar{\omega}_1 \tag{11-22}$$

for $k = 1, \dots, n$. Further, the gain and loss parameters in the outer resonators are chosen as

$$\gamma_1 = \gamma_0 \sqrt{\cot\left(\frac{\pi}{4} - \varphi\right)} = \bar{\gamma}_1 \,, \tag{11-23}$$

$$\gamma_n = -\gamma_0 \sqrt{\tan\left(\frac{\pi}{4} - \varphi\right)} \,, \tag{11-24}$$

which are parametrised by the angle φ. In contrast to Eqs. (6-33) and (6-34), the coupling constant is replaced by $\gamma_0 \approx 955\,\text{Hz}$ defined in Eq. (11-19), which corresponds to a different choice of the scale of gain and loss. The coupling constant $\kappa \approx 276\,\text{kHz}$ is fixed because of a constant separation distance between adjacent resonators. The remaining parameters of the electrical components are summarised in Table 11-3.

Table 11-3: Parameters for the electric components

Param.	Value
ω_0	2.5 MHz
R	40 Ω
L	20.952 mH
N	100
R_w	29 cm
ρ_w	1 mm
ρ	0.0168 µΩ m

Figure 11-8 shows the real and imaginary parts of the eigenfrequencies of a chain of five resonators. It is immediately clear that the parameters (11-22) to (11-24) are no longer the specific solutions for symmetrised systems as in Section 6-3 because the

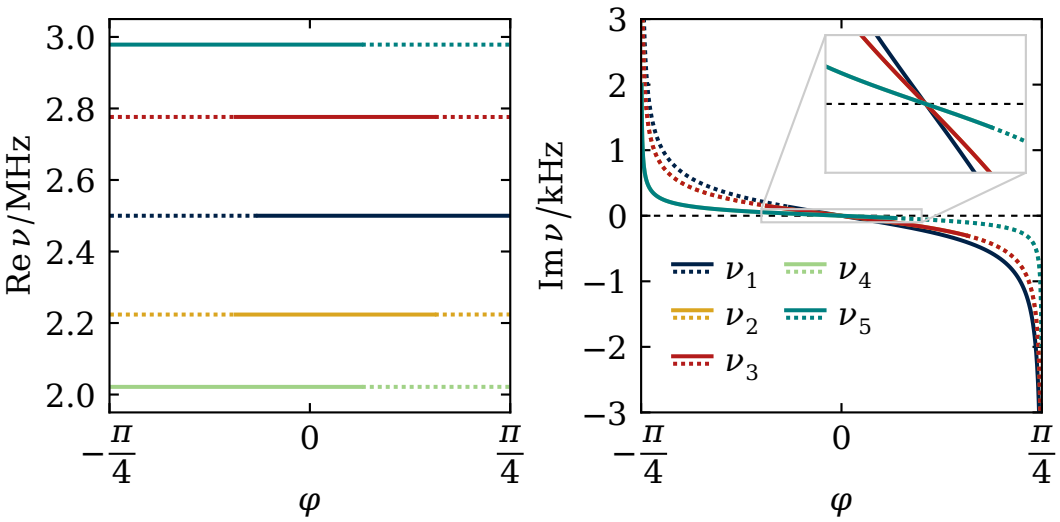

Figure 11-8: Real and imaginary parts of the eigenfrequencies of a chain of five coupled resonators, each separated by $d = 20\,\mathrm{cm}$. The parameters (11-22) to (11-24) are determined by Table 11-3. As before, the solid and dotted lines indicate stable and unstable states, respectively.

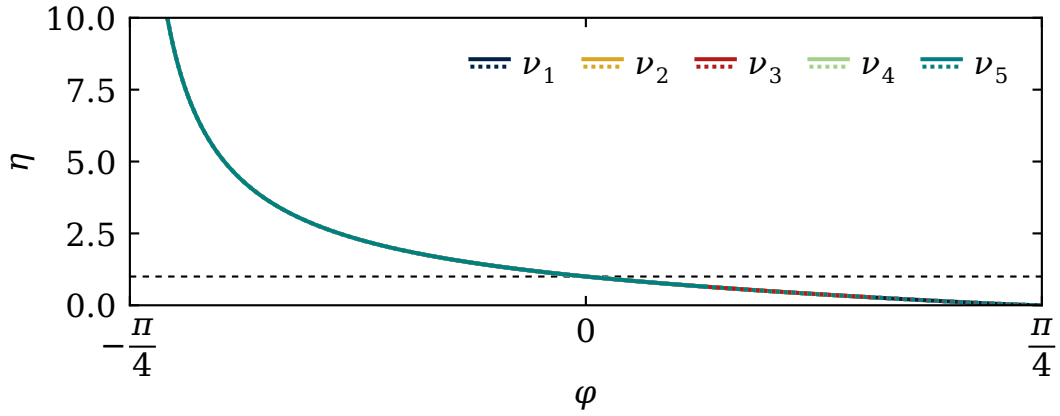

Figure 11-9: WPT efficiency for the stable and unstable solutions of the resonator chain in Fig. 11-8. All states share roughly the same WPT efficiency which is, however, only physically meaningful for the stationary solutions at $\varphi = 0$.

eigenfrequencies are neither real nor do they form complex-conjugate pairs. This is, in particular, due to the physical constraint that the resonance frequencies (11-22) must be non-zero. Nevertheless, the imaginary parts of the eigenfrequencies are still rather small in comparison with the real parts. Moreover, while the real parts of the eigenfrequencies do not noticeably change with respect to their orders of magnitude, the imaginary parts vanish only for $\varphi = 0$ where the parameters (11-23) and (11-24) become $\mathcal{PT}$-symmetric, *i.e.* $\gamma_1 = -\gamma_n$. The farer away the system is from this parameter, the stronger the solutions deviate from a stationary ones. As discussed in Section 11-2, the efficiency of the power transfer of the $\mathcal{PT}$-symmetric systems becomes optimal since the physical and the model parameters are in the same order of magnitude again.[18] This can be observed in Fig. 11-9, where all states are, in fact, described roughly by the same WPT efficiency curve.

[18] *cf.* Eqs. (11-22) and (11-23)

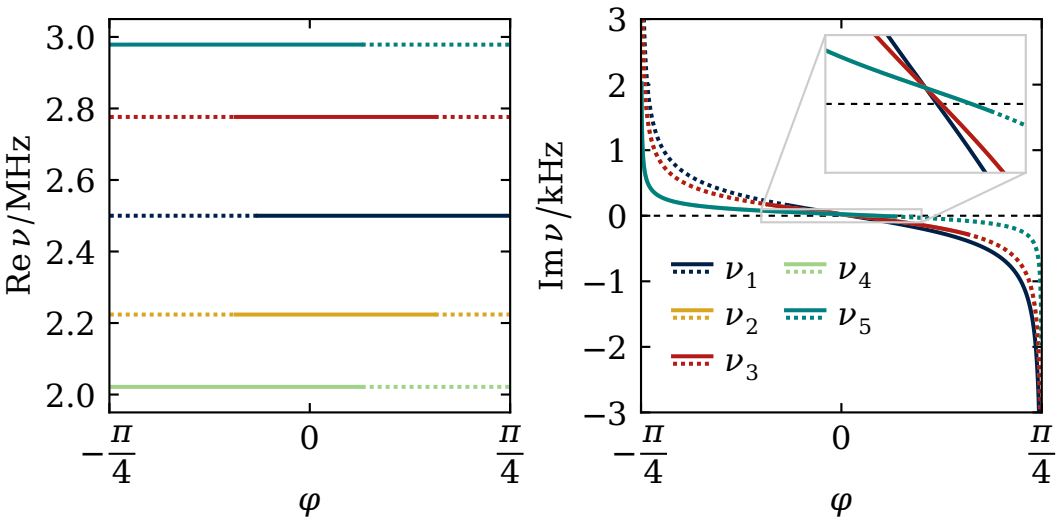

Figure 11-10: Eigenfrequencies of the resonator chain in Fig. 11-8, but with an additional, intrinsic loss. Note that the inset which shows the zeros of the imaginary part uses exactly the same domain as the corresponding inset in Fig. 11-8.

For any real circuit, though, there occurs an intrinsic loss, as discussed in Section 10-2, that has been ignored so far. As an example the resistance of the wire loop is taken into account, which can be calculated via Eq. (10-11). For this reason Table 11-3 also introduces the resistivity ρ of copper taken from Ref. [297]. Hence, in addition to the gain and loss terms in the outer resonators due to Eqs. (11-23) and (11-24), an intrinsic loss term with $\gamma_\mathrm{w} \approx 232\,\mathrm{kHz}$ defined by Eqs. (10-11) and (11-19) is introduced; for the sake of argument, it is assumed that this loss factor is equal in all resonators, ignoring the fact that the inner resonators contain two identical wire loops. The real parts of the eigenfrequencies of the coupled resonators are unchanged as shown in Fig. 11-10. However, the imaginary parts are shifted upwards, so that stable stationary solutions exist for $\varphi \neq 0$. Due to the intrinsic loss in all resonators, none of these solutions can correspond to a $\mathcal{PT}$-symmetric Hamiltonian, *i.e.* they are genuine stationary solutions of an asymmetric potential and correspond to the symmetrised quantum transport chains in Section 6-3.

The efficiency shown in Fig. 11-9 is almost unchanged by the introduction of a small intrinsic loss and can thus be used as a good approximation. Since the stationary solutions of the resonator chain are shifted towards larger values of φ, the corresponding efficiency becomes smaller; this is intuitive, as the WPT efficiency of a stable state cannot exceed unity. Conversely, physical solutions

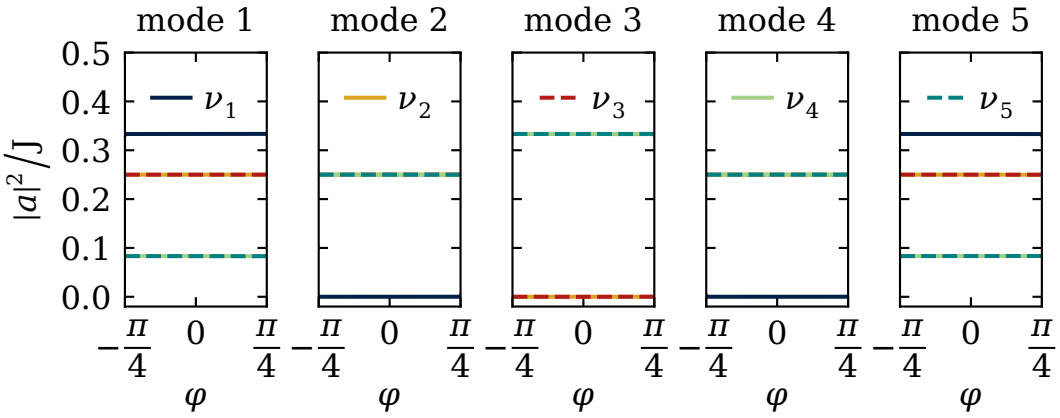

Figure 11-11: The energies of the resonators are approximately equal for Figs. 11-8 and 11-10. Note that ν_1 is non-zero in the third resonator and ν_2, ν_3 are non-zero in the second and fourth resonators; thus, the energy distribution is non-trivial as in Section 6-3.

can only exist for $\varphi \leq 0$ under the assumption that changes to the system preserve the WPT efficiency approximately.

To conclude this discussion, the distribution of the energy in the resonator chain is shown in Fig. 11-11 for the different solutions in Figs. 11-8 and 11-10, *i.e.* the intrinsic loss has only a minor effect on the absolute square of the mode amplitudes. Further, the energies are approximately constant with respect to the parameter φ and — similar to the quantum transport chains in Section 6-3 — all of them are non-trivial, meaning that energy is stored at least in one of the inner resonators. Therefore, the resonator chain does not effectively form a two-resonator system as the one shown in Fig. 11-1. However, the state with $\operatorname{Re}\nu_1 = \omega_0$ effectively forms a three-mode system because[19] $(|a_1|^2)_2 = (|a_1|^2)_4 = 0$; analogously, $(|a_2|^2)_3 = (|a_3|^2)_3 = 0$, *i.e.* these states effectively form a four-mode system.

[19] Here, $(|a_k|^2)_l$ means the absolute square of the l-th component of the k-th eigenvector.

Conclusions and Outlook 12

There is nothing more to be said or to be done tonight.

Sherlock Holmes
—The Five Orange Pips

In this thesis effectively open systems with gain and loss were discussed both within QM and ED. In theory, gain and loss can be introduced via complex potentials which render the Hamiltonian non-Hermitian. The effective description of open systems is of practical importance, as it allows for an elegant and efficient description of otherwise tremendously complicated systems.[1]

For NHQM[2] the rather general concept of symmetrisation was introduced in Chapter 5 as a tool for obtaining physical systems and states for not necessarily physical types of non-Hermitian Hamiltonians. Physical spectra of non-Hermitian Hamiltonians consist of real or complex-conjugate eigenvalues. Such systems are required to satisfy the symmetrisation conditions (5-14) and (5-15) with the symmetrisation operators which can be derived directly[3] or within the framework of SUSY QM.[4] In simple cases the symmetrisation operators also define a metric.[5]

In contrast to actual symmetries[6] like $\mathcal{PT}$ symmetry, symmetrised systems allow for completely asymmetric potentials with no apparent symmetries or structure. This generalisation proves to be useful for obtaining physically meaningful, non-Hermitian quantum systems which are, for example, asymmetric by nature or become asymmetric because an imposed symmetry is hard to maintain.[7] Further, in contrast to similar theories, symmetrisation as a tool allows for applications to systems with incomplete spectral properties, *i.e.* only a specific part of the spectrum is real or complex-conjugate. This occurs, for example, if only a subspace of the Hilbert space is physically meaningful, while the remaining

[1] *cf.* Section 4-6

[2] *cf.* Chapter 4

[3] *cf.* Section 5-3 b)

[4] *cf.* Section 5-2

[5] *cf.* Section 4-4

[6] *cf.* Section 5-3 a)

[7] *cf.* Chapter 8

states can be considered to be consequences of the system being described effectively. Such scenarios require for the concept of semi-symmetrisation, which involves semi-inverse symmetrisation operators, and is particularly useful in cases where only a number of specific states is required in an application; an example is given by WPT considered in the second part of the thesis. However, there are also systems which are inherently just semi-symmetrisable. The two-mode system discussed in Section 6-1 possesses — apart from the $\mathcal{PT}$-symmetric case — only one stationary state. This is a consequence of the limited number of parameters and this property does not occur for higher-dimensional systems with at least three modes.[8] This also holds, in principle, for spatially extended systems as discussed in Section 6-4 and Ref. [180]. However, the construction of symmetrised systems can be rather difficult or even impossible with analytical means, which was discussed in Sections 6-2, 6-4 and 7-3.

[8] *cf.* Section 6-2

The parameters of symmetric and symmetrised systems must also satisfy specific relations due to the symmetrisation conditions, *e.g.* see Eq. (6-16), which, in the latter case, correspond to unobvious symmetries.[9] There are limits, though: While symmetrisation occurs within extended regions in the parameter space, there also exist regions for which a system is not symmetrisable; this can best be seen in Figs. 6-3, 6-4 and 6-7. Although their existence is clear from a mathematical perspective,[10] there seems to be no distinctly physical cause. The reason due to which a human being is unable to recognise patterns and structures in symmetrised systems can be ascribed to the fact that they are *unintuitive*. That is, similar as for QM itself, our everyday lives do not prepare us for these tasks and we thus have to rely on rather abstract mathematics for their identification and description. In recent years, however, computational techniques were developed to circumvent these issues.

[9] *cf.* Section 6-2

[10] There no longer exist real solutions for the parameters for which the symmetrisation conditions are satisfied, *cf.* Section 6-1 d).

Nowadays, *machine learning*[11] and similar technologies can be used to recognise and reproduce structures in vast amounts of data; this makes them particularly useful for image and video processing. However, such algorithms can also be used to extract physical laws [299; 300]. Machine learning proves to be increasingly useful

[11] *e.g.* see Ref. [298] for an overview

for tackling hard problems, like protein folding [301], which are difficult to treat numerically with usual means. Another example of such a type of problem are *many-body quantum systems* [302–304]. The explicit treatment of even just medium-sized many-body systems is quite difficult due to the vast number of degrees of freedom involved. For larger systems one must rely entirely on approximations like the *Bogoliubov back-reaction* [193; 305–307]. In the context of this thesis machine learning concepts could also prove to be useful in recognising the unobvious symmetries and patterns of symmetrised systems. Hence, physical systems could be identified and reproduced in arbitrary environments by a suitably trained *neural network*. This could pave the way for future technical applications.

Another but rather academic application for symmetrisation might be in open many-body quantum systems themselves, where gain and loss usually are introduced via *Lindblad superoperators* [308]. Such a system can be described by a *quantum master equation* [309; 310]. It has already been shown that the characteristic and dynamical properties of such systems correspond to the $\mathcal{PT}$-symmetric models in the mean-field approximation [309]. However, the concept of $\mathcal{PT}$ symmetry is not applicable to many-body quantum systems directly. This is because for small numbers of particles a natural imbalance between gain and loss terms occurs due to differences in the creation and annihilation operators acting on *Fock states* [309],

$$
\begin{aligned}
a_k^\dagger \left|\dots, n_k, \dots\right\rangle &= \sqrt{n_k + 1}\left|\dots, n_k + 1, \dots\right\rangle \,, \\
a_k \left|\dots, n_k, \dots\right\rangle &= \sqrt{n_k}\left|\dots, n_k - 1, \dots\right\rangle \,,
\end{aligned}
$$

which describe the microscopic mechanisms for gain and loss. To compensate for this, the gain-loss terms must be chosen asymmetrically, so that the model formally is not $\mathcal{PT}$-symmetric. Hence, it might be worthwhile to investigate whether or not many-body systems can instead be symmetrised in a similar manner as their counterparts in the mean field discussed in Chapters 6 and 7.

The description of a many-body system is also relevant, in particular, for experiments with BECs as described in Chapter 8, which involve non-linear interaction terms of the form discussed in

Chapter 7. It can be expected that the self-stabilising mechanism, which occurs in the mean-field limit,[12] also occurs in many-body systems. However, it is unclear how robust this phenomenon really is, in particular, for a smaller number of condensate particles, where unique many-body properties start playing a role.[13] Recently, a simplified theory for the theoretical description of BECs and their simulation via many-body calculations was published [311], which can provide accurate results even in strongly interacting regimes; this could provide the means to transfer the concept of symmetrisation to the realm of many-body physics.

[12] *cf.* Section 7-4 b)

[13] *e.g.* see Refs. [193; 264]

Nevertheless, the realisation of such systems within QM is still demanding as discussed in Chapter 8. Yet, the concepts of symmetries and symmetrisation can be transferred from QM to various different wave-mechanical systems. The second part of this thesis dealt with the explicit example of a system of inductively coupled resonant circuits. With *coupled mode theory* a matrix model can be derived which is mathematically equivalent to the discrete, linear Schrödinger equation.[14] Hence, by mapping the parameters of the quantum models to the electrodynamic models, all results described in Chapters 5 and 6 can be transferred with only minor restrictions due to the electrical components of the circuits.

[14] *cf.* Section 10-5

A practical and important technical application of such systems is WPT, which is discussed in Chapter 11. Usually, efficient and robust WPT requires the active tuning of the system parameters [289; 312], which can be used, for example, to adapt the circuit for different separation distances and other forms of misalignments. This may be convenient for some applications of WPT where the separation distance is not necessarily fixed; however, active tuning is necessary for applications like the wireless powering of vehicles,[15] where the distance between the coupled systems varies dynamically. The power transfer in an exactly $\mathcal{PT}$-symmetric WPT system can be optimal independently of the separation distance.[16] In principle, this does not necessarily require active tuning of the electric components. However, it still requires prior knowledge about the secondary circuit and the specific load, which must be matched perfectly by the primary circuit via the incident wave; otherwise,

[15] *e.g.* see Ref. [313]

[16] *cf.* Section 11-2

the $\mathcal{PT}$ symmetry is broken immediately. In contrast, asymmetric systems in combination with non-linear effects can provide a self-stabilising mechanism which is discussed in Section 11-3 and works similarly to the corresponding effect for quantum systems discussed in Chapter 7. Yet, this also requires some prior knowledge or an initial exchange of information for choosing a suitable incident wave. Moreover, the examples discussed in Section 11-3 are not quite efficient. This is because a system of coupled resonators with non-linear in-coupling seems to become unstable rather easily. Thus, Chapter 11 serves as a proof of concept rather than a thoroughful evaluation. To determine whether or not the concepts from NHQM are useful and pioneering in the field of WPT requires for further studies. Nevertheless, such systems are a suitable and accessible platform for the application of symmetries and symmetrisation introduced in this thesis.

The application of WPT in Chapter 11 reveals and illustrates the fundamental differences between an actual symmetry[17] and symmetrisation. A symmetry can be considered as a property of the system which holds as long as it is unbroken. Therefore, WPT can be optimal for an extended range of separation distances. Symmetrisation, on the other hand, can be used for achieving a specific state of an individual system, which here corresponds to a specific separation distance between the coupled circuits at a time. Another fundamental difference occurs for two-mode systems in general,[18] where symmetrised but asymmetrically chosen parameters allow for individual stationary states with real eigenvalues, whereas a $\mathcal{PT}$-symmetric two-mode system may possess an entirely real spectrum. Both of these differences stem from the fact that the $\mathcal{PT}$ operator is independent of the system, while the symmetrisation operators are not;[19] they are constructed for a system with specific parameters and thus cannot be applied if a parameter changes. Therefore, symmetry and symmetrisation should be considered as a property and as a tool, respectively.

[17] *i.e.* $\mathcal{PT}$

[18] *cf.* Section 6-1

[19] *cf.* Section 5-3 b)

Although this thesis attempts to give an overview about symmetries and related concepts in physical but non-Hermitian systems, much about their roles and relations is still unclear.[20] The investigation of non-Hermitian systems — NHQM in particular — and the

[20] *cf.* Ref. [314]

symmetries within them is already a popular and ongoing field of research nowadays, which yields interesting and intriguing results. Surely, his trend will continue and with it the quest for balancing gain and loss.

Appendices

Notations

A

A-1 Derivatives

type	notation used by			
	Leibniz	Euler	Lagrange	Newton
first-order	$\frac{\mathrm{d}f}{\mathrm{d}t}$	$\partial_t f$	f'	$\dot{f}$
second-order	$\frac{\mathrm{d}^2 f}{\mathrm{d}t^2}$	$\partial_t^2 f$	f''	$\ddot{f}$
mixed	$\frac{\mathrm{d}^2 f}{\mathrm{d}x\mathrm{d}y}$	$\partial_{xy} f$	$f'_,$	

Table A-1: Common and uncommon notations for different derivatives. The rather unusual notation for mixed derivatives in Lagrange's notation is used in Ref. [315].

A-2 Bi-orthogonal notation

The common notation for quantum states introduced by Paul Dirac in 1939 [316] describes vectors in Hilbert spaces by kets $|\psi\rangle$ and the co-vectors by bras $\langle\psi|$. Bras and kets are related by the operation of Hermitian adjungation. Further, the inner product is given by a simple bra-ket $\langle\psi|\psi\rangle$. This notation is elegant and efficient when dealing with standard QM in which operators are bound to be Hermitian.

However, when dealing with a non-Hermitian operator $\mathcal{H}$, there is not only the duality between bras and kets, which corresponds to $\mathcal{H}$ and $\mathcal{H}^\dagger$, but one must also distinguish between left-hand and right-hand eigenstates of $\mathcal{H}$. This requires for another layer of notation and provides a typographic challenge: On the one hand, the notation should be as explicitly as possible, so that the reader may quickly understand the meaning of an expression; on the other hand, the notation should also be as simple as possible,[I] so that

[I] *cf. Occam's razor* or *lex parsimoniae*

complex expressions will not become overly cluttered.

The simplest solution — used in Ref. [83] and subsequent publications, for example — is to use different symbols for left-hand and right-hand states, *e.g.* $|\psi\rangle$ and $|\varphi\rangle$. While this works well with Dirac's notation, the author is forced to use specific symbols consistently and exclusively, which makes this kind of notation rather inflexible. Further, the reader is forced to remember which symbols are used for left-hand and which symbols are used for right-hand states.

In Table A-2 different notations for bi-orthogonal states are collected. The entries are ordered roughly by their expressiveness from top to bottom and, at the same time, by their simplicity from bottom to top. While the first notation is readily understandable because of the indices R and L, it takes away from the elegance of Dirac's notation. The next two solutions modify Dirac's notation further by introducing new delimiters; they also explicitly highlight the fact that a new inner product $\langle\psi_n|\eta|\psi_m\rangle$ is introduced, where η is the metric operator connecting the left-hand and right-hand states. Although the third notation is elegant and simple, it is not really consistent, as the *c-product* $(\psi_n|\psi_m)$ is indistinguishable from the product of two left-hand states. The last notation is based on the index notation used in relativity theory and leaves the notation of bras and kets unchanged.

To the author the last notation seems to be a good choice for the following reasons: Dirac's notation and its meaning are preserved while another simple layer of information is introduced by the positioning of the indices; *i.e.* *subscripts* are used for right-hand states and *superscripts* are used for left-hand states. Further, the

Table A-2: Different possible notations for bi-orthogonal states inspired by literature. The index η indicates that left and right states are related by a metric operator with the same symbol.

notation					used in
left states		right states		inner product	
${}_{\mathrm{L}}\langle\psi_n|$	$|\psi_n\rangle_{\mathrm{L}}$	${}_{\mathrm{R}}\langle\psi_n|$	$|\psi_n\rangle_{\mathrm{R}}$	${}_{\mathrm{L}}\langle\psi_n|\psi_m\rangle_{\mathrm{R}}$	[84]
$\langle\!\langle\psi_n|$	$|\psi_n\rangle\!\rangle$	$\langle\psi_n|$	$|\psi_n\rangle$	$\langle\!\langle\psi_n|\psi_m\rangle\!\rangle_\eta$	[83]
$(\psi_n|$	$|\psi_n)$	$\langle\psi_n|$	$|\psi_n\rangle$	$(\psi_n|\psi_m)$	[58]
$\langle\psi^n|$	$|\psi^n\rangle$	$\langle\psi_n|$	$|\psi_n\rangle$	$\langle\psi^n|\psi_m\rangle$	[317]

meaning of an expression can readily be understood by any reader with some education in physics, since the notations are already familiar. To obtain a corresponding representation of objects without indices, one may lend on a notation used in quantum field theories, where left-hand mathematical objects are *underlined*, while right-hand mathematical objects are *overlined*. Last but not least, a corresponding notation for norms could be introduced by drawing on the notation used for flooring[2] and ceiling.[3] This allows for a simple, compact, and mostly consistent notation that is illustrated with several examples in the following section.

[2] lower-angled vertical bars

[3] upper-angled vertical bars

a) Examples

1) Right-hand representations of bras and kets with indices are indicated by subscripts,

$$\langle \psi_n | \,, \quad | \psi_n \rangle \,,$$

and otherwise by underlining,

$$\langle \underline{\psi} | \,, \quad | \underline{\psi} \rangle \,.$$

2) Left-hand representations of bras and kets with indices are indicated by superscripts,

$$\langle \psi^n | \,, \quad | \psi^n \rangle \,,$$

and otherwise by overlining,

$$\langle \overline{\psi} | \,, \quad | \overline{\psi} \rangle \,.$$

3) States are orthogonal with respect to the mixed inner product

$$\langle \psi^n | \psi_m \rangle \propto \delta_{nm} \,.$$

4) It is important with respect to which inner product physical quantities are defined,

$$\lfloor \psi \rfloor \equiv \langle \underline{\psi} | \underline{\psi} \rangle \overset{?}{\leftarrow} |\psi|^2 \overset{?}{\rightarrow} \langle \overline{\psi} | \underline{\psi} \rangle \equiv \lceil \psi \rfloor \, .$$

5) It is immediately clear to which handedness a mathematical objects belongs, *i.e.*

$$\underline{\rho} = \sum_E \underline{p}_E \, |\underline{E}\rangle\langle\underline{E}| \, ,$$
$$\overline{\rho} = \sum_E \overline{p}_E \, |\overline{E}\rangle\langle\overline{E}| \, .$$

6) Even complex expressions like matrix elements are still readable,

$$\overline{\rho}_{kl} = \sum_n \left\langle \varphi_k | \psi^n \right\rangle \left\langle \psi^n | \varphi_l \right\rangle \, ,$$
$$\underline{\rho}^{kl} = \sum_n \left\langle \varphi^k \middle| \psi_n \right\rangle \left\langle \psi_n \middle| \varphi^l \right\rangle \, .$$

B Physical operators in quantum mechanics

Noether's theorem connects the emergence of continuous symmetries to the existence of conserved quantities. As discussed in Section 2-2 a), rotations and boosts are the fundamental symmetries of the Lorentz group. However, the representations used in this section are all finite-dimensional, *i.e.* the transformations are represented by matrices acting on constant objects. However, in most situations the objects will change in space and time. Hence, for more advanced theories an infinite-dimensional representation of the Lorentz group has to be considered — the *field representation* — in which the generators are given by differential operators.

The fundamental symmetries of spacetime are translations, rotations, and boosts.[I] Each of these symmetries possesses its own symmetry generators which are listed in Table B-1. In QM the operators that correspond to physical quantities can be identified with the symmetry generators. Hence, in position space one finds

[I] *cf.* Section 2-2 c)

$$\hat{x}_k = x_k \,, \tag{B-1}$$

$$\hat{p}_k = -\mathrm{i}\partial_{x_k} \,, \tag{B-2}$$

$$\hat{E} = \mathrm{i}\partial_t \,, \tag{B-3}$$

$$\hat{L} = \frac{\mathrm{i}}{2}\epsilon_{klm}\left(x_l\partial_{x_m} - x_m\partial_{x_l}\right) . \tag{B-4}$$

symmetry	generator	conserved quantity
temporal translations	$\mathrm{i}\partial_0$	E
spatial translations	$-\mathrm{i}\partial_k$	$\mathbf{p}$
rotations	$\frac{\mathrm{i}}{2}\epsilon_{klm}(x^l\partial^m - x^m\partial^l)$	$\mathbf{L}$
boosts	$\mathrm{i}(x^0\partial_k - x_k\partial^0)$	$t\mathbf{p} - \mathbf{x}E \equiv 0$

Table B-1: Physical quantities and their symmetry generators [15]. Each of these symmetries can be understood as a translation. Note that the conserved quantity of boosts is zero for a suitable choice of t.

These operators act on physical states that are elements of infinite-dimensional Hilbert spaces. From Eqs. (B-1) and (B-2) also the fundamental commutator relation

$$[\hat{x}_k, \hat{p}_l] = \mathrm{i}\delta_{kl} \tag{B-5}$$

can be obtained.

Note that, although there exists no symmetry concerning the conservation of the position itself, the identification (B-1) can be made using the conserved quantity of boosts from Table B-1 and Eqs. (B-2) to (B-4), *cf.* Ref. [15] and references therein.

B-1 Boundedness

While the position-space representation of QM corresponds to an infinite-dimensional Hilbert space, the physical operators defined on it are unbounded. In contrast, physical operators defined on finite-dimensional Hilbert spaces are bounded. To see this, consider an operator O defined on an n-dimensional complex vector space H. By choosing a basis $\{\hat{\mathbf{e}}_1, \dots, \hat{\mathbf{e}}_n\}$ of the vector space, the linear transformation defined by O is given by

$$Ox = \sum_{i=1}^{n} x_i O\hat{\mathbf{e}}_i \,.$$

With the *triangle inequality* the norm can be written as

$$\|Ox\| = \left\| \sum_{i=1}^{n} x_i O\hat{\mathbf{e}}_i \right\| \leq \sum_{i=1}^{n} |x_i| \|O\hat{\mathbf{e}}_i\| \leq M \sum_{i=1}^{n} |x_i| \,. \tag{B-6}$$

In the last step each norm of the images of the basis vectors is replaced by the their maximum $M = \sup_j \|O\hat{\mathbf{e}}_j\|$, respectively.

Because all norms on finite-dimensional vector spaces are equivalent, that is

$$\widetilde{C}\|x\| \leq \sum_{i=1}^{n} |x_i| \leq C\|x\| \,,$$

Eq. (B-6) is bounded from above, *i.e.*

$$\|Ox\| \leq \lambda \|x\|$$

with $\lambda = CM$, which means that O is bounded. A more general statement, which also holds in infinite dimensions, is made by the *Hellinger–Toeplitz theorem*: Any operator which is Hermitian with respect to a given inner product and which is defined on the entire Hilbert space that corresponds to this inner product is bounded [318].

From a more physical point of view it is often reasonable to assume the boundedness of an operator which describes an observable, even though the underlying Hilbert space is infinite-dimensional. As argued in Refs. [84; 319], in most experiments only a function of the observable $f(O)$ is measured. Even if O is unbounded, the function $f(O)$ might be bounded and yields the same information as O if it is invertible.

B-2 Matrix representations

Matrix representations are an important concept in QM and can simplify the understanding of the abstract concept of operators. Consider an orthonormal basis $\{\hat{e}_k\}$ which satisfies the *closure relation*

$$\sum_k |\hat{e}_k\rangle\langle\hat{e}_k| = \mathbb{1}\,.$$

Further, consider an operator O and its eigenstates $\{\varphi_k\}$, which can be expanded in the orthonormal basis with complex coefficients φ_k,

$$|\varphi_k\rangle = \sum_l \varphi_l |\hat{e}_l\rangle$$

The operator O satisfies an eigenvalue equation

$$O|\varphi_k\rangle = o_k |\varphi_k\rangle \tag{B-7}$$

with the corresponding eigenvalues o_k. Multiplied by $\langle \hat{e}_l |$, the eigenvalue equation (B-7) yields

$$\sum_k O_{lk} \varphi_k = o_k \varphi_k \delta_{lk} \,, \tag{B-8}$$

where

$$O_{lk} = \langle \hat{e}_l | \mathcal{H} | \hat{e}_k \rangle \tag{B-9}$$

are the elements of the operator matrix and $\delta_{lk} = \langle \hat{e}_l | \hat{e}_k \rangle$.

In general, Eq. (B-8) is an infinite-dimensional matrix equation. However, a finite-dimensional representation can be used as an approximation; it converges towards the exact solution if the dimension goes to infinity. If the spectrum of the operator O is bounded from below, then the eigenvalues of a finite-dimensional matrix approximation are upper bounds to the exact eigenvalues of O. This property is called the *Hylleraas–Undheim–MacDonald linear variational theorem* [320; 321].

B-3 The Hermitian adjoint

Consider a general complex matrix O that represents a physical operator O. The matrix elements of O are given by Eq. (B-9) with the orthogonal basis $\{\hat{e}_k\}$. Since

$$\left\langle \hat{e}_k \middle| O^\dagger \hat{e}_l \right\rangle = \left\langle O^\dagger \hat{e}_l \middle| \hat{e}_k \right\rangle^* = \langle \hat{e}_l | O \hat{e}_k \rangle^* \,,$$

one finds that

$$\mathrm{O}^\dagger = \left(\mathrm{O}^\mathsf{T}\right)^* , \tag{B-10}$$

which is the usual definition of the *Hermitian adjoint*.

However, one has to keep in mind that the property (B-10) holds for the matrix representation of the operator, but not necessarily for the operator itself. This can easily be seen by trying to express

O^{T} in a similar fashion,

$$\langle \hat{e}_l | O \hat{e}_k \rangle = \left\langle \hat{e}_k \middle| O^\dagger \hat{e}_l \right\rangle^* \neq \left\langle \hat{e}_k \middle| \left(O^\dagger\right)^* \hat{e}_l \right\rangle = \left\langle \hat{e}_k \middle| O^{\mathsf{T}} \hat{e}_l \right\rangle . \tag{B-11}$$

Only if the basis functions are real, the inequality in Eq. (B-11) becomes an equality, so that Eq. (B-10) holds for the corresponding operator.

Wigner's theorem

C

Wigner's theorem states that the transformations T which leave the inner product unchanged, that is

$$|\langle T\phi|T\psi\rangle| = |\langle\tilde{\psi}|\psi\rangle|\,, \tag{C-1}$$

are either unitary or anti-unitary [35]. A rather simple derivation of this statement is given in Ref. [43], which is summarised in the following.

To find the properties of T, it is useful to first consider the simplest possible Hilbert space $\mathcal{H} = \mathbb{C}$, in which all states $|\psi\rangle$ are just complex numbers ψ. Then, a transformation $T : \mathbb{C} \to \mathbb{C}$ can be considered as a function of either a single complex argument or two real arguments,[I]

$$T(\operatorname{Re} z, \operatorname{Im} z) = T\left(\frac{z+z^*}{2}, \frac{z-z^*}{2\mathrm{i}}\right) \equiv T\left(z, z^*\right).$$

[I] $T(z, z^*)$ has to be understood as a notation only. However, $T(z, \bar{z})$ defines an analytic continuation for $\bar{z} \neq z^*$.

In this sense, Eq. (C-1) reads

$$\left|T^*\left(\phi, \phi^*\right)T\left(\psi, \psi^*\right)\right| = \left|\phi^*\psi\right|. \tag{C-2}$$

For $|\phi^*\psi| \neq 0$, Eq. (C-2) can be written as $|Q| = 1$ with the solutions $Q = \exp(\pm\mathrm{i}\theta)$. Therefore,

$$T^*\left(\phi, \phi^*\right)T\left(\psi, \psi^*\right) = \phi^*\psi\, \mathrm{e}^{\mathrm{i}\theta(\phi,\phi^*,\psi,\psi^*)}\,, \tag{C-3}$$

$$\bar{T}^*\left(\psi, \psi^*\right)\bar{T}\left(\phi, \phi^*\right) = \phi^*\psi\, \mathrm{e}^{\mathrm{i}\bar{\theta}(\psi,\psi^*,\phi,\phi^*)}\,. \tag{C-4}$$

Equations (C-3) and (C-4) are the representations of Q and Q^* for $|Q| = 1$, so that $\bar{\theta}(\psi, \psi^*, \phi, \phi^*) = -\theta(\phi, \phi^*, \psi, \psi^*)$. However, for the following argument θ and $\bar{\theta}$ can be considered as distinct functions that are twice differentiable.

It proves useful to redefine the phase of $T(z, z^*)$,

$$\tilde{T}\left(z, z^*\right) = T\left(z, z^*\right)\mathrm{e}^{\mathrm{i}\alpha(z,z^*)}\,,$$

so that

$$\tilde{T}^*\left(\phi,\phi^*\right)\tilde{T}\left(\psi,\psi^*\right) = \phi^*\psi\,\mathrm{e}^{\mathrm{i}\tilde{\theta}\left(\phi,\phi^*,\psi,\psi^*\right)},$$
$$\tilde{\bar{T}}^*\left(\psi,\psi^*\right)\tilde{\bar{T}}\left(\phi,\phi^*\right) = \phi^*\psi\,\mathrm{e}^{\mathrm{i}\tilde{\bar{\theta}}\left(\psi,\psi^*,\phi,\phi^*\right)}$$

with

$$\tilde{\theta}\left(\phi,\phi^*,\psi,\psi^*\right) = \theta\left(\phi,\phi^*,\psi,\psi^*\right) - \alpha\left(\phi,\phi^*\right) + \alpha\left(\psi,\psi^*\right),$$
$$\tilde{\bar{\theta}}\left(\psi,\psi^*,\phi,\phi^*\right) = \bar{\theta}\left(\psi,\psi^*,\phi,\phi^*\right) - \bar{\alpha}\left(\psi,\psi^*\right) + \bar{\alpha}\left(\phi,\phi^*\right).$$

By choosing $\alpha(\psi,\psi^*) = -\theta(0,0,\psi,\psi^*)$, the term $\tilde{\theta}(0,0,\psi,\psi^*)$ can be cancelled. In the same manner $\bar{\alpha}(\psi,\psi^*) = \bar{\theta}(\psi,\psi^*,0,0)$ cancels the term $\tilde{\bar{\theta}}(\psi,\psi^*,0,0)$. Therefore,

(C-5) $$\theta\left(0,0,\psi,\psi^*\right) = 0\,,\ \frac{\mathrm{d}}{\mathrm{d}\psi}\theta\left(0,0,\psi,\psi^*\right) = \frac{\mathrm{d}}{\mathrm{d}\psi^*}\theta\left(0,0,\psi,\psi^*\right) = 0\,,$$

(C-6) $$\bar{\theta}\left(\psi,\psi^*,0,0\right) = 0\,,\ \frac{\mathrm{d}}{\mathrm{d}\psi}\bar{\theta}\left(\psi,\psi^*,0,0\right) = \frac{\mathrm{d}}{\mathrm{d}\psi^*}\bar{\theta}\left(\psi,\psi^*,0,0\right) = 0$$

for all choices of ψ without a loss of generality.

Finally, Eqs. (C-3) and (C-4) can be differentiated with respect to ψ and ϕ^* by using the complex derivatives

$$\frac{\mathrm{d}}{\mathrm{d}z} = \frac{\mathrm{d}x}{\mathrm{d}z}\frac{\mathrm{d}}{\mathrm{d}x} + \frac{\mathrm{d}y}{\mathrm{d}z}\frac{\mathrm{d}}{\mathrm{d}y} = \frac{1}{2}\left(\frac{\mathrm{d}}{\mathrm{d}x} - \mathrm{i}\frac{\mathrm{d}}{\mathrm{d}y}\right),$$
$$\frac{\mathrm{d}}{\mathrm{d}z^*} = \frac{\mathrm{d}x}{\mathrm{d}z^*}\frac{\mathrm{d}}{\mathrm{d}x} + \frac{\mathrm{d}y}{\mathrm{d}z^*}\frac{\mathrm{d}}{\mathrm{d}y} = \frac{1}{2}\left(\frac{\mathrm{d}}{\mathrm{d}x} + \mathrm{i}\frac{\mathrm{d}}{\mathrm{d}y}\right),$$

where $x = (z+z^*)/2$ and $y = (z-z^*)/2\mathrm{i}$ are the real and the imaginary part of z, respectively.

1) After the differentiation of Eq. (C-3), the left-hand side reads

$$\frac{\mathrm{d}}{\mathrm{d}\phi^*}\frac{\mathrm{d}}{\mathrm{d}\psi}T^*\left(\phi,\phi^*\right)T\left(\psi,\psi^*\right) = \left[\frac{\mathrm{d}}{\mathrm{d}\phi}T\left(\phi,\phi^*\right)\right]^*\frac{\mathrm{d}}{\mathrm{d}\psi}T\left(\psi,\psi^*\right).$$

The term on the right-hand side is given by

(C-7) $$\left[1 + \mathrm{i}\psi\frac{\mathrm{d}\theta}{\mathrm{d}\psi} + \mathrm{i}\phi^*\frac{\mathrm{d}\theta}{\mathrm{d}\phi^*} - \phi^*\frac{\mathrm{d}\theta}{\mathrm{d}\phi^*}\psi\frac{\mathrm{d}\theta}{\mathrm{d}\psi} + \mathrm{i}\phi^*\psi\frac{\mathrm{d}^2\theta}{\mathrm{d}\phi^*\,\mathrm{d}\psi}\right]\mathrm{e}^{\mathrm{i}\theta},$$

where the arguments of θ were omitted in favour of a clearer visual representation. For $\phi = \phi^* = 0$, the right-hand side becomes unity because of Eq. (C-5). Thus,

$$\left[\frac{\mathrm{d}}{\mathrm{d}\psi} T\left(\psi, \psi^*\right)\Big|_{\psi=\psi^*=0}\right]^* \frac{\mathrm{d}}{\mathrm{d}\psi} T\left(\psi, \psi^*\right) = 1\,, \tag{C-8}$$

where the tilde was omitted for convenience. Since this equation holds for all ψ, the transformation $T(\psi, \psi^*)$ is linear in ψ, so that

$$T\left(\psi, \psi^*\right) = \frac{\mathrm{d}}{\mathrm{d}\psi} T\left(\psi, \psi^*\right)\Big|_{\psi=\psi^*=0} \psi\,, \tag{C-9}$$

since $T(0, 0) = 0$ due to Eq. (C-3).

2) The differentiation of Eq. (C-4) yields a similar result. In fact, the right-hand side does not change at all, as all terms in the counterpart of Eq. (C-7) which contain $\bar{\theta}$ or its derivatives vanish according to Eq. (C-6). This finally yields

$$\left[\frac{\mathrm{d}}{\mathrm{d}\psi^*} \overline{T}\left(\psi, \psi^*\right)\Big|_{\psi=\psi^*=0}\right]^* \frac{\mathrm{d}}{\mathrm{d}\psi^*} \overline{T}\left(\psi, \psi^*\right) = 1\,. \tag{C-10}$$

In this case, $\overline{T}(\psi, \psi^*)$ depends linearly on ψ^* and is therefore *anti-linear*,

$$\overline{T}\left(\psi, \psi^*\right) = \frac{\mathrm{d}}{\mathrm{d}\psi^*} \overline{T}\left(\psi, \psi^*\right)\Big|_{\psi=\psi^*=0} \psi^*\,. \tag{C-11}$$

The generalisation of this concept to any Hilbert space is straightforward [43]. Consider

$$\langle\phi|\psi\rangle = \sum_n \langle\phi|\varphi_n\rangle\langle\varphi_n|\psi\rangle = \sum_n \phi_n^* \varphi_n \equiv \phi^* \psi\,,$$

where ψ and ϕ are sequences of the projections of the states $|\psi\rangle$ and $|\phi\rangle$ onto the basis states φ_n. Then,

$$\langle\varphi_n|T\psi\rangle = \sum_m \langle\varphi_n|\mathcal{U}|\varphi_m\rangle\langle\varphi_m|\psi\rangle = \sum_m \mathcal{U}_{nm}\psi_m$$

with

$$\mathcal{U}_{nm} = \left(\frac{\mathrm{d}}{\mathrm{d}\psi} T\left(\psi, \psi^*\right)\Big|_{\psi=\psi^*=0} \right)_{nm} .$$

according to Eq. (C-9). The property (C-8) shows that the operator $\mathcal{U}$ is *unitary*, *i.e.*

$$\begin{aligned} \mathcal{U}^\dagger \mathcal{U} = \mathcal{U}\mathcal{U}^\dagger = \mathbb{1} \,, \\ \mathcal{U}(a\,|\alpha\rangle + b\,|\beta\rangle) = a\mathcal{U}\,|\alpha\rangle + b\mathcal{U}\,|\beta\rangle \,. \end{aligned}$$

The same argumentation holds for Eq. (C-11), which yields

$$\left\langle \varphi_n | \overline{T}\,\psi \right\rangle = \sum_m \langle \varphi_n | \mathcal{A} | \varphi_m \rangle \langle \varphi_m | \psi \rangle = \sum_m \mathcal{A}_{nm} \psi_m$$

with

$$\mathcal{A}_{nm} = \left(\frac{\mathrm{d}}{\mathrm{d}\psi^*} \overline{T}\left(\psi, \psi^*\right)\Big|_{\psi=\psi^*=0} \right)_{nm} .$$

[2] *cf.* Eq. (2-42)

Equation (C-10) shows that the operator $\mathcal{A}$ is *anti-unitary*, *i.e.*[2]

$$\begin{aligned} \mathcal{A}^\dagger \mathcal{A} = \mathcal{A}\mathcal{A}^\dagger = \mathbb{1} \,, \\ \mathcal{A}(a\,|\alpha\rangle + b\,|\beta\rangle) = a^*\mathcal{A}\,|\alpha\rangle + b^*\mathcal{A}\,|\beta\rangle \,, \end{aligned}$$

where the adjoint of $\mathcal{A}$ must not be understood in the ordinary sense, but is instead defined by $\langle \phi | \mathcal{A}\psi \rangle = \langle \mathcal{A}\phi | \psi \rangle^*$.

Avoided crossing theorem

D

Consider a Hamiltonian $\mathcal{H}_0$ with at least two eigenvalues E_1 and E_2 that are closely together but not identical, *i.e.* $|E_1 - E_2| \ll 1$; their corresponding eigenstates are $|\psi_1\rangle$ and $|\psi_2\rangle$. One may ask in which cases the eigenvalues intersect on the variation of some parameters of the system. Or in other words, in which cases do the energy levels cross?

To investigate this, one might follow the argumentation in Ref. [322] by considering a general perturbation $\mathcal{H}_1$ which depends on a set of parameters $\{r_1, \dots, r_n\}$ for $n \geq 1$ and defines a new Hamiltonian

$$\mathcal{H}(r_1, \dots, r_n) = \mathcal{H}_0 + \mathcal{H}_1(r_1, \dots, r_n)\,. \tag{D-1}$$

As a first approximation the superposition $|\psi\rangle = a\,|\psi_1\rangle + b\,|\psi_2\rangle$ may be chosen as an ansatz for a perturbed eigenstate of the Hamiltonian (D-1). The corresponding Schrödinger equation then reads

$$a(E_1 - E + \mathcal{H}_1)\,|\psi_1\rangle + b(E_2 - E + \mathcal{H}_1)\,|\psi_2\rangle = 0\,, \tag{D-2}$$

where E is the eigenvalue of $|\psi\rangle$. By multiplying Eq. (D-2) by $\langle\psi_1|$ and $\langle\psi_2|$, respectively, one finds the linear system of equations

$$\begin{pmatrix} E_1 - E + P_{11} & P_{12} \\ P_{21} & E_2 - E + P_{22} \end{pmatrix} \begin{pmatrix} a \\ b \end{pmatrix} = 0\,,$$

where $P_{nm} = \langle\psi_n|\mathcal{H}_1|\psi_m\rangle$ are the matrix elements of the perturbation. A solution for this system of equations exists only if the determinant of the coefficient matrix vanishes. This yields an equation for the perturbed eigenvalue,

$$E = \frac{1}{2}(E_1 + E_2 + P_{11} + P_{22}) \pm \sqrt{\frac{1}{4}(E_1 - E_2 + P_{11} - P_{22})^2 + P_{12}P_{21}}\,.$$

The eigenvalues coincide if the square root vanishes. Since the two terms under the square root are independent, both of them must vanish simultaneously, which implies

$$E_1 - E_2 + P_{11} - P_{22} = 0\,, \tag{D-3}$$

$$P_{12}P_{21} = 0\,. \tag{D-4}$$

Note that $P_{12} = P_{21}$ for a Hermitian perturbation, *i.e.* $\mathcal{H}_1^\dagger = \mathcal{H}_1$. However, it is not necessary to require such a property here.

Now, consider the one-dimensional case with $n = 1$ first. For one parameter, namely r_1, there exists no possibility to satisfy both Eqs. (D-3) and (D-4) simultaneously in general. However, the off-diagonal elements in Eq. (D-4) vanish identically if the states have different symmetries [322], so that only Eq. (D-3) has to be satisfied. The reason can be understood within the framework of group theory: Consider an operator O of a scalar, physical quantity. Such an operator is by definition invariant under all symmetry transformations. The matrix elements of O are given by

$$O_{nm} = \left\langle \psi_n^{(\alpha)} \middle| O \middle| \psi_m^{(\beta)} \right\rangle\,, \tag{D-5}$$

where α and β indicate that the respective state belongs to a certain set of degenerate energy levels. Let the irreducible representations of their corresponding symmetry groups be $D^{(\alpha)}$ and $D^{(\beta)}$. Since O is invariant with respect to all symmetry transformations, the matrix elements (D-5) belong to the representation given by the direct product $D^{(\alpha)} \otimes D^{(\beta)}$. If $\alpha = \beta$, this representation contains the trivial representation which maps each element to $\mathbb{1}$. In this case Eq. (D-5) reads

$$O_{nm} = O\delta_{nm}\,,$$

where O is a constant [322]. If $\alpha \neq \beta$, on the other hand, then $D^{(\alpha)} \otimes D^{(\beta)}$ does not contain the trivial representation. Thus, the matrix elements (D-5) must vanish, as there would occur changes under a symmetry transformation otherwise.

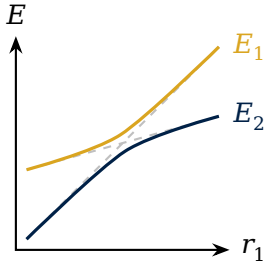

Figure D-1: Avoided crossing of two energy levels

As a conclusion, two energy levels cannot cross if they possess the same symmetry [323]; this statement is called the *avoided*

crossing theorem and it is the origin of *selection rules*. Despite this being said, two energy levels might still cross within perturbational calculations in low order. However, they will move apart on calculating the next order of the approximation [322] as shown in Fig. D-1; this is a typical example of an *avoided crossing*.

For multiple parameters, *i.e.* $n > 1$, Eqs. (D-3) and (D-4) can both be satisfied in general, so that there are crossings of the energy levels. From a geometric point of view the crossings appear on a $(n-2)$-dimensional manifold in the n-dimensional parameter space defined by $\{r_1, \dots, r_n\}$. If the energy levels possess different symmetries, then there again remains only the conditional equation (D-3). Thus, in this case the dimension of the crossing manifold is $n-1$.

However, the *accidental* crossing of two eigenvalues which are sharing the same symmetry is not completely excluded by the avoided crossing theorem [58; 324–327]; though, this occurs rather rarely and is thus quite unlikely in QM according to Ref. [58]. Such accidental crossings are associated with *hidden symmetries* of a system, which are often more of a mathematical phenomenon than of real physical relevance.

Gaussian potential matrix approximation

E

E-1 Frozen Gaussian ansatz

Consider the Schrödinger equation $\mathrm{i}\,|\dot{\psi}\rangle = \mathcal{H}\,|\psi\rangle$ with a potentially non-Hermitian Hamiltonian $\mathcal{H}$. The *frozen Gaussian ansatz*[I] reads

[I] *e.g.* see Ref. [209]

$$|\psi\rangle = \sum_{k=1}^{n} c_k(t)\,|g_k\rangle \tag{E-1}$$

with the time-dependent complex coefficients c_k and Gaussian functions $g_k(\mathbf{r}) = \langle r|\psi\rangle$. The insertion of the ansatz (E-1) into the Schrödinger equation and a multiplication by $\langle g_l|$ yields

$$\mathrm{i}\sum_{k=1}^{n} \underbrace{\langle g_l|g_r\rangle}_{\equiv K_{lk}} \dot{c}_k(t) = \sum_{k=1}^{n} \underbrace{\langle g_l|\mathcal{H}|g_k\rangle}_{\equiv H_{lk}} c_k(t)\,,$$

which can be written as the matrix equation

$$\mathrm{i}K\dot{\mathbf{v}}(t) = H\mathbf{v}(t) \tag{E-2}$$

with $\mathbf{v}(t) = (c_1(t), \ldots, c_n(t))^{\mathsf{T}}$.

The calculation for the corresponding time-independent Schrödinger equation[2] is straightforward and yields

[2] *cf.* Eq. (2-39)

$$H\mathbf{v} = EK\mathbf{v}\,. \tag{E-3}$$

E-2 Symmetric orthogonalisation

If K is a real-valued diagonal matrix, then Eq. (E-3) can be written in Schrödinger form via *symmetric orthogonalisation* [209; 328],

$$\underbrace{K^{-1/2} H K^{-1/2}}_{\equiv \mathcal{H}_{\text{eff}}} \underbrace{\sqrt{K}\mathbf{v}}_{\equiv |\psi\rangle_{\text{eff}}} = E \underbrace{\sqrt{K}\mathbf{v}}_{\equiv |\psi\rangle_{\text{eff}}} ,$$

where $K^{-1/2}$ is the square root of K^{-1} with the diagonal elements $1/\sqrt{k}$ for every diagonal element k of K. This can be generalised for non-diagonal matrices K with $K^{-1/2} \to X$, so that $XKX = \mathbb{1}$ holds in general. Then

$$\underbrace{XHX}_{\equiv \mathcal{H}_{\text{eff}}} \underbrace{X^{-1}\mathbf{v}}_{\equiv |\psi\rangle_{\text{eff}}} = E \underbrace{XKX}_{=\mathbb{1}} \underbrace{X^{-1}\mathbf{v}}_{\equiv |\psi\rangle_{\text{eff}}} .$$

This is possible due to K being Hermitian, *i.e.*

$$K_{lk} = \langle g_l | g_k \rangle = \langle g_k | g_l \rangle^* = K^*_{kl} .$$

Therefore, K is similar to a real-valued diagonal matrix $D = U^\dagger K U$, where U is a unitary matrix. This holds for any arbitrary function of K and thus $X = U D^{-1/2} U^\dagger$ is Hermitian with

$$XKX = U D^{-1/2} \underbrace{U^\dagger K U}_{=D} D^{-1/2} U^\dagger = U U^\dagger = \mathbb{1} .$$

Of course, this line of argument is applicable analogously in the time-dependent case using Eq. (E-2).

Remarks

— The symmetric orthogonalisation can be considered as an *LDL Cholesky decomposition* of K with a lower triangular matrix U.

— The effective Hamiltonian $\mathcal{H}_{\text{eff}}$ is Hermitian if H is Hermitian.

— The norm of the effective wave function $|\psi_{\text{eff}}\rangle$ is well defined, *i.e.*

$$\langle\psi|\psi\rangle = \mathbf{v}^\dagger K\,\mathbf{v} = \psi_{\text{eff}}^\dagger \psi_{\text{eff}}\,.$$

— K is a *metric operator* and defines the norm $\langle\nu|K|\nu\rangle$.

Delta potentials

F

A simple spatial extension of the two-dimensional, non-Hermitian matrix model is a complex, one-dimensional double-delta potential as shown in Fig. F-1. Such a potential can be written as

$$V(x) = \Delta_1 \delta\left(x + \frac{a}{2}\right) + \Delta_2 \delta\left(x - \frac{a}{2}\right), \tag{F-1}$$

where $\Delta_1 = \epsilon_1 + \mathrm{i}\gamma_1$ and $\Delta_2 = \epsilon_2 + \mathrm{i}\gamma_2$, *i.e.* ϵ_1, ϵ_2 and γ_1, γ_2 are the real and imaginary parts of the delta peaks at the positions $x = \pm a/2$, respectively. The corresponding time-independent Schrödinger equation reads

$$\mathcal{H}\psi(x) = \mu\psi(x) \tag{F-2}$$

with the Hamiltonian

$$\mathcal{H} = -\partial_x^2 + V(x)\,.$$

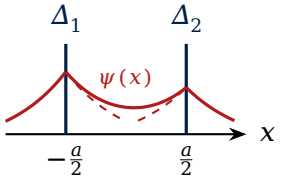

Figure F-1: The wave function in a double-delta potential

In the potential-free case the Schrödinger equation reduces to

$$\partial_x^2 \psi(x) = k^2 \psi(x)$$

with $k = \sqrt{-\mu}$. Therefore, the ansatz for the wave function in between and outside of the delta peaks reads

$$\psi(x) = \begin{cases} \psi_1' \, \mathrm{e}^{kx}\,, & x < -\frac{a}{2} \\ \psi_1 \, \mathrm{e}^{-kx} + \psi_2 \, \mathrm{e}^{kx}\,, & |x| \leq \frac{a}{2} \\ \psi_2' \, \mathrm{e}^{-kx}\,, & x > \frac{a}{2} \end{cases}, \tag{F-3}$$

assuming that $\mathrm{Re}\, k \geq 0$. This assumption corresponds to bound states with real, negative energies. In general, though, μ is complex for the potential (F-1).

The wave function must be continuous at $x = \pm a/2$, *i.e.*

$$\psi_1 \, \mathrm{e}^{\frac{ka}{2}} + \psi_2 \, \mathrm{e}^{-\frac{ka}{2}} = \psi_1' \, \mathrm{e}^{-\frac{ka}{2}}\,, \tag{F-4}$$

(F-5) $$\psi_1 \, \mathrm{e}^{-\frac{ka}{2}} + \psi_2 \, \mathrm{e}^{\frac{ka}{2}} = \psi_2' \, \mathrm{e}^{-\frac{ka}{2}} \, .$$

Another set of equations can be found by integrating the Schrödinger equation (F-2) in the proximity around the delta peaks, that is

$$\lim_{\epsilon \to 0} \left(\partial_x \psi(x) \big|_{-\frac{a}{2}-\epsilon} - \partial_x \psi(x) \big|_{-\frac{a}{2}+\epsilon} \right) = \Delta_1 \psi\left(\frac{a}{2}\right) ,$$
$$\lim_{\epsilon \to 0} \left(\partial_x \psi(x) \big|_{\frac{a}{2}-\epsilon} - \partial_x \psi(x) \big|_{\frac{a}{2}+\epsilon} \right) = \Delta_2 \psi\left(\frac{a}{2}\right) ,$$

By using Eqs. (F-3) to (F-5), one finally finds

(F-6) $$\begin{pmatrix} \left(1 + \frac{2k}{\Delta_2}\right) \mathrm{e}^{ka} & 1 \\ 1 & \left(1 + \frac{2k}{\Delta_1}\right) \mathrm{e}^{ka} \end{pmatrix} \begin{pmatrix} \psi_1 \\ \psi_2 \end{pmatrix} = 0 \, .$$

Equation (F-6) is a conditional equation for the coefficients of the wave function in between the two delta peaks and yields a solution only if the determinant of the coefficient matrix vanishes, *i.e.*

$$\left(1 + \frac{2k}{\Delta_1}\right)\left(1 + \frac{2k}{\Delta_2}\right) = \mathrm{e}^{-2ka} \, .$$

Steady-state solutions

Assuming that the solutions of Eq. (F-6) are both bound, *i.e.* $\mu < 0$, and stationary, *i.e.* $\mu \in \mathbb{R}$, then one finds that $k \in \mathbb{R}$. If $\Delta_1 \Delta_2 \neq 0$, Eq. (F-6) can be written in the form of two real equations

(F-7) $$4k^2 + 2k(\epsilon_1 + \epsilon_2) = (\epsilon_1 \epsilon_2 - \gamma_1 \gamma_2)\left(\mathrm{e}^{-2ka} - 1\right) ,$$

(F-8) $$2k(\gamma_1 + \gamma_2) = (\epsilon_1 \gamma_2 + \gamma_1 \epsilon_2)\left(\mathrm{e}^{-2ka} - 1\right) .$$

Now, consider the following cases:

1) For $\epsilon_1 = \epsilon_2$ and $\gamma_1 = -\gamma_2$, Eq. (F-8) vanishes completely and two real solutions may occur due to Eq. (F-7). As discussed in Section 5-5, a potential with a symmetric real and an anti-symmetric imaginary part is $\mathcal{PT}$-symmetric.

2) In all other cases one of the solutions is always the trivial solution with $k = 0$; its corresponding wave function vanishes everywhere due to the normalisability and continuity conditions. The reason for this is quite simple: The solutions of Eqs. (F-7) and (F-8) are the common intersections of a straight line, a parabola, and an exponential function. Both equations are solved trivially by $k = 0$, though, only Eq. (F-7) allows also for other solutions. Therefore, Eq. (F-8) must vanish, which corresponds again to the first case.

Bi-complex numbers

G

Consider an ordinary complex number $z \in \mathbb{C}$ which can be written as

$$z = x + \mathrm{i}\, y \tag{G-1}$$

with the coefficients $x, y \in \mathbb{R}$. The imaginary unit is defined as usual by $\mathrm{i}^2 = -1$.

A *bi-complex number* is obtained when the real coefficients in Eq. (G-1) become complex themselves with respect to another imaginary unit j, *i.e.*

$$z = \big(x_1 + \mathrm{j}\, x_\mathrm{j}\big) + \mathrm{i}\big(y_1 + \mathrm{j}\, y_\mathrm{j}\big) \equiv z_1 + \mathrm{i}\, z_\mathrm{i} + \mathrm{j}\, z_\mathrm{j} + \mathrm{k}\, z_\mathrm{k}\,, \tag{G-2}$$

where $\mathrm{k} = \mathrm{ij}$. Equation (G-2) is called the *vector representation* of a bi-complex number. Because j is an ordinary imaginary unit, it is also defined by $\mathrm{j}^2 = -1$. Therefore,

$$\mathrm{k}^2 = \mathrm{i}^2\mathrm{j}^2 = 1\,,$$

i.e. k is not an imaginary unit but just an abbreviation. Of course, i and j are freely interchangeable, so none of them is distinguished.

Note that this procedure can be repeated n times, so that hyper-complex numbers with 2^{n+1} coefficients are formed, *i.e.* $n = 0$ corresponds to the usual complex numbers and $n = 1$ to bi-complex numbers.

G-1 Idempotent basis

In principle, Eq. (G-2) summarises all there is to know about bi-complex numbers already. However, there exists a bi-complex representation with particular favourable properties, which can be used to simplify bi-complex calculations. To find it, consider the

special bi-complex numbers

$$e_{\pm} = \frac{1 \pm k}{2} . \tag{G-3}$$

These numbers are quite interesting because

1) they are *zero divisors* and thus form sort of an "orthogonal basis", *i.e.*

$$e_+ e_- = 0 , \tag{G-4}$$

2) they are *idempotent*, meaning

$$e_{\pm}^2 = e_{\pm} . \tag{G-5}$$

Therefore, the numbers (G-3) are called the *idempotent basis* of bi-complex numbers. With the basis elements (G-3) the bi-complex number (G-2) can be written in its *idempotent representation*

$$z = z_+ e_+ + z_- e_- \tag{G-6}$$

with $z_{\pm} \in \mathbb{C}$. Because none of the two imaginary units is distinguished, the complex coefficients can be expressed either with respect to i, that is

$$z_{\pm} = (z_1 \pm z_k) + i\left(z_i \mp z_j\right) ,$$

or with respect to j, that is

$$z_{\pm} = (z_1 \pm z_k) + j\left(z_i \mp z_j\right) .$$

G-2 Bi-complex conjugation

Since bi-complex numbers possess two imaginary units, there exist also two different methods for complex conjugation.

1) The usual complex conjugation with respect to i reads

$$z^* = z_1 - \mathrm{i}z_\mathrm{i} + \mathrm{j}z_\mathrm{j} - \mathrm{k}z_\mathrm{k} = z_-^*\mathrm{e}_+ + z_+^*\mathrm{e}_- \,. \tag{G-7}$$

2) The complex conjugation with respect to j is defined as

$$\bar{z} = z_1 + \mathrm{i}z_\mathrm{i} - \mathrm{j}z_\mathrm{j} - \mathrm{k}z_\mathrm{k} = \overline{z_-}\mathrm{e}_+ + \overline{z_+}\mathrm{e}_- \,. \tag{G-8}$$

Both of these complex conjugations also change the sign of k and thus exchange the idempotent basis elements (G-3).

By combining the complex conjugations (G-7) and (G-8), a third method for complex conjugation — the *bi-complex conjugation* — can be constructed,

$$\bar{z}^* = z_1 - \mathrm{i}z_\mathrm{i} - \mathrm{j}z_\mathrm{j} + \mathrm{k}z_\mathrm{k} = \overline{z_+}^*\mathrm{e}_+ + \overline{z_-}^*\mathrm{e}_- \,.$$

G-3 Bi-complex exponential function

The exponential function can be defined via the limit of the sequence

$$\mathrm{e}^z = \lim_{n\to\infty}\left(1 + \frac{z}{n}\right)^n .$$

Because of the properties (G-4) and (G-5) of the idempotent representation, the exponential function of a bi-complex number of the form (G-6) is given by

$$\begin{aligned}\mathrm{e}^z &= \lim_{n\to\infty}\left[\left(1 + \frac{z_+}{n}\right)\mathrm{e}_+ + \left(1 + \frac{z_-}{n}\right)\mathrm{e}_-\right]^n \\ &= \lim_{n\to\infty}\left(1 + \frac{z_+}{n}\right)^n \mathrm{e}_+ + \lim_{n\to\infty}\left(1 + \frac{z_-}{n}\right)^n \mathrm{e}_- \\ &= \mathrm{e}^{z_+}\mathrm{e}_+ + \mathrm{e}^{z_-}\mathrm{e}_- \,.\end{aligned} \tag{G-9}$$

The same line of thought can be used to derive the bi-complex representations of every function that can be written as a power series.[I]

[I] *e.g.* see Ref. [329]

Inductances of wire loops

H

H-1 The Neumann formula

The flux of a magnetic field $\mathbf{B}$ through a surface S is given by[1]

$$\phi = \int_S \mathbf{B} \cdot \mathrm{d}\mathbf{S} = \int_{\partial S} \mathbf{A} \cdot \mathrm{d}\mathbf{l} \; .$$

[1] *Stoke's theorem* is used in the second step with $\mathbf{A} = \nabla \times \mathbf{B}$.

Here, $\mathbf{A}$ is the retarded vector potential in the *Lorenz gauge*,[2]

$$\mathbf{A}(\mathbf{r}) = \frac{\mu_0}{4\pi} \int_V \frac{\mathbf{J}(\mathbf{r}')}{|\mathbf{r} - \mathbf{r}'|} \mathrm{d}^3\mathbf{r}' \; ,$$

[2] The Lorenz gauge is relativistically invariant and is thus particularly suited for fast changes of the fields, which, for example, occur for alternating electric currents.

which is created by a current $\mathbf{J}$ through a volume V. For a thin element of wire of length l the vector potential can be written as

$$\mathbf{A}(\mathbf{r}) \approx \frac{\mu_0}{4\pi} \int_l \frac{I(l')\,\mathrm{d}l'}{|\mathbf{r} - \mathbf{r}'|} \hat{\mathbf{e}}_{l'} \; ,$$

where

$$I(l')\hat{\mathbf{e}}_{l'} = \int_a \mathbf{J}(\mathbf{r}')\,\mathrm{d}a'$$

is the current through the small wire cross section[3] a. Further, if the current is isotropic along the wire, one finally finds

[3] *i.e.* $\mathbf{r}' \approx$ const.

$$\mathbf{A}(\mathbf{r}) = \frac{\mu_0 I}{4\pi} \int_l \frac{\mathrm{d}l'}{|\mathbf{r} - \mathbf{r}'|} \; . \qquad \text{(H-1)}$$

Now, consider two thin wire loops which enclose the areas A_1 and A_2, respectively. The flux ϕ_{12} through the secondary area A_2 of the magnetic field $\mathbf{B}_1$ created by a current I_1, which is flowing through the primary wire loop, is given by Eq. (H-1); it can also be

expressed as

$$\phi_{12} = M_{12} I_1 \,, \tag{H-2}$$

where

$$M_{12} = \frac{\mu_0}{4\pi} \int\limits_{\partial A_1} \int\limits_{\partial A_2} \frac{\mathrm{d}\mathbf{l}_1 \cdot \mathrm{d}\mathbf{l}_2}{|\mathbf{r}_1 - \mathbf{r}_2|} \tag{H-3}$$

is the *mutual inductance* between the two wire loops. Equation (H-3) is called the *Neumann formula*. Since the dot product is commutative, it is immediately clear that $M_{12} = M_{21} \equiv M$, *i.e.* the coupling is symmetric; in fact, this is a demonstration of the *reciprocity theorem*.

The reciprocity theorem states that the interchange of excitation and response does not affect the result [330]. For example, the magnetic flux (H-2) with the mutual inductance (H-3) is invariant under the exchange of the two areas, *i.e.* it does not matter through which boundary the current flows that causes the magnetic field.

Note that the definition (H-2) of the mutual inductance is completely analogous to the usual definition of the self-inductance[4] via the voltage induced in the secondary wire loop by the current in the primary wire loop, *i.e.* $U_{12} = -M_{12}\dot{I}_{12} = -\dot{\phi}_{12}$.

[4] *cf.* Appendix H-3

H-2 Mutual inductance

In the following, some explicit expressions of the mutual inductance for different geometric arrangement of two wire loops[5] are given. For this, the *Neumann formula* (H-3) with the line elements

[5] *cf.* Fig. 10-5

$$\mathrm{d}\mathbf{l}_k = \begin{pmatrix} -R_k \sin\varphi_k \\ R_k \cos\varphi_k \\ 0 \end{pmatrix} \mathrm{d}l_k \tag{H-4}$$

for $k = 1, 2$ is used.

First, consider two wire loops which are aligned in the x-y plane and which are separated in the z direction by the distance d, *i.e.*

$$\mathbf{d} = (0, 0, d)^\mathsf{T} .$$

With

$$\mathbf{r}_1 = \begin{pmatrix} R_1 \cos\varphi_1 \\ R_1 \sin\varphi_1 \\ 0 \end{pmatrix}, \qquad \text{(H-5)}$$

$$\mathbf{r}_2 = \begin{pmatrix} R_2 \cos\varphi_2 \\ R_2 \sin\varphi_2 \\ d \end{pmatrix},$$

where the origin is set to the centre of the primary loop, one finds

$$M(d) = \frac{\mu_0}{4\pi} \int_{\varphi_1=0}^{2\pi} \int_{\varphi_2=0}^{2\pi} \frac{R_1 R_2 \cos(\varphi_1 - \varphi_2)\,\mathrm{d}\varphi_1\,\mathrm{d}\varphi_2}{\sqrt{R_1^2 + R_2^2 - 2R_1R_2\cos(\varphi_1 - \varphi_2) + d^2}} . \qquad \text{(H-6)}$$

a) Misalignment

Now, consider the same arrangement with an additional misalignment in the x direction, *i.e.*

$$\mathbf{d} = (\delta, 0, d)^\mathsf{T} .$$

Hence,

$$\mathbf{r}_1 = \begin{pmatrix} R_1 \cos\varphi_1 \\ R_1 \sin\varphi_1 \\ 0 \end{pmatrix},$$

$$\mathbf{r}_2 = \begin{pmatrix} R_2 \cos\varphi_2 + \delta \\ R_2 \sin\varphi_2 \\ d \end{pmatrix}.$$

After a short calculation one finds

$$M(d,\delta) = \frac{\mu_0}{4\pi} \int_{\varphi_1=0}^{2\pi} \int_{\varphi_2=0}^{2\pi} \frac{R_1 R_2 \cos(\varphi_1 - \varphi_2)\,\mathrm{d}\varphi_1\,\mathrm{d}\varphi_2}{\sqrt{R_1^2 + R_2^2 - 2R_1 R_2 \cos(\varphi_1 - \varphi_2) + d^2 + \mu(\delta)}}\,,$$

which equals Eq. (H-6) up to the additional term

$$\mu(\delta) = \delta(\delta - 2R_1 \cos\varphi_1 + R_2 \cos\varphi_2)\,.$$

b) Rotation

Last but not least, the case is considered in which the two loops are not aligned parallel to one another. For this, a rotation of the secondary loop around its x axis is introduced via the rotation matrix

$$R_x = \begin{pmatrix} 1 & 0 & 0 \\ 0 & \cos\vartheta & -\sin\vartheta \\ 0 & \sin\vartheta & \cos\vartheta \end{pmatrix}.$$

Then,

$$\mathbf{r}_1 = \begin{pmatrix} R_1 \cos\varphi_1 \\ R_1 \sin\varphi_1 \\ 0 \end{pmatrix},$$

$$\mathbf{r}_2 = R_x \begin{pmatrix} R_2 \cos\varphi_2 \\ R_2 \sin\varphi_2 \\ d \end{pmatrix} = \begin{pmatrix} R_2 \cos\varphi_2 \\ R_2 \sin\varphi_2 \cos\vartheta \\ d + R_2 \sin\varphi_2 \sin\vartheta \end{pmatrix}.$$

In this case also the line element for the secondary loop must be rotated accordingly, *i.e.*

$$\mathrm{d}\mathbf{l}_2 = R_x \begin{pmatrix} -R_2 \sin\varphi_2 \\ R_2 \cos\varphi_2 \\ 0 \end{pmatrix} \mathrm{d}l_2 = \begin{pmatrix} -R_2 \sin\varphi_2 \\ R_2 \cos\varphi_2 \cos\vartheta \\ R_2 \cos\varphi_2 \sin\vartheta \end{pmatrix} \mathrm{d}l_2\,.$$

Therefore, the mutual inductance reads

$$M(d,\vartheta) = \frac{\mu_0}{4\pi} \int_{\varphi_1=0}^{2\pi} \int_{\varphi_2=0}^{2\pi} \frac{R_1 R_2 \,\mathrm{d}\varphi_1 \,\mathrm{d}\varphi_2}{\sqrt{\mu(d,\vartheta)}} (\sin\varphi_1 \sin\varphi_2 + \cos\varphi_1 \cos\varphi_2 \cos\vartheta) \,,$$

where

$$\mu(d,\vartheta) = (R_1\cos\varphi_1 - R_1\cos\varphi_2)^2 + (R_1\sin\varphi_1 - R_2\sin\varphi_2\cos\vartheta)^2 + (d + R_2\sin\varphi_2\sin\vartheta)^2 \,.$$

H-3 Self-inductance

In principle, the self-inductance of a wire loop should be equal to the mutual inductance of two *identical* wire loops at distance $d = 0$; hence, it should be calculable via the Neumann formula (10-21). However, for $\mathbf{r}_1 = \mathbf{r}_2$ the integrand diverges, so that the calculation is not straightforward unfortunately. However, the Neumann formula can be used by dividing the integral into two different parts,

$$L = \frac{\mu_0}{4\pi} \int_{\partial A} \int_{\partial A} \frac{\mathrm{d}\mathbf{l}\cdot\mathrm{d}\mathbf{l}'}{|\mathbf{r}-\mathbf{r}'|}\bigg|_{|\mathbf{r}-\mathbf{r}'|>\epsilon} + \frac{\mu_0}{4\pi} \int_{\partial A} \int_{\partial A} \frac{\mathrm{d}\mathbf{l}\cdot\mathrm{d}\mathbf{l}'}{|\mathbf{r}-\mathbf{r}'|}\bigg|_{|\mathbf{r}-\mathbf{r}'|<\epsilon} \,,$$

where ϵ is small compared to the radii of the wire loops. The second term, which contains all divergences, can be replaced by the inductances of straight wire segments [331], which yields

$$\int_{\partial A} \int_{\partial A} \frac{\mathrm{d}\mathbf{l}\cdot\mathrm{d}\mathbf{l}'}{|\mathbf{r}-\mathbf{r}'|}\bigg|_{|\mathbf{r}-\mathbf{r}'|<\epsilon} \approx \frac{L}{2} \,,$$

where the current is assumed to be equally distributed throughout the wire.

Alternatively, the self-inductance of a wire loop with a finite wire radius ρ can also be calculated via the *Biot–Savart law*

$$\mathbf{B}(\mathbf{r}) = \frac{\mu_0 I}{4\pi} \int\limits_{\partial A} \frac{\mathrm{d}\mathbf{l}' \times (\mathbf{r} - \mathbf{r}')}{|\mathbf{r} - \mathbf{r}'|^3} \,. \tag{H-7}$$

The line element $\mathrm{d}\mathbf{l}'$ and the vector $\mathbf{r}'$ are of the forms (H-4) and (H-5), respectively. It can be shown that the magnetic flux is given by

$$\begin{aligned} \phi &= \int\limits_A \mathbf{B} \cdot \mathrm{d}\mathbf{A} = \mu_0 I R \int\limits_{\varphi=0}^{\pi} \int\limits_{r=0}^{R-\rho} \frac{(R - r\cos\varphi) r \,\mathrm{d}r \,\mathrm{d}\varphi}{R^2 + r^2 - 2Rr\cos\varphi} \\ &\triangleq \mu_0 I R (R-\rho) \int\limits_{\varphi=0}^{\pi} \frac{\cos\varphi \,\mathrm{d}\varphi}{\sqrt{R^2 + (R-\rho)^2 - 2R(R-\rho)\cos\varphi}} \,, \end{aligned} \tag{H-8}$$

where the last term describes just the magnetic flux over the area of the wire loop [332]. Though, this integral is elliptic and cannot be evaluated directly. Yet, by rewriting Eq. (H-8) as

$$\phi = \frac{\mu_0 I}{2} \sqrt{R(R-\rho)} m^2 \int\limits_{\varphi=0}^{\pi} \frac{\cos\varphi \,\mathrm{d}\varphi}{\sqrt{1 - \frac{m^2}{2}(\cos\varphi + 1)}}$$

with $m^2 = 4R(R-\rho)/(2R-\rho)^2$ and by using a change of the variable $\varphi = \pi - 2\vartheta$, one finds

$$\phi = \mu_0 I \sqrt{R(R-\rho)} \left[\left(\frac{2}{m} - m \right) K(m) - \frac{2}{m} E(m) \right]$$

with the *complete elliptic integrals* of the *first* and *second kind*

$$\begin{aligned} K(m) &= \int\limits_0^{\pi/2} \frac{\mathrm{d}\vartheta}{\sqrt{1 - m^2 \sin^2\vartheta}} \,, \\ E(m) &= \int\limits_0^{\pi/2} \sqrt{1 - m^2 \sin^2\vartheta} \,\mathrm{d}\vartheta \,. \end{aligned}$$

For $\rho \ll R$ the factor m can be approximated by $m \approx 1$, which implies $E(m \approx 1) \approx 1$ and

$$K(m \approx 1) \approx \ln\left(\frac{8R}{\rho} - 4\right).$$

The self-inductance L and the magnetic flux ϕ are related by *Faraday's induction law* $U_{\text{ind}} = -L\dot{I} = -\dot{\phi}$. Thus,

$$L = \frac{\phi}{I} \approx \mu_0 R\left[\ln\left(\frac{8R}{\rho} - 4\right) - 2\right].$$

Further, since $R/\rho \gg 1$, the last term in the logarithm can be omitted, which yields the well-known expression

$$L = \mu_0 R\left(\ln\frac{8R}{\rho} - 2\right)$$

for the self-inductance of a thin wire loop with radius R and wire radius ρ.

Glossaries

Acronyms

BdGE	Bogoliubov–de Gennes equations
BEC	Bose–Einstein condensate
ED	electrodynamics
EP	exceptional point
GPE	Gross–Pitaevskii equation
NHQM	non-Hermitian quantum mechanics
NLSE	non-linear Schrödinger equation
QM	quantum mechanics
SUSY	supersymmetry
WPT	wireless power transfer

Abbreviations

cf.	*confer*	meaning “compare”
e.g.	*exempli gratia*	meaning “for example”
et al.	*et alii*	meaning “and others”
etc.	*et cetera*	meaning “and so forth”
i.e.	*id est*	meaning “that is to say”
vs.	*versus*	meaning “against”

Foreign terms

a priori	meaning “from the start”
per se	meaning “by itself”
vice versa	meaning “in reverse”

Bibliography

[1] C. Bender, R. Tateo, P. Dorey, T. Dunning, G. Lévai, S. Kuzhel, A. Fring, H. Jones and D. Hook, »*PT Symmetry in Quantum and Classical Physics*« (WORLD SCIENTIFIC Publishing Company Incorporated, 2019)

[2] E. Schrödinger, »*Die gegenwärtige Situation in der Quantenmechanik*«, Die Wiss. **23**, 807–812 (1935)

[3] K. Kry and R. A. Casey, »*The effect of hiding enrichment on stress levels and behaviour of domestic cats (Felis sylvestris catus) in a shelter setting and the implications for adoption potential*«, Anim. Welf. **16**, 375–383 (2007)

[4] C. Vinke, L. Godijn and W. van der Leij, »*Will a hiding box provide stress reduction for shelter cats?*«, Appl. Anim. Behav. Sci. **160**, 86–93 (2014)

[5] J. L. Stella and C. C. Croney, »*Environmental Aspects of Domestic Cat Care and Management: Implications for Cat Welfare*«, Sci. World J. **2016**, 1–7 (2016)

[6] L. Campbell and W. Garnett, »*The Life of James Clerk Maxwell*« (Cambridge University Press, 2009)

[7] R. W. Batterman, »*Falling cats, parallel parking, and polarized light*«, Stud. Hist. Philos. Sci. B: Stud. Hist. Philos. Mod. Phys. **34**, 527–557 (2003)

[8] R. A. J. Matthews, »*Tumbling toast, Murphy's Law and the fundamental constants*«, Eur. J. Phys. **16**, 172–176 (1995)

[9] D. McDonald, »*How Does a Cat Fall on Its Feet*«, New Sci. **7**, 1647–1649 (1960)

[10] T. Kane and M. Scher, »*A dynamical explanation of the falling cat phenomenon*«, Int. J. Solids Struct. **5**, 663–670 (1969)

[11] R. Montgomery, »*Gauge Theory of The Falling Cat*«, in »*Dynamics and Control of Mechanical Systems*«, edited by M. J. Enos (American Mathematical Society, July 1993), pp. 193–218

[12] A. Arabyan and D. Tsai, »*A distributed control model for the air-righting reflex of a cat*«, Log. Cybern. **79**, 393–401 (1998)

[13] L. J. Maczewsky, K. Wang, A. A. Dovgiy, A. E. Miroshnichenko, A. Moroz, M. Ehrhardt, M. Heinrich, D. N. Christodoulides, A. Szameit and A. A. Sukhorukov, »*Synthesizing multi-dimensional excitation dynamics and localization transition in one-dimensional lattices*«, Nat. Photonics **14**, 76–81 (2019)

[14] N. Jeevanjee, »*An Introduction to Tensors and Group Theory for Physicists*«, 2nd ed. (Birkhäuser Basel, 2015)

[15] J. Schwichtenberg, »*Physics from Symmetry*«, 2nd ed., Undergraduate Lecture Notes in Physics (Springer International Publishing, 2018)

[16] A. Einstein, »*Zur Elektrodynamik bewegter Körper*«, Ann. Phys. **322**, 891–921 (1905)

[17] M. Kaku, »*Einstein's Cosmos: How Albert Einstein's Vision Transformed Our Understanding of Space and Time*« (W. W. Norton & Company, 2004)

[18] M. Robinson, »*Symmetry and the Standard Model*« (Springer New York, 2011)

[19] W. Greiner, »*Relativistic Quantum Mechanics. Wave Equations*« (Springer, July 2000)

[20] S. Hossenfelder, »*A derivation of Born's rule from symmetry*«, Ann. Phys. **425**, 168394 (2021)

[21] Y. Aharonov and D. Bohm, »*Significance of Electromagnetic Potentials in the Quantum Theory*«, Phys. Rev. **115**, 485–491 (1959)

[22] R. G. Chambers, »*Shift of an Electron Interference Pattern by Enclosed Magnetic Flux*«, Phys. Rev. Lett. **5**, 3–5 (1960)

[23] H. Batelaan and A. Tonomura, »*The Aharonov–Bohm effects: Variations on a subtle theme*«, Phys. Today **62**, 38–43 (2009)

[24] J. D. Jackson, »*Classical electrodynamics*«, 3rd (Wiley, New York, 1999)

[25] D. B. Malament, »*On the time reversal invariance of classical electromagnetic theory*«, Stud. Hist. Philos. Sci. B: Stud. Hist. Philos. Mod. Phys. **35**, 295–315 (2004)

[26] I. I. Geru, »*Time-Reversal Symmetry*« (Springer International Publishing, 2018)

[27] T. D. Lee and C. N. Yang, »*Question of Parity Conservation in Weak Interactions*«, Phys. Rev. **104**, 254–258 (1956)

[28] C. S. Wu, E. Ambler, R. W. Hayward, D. D. Hoppes and R. P. Hudson, »*Experimental Test of Parity Conservation in Beta Decay*«, Phys. Rev. **105**, 1413–1415 (1957)

[29] J. H. Christenson, J. W. Cronin, V. L. Fitch and R. Turlay, »*Evidence for the 2π Decay of the K_2^0 Meson*«, Phys. Rev. Lett. **13**, 138–140 (1964)

[30] G. Lüders, »*On the Equivalence of Invariance under Time Reversal and under Particle-Antiparticle Conjugation for Relativistic Field Theories*«, R. Dan. Acad. Sci. Lett. **28**, 1–17 (1954)

[31] W. Pauli, »*Exclusion principle, Lorentz group and reflection of space-time and charge*«, in »*Niels Bohr and the Development of Physics*«, edited by W. Pauli, L. Rosenfeld and V. Weisskopf (McGraw-Hill, New York, 1955), pp. 30–51

[32] V. A. Kostelecký and N. Russell, »*Data tables for Lorentz and CPT violation*«, Rev. Mod. Phys. **83**, 11–31 (2011)

[33] R. Jost, »*Das Pauli-Prinzip und die Lorentzgruppe*«, in »*Theoretical Physics in the Twentieth Century*«, edited by M. Fierz and V. Weisskopf (Interscience, New York, 1960)

[34] O. W. Greenberg, »*CPT Violation Implies Violation of Lorentz Invariance*«, Phys. Rev. Lett. **89**, 231602 (2002)

[35] E. Wigner, »*Gruppentheorie und ihre Anwendung auf die Quantenmechanik der Atomspektren*«, Vol. 85, Die Wissenschaft; Sammlung von Einzeldarstellungen aus den Gebieten der Naturwissenschaft und Technik (Friedrich Vieweg und Sohn, Braunschweig, 1931)

[36] R. Simon, N. Mukunda, S. Chaturvedi and V. Srinivasan, »*Two elementary proofs of the Wigner theorem on symmetry in quantum mechanics*«, Phys. Lett. A **372**, 6847–6852 (2008); R. Simon, N. Mukunda, S. Chaturvedi, V. Srinivasan and J. Hamhalter, »*Comment on: Two elementary proofs of the Wigner theorem on symmetry in quantum mechanics [Phys. Lett. A 372 (2008) 6847]*«, Phys. Lett. A **378**, 2332–2335 (2014)

[37] E. P. Wigner, »*Phenomenological Distinction between Unitary and Antiunitary Symmetry Operators*«, J. Math. Phys. **1**, 414–416 (1960)

[38] A. Messiah, »*Quantum Mechanics*«, Vol. 2, Quantum Mechanics (North-Holland Publishing Company, Amsterdam, 1961)

[39] V. Bargmann, »*Note on Wigner's Theorem on Symmetry Operations*«, J. Math. Phys. **5**, 862–868 (1964)

[40] L. Fonda and G. Ghirardi, »*Symmetry principles in quantum physics*«, Theoretical physics (M. Dekker, 1970)

[41] L. Molnár, »*An algebraic approach to Wigner's unitary-antiunitary theorem*«, arXiv e-prints, arXiv:math/9808033 (1998)

[42] G. Chevalier, »*Wigner's theorem and its generalizations*«, in »*Handbook of Quantum Logic and Quantum Structures*«, edited by K. Engesser, D. M. Gabbay and D. Lehmann (Elsevier Science B.V., Amsterdam, 2007), pp. 429–475

[43] A. Mouchet, »*An alternative proof of Wigner theorem on quantum transformations based on elementary complex analysis*«, Phys. Lett. A **377**, 2709–2711 (2013)

[44] S. Mazur and S. Ulam, »*Sur less transformations isométriques d'espaces vectoriels normés*«, C. R. Acad. Sci. **194**, 946–948 (1932)

[45] W. Pauli, »*Wave Mechanics: Volume 5 of Pauli Lectures on Physics*«, Pauli Lectures on Physics (MIT Press, 1973)

[46] D. Marolf and H. Maxfield, »*Observations of Hawking radiation: the Page curve and baby universes*«, arXiv e-prints, arXiv:hep–th/2010.06602 (2020)

[47] G. Musser, »*The Most Famous Paradox in Physics Nears Its End*«, Quanta Magazine, (29th Oct. 2020) https://www.quantamagazine.org/the-black-hole-information-paradox-comes-to-an-end-20201029

[48] H. Kalka and G. Soff, »*Supersymmetrie*« (Vieweg+Teubner Verlag, 1997)

[49] L. Infeld and T. E. Hull, »*The Factorization Method*«, Rev. Mod. Phys. **23**, 21–68 (1951)

[50] L. É. Gendenshteĭn and I. V. Krive, »*Supersymmetry in quantum mechanics*«, Sov. Phys. Uspekhi **28**, 645–666 (1985)

[51] M. Gianfreda, »*PT-symmetric Interpretation of Open Quantum and Classical Systems*«, Open Quantum Systems: From atomic nuclei to ultracold atoms and quantum optics, European Centre for Theoretical Studies in Nuclear Physics and Related Areas, Trento, Italy, 11th July 2017

[52] P. A. M. Dirac, »*The Principles of Quantum Mechanics*«, International series of monographs on physics (Oxford, England) (Clarendon Press, Oxford, UK, 1930)

[53] J. von Neumann, »*Mathematische Grundlagen der Quantenmechanik*« (Springer, Berlin, 1932)

[54] M. H. Stone, »*Linear Transformations in Hilbert Space: III. Operational Methods and Group Theory*«, Proc. Natl. Acad. Sci. U.S.A. **16**, 172–175 (1930)

[55] M. Fox, »*Optical Properties of Solids*«, Oxford Master Series in Physics (OUP Oxford, 2010)

[56] K. Wright, »*Q&A: Defects Wanted; Apply Here*«, Physics **12** (2019)

[57] C. M. Bender, D. C. Brody and H. F. Jones, »*Complex Extension of Quantum Mechanics*«, Phys. Rev. Lett. **89**, 270401 (2002)

[58] N. Moiseyev, »*Non-Hermitian Quantum Mechanics*« (Cambridge University Press, 2011)

[59] M. Jakob and S. Stenholm, »*Variational functions in driven open quantum systems*«, Phys. Rev. A **67**, 032111 (2003)

[60] S. Stenholm and M. Jakob, »*Time inversion in dynamical systems*«, Ann. Phys. **310**, 106–126 (2004)

[61] Z. Wen and C. M. Bender, »*$\mathcal{PT}$-symmetric potentials having continuous spectra*«, J. Phys. A: Math. Theor. **53**, 375302 (2020)

[62] C. M. Bender, M. Gianfreda, N. Hassanpour and H. F. Jones, »*Comment on "On the Lagrangian and Hamiltonian description of the damped linear harmonic oscillator" [J. Math. Phys. 48, 032701 (2007)]*«, J. Math. Phys. **57**, 084101 (2016)

[63] M. M. Sternheim and J. F. Walker, »*Non-Hermitian Hamiltonians, Decaying States, and Perturbation Theory*«, Phys. Rev. C **6**, 114–121 (1972)

[64] R. M. Young, »*On complete biorthogonal systems*«, Proc. Am. Math. Soc. **83**, 537–537 (1981)

[65] D. C. Brody, »*Biorthogonal quantum mechanics*«, J. Phys. A: Math. Theor. **47**, 035305 (2013)

[66] P. M. Morse and H. Feshbach, »*Methods of theoretical physics*« (McGraw-Hill, 1953)

[67] F. H. M. Faisal and J. V. Moloney, »*Time-dependent theory of non-Hermitian Schrodinger equation: Application to multiphoton-induced ionisation decay of atoms*«, J. Phys. B **14**, 3603–3620 (1981)

[68] A. I. Nesterov, »*Non-Hermitian Quantum Systems and Time-Optimal Quantum Evolution*«, SIGMA **5** (2009)

[69] N. Moiseyev and S. Friedland, »*Association of resonance states with the incomplete spectrum of finite complex-scaled Hamiltonian matrices*«, Phys. Rev. A **22**, 618–624 (1980)

[70] T. Kato, »*Perturbation Theory for Linear Operators*« (Springer Berlin Heidelberg, 1995)

[71] W. Heiss and H. Harney, »*The chirality of exceptional points*«, Eur. Phys. J. D **17**, 149–151 (2001)

[72] W. D. Heiss, »*The physics of exceptional points*«, J. Phys. A: Math. Theor. **45**, 444016 (2012)

[73] N. Moiseyev and A. A. Mailybaev, »*Effects of Exceptional Points in PT-Symmetric Waveguides*«, in »*Springer Tracts in Modern Physics*«, edited by M. Bhattacharya, Y. Chen, A. Fujimori, M. Getzlaff, T. Mannel, E. Mucciolo, W. Stwalley and J. Yang (Springer Singapore, 2018), pp. 237–259

[74] F. Bagarello, R. Passante and C. Trapani, »*Non-Hermitian Hamiltonians in Quantum Physics*« (Springer International Publishing, 2016)

[75] C. Dembowski, H.-D. Gräf, H. L. Harney, A. Heine, W. D. Heiss, H. Rehfeld and A. Richter, »*Experimental Observation of the Topological Structure of Exceptional Points*«, Phys. Rev. Lett. **86**, 787–790 (2001)

[76] C. Dembowski, B. Dietz, H.-D. Gräf, H. L. Harney, A. Heine, W. D. Heiss and A. Richter, »*Observation of a Chiral State in a Microwave Cavity*«, Phys. Rev. Lett. **90**, 034101 (2003)

[77] P. A. M. Dirac, »*Bakerian Lecture—The physical interpretation of quantum mechanics*«, Proc. R. Soc. Lond. A **180**, 1–40 (1942)

[78] W. Pauli, »*On Dirac's New Method of Field Quantization*«, Rev. Mod. Phys. **15**, 175–207 (1943)

[79] L. Pontryagin, »*Hermitian operators in a space with indefinite metric*«, Izy. Akad Nauk. SSSR Mat. **8**, (russian), 243280 (1944)

[80] M. G. Krein, »*On an application of the fixed point principle in the theory of linear transformations of spaces with an indefinite metric*«, Uspekhi Mat. Nauk. **5**, (russian), 180–190 (1950)

[81] H. Langer, »*Zur Spektraltheorie J-selbstadjungierter Operatoren*«, Math. Ann. **146**, 60–85 (1962)

[82] T. Y. Azizov and I. S. Iokhvidov, »*Linear operators in spaces with an indefinite metric and their applications*«, Itogi Nauk. Tekhn. Mat. Anal. **17**, (russian), 113–205 (1979)

[83] A. Mostafazadeh, »*Pseudo-Hermiticity versus PT symmetry: The necessary condition for the reality of the spectrum of a non-Hermitian Hamiltonian*«, J. Math. Phys. **43**, 205–214 (2002); »*Pseudo-Hermiticity versus PT-symmetry. II. A complete characterization of non-Hermitian Hamiltonians with a real spectrum*«, J. Math. Phys. **43**, 2814–2816 (2002); »*Pseudo-Hermiticity versus PT-symmetry III: Equivalence of pseudo-Hermiticity and the presence of antilinear symmetries*«, J. Math. Phys. **43**, 3944–3951 (2002)

[84] F. Scholtz, H. Geyer and F. Hahne, »*Quasi-Hermitian operators in quantum mechanics and the variational principle*«, Ann. Phys. **213**, 74–101 (1992)

[85] R. Kretschmer and L. Szymanowski, »*Quasi-Hermiticity in infinite-dimensional Hilbert spaces*«, Phys. Lett. A **325**, 112–117 (2004)

[86] A. Mostafazadeh, »*Pseudo-Hermitian Representation of Quantum Mechanics*«, Int. J. Geom. Meth. Mod. Phys **07**, 1191–1306 (2010)

[87] A. Mostafazadeh, »*Time-dependent pseudo-Hermitian Hamiltonians defining a unitary quantum system and uniqueness of the metric operator*«, Phys. Lett. B **650**, 208–212 (2007)

[88] A. Mostafazadeh, »*Pseudounitary operators and pseudounitary quantum dynamics*«, J. Math. Phys. **45**, 932–946 (2004)

[89] R. Santra and L. S. Cederbaum, »*Non-Hermitian electronic theory and applications to clusters*«, Phys. Rep. **368**, 1–117 (2002)

[90] M. Naimark, »*Linear Differential Operators*«, Part 2 (Larousse Harrap Publishers, 1968)

[91] H.-P. Breuer and F. Petruccione, »*The Theory of Open Quantum Systems*« (Oxford University Press, New York, 2002)

[92] H. Feshbach, »*Unified theory of nuclear reactions*«, Ann. Phys. **5**, 357–390 (1958)

[93] H. Feshbach, »*A unified theory of nuclear reactions. II*«, Ann. Phys. **19**, 287–313 (1962)

[94] I. Rotter, »*A non-Hermitian Hamilton operator and the physics of open quantum systems*«, J. Phys. A: Math. Theor. **42**, 153001 (2009)

[95] O. Christensen, »*Frames, Riesz bases, and discrete Gabor/wavelet expansions*«, Bull. Am. Math. Soc. **38**, 273–292 (2001)

[96] B. Mityagin and P. Siegl, »*Root System of Singular Perturbations of the Harmonic Oscillator Type Operators*«, Lett. Math. Phys. **106**, 147–167 (2015)

[97] H. F. Jones, »*Interface between Hermitian and non-Hermitian Hamiltonians in a model calculation*«, Phys. Rev. D **78**, 065032 (2008)

[98] J. Mecklin, ed., »*Closer than ever: It is 100 seconds to midnight, 2020 Doomsday Clock Statement*«, Bulletin of the Atomic Scientists, (23rd Jan. 2020) `https://thebulletin.org/doomsday-clock/`

[99] C. M. Bender and S. Boettcher, »*Real Spectra in Non-Hermitian Hamiltonians Having $\mathcal{PT}$ Symmetry*«, Phys. Rev. Lett. **80**, 5243–5246 (1998)

[100] M. Znojil, »*Should Symmetric Quantum Mechanics Be Interpreted as Nonlinear?*«, J. Nonlinear Math. Phys. **9**, 122–133 (2002)

[101] M. Znojil, »*Conservation of pseudo-norm in PT symmetric quantum mechanics*«, Rendic. Circ. Mat. Palermo II Suppl. **72**, 211–218 (2004)

[102] C. M. Bender, D. C. Brody and H. F. Jones, »*Must a Hamiltonian be Hermitian?*«, Am. J. Phys. **71**, 1095–1102 (2003)

[103] S. Albeverio and S. Kuzhel, »*One-dimensional Schrödinger operators with -symmetric zero-range potentials*«, J. Phys. A: Math. Gen. **38**, 4975–4988 (2005)

[104] C. M. Bender, »*Making sense of non-Hermitian Hamiltonians*«, Rep. Prog. Phys. **70**, 947–1018 (2007)

[105] D. Christodoulides and J. Yang, »*Parity-time Symmetry and Its Applications*« (Springer Singapore, 2018)

[106] A. Guo, G. J. Salamo, D. Duchesne, R. Morandotti, M. Volatier-Ravat, V. Aimez, G. A. Siviloglou and D. N. Christodoulides, »*Observation of $\mathcal{PT}$-Symmetry Breaking in Complex Optical Potentials*«, Phys. Rev. Lett. **103**, 093902 (2009)

[107] C. M. Bender, B. K. Berntson, D. Parker and E. Samuel, »*Observation of PT phase transition in a simple mechanical system*«, Am. J. Phys. **81**, 173–179 (2013)

[108] J. Schindler, A. Li, M. C. Zheng, F. M. Ellis and T. Kottos, »*Experimental study of active LRC circuits with $\mathcal{PT}$ symmetries*«, Phys. Rev. A **84**, 040101 (2011)

[109] J. Schindler, Z. Lin, J. M. Lee, H. Ramezani, F. M. Ellis and T. Kottos, »*$\mathcal{PT}$-symmetric electronics*«, J. Phys. A: Math. Theor. **45**, 444029 (2012)

[110] J. Li, A. K. Harter, J. Liu, L. de Melo, Y. N. Joglekar and L. Luo, »*Observation of parity-time symmetry breaking transitions in a dissipative Floquet system of ultracold atoms*«, Nat. Commun. **10** (2019)

[111] Y. Wu, W. Liu, J. Geng, X. Song, X. Ye, C.-K. Duan, X. Rong and J. Du, »*Observation of parity-time symmetry breaking in a single-spin system*«, Science **364**, 878–880 (2019)

[112] M. Naghiloo, M. Abbasi, Y. N. Joglekar and K. W. Murch, »*Quantum state tomography across the exceptional point in a single dissipative qubit*«, Nat. Phys. (2019)

[113] W.-C. Gao, C. Zheng, L. Liu, T. Wang and C. Wang, »*Experimental simulation of the Parity-Time-symmetric dynamics using photonics qubits*«, arXiv e-prints, arXiv:quant–ph/2004.08985 (2020)

[114] R. Gutöhrlein, H. Cartarius, J. Main and G. Wunner, »*Bifurcations and exceptional points in a $\mathcal{PT}$-symmetric dipolar Bose–Einstein condensate*«, J. Phys. A: Math. Theor. **49**, 485301 (2016)

[115] J. Schnabel, H. Cartarius, J. Main, G. Wunner and W. D. Heiss, »*Simple models of three coupled PT-symmetric wave guides allowing for third-order exceptional points*«, Acta Polytech. **57**, 454 (2017)

[116] L. Pan, S. Chen and X. Cui, »*High-order exceptional points in ultracold Bose gases*«, Phys. Rev. A **99**, 011601(R) (2019)

[117] W. R. Sweeney, C. W. Hsu, S. Rotter and A. D. Stone, »*Perfectly Absorbing Exceptional Points and Chiral Absorbers*«, Phys. Rev. Lett. **122**, 093901 (2019)

[118] J. Rubinstein, P. Sternberg and Q. Ma, »*Bifurcation Diagram and Pattern Formation of Phase Slip Centers in Superconducting Wires Driven with Electric Currents*«, Phys. Rev. Lett. **99**, 167003 (2007)

[119] N. M. Chtchelkatchev, A. A. Golubov, T. I. Baturina and V. M. Vinokur, »*Stimulation of the Fluctuation Superconductivity by $\mathcal{PT}$ Symmetry*«, Phys. Rev. Lett. **109**, 150405 (2012)

[120] Y. D. Chong, L. Ge and A. D. Stone, »*$\mathcal{PT}$-Symmetry Breaking and Laser-Absorber Modes in Optical Scattering Systems*«, Phys. Rev. Lett. **106**, 093902 (2011)

[121] M. Liertzer, L. Ge, A. Cerjan, A. D. Stone, H. E. Türeci and S. Rotter, »*Pump-Induced Exceptional Points in Lasers*«, Phys. Rev. Lett. **108**, 173901 (2012)

[122] A. Regensburger, C. Bersch, M.-A. Miri, G. Onishchukov, D. N. Christodoulides and U. Peschel, »*Parity-time synthetic photonic lattices*«, Nature **488**, 167–171 (2012)

[123] G. Castaldi, S. Savoia, V. Galdi, A. Alù and N. Engheta, »*$\mathcal{PT}$ Metamaterials via Complex-Coordinate Transformation Optics*«, Phys. Rev. Lett. **110**, 173901 (2013)

[124] C. Zheng, L. Hao and G. L. Long, »*Observation of a fast evolution in a parity-time-symmetric system*«, Philos. Trans. R. Soc. Lond. A **371**, 20120053 (2013)

[125] S. Assawaworrarit, X. Yu and S. Fan, »*Robust wireless power transfer using a nonlinear parity-time-symmetric circuit*«, Nature **546**, 387–390 (2017)

[126] M. Sakhdari, M. Hajizadegan and P.-Y. Chen, »*Robust extended-range wireless power transfer using a higher-order PT-symmetric platform*«, Phys. Rev. Res. **2**, 013152 (2020)

[127] C. M. Bender, D. C. Brody and M. P. Müller, »*Hamiltonian for the Zeros of the Riemann Zeta Function*«, Phys. Rev. Lett. **118**, 130201 (2017)

[128] C. M. Bender and D. C. Brody, »*Asymptotic analysis on a pseudo-Hermitian Riemann-zeta Hamiltonian*«, J. Phys. A: Math. Theor. **51**, 135203 (2018)

[129] S. Nixon and J. Yang, »*All-real spectra in optical systems with arbitrary gain-and-loss distributions*«, Phys. Rev. A **93**, 031802 (2016)

[130] A. Mostafazadeh and H. Mehri-Dehnavi, »*Spectral singularities, biorthonormal systems and a two-parameter family of complex point interactions*«, J. Phys. A: Math. Theor. **42**, 125303 (2009)

[131] D. A. Zezyulin and V. V. Konotop, »*A universal form of localized complex potentials with spectral singularities*«, New J. Phys. **22**, 013057 (2020)

[132] V. V. Konotop and D. Zezyulin, »*Construction of potentials with multiple spectral singularities*«, J. Phys. A: Math. Theor. (2020)

[133] L. Ge and H. E. Türeci, »*Antisymmetric $\mathcal{PT}$-photonic structures with balanced positive- and negative-index materials*«, Phys. Rev. A **88**, 053810 (2013)

[134] J.-H. Wu, M. Artoni and G. C. La Rocca, »*Non-Hermitian Degeneracies and Unidirectional Reflectionless Atomic Lattices*«, Phys. Rev. Lett. **113**, 123004 (2014)

[135] A. Ruschhaupt, T. Dowdall, M. A. Simón and J. G. Muga, »*Asymmetric scattering by non-Hermitian potentials*«, Europhys. Lett. **120**, 20001 (2018)

[136] M. A. Simón, A. Buendía, A. Kiely, A. Mostafazadeh and J. G. Muga, »*S-matrix pole symmetries for non-Hermitian scattering Hamiltonians*«, Phys. Rev. A **99**, 052110 (2019)

[137] K. G. Makris, Z. H. Musslimani, D. N. Christodoulides and S. Rotter, »*Constant-intensity waves and their modulation instability in non-Hermitian potentials*«, Nat. Commun. **6**, 7257 (2015)

[138] A. Brandstötter, K. G. Makris and S. Rotter, »*Scattering-free pulse propagation through invisible non-Hermitian media*«, Phys. Rev. B **99**, 115402 (2019)

[139] E. Rivet, A. Brandstötter, K. G. Makris, H. Lissek, S. Rotter and R. Fleury, »*Constant-pressure sound waves in non-Hermitian disordered media*«, Nat. Phys. **14**, 942–947 (2018)

[140] S. Stenholm, »*Variational Functions in Open Systems*«, Ann. Phys. **302**, 142–157 (2002)

[141] P. Peng, W. Cao, C. Shen, W. Qu, J. Wen, L. Jiang and Y. Xiao, »*Anti-parity-time symmetry with flying atoms*«, Nat. Phys. **12**, 1139–1145 (2016)

[142] Y. Choi, C. Hahn, J. W. Yoon and S. H. Song, »*Observation of an anti-PT-symmetric exceptional point and energy-difference conserving dynamics in electrical circuit resonators*«, Nat. Commun. **9**, 2182 (2018)

[143] Y. Li, Y.-G. Peng, L. Han, M.-A. Miri, W. Li, M. Xiao, X.-F. Zhu, J. Zhao, A. Alù, S. Fan and C.-W. Qiu, »*Anti-parity-time symmetry in diffusive systems*«, Science **364**, 170–173 (2019)

[144] M. Wadati, »*Construction of Parity-Time Symmetric Potential through the Soliton Theory*«, J. Phys. Soc. Jpn. **77**, 074005 (2008)

[145] E. N. Tsoy, I. M. Allayarov and F. K. Abdullaev, »*Stable localized modes in asymmetric waveguides with gain and loss*«, Opt. Lett. **39**, 4215–4218 (2014)

[146] V. V. Konotop and D. A. Zezyulin, »*Families of stationary modes in complex potentials*«, Opt. Lett. **39**, 5535–5538 (2014)

[147] S. Nixon and J. Yang, »*Nonlinear light behaviors near phase transition in non-parity-time-symmetric complex waveguides*«, Opt. Lett. **41**, 2747–2750 (2016)

[148] J. Yang, »*Classes of non-parity-time-symmetric optical potentials with exceptional-point-free phase transitions*«, Opt. Lett. **42**, 4067–4070 (2017)

[149] L.-L. Zhang, Z.-Z. Li, G.-H. Zhan, G.-Y. Yi and W.-J. Gong, »*Eigenenergies and quantum transport properties in a non-Hermitian quantum-dot chain with side-coupled dots*«, Phys. Rev. A **99**, 032119 (2019)

[150] P. Lunt, D. Haag, D. Dast, H. Cartarius and G. Wunner, »*Balanced gain and loss in Bose–Einstein condensates without $\mathcal{PT}$ symmetry*«, Phys. Rev. A **96**, 023614 (2017)

[151] M. Simón, Á. Buendía and J. Muga, »*Symmetries and invariants for non-Hermitian Hamiltonians*«, Mathematics **6**, 111 (2018)

[152] L. Solombrino, »*Weak pseudo-Hermiticity and antilinear commutant*«, J. Math. Phys. **43**, 5439–5445 (2002)

[153] E. P. Wigner, »*Normal Form of Antiunitary Operators*«, J. Math. Phys. **1**, 409–413 (1960)

[154] P. Siegl, »*The non-equivalence of pseudo-Hermiticity and presence of antilinear symmetry*«, Pramana **73**, 279 (2009)

[155] A. Mostafazadeh, »*Is weak pseudo-Hermiticity weaker than pseudo-Hermiticity?*«, J. Math. Phys. **47**, 092101 (2006)

[156] W. T. Reid, »*Symmetrizable completely continuous linear transformations in Hilbert space*«, Duke Math. J. **18**, 41–56 (1951)

[157] D. Dizdarevic, H. Cartarius, J. Main and G. Wunner, »*Balancing gain and loss in symmetrised multi-well potentials*«, J. Phys. A: Math. Theor. **53**, 405304 (2020)

[158] G. Darboux, »*Sur une proposition relative aux équations linéaires*«, C. R. Acad. Sci. Paris **94**, 1456–1459 (1882)

[159] F. Cannata, G. Junker and J. Trost, »*Schrödinger operators with complex potential but real spectrum*«, Phys. Lett. A **246**, 219–226 (1998)

[160] J. Dieudonné, »*Quasi-Hermitian operators*«, in »*Proceedings of the International Symposium on Linear Spaces*« (1961), pp. 115–122

[161] R. Kühne, »*Über eine Klasse J-selbstadjungierter Operatoren*«, Math. Ann. **154**, 56–69 (1964)

[162] M. Pease, »*Methods of Matrix Algebra*«, Mathematics in science and engineering (Academic Press, 1965)

[163] M. Froissart, »*Covariant formalism of a field with indefinite metric*«, Nuovo Cim. **14**, 197–204 (1959)

[164] T. Lee and G. Wick, »*Negative metric and the unitarity of the S-matrix*«, Nucl. Phys. B **9**, 209–243 (1969)

[165] S. Albeverio and S. Kushel, »*Pseudo-Hermiticity and Theory of Singular Perturbations*«, Lett. Math. Phys. **67**, 223–238 (2004)

[166] J. Feinberg and A. Zee, »*Non-Hermitian localization and delocalization*«, Phys. Rev. E **59**, 6433–6443 (1999)

[167] A. V. Smilga, »*Physics of crypto-Hermitian and crypto-supersymmetric field theories*«, Phys. Rev. D **77**, 061701 (2008)

[168] A. V. Smilga, »*Cryptogauge symmetry and cryptoghosts for crypto-Hermitian Hamiltonians*«, J. Phys. A: Math. Theor. **41**, 244026 (2008)

[169] S. Sun and X. Ma, »*Generalized hermitian operators*«, Linear Algebr. Appl. **433**, 737–749 (2010)

[170] C. M. Bender and P. D. Mannheim, »*PT symmetry and necessary and sufficient conditions for the reality of energy eigenvalues*«, Phys. Lett. A **374**, 1616–1620 (2010)

[171] H. Langer and C. Tretter, »*A Krein Space Approach to PT-symmetry*«, Czechoslov. J. Phys. **54**, 1113–1120 (2004)

[172] C. M. Bender, M. V. Berry and A. Mandilara, »*Generalized PT symmetry and real spectra*«, J. Phys. A: Math. Theor. **35**, L467–L471 (2002)

[173] M. A. Nielsen and I. L. Chuang, »*Quantum Computation and Quantum Information: 10th Anniversary Edition*«, 10th (Cambridge University Press, New York, 2011)

[174] A. Mostafazadeh, »*Hilbert space structures on the solution space of Klein Gordon-type evolution equations*«, Class. Quantum Gravity **20**, 155–171 (2002)

[175] S. Sundar Mukherjee and P. Roy, »*On Pseudo-Hermitian Hamiltonians*«, arXiv e-prints, arXiv:quant–ph/1401.5255 (2014)

[176] D. C. Brody, »*PT-symmetry, indefinite metric, and nonlinear quantum mechanics*«, J. Phys. A: Math. Theor. **50**, 485202 (2017)

[177] J. S. Frame, »*Part I—Matrix operations and generalized inverses*«, IEEE Spectr. **1**, 209–220 (1964)

[178] C. M. Bender, S. Boettcher and P. N. Meisinger, »*PT-symmetric quantum mechanics*«, J. Math. Phys. **40**, 2201–2229 (1999)

[179] F. Kogel, S. Kotzur, D. Dizdarevic, J. Main and G. Wunner, »*Realization of $\mathcal{PT}$-symmetric and $\mathcal{PT}$-symmetry-broken states in static optical-lattice potentials*«, Phys. Rev. A **99**, 063610 (2019)

[180] S. Altinisik, D. Dizdarevic and J. Main, »*Balanced gain and loss in spatially extended non-$\mathcal{PT}$-symmetric multiwell potentials*«, Phys. Rev. A **100**, 063639 (2019)

[181] E. Angerson, Z. Bai, J. Dongarra, A. Greenbaum, A. McKenney, J. Du Croz, S. Hammarling, J. Demmel, C. Bischof and D. Sorensen, »*LAPACK: A portable linear algebra library for high-performance computers*«, in »*Supercomputing '90: Proceedings of the 1990 ACM/IEEE Conference on Supercomputing*« (1990), pp. 2–11

[182] E. Anderson, Z. Bai, C. Bischof, S. Blackford, J. Demmel, J. Dongarra, J. Du Croz, A. Greenbaum, S. Hammarling, A. McKenney and D. Sorensen, »*LAPACK Users' Guide*«, Third (Society for Industrial and Applied Mathematics, Philadelphia, 1999)

[183] E. M. Graefe, H. J. Korsch and A. E. Niederle, »*Mean-Field Dynamics of a Non-Hermitian Bose–Hubbard Dimer*«, Phys. Rev. Lett. **101**, 150408 (2008)

[184] C. E. Rüter, K. G. Makris, R. El-Ganainy, D. N. Christodoulides, M. Segev and D. Kip, »*Observation of parity-time symmetry in optics*«, Nat. Phys. **6**, 192–195 (2010)

[185] H. Cartarius and G. Wunner, »*Model of a $\mathcal{PT}$-symmetric Bose–Einstein condensate in a δ-function double-well potential*«, Phys. Rev. A **86**, 013612 (2012)

[186] E.-M. Graefe, »*Stationary states of a PT symmetric two-mode Bose–Einstein condensate*«, J. Phys. A: Math. Theor. **45**, 444015 (2012)

[187] D. Dast, D. Haag, H. Cartarius, G. Wunner, R. Eichler and J. Main, »*A Bose–Einstein condensate in a $\mathcal{PT}$ symmetric double well*«, Fortschr. Phys. **61**, 124–139 (2012)

[188] K. Ding, G. Ma, M. Xiao, Z. Q. Zhang and C. T. Chan, »*Emergence, Coalescence, and Topological Properties of Multiple Exceptional Points and Their Experimental Realization*«, Phys. Rev. X **6**, 021007 (2016)

[189] Z.-Z. Liu, Q. Zhang, Y. Chen and J.-J. Xiao, »*General coupled-mode analysis of a geometrically symmetric waveguide array with nonuniform gain and loss*«, Photonics Res. **5**, 57 (2017)

[190] A. Trombettoni and A. Smerzi, »*Discrete Solitons and Breathers with Dilute Bose–Einstein Condensates*«, Phys. Rev. Lett. **86**, 2353–2356 (2001)

[191] A. Smerzi and A. Trombettoni, »*Nonlinear tight-binding approximation for Bose–Einstein condensates in a lattice*«, Phys. Rev. A **68**, 023613 (2003)

[192] M. Kreibich, J. Main, H. Cartarius and G. Wunner, »*Realizing $\mathcal{PT}$-symmetric non-Hermiticity with ultracold atoms and Hermitian multiwell potentials*«, Phys. Rev. A **90**, 033630 (2014)

[193] D. Dizdarevic, J. Main, K. Alpin, J. Reiff, D. Dast, H. Cartarius and G. Wunner, »*Realization of balanced gain and loss in a time-dependent four-mode Bose–Hubbard model*«, Phys. Rev. A **97**, 013623 (2018)

[194] E. M. Graefe, U. Günther, H. J. Korsch and A. E. Niederle, »*A non-Hermitian $\mathcal{PT}$ symmetric Bose–Hubbard model: eigenvalue rings from unfolding higher-order exceptional points*«, J. Phys. A: Math. Theor. **41**, 255206 (2008)

[195] E.-M. Graefe, H. J. Korsch and A. E. Niederle, »*Quantum-classical correspondence for a non-Hermitian Bose–Hubbard dimer*«, Phys. Rev. A **82**, 013629 (2010)

[196] W. D. Heiss, H. Cartarius, G. Wunner and J. Main, »*Spectral singularities in $\mathcal{PT}$-symmetric Bose–Einstein condensates*«, J. Phys. A: Math. Theor. **46**, 275307 (2013)

[197] A. A. T. Durst, »*Symmetrisierbare Hamilton-Operatoren für ausgeglichen Gewinn und Verlust bei Bose–Einstein-Kondensaten in drei und mehr Mulden*«, BA thesis (Universität Stuttgart, 2019)

[198] G. B. Price, »*An Introduction to Multicomplex Spaces and Functions*« (Marcel Dekker, New York, 1991)

[199] W. R. Hamilton, »*LXIX. On quaternions; or on a new system of imaginaries in algebra*«, Lond. Edinb. Dublin Philos. Mag. J. Sci. **30**, 458–461 (1847)

[200] D. Rochon and S. Tremblay, »*Bicomplex Quantum Mechanics: I. The Generalized Schrödinger Equation*«, Adv. Appl. Clifford Algebr. **14**, 231–248 (2004)

[201] D. Rochon and S. Tremblay, »*Bicomplex Quantum Mechanics: II. The Hilbert Space*«, Adv. Appl. Clifford Algebr. **16**, 135–157 (2006)

[202] L. S. Simeonov and N. V. Vitanov, »*Dynamical invariants for pseudo-Hermitian Hamiltonians*«, Phys. Rev. A **93**, 012123 (2016)

[203] T. Poston and I. Stewart, »*Catastrophe Theory and Its Applications*« (Pitman, London, 1978)

[204] G. Demange and E.-M. Graefe, »*Signatures of three coalescing eigenfunctions*«, J. Phys. A: Math. Theor. **45**, 025303 (2011)

[205] R. Gutöhrlein, J. Main, H. Cartarius and G. Wunner, »*Bifurcations and exceptional points in dipolar Bose–Einstein condensates*«, J. Phys. A: Math. Theor. **46**, 305001 (2013)

[206] M. Am-Shallem, R. Kosloff and N. Moiseyev, »*Exceptional points for parameter estimation in open quantum systems: analysis of the Bloch equations*«, New J. Phys. **17**, 113036 (2015)

[207] D. Dizdarevic, D. Dast, D. Haag, J. Main, H. Cartarius and G. Wunner, »*Cusp bifurcation in the eigenvalue spectrum of $\mathcal{PT}$-symmetric Bose–Einstein condensates*«, Phys. Rev. A **91**, 033636 (2015)

[208] D. Dast, D. Haag, H. Cartarius, J. Main and G. Wunner, »*Eigenvalue structure of a Bose–Einstein condensate in a $\mathcal{PT}$-symmetric double well*«, J. Phys. A: Math. Theor. **46**, 375301 (2013)

[209] M. Kreibich, J. Main, H. Cartarius and G. Wunner, »*Tilted optical lattices with defects as realizations of $\mathcal{PT}$ symmetry in Bose–Einstein condensates*«, Phys. Rev. A **93**, 023624 (2016)

[210] D. Jaksch, C. Bruder, J. I. Cirac, C. W. Gardiner and P. Zoller, »*Cold Bosonic Atoms in Optical Lattices*«, Phys. Rev. Lett. **81**, 3108–3111 (1998)

[211] M. Kreibich, »*Realizations of $\mathcal{PT}$-symmetric Bose–Einstein condensates with time-dependent Hermitian potentials*«, PhD thesis (Universität Stuttgart, 2015)

[212] S. Altinisik, »*Ausgeglichener Gewinn und Verlust in ausgedehnten nicht $\mathcal{PT}$-symmetrischen Mehrmuldenpotentialen*«, MA thesis (Universität Stuttgart, 2019)

[213] A. Scott, »*Encyclopedia of Nonlinear Science*« (Routledge, 2005)

[214] E. P. Gross, »*Structure of a quantized vortex in boson systems*«, Nuovo Cim. **20**, 454–477 (1961)

[215] L. P. Pitaevskii, »*Vortex Lines in an Imperfect Bose Gas*«, Sov. Phys. JETP **13**, 451 (1961)

[216] O. Morsch and M. Oberthaler, »*Dynamics of Bose–Einstein condensates in optical lattices*«, Rev. Mod. Phys. **78**, 179–215 (2006)

[217] J. Eilbeck, P. Lomdahl and A. Scott, »*The discrete self-trapping equation*«, Phys. D **16**, 318–338 (1985)

[218] V. M. Kenkre and D. K. Campbell, »*Self-trapping on a dimer: Time-dependent solutions of a discrete nonlinear Schrödinger equation*«, Phys. Rev. B **34**, 4959–4961 (1986)

[219] G. Agrawal, »*Applications of Nonlinear Fiber Optics*« (Elsevier, Amsterdam, 2001)

[220] H. Ramezani, T. Kottos, R. El-Ganainy and D. N. Christodoulides, »*Unidirectional nonlinear $\mathcal{PT}$-symmetric optical structures*«, Phys. Rev. A **82**, 043803 (2010)

[221] T. Holstein, »*Studies of polaron motion*«, Ann. Phys. **8**, 325–342 (1959)

[222] T. Holstein, »*Studies of polaron motion*«, Ann. Phys. **8**, 343–389 (1959)

[223] D. K. Campbell, A. R. Bishop and K. Fesser, »*Polarons in quasi-one-dimensional systems*«, Phys. Rev. B **26**, 6862–6874 (1982)

[224] Y. Toyozawa, »*Localization and Delocalization of an Exciton in the Phonon Field*«, in »*Organic Molecular Aggregates*«, edited by P. Reineker, H. Haken and H. C. Wolf (1983), pp. 90–106

[225] A. V. Gurevich, »*Nonlinear Phenomena in the Ionosphere*« (Springer Berlin Heidelberg, 1978)

[226] A. Davydov, »*The theory of contraction of proteins under their excitation*«, J. Theor. Biol. **38**, 559–569 (1973)

[227] V. E. Zakharov and A. B. Shabat, »*Exact theory of two-dimensional self-focusing and one-dimensional self-modulation of waves in nonlinear media*«, Sov. Phys. JETP **34**, translated from Ž. Èksper. Teoret. Fiz. 61 (1971), no. 1, 118–134 (russian), 62–69 (1972)

[228] R. Martin, R. Martin and C. U. Press, »*Electronic Structure: Basic Theory and Practical Methods*« (Cambridge University Press, 2004)

[229] Y. Saad, J. R. Chelikowsky and S. M. Shontz, »*Numerical Methods for Electronic Structure Calculations of Materials*«, SIAM Rev. **52**, 3–54 (2010)

[230] E. Jarlebring, S. Kvaal and W. Michiels, »*An Inverse Iteration Method for Eigenvalue Problems with Eigenvector Nonlinearities*«, SIAM J. Sci. Comput. **36**, A1978–A2001 (2014)

[231] Y. Cai, L.-H. Zhang, Z. Bai and R.-C. Li, »*On an Eigenvector-Dependent Nonlinear Eigenvalue Problem*«, SIAM J. Matrix Anal. Appl. **39**, 1360–1382 (2018)

[232] H. Kramers, »*Brownian motion in a field of force and the diffusion model of chemical reactions*«, Physica **7**, 284–304 (1940)

[233] H. Eyring, »*The Activated Complex in Chemical Reactions*«, J. Chem. Phys. **3**, 107–115 (1935)

[234] P. Hänggi, P. Talkner and M. Borkovec, »*Reaction-rate theory: fifty years after Kramers*«, Rev. Mod. Phys. **62**, 251–341 (1990)

[235] P.-G. De Gennes, »*Superconductivity of Metals and Alloys*« (Addison-Wesley Publishing Company, Redwood City, 1966)

[236] A. Löhle, H. Cartarius, D. Haag, D. Dast, J. Main and G. W. Wunner, »*Stability of Bose–Einstein condensates in a PT-symmetric double-δ potential close to branch points*«, Acta Polytech. **54**, 133–138 (2014)

[237] S. Klaiman, U. Günther and N. Moiseyev, »*Visualization of Branch Points in $\mathcal{PT}$-Symmetric Waveguides*«, Phys. Rev. Lett. **101**, 080402 (2008)

[238] Z. H. Musslimani, K. G. Makris, R. El-Ganainy and D. N. Christodoulides, »*Optical Solitons in $\mathcal{PT}$ Periodic Potentials*«, Phys. Rev. Lett. **100**, 030402 (2008)

[239] K. G. Makris, R. El-Ganainy, D. N. Christodoulides and Z. H. Musslimani, »*$\mathcal{PT}$-symmetric optical lattices*«, Phys. Rev. A **81**, 063807 (2010)

[240] B. Peng, Ş. K. Özdemir, F. Lei, F. Monifi, M. Gianfreda, G. L. Long, S. Fan, F. Nori, C. M. Bender and L. Yang, »*Parity–time-symmetric whispering-gallery microcavities*«, Nat. Phys. **10**, 394–398 (2014)

[241] S. Weimann, M. Kremer, Y. Plotnik, Y. Lumer, S. Nolte, K. G. Makris, M. Segev, M. C. Rechtsman and A. Szameit, »*Topologically protected bound states in photonic parity–time-symmetric crystals*«, Nat. Mater. **16**, 433–438 (2016)

[242] R. Gutöhrlein, J. Schnabel, I. Iskandarov, H. Cartarius, J. Main and G. Wunner, »*Realizing $\mathcal{PT}$-symmetric BEC subsystems in closed Hermitian systems*«, J. Phys. A: Math. Theor. **48**, 335302 (2015)

[243] Y. Shin, G.-B. Jo, M. Saba, T. A. Pasquini, W. Ketterle and D. E. Pritchard, »*Optical Weak Link between Two Spatially Separated Bose–Einstein Condensates*«, Phys. Rev. Lett. **95**, 170402 (2005)

[244] R. Gati, M. Albiez, J. Fölling, B. Hemmerling and M. K. Oberthaler, »*Realization of a single Josephson junction for Bose–Einstein condensates*«, Appl. Phys. B **82**, 207–210 (2006)

[245] N. P. Robins, C. Figl, M. Jeppesen, G. R. Dennis and J. D. Close, »*A pumped atom laser*«, Nat. Phys. **4**, 731–736 (2008)

[246] T. Gericke, P. Wurtz, D. Reitz, T. Langen and H. Ott, »*High-resolution scanning electron microscopy of an ultracold quantum gas*«, Nat. Phys. **4**, 949–953 (2008)

[247] Y. Kagan, A. E. Muryshev and G. V. Shlyapnikov, »*Collapse and Bose–Einstein Condensation in a Trapped Bose Gas with Negative Scattering Length*«, Phys. Rev. Lett. **81**, 933–937 (1998)

[248] M. H. Anderson, J. R. Ensher, M. R. Matthews, C. E. Wieman and E. A. Cornell, »*Observation of Bose–Einstein Condensation in a Dilute Atomic Vapor*«, Science **269**, 198–201 (1995)

[249] D. C. Aveline, J. R. Williams, E. R. Elliott, C. Dutenhoffer, J. R. Kellogg, J. M. Kohel, N. E. Lay, K. Oudrhiri, R. F. Shotwell, N. Yu and R. J. Thompson, »*Observation of Bose–Einstein condensates in an Earth-orbiting research lab*«, Nature **582**, 193–197 (2020)

[250] S. O. Demokritov, V. E. Demidov, O. Dzyapko, G. A. Melkov, A. A. Serga, B. Hillebrands and A. N. Slavin, »*Bose–Einstein condensation of quasi-equilibrium magnons at room temperature under pumping*«, Nature **443**, 430–433 (2006)

[251] I. V. Borisenko, B. Divinskiy, V. E. Demidov, G. Li, T. Nattermann, V. L. Pokrovsky and S. O. Demokritov, »*Direct evidence of spatial stability of Bose–Einstein condensate of magnons*«, Nat. Commun. **11** (2020)

[252] M. Schneider, T. Brächer, D. Breitbach, V. Lauer, P. Pirro, D. A. Bozhko, H. Y. Musiienko-Shmarova, B. Heinz, Q. Wang, T. Meyer, F. Heussner, S. Keller, E. T. Papaioannou, B. Lägel, T. Löber, C. Dubs, A. N. Slavin, V. S. Tiberkevich, A. A. Serga, B. Hillebrands and A. V. Chumak, »*Bose–Einstein condensation of quasiparticles by rapid cooling*«, Nat. Nanotechnol. (2020)

[253] S. Burger, F. S. Cataliotti, C. Fort, F. Minardi, M. Inguscio, M. L. Chiofalo and M. P. Tosi, »*Superfluid and Dissipative Dynamics of a Bose–Einstein Condensate in a Periodic Optical Potential*«, Phys. Rev. Lett. **86**, 4447–4450 (2001)

[254] F. S. Cataliotti, S. Burger, C. Fort, P. Maddaloni, F. Minardi, A. Trombettoni, A. Smerzi and M. Inguscio, »*Josephson Junction Arrays with Bose–Einstein Condensates*«, Science **293**, 843–846 (2001)

[255] K. Henderson, C. Ryu, C. MacCormick and M. G. Boshier, »*Experimental demonstration of painting arbitrary and dynamic potentials for Bose–Einstein condensates*«, New J. Phys. **11**, 043030 (2009)

[256] S. Peil, J. V. Porto, B. L. Tolra, J. M. Obrecht, B. E. King, M. Subbotin, S. L. Rolston and W. D. Phillips, »*Patterned loading of a Bose–Einstein condensate into an optical lattice*«, Phys. Rev. A **67**, 051603 (2003)

[257] H. Cartarius, D. Haag, D. Dast and G. Wunner, »*Nonlinear Schrödinger equation for a $\mathcal{PT}$-symmetric delta-function double well*«, J. Phys. A: Math. Theor. **45**, 444008 (2012)

[258] D. Haag, D. Dast, A. Löhle, H. Cartarius, J. Main and G. Wunner, »*Nonlinear quantum dynamics in a $\mathcal{PT}$-symmetric double well*«, Phys. Rev. A **89**, 023601 (2014)

[259] D. Döring, G. R. Dennis, N. P. Robins, M. Jeppesen, C. Figl, J. J. Hope and J. D. Close, »*Pulsed pumping of a Bose–Einstein condensate*«, Phys. Rev. A **79**, 063630 (2009)

[260] P. Würtz, T. Langen, T. Gericke, A. Koglbauer and H. Ott, »*Experimental Demonstration of Single-Site Addressability in a Two-Dimensional Optical Lattice*«, Phys. Rev. Lett. **103**, 080404 (2009)

[261] G. Barontini, R. Labouvie, F. Stubenrauch, A. Vogler, V. Guarrera and H. Ott, »*Controlling the Dynamics of an Open Many-Body Quantum System with Localized Dissipation*«, Phys. Rev. Lett. **110**, 035302 (2013)

[262] F. Single, H. Cartarius, G. Wunner and J. Main, »*Coupling approach for the realization of a $\mathcal{PT}$-symmetric potential for a Bose–Einstein condensate in a double well*«, Phys. Rev. A **90**, 042123 (2014)

[263] M. Kreibich, J. Main, H. Cartarius and G. Wunner, »*Hermitian four-well potential as a realization of a $\mathcal{PT}$-symmetric system*«, Phys. Rev. A **87**, 051601 (2013)

[264] T. Mathea, D. Dast, D. Dizdarevic, H. Cartarius, J. Main and G. Wunner, »*Using mixed many-body particle states to generate exact $\mathcal{PT}$-symmetry in a time-dependent four-well system*«, J. Phys. A: Math. Theor. **51**, 315303 (2018)

[265] R. Labouvie, B. Santra, S. Heun and H. Ott, »*Bistability in a Driven-Dissipative Superfluid*«, Phys. Rev. Lett. **116**, 235302 (2016)

[266] N. Tesla, »*Tesla's Tower*«, New York Am. **17**, 12–28 (1904)

[267] Z. Lin, H. Ramezani, T. Eichelkraut, T. Kottos, H. Cao and D. N. Christodoulides, »*Unidirectional Invisibility Induced by $\mathcal{PT}$-Symmetric Periodic Structures*«, Phys. Rev. Lett. **106**, 213901 (2011)

[268] F. Loran and A. Mostafazadeh, »*Unidirectional invisibility and non-reciprocal transmission in two and three dimensions*«, Proc. R. Soc. A: Math. Phys. Eng. Sci. **472**, 20160250 (2016)

[269] B. Lv, J. Fu, B. Wu, R. Li, Q. Zeng, X. Yin, Q. Wu, L. Gao, W. Chen, Z. Wang, Z. Liang, A. Li and R. Ma, »*Unidirectional invisibility induced by parity-time symmetric circuit*«, Sci. Rep. **7** (2017)

[270] N. Tesla, »*The Transmission of Electrical Energy Without Wires*«, Electr. World Eng. (1904)

[271] N. Tesla, »*High frequency oscillators for electro-therapeutic and other purposes*«, Electr. Eng. **26** (1898)

[272] N. Tesla, »*Apparatus for transmission of electrical energy*«, US649621A (1897)

[273] N. Tesla, »*Apparatus for transmitting electrical energy*«, US1119732A (1907)

[274] N. Tesla, »*Experiments with Alternate Currents of Very High Frequency and Their Application to Methods of Artificial Illumination*« (Wildside Press, 2006)

[275] D. Kent, »*Tesla: The Wizard of Electricity*« (Fall River Press, 2013)

[276] S. C. Mukhopadhyay and T. Islam, »*Wearable Sensors*«, 2053-2563 (IOP Publishing, 2017)

[277] S. Valtchev, E. Baikova and L. Jorge, »*Electromagnetic field as the wireless transporter of energy*«, Facta Univ. Ser. Electron. Energ. **25**, 171–181 (2012)

[278] R. Pudur, V. Hanumante, S. Shukla and K. Kumar, »*Wireless Power Transmission: A survey*«, in »*International Conference on Recent Advances and Innovations in Engineering (ICRAIE-2014)*« (May 2014)

[279] S. Nikoletseas, Y. Yang and A. Georgiadis, »*Wireless Power Transfer Algorithms, Technologies and Applications in Ad Hoc Communication Networks*« (Springer International Publishing, 2016)

[280] S. R. Hui, »*Past, Present and Future Trends of Non-Radiative Wireless Power Transfer*«, CPSS Trans. Power Electron. Appl. **1**, 83–91 (2016)

[281] W. Brown, »*The History of Power Transmission by Radio Waves*«, IEEE Trans. Microw. Theory Tech. **32**, 1230–1242 (1984)

[282] C. Zierhofer and E. Hochmair, »*High-efficiency coupling-insensitive transcutaneous power and data transmission via an inductive link*«, IEEE Trans. Biomed. Eng. **37**, 716–722 (1990)

[283] L. J. Fernández-Alcázar, R. Kononchuk and T. Kottos, »*Thermal Motors with Enhanced Performance due to Engineered Exceptional Points*«, arXiv e-prints, arXiv:physics.optics/2010.06743 (2020)

[284] H. Haus, »*Waves and Fields in Optoelectronics*«, Prentice-Hall series in solid state physical electronics (Prentice-Hall, 1984)

[285] R. A. Serway, »*Principles of Physics*«, 2nd (Saunders College Pub., Fort Worth, Texas; London, 1998)

[286] F. E. Neumann, »*Allgemeine Gesetze der inducirten elektrischen Ströme*«, Ann. Phys. Chem. **143**, 31–44 (1846)

[287] T. Imura and Y. Hori, »*Maximizing Air Gap and Efficiency of Magnetic Resonant Coupling for Wireless Power Transfer Using Equivalent Circuit and Neumann Formula*«, IEEE Trans. Ind. Electron. **58**, 4746–4752 (2011)

[288] A. Kurs, A. Karalis, R. Moffatt, J. D. Joannopoulos, P. Fisher and M. Soljacic, »*Wireless Power Transfer via Strongly Coupled Magnetic Resonances*«, Science **317**, 83–86 (2007)

[289] X. Yu, T. Skauli, B. Skauli, S. Sandhu, P. B. Catrysse and S. Fan, »*Wireless power transfer in the presence of metallic plates: Experimental results*«, AIP Adv. **3**, 062102 (2013)

[290] H. Haus and W. Huang, »*Coupled-mode theory*«, Proc. IEEE **79**, 1505–1518 (1991)

[291] M. Kiani and M. Ghovanloo, »*The Circuit Theory Behind Coupled-Mode Magnetic Resonance-Based Wireless Power Transmission*«, IEEE Trans. Circuits Syst. I: Regul. Pap. **59**, 2065–2074 (2012)

[292] G. Pierce, »*Principles of Wireless Telegraphy*« (McGraw-Hill Book Company, 1910)

[293] A. Karalis, J. Joannopoulos and M. Soljačić, »*Efficient wireless non-radiative mid-range energy transfer*«, Ann. Phys. **323**, 34–48 (2008)

[294] G. A. Covic and J. T. Boys, »*Inductive Power Transfer*«, Proc. IEEE **101**, 1276–1289 (2013)

[295] J. I. Agbinya, »*Investigation of near field inductive communication system models, channels and experiments*«, Prog. In Electromagn. Res. B **49**, 129–153 (2013)

[296] V. V. Pande, P. D. Doifode, D. S. Kamtekar and P. P. Shingade, »*Wireless power transmission using resonance inductive coupling*«, Int. J. Eng. Res. Appl. **4**, 46–50 (2014)

[297] R. A. Matula, »*Electrical resistivity of copper, gold, palladium, and silver*«, J. Phys. Chem. Ref. Data **8**, 1147–1298 (1979)

[298] G. Carleo, I. Cirac, K. Cranmer, L. Daudet, M. Schuld, N. Tishby, L. Vogt-Maranto and L. Zdeborová, »*Machine learning and the physical sciences*«, Rev. Mod. Phys. **91**, 045002 (2019)

[299] M. Schmidt and H. Lipson, »*Distilling Free-Form Natural Laws from Experimental Data*«, Science **324**, 81–85 (2009)

[300] G. Raayoni, S. Gottlieb, Y. Manor, G. Pisha, Y. Harris, U. Mendlovic, D. Haviv, Y. Hadad and I. Kaminer, »*Generating conjectures on fundamental constants with the Ramanujan Machine*«, Nature **590**, 67–73 (2021)

[301] E. Callaway, »*'It will change everything': DeepMind's AI makes gigantic leap in solving protein structures*«, Nature (2020)

[302] D. Jaschke, S. Montangero and L. D. Carr, »*One-dimensional many-body entangled open quantum systems with tensor network methods*«, Quantum Sci. Technol. **4**, 013001 (2018)

[303] N. Yoshioka and R. Hamazaki, »*Constructing neural stationary states for open quantum many-body systems*«, Phys. Rev. B **99**, 214306 (2019)

[304] M. J. Hartmann and G. Carleo, »*Neural-Network Approach to Dissipative Quantum Many-Body Dynamics*«, Phys. Rev. Lett. **122**, 250502 (2019)

[305] A. Vardi and J. R. Anglin, »*Bose–Einstein Condensates beyond Mean Field Theory: Quantum Backreaction as Decoherence*«, Phys. Rev. Lett. **86**, 568–571 (2001)

[306] J. R. Anglin and A. Vardi, »*Dynamics of a two-mode Bose–Einstein condensate beyond mean-field theory*«, Phys. Rev. A **64**, 013605 (2001)

[307] I. Tikhonenkov, J. R. Anglin and A. Vardi, »*Quantum dynamics of Bose–Hubbard Hamiltonians beyond the Hartree-Fock-Bogoliubov approximation: The Bogoliubov back-reaction approximation*«, Phys. Rev. A **75**, 013613 (2007)

[308] G. Lindblad, »*On the generators of quantum dynamical semigroups*«, Commun. Math. Phys. **48**, 119–130 (1976)

[309] D. Dast, D. Haag, H. Cartarius and G. Wunner, »*Quantum master equation with balanced gain and loss*«, Phys. Rev. A **90**, 052120 (2014)

[310] D. Dast, D. Haag, H. Cartarius and G. Wunner, »*Purity oscillations in Bose–Einstein condensates with balanced gain and loss*«, Phys. Rev. A **93**, 033617 (2016)

[311] C. L. Benavides-Riveros, J. Wolff, M. A. L. Marques and C. Schilling, »*Reduced Density Matrix Functional Theory for Bosons*«, Phys. Rev. Lett. **124**, 180603 (2020)

[312] A. E. Rendon-Nava, J. A. Díaz-Méndez, L. Nino-de-Rivera, W. Calleja-Arriaga, F. Gil-Carrasco and D. Díaz-Alonso, »*Study of the Effect of Distance and Misalignment between Magnetically Coupled Coils for Wireless Power Transfer in Intraocular Pressure Measurement*«, Sci. World J. **2014**, 1–11 (2014)

[313] A. Brecher and D. Arthur, »*Review and Evaluation of Wireless Power Transfer (WPT) for Electric Transit Applications*«, tech. rep., FTA Report No. 0060 (US Department of Transportation, 2014)

[314] K. Kawabata, S. Higashikawa, Z. Gong, Y. Ashida and M. Ueda, »*Topological unification of time-reversal and particle-hole symmetries in non-Hermitian physics*«, Nat. Commun. **10** (2019)

[315] A. De Morgan, »*The Differential and Integral Calculus*«, Library of useful knowledge (R. Baldwin & Cradock, 1842)

[316] P. A. M. Dirac, »*A new notation for quantum mechanics*«, Math. Proc. Camb. Philos. Soc. **35**, 416–418 (1939)

[317] S. Weigert, »*$\mathcal{PT}$-symmetry and its spontaneous breakdown explained by anti-linearity*«, J. Opt. B **5**, S416–S419 (2003)

[318] E. Prugovečki, »*Quantum Mechanics in Hilbert Space*«, Pure and applied mathematics: a series of monographs and textbooks (Academic Press, 1981)

[319] R. Richtmyer, »*Principles of advanced mathematical physics*«, Texts and monographs in physics Volume 1 (Springer Verlag, 1978)

[320] E. A. Hylleraas and B. Undheim, »*Numerische Berechnung der 2S-Terme von Ortho- und Par-Helium*«, Z. Phys. **65**, 759–772 (1930)

[321] J. K. L. MacDonald, »*Successive Approximations by the Rayleigh-Ritz Variation Method*«, Phys. Rev. **43**, 830–833 (1933)

[322] L. D. Landau and L. E. M., »*Quantum Mechanics: Non-relativistic Theory*«, A-W series in advanced physics (Pergamon Press, 1965)

[323] J. von Neumann and E. P. Wigner, »*Über merkwürdige diskrete Eigenwerte*«, in »*The Collected Works of Eugene Paul Wigner*«, edited by A. S. Wightman (Springer Berlin Heidelberg, 1993), pp. 291–293

[324] J. von Neumann and E. P. Wigner, »*Über das Verhalten von Eigenwerten bei adiabatischen Prozessen*«, in »*The Collected Works of Eugene Paul Wigner*«, edited by A. S. Wightman (Springer Berlin Heidelberg, 1993), pp. 294–297

[325] F. Hund, »*Zur Deutung der Molekelspektren. I*«, Z. Phys. **40**, 742–764 (1927)

[326] E. Teller, »*The Crossing of Potential Surfaces.*« J. Phys. Chem. **41**, 109–116 (1937)

[327] H. C. Longuet-Higgins, »*The intersection of potential energy surfaces in polyatomic molecules*«, Proc. R. Soc. London. A. Math. Phys. Sci. **344**, 147–156 (1975)

[328] P.-O. Löwdin, »*On the Non-Orthogonality Problem Connected with the Use of Atomic Wave Functions in the Theory of Molecules and Crystals*«, J. Chem. Phys. **18**, 365–375 (1950)

[329] M. Luna-Elizarrarás, M. Shapiro, D. Struppa and A. Vajiac, »*Bicomplex Numbers and their Elementary Functions*«, CUBO **14**, 61–80 (2012)

[330] I. Mayergoyz and W. Lawson, »*Basic Electric Circuit Theory: A One-Semester Text*« (Elsevier Science, San Diego, 1997)

[331] R. Dengler, »*Self inductance of a wire loop as a curve integral*«, Adv. Electromagn. **5**, 1 (2016)

[332] C. R. Paul, »*Inductance*« (John Wiley & Sons, Inc., Dec. 2009)

[333] M. Znojil, »*Three-Hilbert-Space Formulation of Quantum Mechanics*«, SIGMA **5** (2009); »*Cryptohermitian Picture of Scattering Using Quasilocal Metric Operators*«, SIGMA **5** (2009)

Zusammenfassung in deutscher Sprache

In dieser Arbeit werden Konzepte untersucht und diskutiert, mit denen sich ausgeglichene Gewinne und Verluste in unterschiedlichen Systemen erzeugen lassen. Über Gewinn und Verlust können die Wechselwirkungen eines Systems mit seiner Umgebung auf elegante und effiziente Art und Weise beschrieben werden; sind diese ausgeglichen, so treten stationäre Zustände auf.

Kapitel 2 gibt zuerst einen Überblick über verschiedene Symmetrien innerhalb der Physik und deren Bedeutung. Zur mathematischen Beschreibung von Symmetrien dient die Gruppentheorie. Eine der fundamentalsten und wichtigsten Gruppen in der Physik ist die Lorentz-Gruppe, welche alle Symmetrietransformationen der vierdimensionalen Raumzeit enthält. Diese Lorentz-Transformationen lassen sich in vier Kategorien einteilen, die in Tabelle 2-1 zusammengefasst sind. Wichtig sind hierbei die Operatoren $\mathcal{P}$, $\mathcal{T}$ und $\mathcal{C}$, die Paritäts-, Zeit- und Ladungsumkehr beschreiben; ihre Kombination bildet gemäß des $\mathcal{CPT}$-Theorems[I] die fundamentalste Symmetrieoperation, unter der alle bekannten physikalischen Theorien invariant sind. Die Zeitumkehr ist nochmals ausgezeichnet, da es sich hierbei um eine antilineare Operation handelt, die sich von einer linearen Operation durch eine zusätzliche komplexe Konjugation unterscheidet.[2] Das ist insbesondere in der Quantenmechanik wichtig, da diese über einen komplexen Hilbert-Raum definiert ist.[3] Dabei ist zu beachten, dass Zeitumkehr die Umkehr aller Bewegungen und Trajektorien meint und nicht lediglich die Umkehr der Zeitkoordinate der Raumzeit, was ausführlich in Abschnitt 2-3 a) diskutiert wird.

Aus den verschiedenen Darstellungen der Lorentz-Gruppe[4] lassen sich im Prinzip die Theorien der modernen Physik herleiten. So folgt etwa die Schrödinger-Gleichung (2-38) in der *Quantenmechanik*, abgesehen von dem Faktor $\hbar$, formal aus der Dirac-

[I] vgl. Abschnitt 2-3 b)

[2] vgl. Abschnitt 2-4

[3] In der Quantenmechanik lässt sich Zeitumkehr sogar gänzlich über die komplexe Konjugation definieren.

[4] vgl. Abschnitt 2-2 b)

Gleichung (2-22). Die Maxwell-Gleichungen (2-29) bis (2-32) in der *Elektrodynamik* hingegen ergeben sich aus der Proca-Gleichung (2-24). Diese Arbeit ist thematisch auch entsprechend dieser beiden Theorien geteilt.

Teil 1: Quantensysteme

Im ersten Teil der Arbeit wird Gewinn und Verlust in der Quantenmechanik eingeführt. Üblicherweise beschreibt die Quantentheorie lediglich abgeschlossene Systeme mithilfe Hermitescher Operatoren,[5] deren Eigenwerte reell und damit physikalisch interpretierbar sind. Jedoch lassen sich Wechselwirkungen zwischen einem offenen System und seiner Umgebung auf einfache Weise als Gewinne oder Verluste durch die Einführung eines imaginären Potentials beschreiben, wodurch der zugehörige Hamilton-Operator jedoch nicht mehr Hermitesch ist;[6] solche Operatoren sind im Allgemeinen dann komplex symmetrisch.[7] Diese nicht-Hermitesche Quantentheorie wird in Kapitel 4 beschrieben und unterscheidet sich deutlich von der üblichen, Hermiteschen Quantenmechanik. Der Imaginärteil V_i des Potentials führt zu einer Veränderung der Kontinuitätsgleichung für die Wahrscheinlichkeitsdichte ρ und den Wahrscheinlichkeitsstrom j,

[5] vgl. Abschnitt 4-1

[6] vgl. Abschnitt 4-6

[7] vgl. Abschnitt 4-5

$$\frac{\mathrm{d}\rho}{\mathrm{d}t} + \nabla j = 2V_\mathrm{i}\rho\,. \tag{4-6}$$

Für $V_\mathrm{i} \neq 0$ ist die Wahrscheinlichkeit der Zustände im Allgemeinen nicht mehr erhalten und die zugehörigen Energieeigenwerte sind in diesem Fall komplex.[8] Diese können ähnlich wie ein komplexer Brechungsindex in der Optik als effektive mathematische Beschreibung der Wechselwirkung mit der Umgebung interpretiert werden. Jedoch besitzen nicht-Hermitesche Operatoren eine unübliche mathematische Struktur, welche zu einigen verblüffenden Eigenschaften führt.

[8] vgl. Abschnitt 4-2 b)

Im Gegensatz zu Hermiteschen Operatoren sind die Eigenzustände eines nicht-Hermiteschen Operators $\mathcal{H}$ nicht mehr orthogonal zueinander. Stattdessen bilden die Zustände eine biorthogonale

Basis mit der Eigenschaft

$$\langle \psi^m | \psi_n \rangle = \delta_{nm} \,, \tag{4-14}$$

wobei $|\psi_n\rangle$ eine Lösung der rechtsseitigen Eigenwertgleichung

$$\mathcal{H} \, |\psi_n\rangle = E_n \, |\psi_n\rangle \tag{4-10}$$

und $|\psi^n\rangle$ eine Lösung der linksseitigen Eigenwertgleichung

$$\langle \psi^n | \, \mathcal{H} = \langle \psi^n | \, E_n \tag{4-11}$$

ist.[9] Für einen Hermiteschen Operator $\mathcal{H} = \mathcal{H}^\dagger$ mit reellen Eigenwerten $E_n \in \mathbb{R}$ sind Gln. (4-10) und (4-11) äquivalent, sodass die links- und rechtsseitigen Zustände gleich und damit orthogonal sind. Damit ist die Biorthogonalität eine direkte Verallgemeinerung der Orthogonalität. Für $E_n \in \mathbb{C}$ entspricht die linksseitige Eigenwertgleichung (4-11) dem Adjungierten der rechtsseitigen Eigenwertgleichung (4-10) mit dem Operator $\mathcal{H}^\dagger$ und dem komplex konjugierten Spektrum, bestehend aus den Eigenwerten E_n^*.

[9] Die spezifische Notation für links- und rechtsseitige Zustände ist in Anhang A-2 beschrieben.

In nicht-Hermiteschen Quantensystemen kann es zur gleichzeitigen Entartung von Eigenwerten und Eigenzuständen kommen. Da die Biorthogonalität (4-14) erhalten bleibt, sind solche Zustände formal orthogonal zu sich selbst und nicht mehr normierbar.[10] Dieses Phänomen der Selbstorthogonalität[11] ist ausschließlich in nicht-Hermiteschen Systemen an sogenannten exzeptionellen Punkten zu finden, an denen eine spontane Symmetriebrechung auftritt. Bei der Umkreisung eines exzeptionellen Punktes werden die Eigenwerte vertauscht. Es bedarf mehrerer Umkreisungen um die Ausgangssituation wieder herzustellen. Dieses Phänomen entsteht durch die einzigartige Topologie der Eigenwertlösungen eines nicht-Hermiteschen Operators in der komplexen Ebene um den exzeptionellen Punkt; diese liegen auf unterschiedlichen Riemann-Blättern, was in Abb. 4-1 für zwei Eigenwerte skizziert ist. Abschnitt 4-3 a) enthält auch eine einfache Modellrechnung, um dieses Phänomen explizit zu zeigen.

[10] vgl. Abschnitt 4-3 b)

[11] vgl. Abschnitt 4-3 a)

Durch das Noether-Theorem[12] sind Symmetrien üblicherweise mit dem Auftreten von Erhaltungsgrößen verbunden. Das gilt

[12] vgl. Abschnitt 2-1 c)

jedoch nur für kontinuierliche Symmetrien, die sich über infinitesimale Transformationen beschreiben lassen und damit eine Lie-Gruppe[13] bilden. Jedoch kann auch zwischen bestimmten diskreten Symmetrien und der Erhaltung der Wahrscheinlichkeit in der nicht-Hermiteschen Quantenmechanik ein Zusammenhang hergestellt werden. In Kapitel 5 werden daher solche Symmetrien und andere Konzepte besprochen, welche trotz der Anwesenheit eines komplexen Potentials[14] zu einer Erhaltung der Wahrscheinlichkeit in nicht-Hermiteschen Quantensystemen führen. Das ist genau dann der Fall, wenn der entsprechende Energieeigenwert reell ist. Reelle Eigenwerte treten als Spezialfälle in Anwesenheit einer antiunitären Symmetrie auf,[15] was sich über die Symmetriebedingung

[13] vgl. Abschnitt 2-1 b)

[14] vgl. Gl. (4-6)

[15] vgl. Abschnitt 5-3 a)

$$[\mathcal{A}, \mathcal{H}] = 0 \tag{5-24}$$

als Kommutator mit dem Hamilton-Operator $\mathcal{H}$ fordern lässt. Hierbei ist $\mathcal{A}$ ein antilinearer Operator, der mit dem physikalisch fundamentalsten antilinearen Operator $\mathcal{T}$ für die Zeitumkehr verknüpft ist.

Die wohl bekannteste Symmetrie in diesem Zusammenhang ist die $\mathcal{PT}$-Symmetrie mit $\mathcal{A} = \mathcal{PT}$, welche ausführlich in Abschnitt 5-1 eingeführt wird. Die Wirkung des $\mathcal{PT}$-Operators entspricht einer Spiegelung des Raums zusammen mit einer komplexen Konjugation,

$$\mathcal{PT}: \quad \hat{x} \to -\hat{x}\,, \quad \mathrm{i} \to -\mathrm{i}\,. \tag{5-2}$$

Durch Anwendung des $\mathcal{PT}$-Operators auf die Eigenwertgleichungen (4-10) und (4-11) lässt sich zeigen, dass für jeden Eigenwert E_n eines $\mathcal{PT}$-symmetrischen Hamilton-Operators, der Gl. (5-1) erfüllt, auch E_n^* ein Teil des Spektrums sein muss, sodass die Eigenwerte in komplex konjugierten Paaren auftreten. Ist die $\mathcal{PT}$-Symmetrie exakt, so sind die Eigenwerte sogar reell. Treffen sich zwei reelle Eigenwerte, so können diese durch spontane Brechung der $\mathcal{PT}$-Symmetrie an einem exzeptionellen Punkt in ein Paar komplex konjugierter Eigenwerte aufspalten. Diese Eigenschaften bleiben auch bei anderen antiunitären Symmetrien erhalten, die einer Verallgemeinerung des $\mathcal{PT}$-Operators entsprechen. Jedoch besticht gerade die $\mathcal{PT}$-Symmetrie durch ihre Einfachheit; $\mathcal{PT}$-symmetri-

sche, komplexe Potentiale besitzen etwa stets einen symmetrischen Realteil und einen antisymmetrischen Imaginärteil[16] bezüglich des Ortes $\hat{x}$.

[16] vgl. Gl. (5-3)

Eine weitere bekannte Symmetrie ist die Supersymmetrie, deren Grundlagen in Abschnitt 2-5 beschrieben werden. Üblicherweise bezeichnet sie die Symmetrie zwischen Bosonen und Fermionen und findet somit Anwendung in der Quantenfeldtheorie. Jedoch lässt sich Supersymmetrie auch auf die Quantenmechanik[17] und insbesondere auf die nicht-Hermitesche Quantenmechanik[18] anwenden. In nicht-Hermiteschen Systemen können die links- und die rechtsseitigen, biorthogonalen Zustände als bosonische und fermionische Zustände mit einer gebrochenen Supersymmetrie interpretiert werden.[19] Auch in diesem Fall besteht das Spektrum des Hamilton-Operators aus reellen und Paaren zueinander komplex konjugierter Eigenwerte.[20] Die Zustände, die zum selben reellen Energieeigenwert gehören, lassen sich durch die Symmetrisierungsoperatoren (5-37) und (5-38), welche die Beziehungen

[17] vgl. Abschnitt 2-5 d)

[18] vgl. Abschnitt 5-2

[19] vgl. Abb. 2-7 und 2-9

[20] im Folgenden kurz als „komplex konjugiertes Spektrum“ bezeichnet

$$\mathcal{H}\underline{S} = \underline{S}\mathcal{H}^\dagger\,, \tag{5-14}$$

$$\overline{S}\mathcal{H} = \mathcal{H}^\dagger\overline{S} \tag{5-15}$$

erfüllen, ineinander überführen. Im Allgemeinen werden jedoch jeweils die Zustände zu den zueinander komplex konjugierten Eigenwerten durch die Symmetrisierungsoperatoren (5-43) und (5-44) ineinander überführt. Sind die Symmetrisierungsoperatoren zusätzlich noch invertierbar und invers zueinander, so lassen sich Gln. (5-14) und (5-15) schreiben als

$$\underline{S}\mathcal{H}^\dagger\overline{S} = \mathcal{H}\,, \tag{5-30}$$

was eine Verallgemeinerung der Hermitezitätsbedingung darstellt.[21] Die Symmetrisierungsoperatoren stellen hierbei eine Metrik dar.[22]

[21] vgl. Abschnitt 4-4 a)

[22] vgl. Abschnitt 4-4

Gleichungen (5-14), (5-15) und (5-24) sind miteinander verknüpft.[23] Jedoch stellen die Bedingungen (5-14) und (5-15) keine Symmetriebedingungen dar, wodurch der Hamilton-Operator keine offensichtlichen Symmetrien aufweisen muss; daher wird dieses Konzept in dieser Arbeit als „Symmetrisierung“ bezeichnet und

[23] vgl. Abschnitt 5-3 d)

ist in Abschnitt 5-3 beschrieben. Sowohl im Fall eines symmetrischen als auch eines symmetrisierten Quantensystems sind die Koeffizienten des charakteristischen Polynoms reell,[24] was eine notwendige Bedingung für das Auftreten eines komplex konjugierten Spektrums ist. Jedoch lassen sich die Symmetrisierungsbedingungen (5-14) und (5-15) auch dann anwenden, wenn nur ein Teil des Spektrums komplex konjugiert ist.[25] Umgekehrt lassen sich damit etwa nicht-Hermitesche Systeme finden, die reelle Eigenwerte und damit ausgeglichenen Gewinn und Verlust aufweisen. Die Symmetrisierungsoperatoren sind in diesem Fall nicht mehr invertierbar und nur noch semiinvers zueinander; entsprechend wird diese Verallgemeinerung der Symmetrisierung als Semisymmetrisierung bezeichnet und in Abschnitt 5-4 anhand eines einfachen Beispiels besprochen.

[24] vgl. Abschnitt 5-3 c)

[25] Die übrigen Eigenwerte sind hierbei isoliert komplex.

Die Konzepte der $\mathcal{PT}$-Symmetrie sowie der Symmetrisierung und Semisymmetrisierung werden in Kapitel 6 auf lineare, eindimensionale Mehrmuldenpotentiale mit lokalisierten Gewinnen und Verlusten, wie in Abb. 6-1 dargestellt, angewandt. Hierbei zeigt sich, dass Symmetrisierung als eine eigenständige Methode angesehen werden kann. Lokalisierte Gewinne und Verluste können nicht mithilfe der Symmetrisierungsoperatoren aus der nicht-Hermiteschen Supersymmetrie beschrieben werden,[26] welche notwendigerweise durch Differentialoperatoren gegeben sind.[27] Im einfachsten Fall kann ein Zweimuldenpotential mit dem diskreten, komplex symmetrischen Hamilton-Operator

[26] vgl. Abschnitt 5-5

[27] vgl. Abschnitt 5-2 b)

$$\mathcal{H} = \begin{pmatrix} \epsilon_1 + \mathrm{i}\gamma_1 & -J \\ -J & \epsilon_2 + \mathrm{i}\gamma_2 \end{pmatrix} \tag{6-9}$$

beschrieben werden; für $\epsilon_1 = \epsilon_2$ und $\gamma_1 = -\gamma_2$ ist dieser $\mathcal{PT}$-symmetrisch. Abbildung 6-2 zeigt ein typisches Spektrum eines $\mathcal{PT}$-symmetrischen Systems, in dem alle Eigenwerte reell sind, solange die $\mathcal{PT}$-Symmetrie für geringere Gewinne und Verluste ungebrochen ist. Jedoch lassen sich auch abseits der $\mathcal{PT}$-Symmetrie reelle Eigenwerte finden, wenn folgender Zusammenhang gilt,

$$\epsilon_1 - \epsilon_2 = \pm(\gamma_1 + \gamma_2)\sqrt{-\frac{J^2}{\gamma_1\gamma_2} - 1}\,. \tag{6-16}$$

Die $\mathcal{PT}$-symmetrischen Systeme sind hierbei ein Spezialfall dieser Zweimodensysteme, die, wie in Abb. 6-3 und 6-4 gezeigt, semisymmetrisiert sind, sodass nur jeweils ein reeller und ein komplexer Eigenwert auftreten. Tatsächlich zeigt sich, dass ein Zweimodensystem der Form (6-9) nur dann zwei reelle Eigenwerte besitzen kann, wenn der Hamilton-Operator (6-9) Hermitesch oder $\mathcal{PT}$-symmetrisch ist. Das kann auf die geringe Anzahl an freien Parametern zurückgeführt werden und tritt bei Drei- und Mehrmodensystemen nicht mehr auf.

Darüber hinaus lassen sich solche Systeme nicht für alle Parameterkombinationen symmetrisieren, da sich die Symmetrisierungsbedingungen nicht mehr erfüllen lassen, sodass Gl. (6-16) keine reellen Werte mehr liefert. Diese Bereiche sind in Abb. 6-3 und 6-4 schraffiert dargestellt und lassen sich in zwei Kategorien einteilen:

1) Sowohl Gewinn als auch Verlust müssen auftreten und sich ausgleichen. Daher müssen γ_1 und γ_2 unterschiedliche Vorzeichen haben.

2) Werden Gewinn und Verlust zu groß, so kommt es zu einer Brechung der Symmetrisierung.

Mithilfe bikomplexer Zahlen[28] lässt sich zeigen, dass auch in diesen Fällen symmetrisierte Lösungen existieren, welche die physikalischen Lösungen analytisch fortsetzen. Das ist gut ersichtlich bei einem Vergleich der Abbildungen 6-3, 6-5 und 6-6. Hierbei zeigt sich nochmals ein deutlicher Unterschied zwischen den oben besprochenen Kategorien: Während sich die bikomplexen Lösungen im Falle der Brechung der Symmetrisierung stetig an die physikalischen Lösungen anschließen, so treten Unstetigkeiten in den Bereichen auf, in denen nur Gewinne oder nur Verluste vorliegen.

[28] vgl. Anhang G

Auf ähnliche Art und Weise lassen sich auch Mehrmodensysteme beschreiben. In Abb. 6-7 sind die Bereiche des Parameterraums dargestellt, in denen symmetrisierte Dreimodensysteme der Form (6-22) existieren. Im Gegensatz zum Zweimodensystem sind diese Bereiche jedoch vollkommen getrennt von den $\mathcal{PT}$-symmetrischen Lösungen.[29] Jedoch ergibt sich auch hierbei als Spezialfall eine Symmetrie, die Anti-$\mathcal{PT}$-Symmetrie.[30] Außerdem treten in den

[29] vgl. Abb. 6-4 und 6-7

[30] vgl. Abb. 6-9

symmetrisierten Dreimodensystemen auch jeweils exzeptionelle Punkte zwischen dem Grundzustand und dem ersten angeregten Zustand sowie zwischen den beiden angeregten Zuständen auf. Hierbei handelt es sich um exzeptionelle Punkte zweiter Ordnung,[31] die im Parameterraum eine zusammenlaufen und einen exzeptionellen Punkt dritter Ordnung bilden.[32] Hierbei entsteht die Form einer Spitze, in deren Bereich drei reelle Eigenwerte auftreten, wohingegen außerhalb nur ein Eigenwert reell ist und die übrigen beiden zueinander komplex konjugiert sind.

[31] vgl. Abb. 4-1

[32] vgl. Abb. 6-8

Eine besondere Art von Mehrmodensystemen wird in Abschnitt 6-2 untersucht, in dem nur die äußeren Mulden Gewinn und Verlust erfahren. Die Parameter dieser Mulden werden gemäß Gln. (6-32) bis (6-34) gewählt, was dem Rand in Abb. 6-4 entspricht, an dem die Symmetrisierung gebrochen wird. Die inneren Mulden sind hingegen alle identisch gemäß Gl. (6-31). Das Spektrum eines solchen Mehrmuldenpotentials ist in Abb. 6-10 dargestellt. Die besondere Eigenschaft besteht hierbei darin, dass die Eigenwerte bis auf einen Zustand reell sind. Dies gilt unabhängig von der Anzahl der inneren Mulden. Solche Systeme eignen sich daher zur Realisierung von Transportketten, bei denen etwa Teilchen am einen Ende ein- und am anderen Ende ausgekoppelt werden, sodass ein konstanter Strom entsteht, der den Gewinn und den Verlust ausgleicht.

Neben linearen Quantensystemen werden in dieser Arbeit in Kapitel 7 auch nichtlineare Systeme mit einem zusätzlichen Term der Form

$$f(\psi) \propto |\psi|^2 = \langle \psi | \psi \rangle \tag{7-2}$$

untersucht. Der zugehörige Hamilton-Operator $\mathcal{H}(\psi)$ hängt damit vom Zustand des Systems ab. Die Eigenwerte und Eigenzustände eines solchen Operators müssen über eine nichtlineare Eigenwertgleichung bestimmt werden, deren Lösung nur in Ausnahmefällen analytisch möglich ist[33] und in der Regel über numerische Verfahren erfolgen muss.[34] Da solche Systeme nicht mehr durch die lineare Algebra beschrieben werden können, ist im Voraus auch nicht klar, wie viele Lösungen ein nichtlineares System besitzt. In einem $\mathcal{PT}$-symmetrischen, nichtlinearen Zweimodensystem der

[33] vgl. Abschnitt 7-4 a)

[34] vgl. Abschnitt 7-1 a)

Form (7-31) treten für bestimmte Parameter beispielsweise bis zu vier Lösungen auf, wie in Abb. 7-3 zu sehen ist. All das erschwert die Beschreibung solcher Systeme und insbesondere auch die Anwendung von Konzepten wie der Symmetrisierung.[35] Daher beschäftigt sich Kapitel 7 nur mit der Untersuchung reeller Energieeigenwerte, was in der Regel einem symmetrischen, symmetrisierten oder semisymmetrisierten System entspricht.

[35] vgl. Abschnitt 7-3

Während die reellen Lösungen eines $\mathcal{PT}$-symmetrischen Zweimodensystems in einem nichtlinearen System,[36] wie in Abb. 7-3 gezeigt, praktisch unverändert über einen breiten Parameterbereich auftreten, so sind reelle Lösungen eines asymmetrischen, nichtlinearen Systems[37] nur noch vereinzelt zu finden. Abbildung 7-6 zeigt, dass stationäre Zustände auch für einen Hamilton-Operator der Form (7-30) und für unterschiedliche Stärken der nichtlinearen Terme auftreten. Jedoch muss hierbei die Stabilität der Lösungen beachtet werden. Stationäre Lösungen nichtlinearer Gleichungen müssen nicht zwangsläufig auch zeitlich stabil gegenüber von Störungen sein.[38] Falls, wie in Abb. 7-1 dargestellt, eine rücktreibende „Kraft“ das System bei einer Störung zurück in den stationären Zustand bringt, ist der Zustand stabil. Ist der Zustand jedoch instabil wie in Abb. 7-2, so entfernt sich das System bei einer Störung bereits zunehmend vom stationären Zustand. Durch Linearisierung kann die lineare Stabilität eines dynamischen Systems gegenüber kleiner Störungen bestimmt werden.[39] Für ein nicht-Hermitesches Quantensystem mit einem Term der Form (7-2) müssen hierbei simultane Störungen der links- und rechtsseitigen Eigenzustände betrachtet werden, welche sich über den Zustandsvektor $\phi = (\underline{\psi}, \overline{\psi})^\mathsf{T}$ beschreiben lassen,

[36] vgl. Abschnitt 7-4 a)

[37] vgl. Abschnitt 7-4 b)

[38] vgl. Abschnitt 7-2

[39] vgl. Abschnitt 7-2 a)

$$\delta\phi(t) = \mathrm{e}^{-\mathrm{i}J(\phi_0)t}\delta\phi(0)\,. \tag{7-14}$$

Die Jacobi-Matrix J ist über Gl. (7-15) definiert und ihre Eigenwerte bestimmen die Stabilität des Systems; sind alle Imaginärteile negativ, so ist der Zustand stabil.

In Abb. 7-7 sind die Stabilitätseigenwerte der Jacobi-Matrix für Lösungen des Zweimodensystems dargestellt. Es lässt sich erkennen, dass es ausgedehnte Parameterbereiche für γ gibt, in denen die Lösungen des nichtlinearen Systems stabil sind.[40] Die

[40] Strenggenommen ist so eine Stabilitätsbetrachtung nur für stationäre Lösungen sinnvoll.

stationären Lösungen γ_s fallen in einen dieser Bereiche, falls die Stärke g der nichtlinearen Terme nicht zu groß ist. Jedoch zeigt sich hierbei noch eine weitere Eigenschaft: Das Betragsquadrat $|\psi|^2$ der Wellenfunktion, das bei γ_s erhalten bleibt, nimmt für $\gamma > \gamma_s$ zu und für $\gamma < \gamma_s$ ab. Gleichzeitig verschiebt sich die Position γ_s einer stationären Lösung mit g zu größeren Werten hin. Da die nichtlinearen Terme in Gl. (7-30) dem Produkt dieser beiden Größen entsprechen, also $g|\psi|^2$, ergibt sich eine zusätzliche Selbststabilisierungswirkung. Wird das System gestört und aus seinem stationären Zustand gebracht, dann verändern die nichtlinearen Terme den Hamilton-Operator so, dass sich das System wieder in einem stationären Zustand befindet. Wie in Abb. 7-11 gezeigt, lassen sich ähnliche Szenarien auch in asymmetrischen Dreimodensystemen finden.[41]

[41] vgl. Abschnitt 7-5

Dieser Selbststabilisierungsmechanismus nichtlinearer Systeme könnte insbesondere in Experimenten von Interesse sein. Das exakte Einstellen und Aufrechterhalten der Parameter eines $\mathcal{PT}$-symmetrischen Systems stellt beispielsweise eine experimentelle Herausforderung dar, insbesondere, wenn Gewinn und Verlust aufgrund ihrer Realisierung von Natur aus unsymmetrisch sind.[42] Das betrifft jedoch auch symmetrisierte Systeme, die ebenfalls auf die exakte Einhaltung von Relationen[43] zwischen den Parametern angewiesen sind. Durch Verwendung eines entsprechenden nichtlinearen Systems lassen sich diese Probleme vermeiden, was etwa die experimentelle Realisierung solcher Zustände in Bose–Einstein-Kondensaten ermöglichen könnte. Der nichtlineare Term (7-2) beschreibt dabei die Kontaktwechselwirkungen zwischen den Kondensatteilchen, deren Stärke sich über Feshbach-Resonanzen beliebig einstellen lässt. Für Bose–Einstein-Kondensate lassen sich sowohl echte[44] als auch effektive[45] Gewinne und Verluste erzeugen. Effektiv offene Mehrmuldenpotentiale lassen sich, wie in Abb. 8-1 dargestellt, durch Einbettung in eine Optische Kette realisieren. Die in dieser Arbeit untersuchten Matrixmodelle sind aber nur eine Näherung realistischer Mehrmuldenpotentiale.[46] Jedoch werden in Abschnitt 6-4 auch räumlich ausgedehnte Potentiale aus Gauß-Funktionen untersucht und gezeigt, dass die Modellrechnungen eine gute Näherung realistischer Potentiale mit entsprechenden Parametern darstellen.

[42] vgl. Kapitel 8

[43] z.B. Gl. (6-16)

[44] vgl. Abschnitt 8-1

[45] vgl. Abschnitt 8-2

[46] vgl. Anhang E

Teil 2: Elektromagnetische Systeme

Die Realisierung von Symmetrien und symmetrisierter Quantensysteme ist schwierig,[47] was man etwa daran erkennen kann, dass $\mathcal{PT}$-Symmetrie vor seiner Realisierung in einem Quantensystem zuerst in verschiedenen anderen, wellenmechanischen Systemen experimentell beobachtet wurde. Das ist möglich, da viele Systeme mathematisch äquivalent zur Schrödinger-Gleichung mit Gewinn und Verlust beschrieben werden können. Ein Beispiel hierfür sind magnetisch gekoppelte, elektrische Schwingkreise, die in Kapitel 10 besprochen werden und eine einfache und zugängliche Basis für die Realisierung von Symmetrien und Symmetrisierung zur Erzeugung von ausgeglichenem Gewinn und Verlust bieten.

[47] vgl. Kapitel 8

Strom und Spannung in einem elektrischen Schwingkreis, im einfachsten Fall bestehend aus einer Spule und einem Kondensator,[48] werden jeweils durch eine Differentialgleichung zweiter Ordnung beschrieben; für die Spannung gilt beispielsweise

[48] vgl. Abb. 10-1

$$\frac{\mathrm{d}^2 U}{\mathrm{d}t^2} + \omega_0^2 U = 0 \tag{10-3}$$

mit der Resonanzfrequenz ω_0. Durch geschickte Kombination von Strom und Spannung lässt sich ein Schwingkreis jedoch auch als ein Einmodensystem schreiben,[49]

[49] vgl. Abschnitt 10-1

$$\frac{\mathrm{d}a}{\mathrm{d}t} = \mathrm{i}\omega_0 a\,, \tag{10-10}$$

wobei $|a|^2$ der im Schwingkreis gespeicherten Energie entspricht. Gewinn[50] und Verlust[51] lassen sich entsprechend in diese Beschreibung einführen. Während Verluste durch die Anwesenheit eines Verbrauchers entstehen und sich einfach über deren Widerstände charakterisieren lassen, erfordert die Erzeugung eines Gewinns eine Koaxialleitung, über die eine einlaufende Welle in den Schwingkreis eingekoppelt wird. Die Koaxialleitung erzeugt gleichzeitig einen Verlust, da ein Teil der eingekoppelten Energie als auslaufende Welle vom Schaltkreis reflektiert wird.[52] Die Effekte der ein- und auslaufenden Wellen lassen sich als effektiver Gewinn

[50] vgl. Abschnitt 10-3

[51] vgl. Abschnitt 10-2

[52] vgl. Abschnitt 10-3 a)

zusammenfassen.[53] Mathematisch lässt sich das analog zum Verlust über einen negativen Widerstand beschreiben, was jedoch eine entsprechend angepasste einlaufende Welle erfordert.[54]

[53] vgl. Abschnitt 10-5 a)

[54] vgl. Gl. (10-31)

Zwei Schwingkreise sind, wie in Abb. 10-4 skizziert, über ihre Spulen magnetisch gekoppelt. Das Magnetfeld, das in einer Spule entsteht, induziert einen Strom in der anderen Spule und umgekehrt. Die Beschreibung dieser Gegenseitigen Induktion erfolgt analog zur Beschreibung der Selbstinduktion.[55] Die gekoppelten Schwingkreise können dann über Gl. (10-29) als Zweimodensystem mit der Kopplungskonstanten κ aus Gl. (10-28) beschrieben werden. Die Stärke der Kopplung hängt dabei von der geometrischen Anordnung der Spulen zueinander ab, wie in Abb. 10-5 und 10-6 gezeigt, und nimmt mit der Entfernung ab. Werden dann noch Gewinn und Verlust eingeführt, so ergibt sich

[55] vgl. Anhang H

$$-\mathrm{i}\mathcal{H} = \begin{pmatrix} \mathrm{i}\bar{\omega}_1 + \bar{\gamma}_1 & \mathrm{i}\kappa \\ \mathrm{i}\kappa & \mathrm{i}\omega_2 - \gamma_2 \end{pmatrix}, \tag{10-32}$$

was äquivalent zum Hamilton-Operator (6-9) mit den Resonanzfrequenzen $\bar{\omega}_1 = -\epsilon_1$, $\omega_2 = -\epsilon_2$ sowie $\bar{\gamma}_1 = \gamma_1$ und $\kappa = J$ ist.[56] Hierbei sind $\bar{\omega}_1$ und $\bar{\gamma}_1$ effektive Modellparameter, welche über die einlaufende Welle frei eingestellt werden können. Damit lassen sich alle oben diskutierten Methoden und Effekte für lineare, nicht-Hermitesche Quantensysteme direkt auf ein System aus gekoppelten Schwingkreisen übertragen.

[56] Die Stärke des Verlustes wird hier durch $\gamma_2 > 0$ beschrieben.

Neben der bloßen Realisierung der in dieser Arbeit besprochenen Symmetrien und Konzepten der Symmetrisierung, können gekoppelte Schwingkreise mit Gewinn und Verlust, wie in Abb. 11-1 gezeigt, auch für die kabellose Übertragung von Energie verwendet werden. Auch hierbei ist der Ausgleich von Gewinnen und Verlusten notwendig, um eine kontinuierliche und effiziente[57] Energieübertragung zu gewährleisten. So zeigt Abb. 11-4 etwa, dass der Wirkungsgrad (11-10) einer kabellosen Energieübertragung optimal ist, solange der Hamilton-Operator (10-32) $\mathcal{PT}$-symmetrisch ist.[58] Das gilt weitgehend unabhängig von der Entfernung der gekoppelten Spulen, was üblicherweise eine aktive Anpassung der Parameter der Schwingkreise erfordern würde. Dabei muss beachtet werden, dass der Wirkungsgrad nicht nur von den Mo-

[57] vgl. Abschnitt 11-1 b)

[58] vgl. Abschnitt 11-2

dellparametern $\bar{\omega}_1$ und $\bar{\gamma}_1$, sondern auch von den physikalischen Parametern ω_1 und γ_1 abhängt, die von den elektrischen Komponenten des Schwingkreises bestimmt werden; liegen diese in derselben Größenordnung, so liegt auch der Wirkungsgrad in der Größenordnung Eins. Obwohl der Wirkungsgrad optimal ist, eignet sich die strahlungslose Energieübertragung mithilfe magnetischer Kopplungen nur für kurze bis mittlere Entfernungen. Für eine kabellose Energieübertragung über Langstrecken muss Laser- oder Mikrowellenstrahlung verwendet werden.

Abgesehen von der Optimierung der Energieübertragung lässt sich auch ein Selbststabilisierungsmechanismus in unsymmetrischen Systemen erzeugen.[59] Die Modellparameter $\bar{\omega}_1$ und $\bar{\gamma}_1$ werden gänzlich durch die Wahl der einlaufenden Welle bestimmt. Somit lassen sich auch beliebige, nichtlineare Terme in dem Schwingkreis erzeugen, in dem eingekoppelt wird,[60] wobei die einlaufende Welle im Allgemeinen der Form (10-38) gehorcht. Wie in Abb. 11-5 gezeigt, gibt es stabile stationäre Lösungen, welche dieselben Eigenschaften aufweisen wie die stationären Zustände des Quantensystems in Abb. 7-6. Daher erfahren auch diese Zustände eine Selbststabilisierung bei geringen Störungen der Entfernung der gekoppelten Spulen. Die Anpassung der einlaufenden Welle wirkt hierbei wie eine Steuerungstechnik. Jedoch werden die stationären Lösungen recht schnell instabil. Außerdem ist der Wirkungsgrad der Energieübertragung, den solche Zustände ermöglichen, wie in Abb. 11-6 gezeigt eher gering. Der Grund hierfür ist, dass die Modellparameter und die physikalischen Parameter nicht in derselben Größenordnung liegen, da andernfalls keine stabilen stationären Zustände gefunden werden konnten.[61]

In Abschnitt 11-4 wird kurz diskutiert, wie sich lange Ketten aus gekoppelten Schwingkreisen bauen lassen, bei denen an einem Ende ein- und am anderen Ende ausgekoppelt werden. Dieses Szenarien sind ähnlich zu den Transportketten, welche in Abschnitt 6-2 diskutiert werden. Jedoch sind die Resonanzfrequenzen der elektrischen Schwingkreise notwendigerweise von Null verschieden, sodass sich durch Verwendung der aus den Quantensystemen bekannten Parametern (11-22) bis (11-24) nur im $\mathcal{PT}$-symmetrischen Fall stationäre Lösungen ergeben.[62] Jedoch zeigt die Berücksichti-

[59] vgl. Abschnitt 11-3

[60] vgl. Abschnitt 10-5 b)

[61] Das schließt deren Existenz jedoch nicht aus.

[62] vgl. Abb. 11-8

gung geringer, intrinsischer Verluste aufgrund des Drahtwiderstandes[63] jeder Spule, dass stabile, stationäre Zustände nur noch für unsymmetrische Parameter möglich sind.[64]

[63] vgl. Gl. (10-11)

[64] vgl. Abb. 11-10

Ausblick

Die Beschreibungen der Quantensysteme in dieser Arbeit erfolgten stets unter dem Aspekt der Einteilchendynamik, wie sie etwa für Bose–Einstein-Kondensate im Grenzfall vieler Teilchen auftritt. Obwohl diese Annahme in typischen Experimenten gerechtfertigt ist, so könnte eine Untersuchung der echten Vielteilchendynamik dennoch interessant sein. Die mikroskopischen Prozesse, welche die Ein- und Auskopplung von Teilchen aus einem Quantensystem beschreiben, sind von Natur aus nicht symmetrisch.[65] Daher lässt sich etwa $\mathcal{PT}$-Symmetrie nicht direkt auf Vielteilchensysteme anwenden. Symmetrisierung könnte hierbei helfen, Zustände in Vielteilchensystemen mit ausgeglichenem Gewinn und Verlust zu finden.

[65] vgl. Kapitel 12

Jedoch ist die Anwendung von Symmetrisierung, je nach System, schwierig und muss rein numerisch erfolgen.[66] Daher könnte man sich den Umstand zunutze machen, dass symmetrisierte Systeme bestimmte Strukturen aufweisen, auch wenn diese nur in wenigen Fällen für Menschen intuitiv erkennbar sind. Das lässt sich etwa an den in Abb. 6-9 dargestellten, anti-$\mathcal{PT}$-symmetrischen Systemen sehen, die einen Spezialfall symmetrisierter Systeme darstellen. Computer hingegen sind in der Lage solche abstrakten Strukturen und Muster zu erkennen. Durch Methoden des maschinellen Lernens könnte auch die Symmetrisierung komplexer Systeme möglich sein,[67] was die Konstruktion beliebiger Systeme mit ausgeglichenen Gewinnen und Verlusten erlauben würde.

[66] vgl Abschnitt 7-3

[67] vgl. Kapitel 12

Index

Z

Danksagung

Leider läßt sich eine wahrhafte Dankbarkeit mit Worten nicht ausdrücken.

Johann Wolfgang von Goethe

An dieser Stelle möchte ich mich bei all den Personen bedanken, ohne die ich diese Arbeit nicht hätte anfertigen können, die mich auf meinem Weg begleitet haben und denen ich zu tiefstem Dank verpflichtet bin:

— Mein großer Dank gilt natürlich Herrn Apl. Prof. Dr. Jörg Main, der nicht zuletzt durch seine Betreuung diese Arbeit überhaupt erst ermöglicht hat, sich jedoch auch stets die Zeit für Fragen und Diskussionen genommen hat. Insbesondere möchte ich mich auch für die Unterstützung bei der Finanzierung meiner Arbeit über die letzten Monate bedanken.

— Ich möchte mich ganz herzlich bei Herrn Prof. Dr. Holger Cartarius bedanken, der mir nicht nur stets ein großes Vorbild war, sondern mit seiner fachlichen Unterstützung, gemeinsamen Diskussionen und Ratschlägen auch maßgeblich zur Themenfindung und zum Gelingen dieser Arbeit beigetragen hat.

— Es wäre mir jedoch nicht möglich gewesen, meine Arbeit ohne die Unterstützung von Herrn Prof. Dr. Wunner anzufertigen, der unsere Zusammenarbeit bei Veröffentlichungen nicht nur mit seinen exzellenten Sprachkenntnissen bereicherte, sondern auch die Möglichkeit einer Finanzierung meiner Promotion gefunden hat.

— Ich möchte mich auch bei Herrn Apl. Prof. Dr. Johannes Roth bedanken, der gleich und mit Interesse zugestimmt hat, den Mitbericht zu dieser Arbeit zu übernehmen.

— Ich möchte mich außerdem bei Herrn Prof. Dr. Ronny Nawrodt für die freudige Übernahme des Prüfungsvorsitzes und für die entspannte Atmosphäre in der Prüfung bedanken.

— Insbesondere möchte ich mich auch bei meinen Eltern bedanken, die mich auf meinem langen Weg stets unterstützt und an mich geglaubt haben.

— Ich bin auch dankbar für all meine Freundinnen und Freunde, die mich während dieser Zeit begleitet haben oder die ich auf diesem Weg kennenlernen durfte.

— Mein Dank gilt zudem allen Mitarbeiterinnen und Mitarbeitern am Institut für Theoretische Physik I, die das ITP1 zu etwas ganz Besonderem gemacht haben, sodass ich mich gleich von Beginn an wohl gefühlt habe und das auch nach vielen Jahren noch tue. Das gilt insbesondere auch für frühere Kolleginnen und Kollegen, mit denen ich in meiner Zeit am ITP1 arbeiten und von welchen ich lernen durfte.

— Ebenso danke ich dem Team des Studienlotsenprojektes, nicht nur, weil mir die Arbeit mit ihnen die Finanzierung meiner Promotion ermöglicht hat, sondern auch für die unterhaltsame und lehrreiche Zeit.

Daniel Dizdarevic

geboren am 12.03.1991 in Göppingen

daniel.dizdarevic@gmx.de

Ausbildung

Allgemeines Abitur **2010**
Erich Kästner Gymnasium Eislingen

B. Sc. Physik **2014**
Institut für Theoretische Physik I Universität Stuttgart
»Bifurkationen in den Eigenwertspektren PT-symmetrischer Bose–Einstein-Kondensate«

M. Sc. Physik **2016**
Institut für Theoretische Physik I Universität Stuttgart
»Realisierung von balanced gain and loss in einem Bose–Hubbard-Modell mit zeitabhängigen Potentialen«

Publikationen

[157] D. Dizdarevic, H. Cartarius, J. Main und G. Wunner, »Balancing gain and loss in symmetrised multi-well potentials«, J. Phys. A: Math. Theor. **53**, 405304 (2020)

[179] F. Kogel, S. Kotzur, D. Dizdarevic, J. Main und G. Wunner, »Realization of $\mathcal{PT}$-symmetric and $\mathcal{PT}$-symmetry-broken states in static optical-lattice potentials«, Phys. Rev. A **99**, 063610 (2019)

[180] S. Altinisik, D. Dizdarevic und J. Main, »Balanced gain and loss in spatially extended non-$\mathcal{PT}$-symmetric multiwell potentials«, Phys. Rev. A **100**, 063639 (2019)

[193] D. Dizdarevic, J. Main, K. Alpin, J. Reiff, D. Dast, H. Cartarius und G. Wunner, »Realization of balanced gain and loss in a time-dependent four-mode Bose–Hubbard model«, Phys. Rev. A **97**, 013623 (2018)

[207] D. Dizdarevic, D. Dast, D. Haag, J. Main, H. Cartarius und G. Wunner, »Cusp bifurcation in the eigenvalue spectrum of $\mathcal{PT}$-symmetric Bose–Einstein condensates«, Phys. Rev. A **91**, 033636 (2015)

[264] T. Mathea, D. Dast, D. Dizdarevic, H. Cartarius, J. Main und G. Wunner, »Using mixed many-body particle states to generate exact $\mathcal{PT}$-symmetry in a time-dependent four-well system«, J. Phys. A: Math. Theor. **51**, 315303 (2018)

Ehrenwörtliche Erklärung

Ich erkläre, dass ich diese Dissertation, abgesehen von den ausdrücklich bezeichneten Hilfsmitteln, selbständig verfasst habe.

Stuttgart, den 31. Mai 2021